

1 **The relationship between ice sheets and submarine mass movements** 2 **in the Nordic Seas during the Quaternary**

3 Ed L. Pope^{1*}, Peter J. Talling², Colm Ó Cofaigh¹

4 ¹*Department of Geography, Durham University, Science Laboratories, South Road, Durham, DH1 3LE,*
5 *UK.*

6 ²*Departments of Earth Science and Geography, Durham University, Science Laboratories, South Road,*
7 *Durham, DH1 3LE, UK.*

8 **Abstract**

9 Quaternary evolution of high-latitude margins has, to a large degree been shaped by the advance
10 and retreat of ice sheets. Our understanding of these margins and the role of ice sheets is
11 predominantly derived from the polar North Atlantic during the Late Weichselian. This region has
12 formed the basis for conceptual models of how glaciated margins work and evolve through time
13 with particular focus on trough-mouth fans, submarine landslides and channel systems. Here, by
14 reviewing the current state of knowledge of the margins of the Nordic Seas during the Quaternary
15 we provide a new set of models for different types of glaciated margin and their deposits. This is
16 achieved by tracking the growth and decay of the Greenland, Barents Sea and Scandinavian Ice
17 Sheets over the last 2.58 Ma and how these ice sheets have influenced sedimentation along their
18 margins. The reconstructed histories show 1) the completeness of records along each ice sheet
19 margin is highly variable. 2) Climatic deterioration and the adoption of 100 kyr cyclicity has had
20 progressive impacts on each ice sheet and the resulting sedimentation and evolution of its related
21 margin. These reconstructions and records on other margins worldwide enable us to identify first
22 order controls on sediment delivery at ice sheet scales, propose new conceptual models for trough-
23 mouth fans and glaciated margin development. We are also able to show how the relationship
24 between large submarine landslide occurrence and ice sheet histories changes on different types of
25 margin.

26 **Keywords:** Glacial history, glaciated continental margins, Nordic Seas, glacimarine sedimentary
27 processes, trough-mouth fans, submarine landslides; ice sheets; Greenland Ice Sheet; Barents Sea
28 Ice Sheet; Scandinavian Ice Sheet

29 *Corresponding author: Edward.Pope@durham.ac.uk

30

31 **1. Introduction**

32 Sediment is transported across our planet most efficiently by ice sheets and submarine mass
33 movements (Boulton, 1978; Hallet et al., 1996; Dowdeswell et al., 2010b; Talling et al., 2014). Rates
34 of erosion by ice sheets and the subsequent transport and deposition of the eroded material in
35 marine settings can be an order of magnitude greater than river catchments with larger areas
36 (Milliman and Meade, 1983; Elverhøi et al., 1998). Once deposited this material is then often
37 reworked by submarine gravity-flow processes. For example large submarine landslides, such as the
38 Storegga Slide that occurred 8.2 ka offshore Norway, can contain several thousand cubic kilometres
39 of predominantly glacial sediments (Haflidason et al., 2005). A clear relationship therefore exists
40 between ice sheet processes, submarine mass movements and the sedimentary architecture of
41 glaciated continental margins (Heezen and Ewing, 1952; Kuvaas and Kristoffersen, 1996; Vorren et
42 al., 1998; Ó Cofaigh et al., 2003). Understanding the links between the two phenomena is therefore
43 crucial to reconstructing ice sheet histories from the sedimentary record, and understanding the
44 evolution of glaciated margins.

45 Delivery of sediment to the marine environment by ice sheets is characterised by the sporadic
46 nature and the exceptional volumes involved. The rate of sediment delivery by ice sheets is a
47 function of the frequency of glaciation and its intensity, internal dynamics and the geology over
48 which the ice is moving, i.e. local lithology and permeability. Over long timescales, the growth and
49 decay of ice sheets is controlled by orbital forcing (Jansen and Sjøholm, 1991; Raymo and Ruddiman,
50 1992; Thiede et al., 1998; Jansen et al., 2000; Ehlers and Gibbard, 2004). At shorter timescales ice
51 sheets can also be affected by sub-orbital forcing, such as reduced thermohaline circulation
52 (Broecker and Denton, 1990; Bond et al., 1999), or the switch on/off of ice streams draining the ice
53 sheet interior (Bennett, 2003; Catania et al., 2006; Dowdeswell et al., 2006b; Christoffersen et al.,
54 2010). Spatially, ice sheet sedimentation also varies according to the position of fast and slow
55 flowing ice (Ottesen et al., 2005), the drift tracks of icebergs (Mugford and Dowdeswell, 2010), the

56 location of meltwater discharge from the ice front (Dowdeswell et al., 2015) and the type of
57 substrate. This temporal and spatial variability should be reflected in the sedimentary history of
58 glaciated margins and therefore provide insights for ice sheet reconstructions. However, to assess
59 this, accurate ice sheet and sedimentation histories need to be reconstructed and diagnostic facies
60 need to be identified.

61 **1.1. Why is it important to understand the links between ice sheet and sedimentation** 62 **histories?**

63 The geological record of high-latitude continental margins contains key information on former ice
64 sheets (Dowdeswell et al., 2016b). Specific landforms and sedimentary sequences have been used to
65 provide information on the extent of palaeo-ice sheets as well as the direction and nature of past ice
66 flow and dynamics (Clark, 1993; Ottesen et al., 2005; Ottesen and Dowdeswell, 2006; Ó Cofaigh et
67 al., 2013a; Jakobsson et al., 2014; Hogan et al., 2016). Multiple sequences of alternating till and pro-
68 /deltaic muds have been used to infer short-term advance and retreat cycles (Funder and Hansen,
69 1996). Eskers and tunnel valleys have been used as indicators of the geometry of past subglacial
70 hydrological systems (Stewart et al., 2013; Greenwood et al., 2016). Trough-mouth fans, covering
71 areas of $10^3 - 10^5 \text{ km}^2$ with volumes of $10^4 - 10^5 \text{ km}^3$, are thought to be indicative of the delivery of
72 large volumes of sediment by fast-flowing ice streams present at the shelf edge (Dowdeswell et al.,
73 1997; Vorren and Laberg, 1997; Canals et al., 2003; Ó Cofaigh et al., 2003; Sejrup et al., 2005). These
74 landform interpretations can subsequently be used to constrain/validate ice sheet models, which in
75 turn can be used to model possible future ice sheet changes (Kleman et al., 1997; Greenwood and
76 Clark, 2009).

77 From an applied perspective, understanding the history of ice sheets and sedimentation along a
78 glaciated margin is important for assessing marine resource potential. Changes in geostatic loading
79 associated with ice sheet growth and decay can lead to the displacement of water or hydrocarbons
80 from low-permeability beds into horizons with superior reservoir properties (Trofimuk et al., 1977;

81 Kjemperud and Fjeldskaar, 1992; Doré and Jensen, 1996). Alternatively ice sheet induced fluid
82 displacement can result in partial failure of oil and gas reservoirs or the displacement of these
83 hydrocarbons into sediments marginal to the ice sheet (Tasianas et al., 2016; Zieba and Grøver,
84 2016). Exhumation of sediments can also adversely impact resource potential as the probability of
85 trapping or sealing hydrocarbons is generally reduced (Doré et al., 2002; Fjeldskaar and Amantov,
86 2017). Upward migration, particularly of free gas, also represents a hazard to resource extraction in
87 terms of drilling and can act as a potential trigger for submarine landslides (Maslin et al., 1998;
88 Pickrill et al., 2001; Chand et al., 2012; Vadakkepuliambatta et al., 2013).

89 **1.1.1. Ice sheets, climate and sedimentation histories**

90 Interpretations of landforms and sedimentary sequences are based on a combination of
91 observations from contemporary glacial environments and interpretations of the environmental
92 conditions that existed under full-glacial conditions. At the most fundamental level these
93 interpretations reflect our understanding of the relationship between glacier dynamics and climate
94 (Hallam, 1989). To first order, glacial sediment delivery and thus landform genesis is often linked to
95 temperature. It is hypothesised that colder climates result in lower basal temperatures in glaciers
96 and ice sheets (Cuffey and Paterson, 2010). These temperatures reduce meltwater production which
97 in turn impacts upon glacial sliding, erosion and therefore sediment transfer (Herman et al., 2011;
98 Egholm et al., 2012; Koppes et al., 2015). At a process scale, processes dominating glacier-influenced
99 delivery of sediment to marine environments are also linked to temperature. Modern/Quaternary
100 interglacial glacial delivery of sediment to marine environments is conceptualised as a continuum
101 between meltwater-dominated (e.g. Southern Alaska) to iceberg-dominated (e.g. West/East
102 Antarctica) environments (Fig. 1a; Dowdeswell et al., 1998). Under full-glacial conditions, the
103 position of each system and thus the dominance of a given mechanism for sediment delivery, shifts
104 its position on the continuum (Fig. 1b; Dowdeswell et al., 2016b).

105 The evolution and history of sedimentation on continental margins should not, however, be
106 conceptualised simply as glacial vs. interglacial conditions. The length and severity of glacial periods
107 has varied throughout the Quaternary (Thiede et al., 1989; Raymo and Nisancioglu, 2003; Ehlers and
108 Gibbard, 2004). At the simplest level, glacial periods can be divided into those which occurred when
109 climate was dominated by 41 kyr cyclicity and those that occurred under 100 kyr cyclicity (Raymo
110 and Nisancioglu, 2003; Tziperman and Gildor, 2003). In terms of erosion and sediment delivery to
111 the continental margin, it has been proposed that the adoption of the 100 kyr climate cycle led to an
112 intensification of glacial erosion and sediment transport (Faleide et al., 2002; Gulick et al., 2015).
113 However, this assertion, linked to the severity and intensity of the 100 kyr cycles is at odds with the
114 understanding of temperature/climate controlling the rate of glacier driven sedimentation. Long-
115 term marine sedimentary records provide one of the few means through which these relationships
116 can be tested over multiple glacial cycles and thus allow us to reconstruct ice sheets and ice sheet
117 processes and their response to variable climatic forcing.

118

119 **1.1.2. Geohazard assessment**

120 Understanding the links between ice sheets and sedimentary processes on continental margins is
121 also critical for hazard assessment. Since the 1929 Grand Banks submarine landslide, increasing
122 numbers of slide scars and deposits have been mapped on previously glaciated margins (Heezen and
123 Ewing, 1952; Bugge, 1983; 1987; Piper and Aksu, 1987; Dowdeswell et al., 1996; Vorren et al., 1998;
124 Hogan et al., 2013). Considered to be one of the main morphological features of glaciated margins,
125 these events have the potential to generate damaging tsunamis and damage local subsea
126 infrastructure (Heezen and Ewing, 1952; Bondevik et al., 1997; 2003; Grauert et al., 2001; Pope et
127 al., 2017a). The Storegga Slide is known to have generated a tsunami with wave run-up heights >20
128 m (Bondevik et al., 2003) while the Grand Banks Slide caused 23 telegraph cable breaks (Piper et al.,
129 1999). The locations of the slides, specifically their often close association with trough-mouth fans,

130 has led to the hypothesis that rapid rates of ice sheet driven sedimentation is a critical factor in the
131 triggering of these slides (Bryn et al., 2003; 2005; Hafliðason et al., 2004; Owen et al., 2007).
132 Understanding the timing and emplacement mechanisms of these slides over multiple glacial cycles
133 relative to changing ice sheet dynamics is therefore crucial to quantifying the potential risk
134 associated with these hazards.

135 **1.2. Previous models linking ice sheet with sedimentation processes and continental margin**
136 **morphology**

137 Conceived in the mid-1990s, an original model (Fig. 2; Dowdeswell et al., 1996) for large-scale
138 sedimentation on glaciated margins was based on a combination of GLORIA imagery, seismic data
139 and models of former ice sheet behaviour. This model linked the sedimentary architecture seen on
140 the margins of the Nordic Seas (i.e. submarine channels, glacigenic debris-flows, etc.) to the
141 extent/velocity of ice delivering sediment to the shelf break (Dowdeswell et al., 1996; Dowdeswell
142 and Siebert, 1999). Low velocity ice associated with low sediment delivery or ice terminating inshore
143 of the shelf edge was hypothesised to be associated with submarine channel systems. Fast flowing
144 ice streams delivering large amounts of sediment were associated with glacigenic debris-flows,
145 submarine landslides and the build-up of trough-mouth fans (Dowdeswell et al., 1996).

146 With the available data this model effectively identified where specific sedimentary features and
147 processes were likely to occur and how they related to palaeo-ice sheets. However, since the
148 inception of this model a number of key advances have been made. First, studies have been able to
149 identify how sedimentation has changed over time on specific sections of a margin (e.g. Solheim et
150 al., 1998; Nygård et al., 2005). This implies that a static model of ice sheet driven sedimentary
151 processes is perhaps not appropriate. Second, there has been growing recognition of the importance
152 of specific processes, such as meltwater delivery of sediment, on glaciated margins (Lekens et al.,
153 2005; Lucchi et al., 2013). These processes therefore may have to be incorporated within a model of
154 glacial margin sedimentation. Third, our understanding of other glaciated margins around the world

155 has improved (Escutia et al., 2000; Ó Cofaigh et al., 2008; 2013; Montelli et al., 2017b). This enables
156 us to analyse whether models of glaciated margins based on observations around the Nordic Seas
157 are applicable to other margins. For these reasons, it is timely to re-evaluate our current models of
158 glaciated margin sedimentation and evolution.

159 **1.3. Why focus on the Nordic Sea?**

160 This study of ice sheet and submarine mass movement histories is focussed initially on their
161 relationship in the Nordic Seas (Fig. 3). We chose to focus on this region for a number of reasons.
162 First, the Nordic Seas and their surrounding margins have been subject to multiple glaciations during
163 the Quaternary. During the Quaternary four major ice sheets, the Greenland, Barents Sea,
164 Scandinavian and the British-Irish ice sheets have grown and decayed on the continents surrounding
165 the Nordic Seas (Ehlers and Gibbard, 2004; Hibbert et al., 2010; Funder et al., 2011; Patton et al.,
166 2015). Each of these ice sheets has different climatic, topographic and geological settings which can
167 affect the processes of ice movement, advance and retreat, and the delivery of sediment (Patton et
168 al., 2016). These contrasts allow us to assess how variable histories of sedimentation are across and
169 between glaciated margins through different glacial cycles.

170 Second, the Nordic Seas and their surrounding land masses are one of the best studied glaciated
171 margins. The economic resources found here, combined with multiple long-running scientific
172 consortia projects (e.g. PONAM and QUEEN) have resulted in regional scale mapping of the surface
173 and sub-surface of the continental shelf and slope (Faleide et al., 1996; Solheim et al., 1998;
174 Svendsen et al., 2004a). Combined with sedimentological studies, this has resulted in one of the
175 most complete records of ice sheet change and the associated history of sedimentation during the
176 Quaternary (Mangerud et al., 1998; Eidvin et al., 2000; Jansen et al., 2000; Svendsen et al., 2004a;
177 and references therein). It is therefore appropriate that any attempt to understand the evolution of
178 glaciated margins should include a detailed study of the margins of the Nordic Seas. The

179 transferability of models based on the Nordic Sea margins to other glaciated margins can
180 subsequently be assessed.

181 **1.4. Aims**

182 The purpose of this study is to draw together various records from around the Nordic Seas to
183 achieve the following aims.

184 1) We aim to reconstruct the growth and decay histories of the Greenland, Barents Sea and
185 Scandinavian ice sheets on the margins of the Nordic Seas and outline the history of sedimentation
186 associated with these ice sheets.

187 2) We compare sedimentary records on different glaciated margins to those from the Nordic Seas in
188 order to understand the appropriateness of models derived from the Nordic Seas for understanding
189 other glaciated margins.

190 3) From these records, we derive a set of general models for ice sheet driven sedimentary processes
191 and landform formation on the continental shelf and slope. These general models for different types
192 of system provide a basis for understanding the evolution of glaciated margins.

193 4) By compiling records of large submarine landslides on glaciated margins, we aim to provide
194 explanations for their spatial distribution and provide conceptual models for understanding their
195 preconditioning and triggering mechanisms.

196 **2. Ice sheet and submarine mass movement histories**

197 The following section will first outline the Late Pliocene history for the Greenland Ice Sheet, Barents
198 Sea Ice Sheet and Scandinavian Ice Sheet. It will then analyse the evolution of each ice sheet during
199 the Quaternary and the associated sedimentation record. First, we focus on the Greenland Ice Sheet;
200 second, the Barents Sea Ice Sheet and last the Scandinavian Ice Sheet.

201 **2.1. Ice sheet histories in the Late Pliocene**

202 The Pliocene spans the period from 5.333 – 2.588 Ma. This period was characterised by significant
203 cooling of high latitude regions (Fronval and Jansen, 1996; Kleiven et al., 2002). The climatic
204 deterioration that occurred during this period led to the expansion of ice sheets around the Nordic
205 Seas (Solheim et al., 1998; Forsberg et al., 1999) and the adoption of orbitally-forced climatic
206 cyclicity (Kleiven et al., 2002). The progression of ice sheet development can be seen in the Ice-
207 Rafted Debris (IRD) histories of ODP sites from around the Nordic Seas (Fig. 3).

208 Sedimentary records show that the Greenland Ice Sheet was the earliest to expand and was the
209 most expansive ice sheet in the region during this period. The earliest and largest IRD peaks (before
210 3 Ma) are recorded at ODP Sites 987 and 907. Located on the Scoresby Sund Trough-Mouth Fan and
211 on the Iceland Plateau (Fig. 4), the IRD records from these cores and the lack of comparable records
212 from sites elsewhere around the Nordic Seas suggest that the Greenland Ice Sheet was producing
213 the largest volumes of IRD during this period (Jansen et al., 1988; 2000; Channell et al., 1999).

214 With the exception of an ice advance ~2.7 Ma (Böse et al., 2012), there is little evidence of ice sheet
215 activity on the Northern European Margin during the Pliocene comparable to the expansion
216 proposed for the Greenland Ice Sheet (Stoker et al., 1994; Böse et al., 2012; Thierens et al., 2012).
217 IRD records on the Yermak Plateau (Sites 910 and 911; Fig. 3) indicate glacial ice growth on the
218 northern, sub-aerially exposed Barents Sea between 3.5 and 2.6 Ma (Rasmussen and Fjeldskaar,
219 1996; Butt et al., 2002). However, IRD records from the Fram Strait indicate that this growth was
220 fairly limited (Knies et al., 2009). Further south, along the Norwegian continental margin, ODP Sites
221 (644 and 642) on the Vøring Plateau indicate growth of Scandinavian glaciers at this time (Spiegler
222 and Jansen, 1989; Jansen and Sjøholm, 1991). However, the IRD flux is two to three orders of
223 magnitude smaller than Quaternary IRD fluxes indicating far less extensive glaciations before 2.58
224 Ma (Jansen and Sjøholm, 1991).

225 **2.1.1. Sedimentary records of ice sheet and submarine mass movement histories: Late** 226 **Pliocene**

227 The impact of ice sheets on the continental shelves of the Nordic Seas varies according to local ice
228 sheet history. The continental shelf of Greenland underwent significant changes during the Late
229 Pliocene. Evidence for repeated glaciation of the shelf comes primarily from IRD records around
230 Greenland (Larsen, 1990; Jansen and Sjøholm, 1991; Larsen et al., 1994). However, this period is also
231 marked by an erosional unconformity across the East Greenland continental shelf, thought to
232 represent a glacial erosion surface and marking the most pronounced depositional change within the
233 geological record of this region (Vanneste et al., 1995; Fig. 5). Correlation of seismic and core records
234 from the Scoresby Sund Trough-Mouth Fan also indicate the presence of glacial debris-flow
235 deposits from this period (Larsen, 1990; Vanneste et al., 1995; Solheim et al., 1998; Butt et al.,
236 2001a). The presence of debris-flow deposits is inferred to be indicative of fast flowing ice reaching
237 the shelf edge and depositing large volumes of sediment. The increased delivery of sediment to the
238 fan during the Late Pliocene is hypothesised to mark the start of the main construction phase of the
239 fan in conjunction with widespread progradation of the continental shelf (Larsen, 1990; Jansen and
240 Raymo, 1996; Solheim et al., 1998).

241 With the exception of a correlatable regional till layer produced by ice sheet advance at ~2.7 Ma,
242 there is no evidence identified as yet of significant Late Pliocene ice sheet influence on the
243 sedimentary evolution of the Scandinavian or Svalbard/Barents Sea continental margins (Sejrup et
244 al., 1996, 2005; Jansen et al., 2000; Lee et al., 2012). There is also no evidence of any link between
245 ice sheet activity and submarine mass movement occurrence at this time.

246 **3. Greenland Ice Sheet**

247 The following section focuses on the evolution of the Greenland Ice Sheet. Specifically it will focus on
248 the sectors of the ice sheet that border the Nordic Seas.

249 **3.1.2.58 – 1.3 Ma**

250 The Greenland Ice Sheet was the largest ice sheet around the Nordic Seas and advanced the furthest
251 onto the shelf during the Early Quaternary. This is suggested by both IRD records close to the
252 Greenland continental shelf and records further out into the Nordic Seas (Thiede et al., 1998; Jansen
253 et al., 2000; Helmke et al., 2003b) as well as erosional unconformities on the continental shelf (Fig.
254 4). These records show the 41 kyr periodicity of Greenland Ice Sheet expansion and contraction and
255 a dominant contribution of IRD into the Nordic Seas compared to other surrounding ice masses
256 (Jansen and Sjøholm, 1991; Jansen et al., 2000; Helmke et al., 2003b).

257 IRD records imply the two largest advances occurred at the start of the Early Quaternary from 2.5 –
258 2.4 Ma and ~2.1 Ma. Subsequent IRD peaks are smaller, suggesting later advances were not as
259 spatially or temporally as extensive or did not produce similar numbers of icebergs (Jansen and
260 Sjøholm, 1991). It appears that the ice sheet did not undergo widespread collapses that
261 characterised the Laurentide and northern European ice sheets in the Late Quaternary (see Fig. 6 for
262 possible margin extent). This is inferred from the amplitude of $\delta^{18}\text{O}$ variations (Lisiecki and Raymo,
263 2007) and the continuous presence of IRD beyond the shelf edge (Jansen et al., 2000).

264 **3.1.1. Sedimentary records of ice sheet and submarine mass movement histories**

265 The initial 2.5 – 2.4 Ma advance left the largest sedimentary signature during the Early Quaternary.
266 This advance is marked by reflector R6 in Fig. 5c which identifies the base of the glacial units in the
267 Scoresby Sund area (Vanneste et al., 1995). This advance was characterised by the emplacement of
268 glacial debris-flow deposits on the Scoresby Sund Trough-Mouth Fan implying a high rate of
269 sediment delivery during this period (Solheim et al., 1998; Channell et al., 1999). Subsequent
270 sedimentation during the period from 2.4 – 1.3 Ma was characterised by silty clays containing
271 variable amounts of IRD, turbidites ranging in thickness from 5 to 60 cm and lower volume glacial
272 debris-flows emplaced on the upper parts of Scoresby Sund Trough-Mouth Fan (Solheim et al., 1998;
273 Wilken and Mienert, 2006). The change in depositional character may be a consequence of lower
274 rates of sediment transport to the shelf edge by continental ice and storage on the shelf. This

275 hypothesis is supported by limited progradation of the shelf edge of only 5 km during the Early
276 Quaternary (Vanneste et al., 1995; Lykke-Andersen, 1998); a rate of progradation 16 times lower
277 than would occur from 1.3 – 0.7 Ma. Alternatively, deposition of sediment by meltwater processes
278 may have led to enhanced turbidity current activity and the transportation of sediment to the deep
279 ocean.

280 **3.2. 1.3 – 0.7 Ma**

281 Compared with the northern European ice sheets, the Greenland Ice Sheet underwent
282 comparatively little change between 1.3 and 0.7 Ma. The ice sheet underwent advance and retreat
283 cycles consistent with climatic forcing. However, the extent of these advances is contentious.

284 Early analysis of the Greenland Ice Sheet during this time period concluded that the ice sheet was
285 relatively stable (Fig. 6b). Neither its advances, nor its retreats were particularly extensive; the ice
286 sheet remaining on or near to the continental shelf (Solheim et al., 1998; Butt et al., 2001a). This
287 scenario was supported by the continuous supply of IRD provided by the Greenland Ice Sheet to sites
288 both within and outside of the Nordic Seas (Larsen, 1990; Larsen et al., 1994; St. John and Krissek,
289 2002; Helmke et al., 2003a). Large IRD peaks that might indicate widespread collapse/retreat of an
290 extensive ice sheet are also less common (Jansen et al., 2000).

291 Subsequent analysis of offshore records has challenged the view of a 'stable' restricted ice sheet
292 (Fig. 6b). Glacigenic debris-flows on the Scoresby Sund Trough-Mouth Fan (Fig. 5d) suggest the ice
293 sheet may in fact have advanced sufficiently during this period to reach the shelf edge. The exact
294 timing of advances to the shelf edge are uncertain (Laberg et al., 2013), but is suggestive of a more
295 dynamic glacial regime, more akin to reconstructions of the Late Quaternary Greenland Ice Sheet
296 (Håkansson et al., 2009; Winkelmann et al., 2010).

297 **3.2.1. Sedimentary records of ice sheet and submarine mass movement histories**

298 Contrasting sedimentary processes are invoked to be associated with the Greenland Ice Sheet
299 between 1.3 and 0.7 Ma. First, glacial debris-flow deposits on the central and southern sides of
300 the Scoresby Sund Trough-Mouth Fan suggest direct input of sediment by an ice stream active at the
301 shelf edge (Laberg et al., 2013; Laberg and Dowdeswell, 2016). Second, the dominant ice sheet
302 driven process responsible for the majority of margin evolution is meltwater delivery of sediment.
303 From 1.3 – 0.6 Ma the East Greenland shelf margin moved seawards by 38 km (Vanneste et al.,
304 1995). This progradation has been attributed to glacial marine deposition through meltwater plumes
305 and turbidity currents (Solheim et al., 1998; Wilken and Mienert, 2006). The delivery of sediment
306 through these processes is also thought to be responsible for vertical aggradation of the shelf by 130
307 m (Vanneste et al., 1995). The predominance of sediment delivery through meltwater processes and
308 the triggering of turbidity currents is also thought to have led to submarine channel formation along
309 the East Greenland Margin during this period (Ó Cofaigh et al., 2004; Wilken and Mienert, 2006;
310 Laberg et al., 2013).

311 The enhanced shelf progradation and aggradation from 1.2 to 0.6 Ma is thought to be a
312 consequence of a period when the Greenland Ice Sheet was particularly erosive (Vanneste et al.,
313 1995; Solheim et al., 1998). The presence of warm-based ice with greater erosive potential is also
314 suggested by margin sedimentation being dominated by meltwater processes.

315 **3.3.0.7 – 0.13 Ma**

316 Repeated glaciations of the Greenland continental shelf are inferred from 0.7 – 0.13 Ma from IRD
317 records but the extent of these advances remains unclear (Solheim et al., 1998; Thiede et al., 1998;
318 Jansen et al., 2000). Between 0.7 – 0.13 Ma background levels of IRD are greater than they were
319 during earlier periods, although IRD pulses are less common (St. John and Krissek, 2002). This could
320 be a consequence of either a larger and more stable ice sheet or a function of greater sea ice
321 coverage preventing IRD reaching the continental shelf (Funder et al., 2011). One exception to this is
322 the Saalian glaciation (Fig. 6c). Terminating at ~130 ka, terrestrial and continental shelf records

323 suggest that the Saalian Greenland Ice Sheet may represent the maximum ice cover achieved during
324 the Late Quaternary (Stein et al., 1996; Funder et al., 1998; Nam and Stein, 1999; Adrielsson and
325 Alexanderson, 2005; Håkansson et al., 2009).

326 **3.3.1. Sedimentary records of ice sheet and submarine mass movement histories**

327 The Late Quaternary is primarily associated with aggradation of sediment on the continental shelf
328 (Fig. 5b; sequence 10 and 11). From 0.7 – 0.13 Ma the continental shelf aggradated over 260 m,
329 whereas progradation is reduced to less than 5 km (Vanneste et al., 1995). This is attributed to the
330 reduced erosional capabilities of successive advancing ice sheets and the increased distance to the
331 shelf edge (ten Brink et al., 1995; Vanneste et al., 1995; Solheim et al., 1998). As a consequence
332 there is limited evidence for submarine mass movement occurrence on or beyond the continental
333 shelf, although this may be a consequence of subsequent erosion by the Saalian and Weichselian ice
334 sheets.

335 The shelf edge Saalian advance led to a phase of intense sediment remobilisation. Glacigenic debris-
336 flows occurred on the southern part of the Scoresby Sund Trough-Mouth Fan (Fig. 5; Dowdeswell et
337 al., 1997; Laberg et al., 2013). However, the volumes of these debris-flows was far smaller than
338 those seen on the Bear Island or North Sea Trough-Mouth Fans during similar periods (Dowdeswell
339 et al., 1997). The shift in location of glacigenic debris-flows on the fan is a consequence of a cross-
340 shelf trough migration. The change of drainage path direction is reflected by a lack of mass
341 movement deposits and the lower sedimentation rate after about 0.78 Ma at ODP Site 987 (Nam et
342 al., 1995; Funder et al., 2011; Laberg et al., 2013).

343 Ice also reached the shelf edge along the section of the Greenland Basin where submarine channels
344 had previously formed between 1.3 and 0.7 Ma (Wilken and Mienert, 2006). The continental margin
345 in this sector was also characterised by limited glacigenic debris-flow emplacement during the
346 Saalian advance. However, unlike earlier advances or indeed the subsequent Weichselian advances,

347 evidence suggests that this submarine channel system was not active and was in fact overridden by
348 glacial debris-flows (Wilken and Mienert, 2006). From this we infer that turbidity currents played
349 a far less pivotal role in sediment transport during the Saalian compared to previous and later glacial
350 advances in this area possibly as a consequence of reduced meltwater input (Wilken and Mienert,
351 2006).

352 **3.4.0.13 – 0 Ma (Weichselian – Present)**

353 Greenland Ice Sheet history during the Weichselian is the best constrained of any period during the
354 Quaternary. Our understanding of the ice sheet is, however, based primarily on a number of key
355 sites and thus reconstructions involve a large amount of interpolation (Funder et al., 1994; 2011).
356 Along the East Greenland Margin, reconstructions are based primarily on sites around Scoresby Sund
357 and Jameson Land (Fig. 4; Funder et al., 2011). The consequence of this is that we are unable to build
358 precise advance and retreat chronologies with the same level of detail that we are able to for the
359 Barents Sea and Scandinavian Ice Sheets (Fig. 6d).

360 Five glacial advances are envisaged in East Greenland. The earliest advances are attributed to Marine
361 Isotope Stage (MIS) 5d and 5b, and are dated using the stratigraphical setting and luminescence
362 dates from glaciolacustrine sediments overlying till beds (Funder et al., 1994; Landvik, 1994;
363 Tveranger et al., 1994). During the MIS 5d, glaciers are believed to have advanced at least onto the
364 inner shelf (Ingólfsson et al., 1994; Landvik et al., 1994; Tveranger et al., 1994). IRD records also
365 suggest an advance during MIS 4 followed by a limited retreat between MIS 4 and 3 (Funder et al.,
366 1998; 2011). In the Scoresby Sund area, the extent of the MIS 4 ice sheet around 60 ka Before
367 Present (BP) has been suggested to be close to the limit of the MIS 2 ice sheet using OSL dating of
368 fluvial and deltaic sediments and IRD on the continental slope (Hansen et al., 1999). IRD peaks during
369 MIS 3 which coincide with heavy and light $\delta^{18}\text{O}$ values are inferred to represent small advance and
370 retreat cycles (Nam et al., 1995; Stein et al., 1996). However, they may also represent fluctuations in

371 sea ice cover along the East Greenland Coast (Gard and Backman, 1990; Nam et al., 1995; Stein et
372 al., 1996).

373 The last glacial advance occurred in MIS 2. IRD records indicate that glaciers in East Greenland
374 reached their maximum extent from 21 – 16 ka BP (Stein et al., 1996). Changes to glacier margin
375 positions may also be indicated by pulses of IRD at ~32.7, ~30.9 – ~29.7, ~27 – ~25.9, ~24.8 –
376 ~23.6, ~21.3 – ~20, ~17.8 – ~16.4 ka cal BP (Funder et al., 1998). However, the extent and style of
377 glaciation of the MIS 2 advance is uncertain. Basal till, streamlined subglacial bedforms and terminal
378 moraines identified from the south east and south west sectors of the Greenland Ice Sheet show
379 that glaciers expanded to the shelf edge (Jennings et al., 2002; 2006; Andrews, 2008; Dowdeswell et
380 al., 2010a; Funder et al., 2011). In contrast, seismic records of the central East Greenland continental
381 shelf show no seismically resolvable layers associated with this advance (Solheim et al., 1998). Two
382 scenarios have been suggested to explain this; (1) glaciers reached the coast and fjord mouths but
383 did not expand greatly onto the continental shelf (Solheim et al., 1998); or (2) glaciers were cold-
384 based with restricted flow and sediment transfer (Funder et al., 1998). However, more recent
385 cosmogenic dating in the Scoresby Sund region has suggested that ice may have reached the outer
386 shelf (Håkansson et al., 2007; 2009). In the northeast sector of the Greenland Ice Sheet, submarine
387 landforms (mega-scale glacial lineations and elongate bedforms) indicate that the MIS 2 ice sheet
388 expanded to at least the middle-outer continental shelf (Evans et al., 2009). Contrary to the
389 suggested restricted flow pattern in the central eastern sector, bathymetric cross-shelf troughs in
390 this sector were filled by warm-based, fast flowing ice. There is also evidence of elongate bedforms
391 to suggest active ice flow across shallow intra-trough regions (Evans et al., 2009).

392 The exact timing of the initial retreat from the MIS 2 maximum is equally contentious. Funder and
393 Hansen (1996) suggested that the ice margin began retreating from the outer part of fjord basins at
394 ca. 17.8 cal ka BP in the central East Greenland sector. The timing is coincident with a marked
395 decrease in IRD in continental slope records (Nam et al., 1995). An alternative scenario proposes

396 that deglaciation occurred shortly before 10 ka BP (Björck et al., 1994a; 1994b). In the northeast
397 sector, glacier retreat is envisaged to occur after 19.5 cal ka BP, marked by an increase in IRD on the
398 continental slope (Nothhold, 1998; Evans et al., 2009).

399 **3.4.1. Sedimentary records of ice sheet and submarine mass movement histories**

400 The sedimentary signature of the Weichselian glaciation along the East Greenland Margin is
401 extremely varied but beyond the shelf break is associated with widespread submarine mass
402 movement occurrence. In more proximal settings, the multiple cycles of ice marginal expansion and
403 contraction can be identified within fjord settings by sedimentary successions. Advances are
404 characterised by tills and overridden/glacially thrust sediments (Tveranger et al., 1994; Funder et al.,
405 1998). Retreats are indicated by pro- and deltaic mud and sand sequences (Funder et al., 1994;
406 1996). Additional sequences include thick laminated fine-grained sediments likely resulting from
407 glacier proximal sediment plumes (Stein et al., 1993; Funder et al., 2011).

408 Beyond the continental shelf, submarine mass movement processes vary by sector. In the Scoresby
409 Sund sector, glacial debris-flows occurred on the southern side of the Scoresby Sund Trough-
410 Mouth Fan (Nam et al., 1995; Dowdeswell et al., 1997). The previously active northern side does not
411 appear to have experienced any mass wasting processes during the Weichselian (Laberg et al.,
412 2013). The number and volume of glacial debris-flows in the Weichselian continued to be far
413 smaller than those seen on other trough-mouth fans around the Nordic Seas indicating a continued
414 reduction in the volume of sediment delivered compared to the period from 1.2 – 0.5 Ma (Vanneste
415 et al., 1995; Dowdeswell et al., 1997).

416 North of the Scoresby Sund Trough-Mouth Fan, glacial debris-flows, turbidity current deposits
417 and extensive channel systems have been identified beyond the shelf break (Fig. 7; Ó Cofaigh et al.,
418 2004; Wilken and Mienert, 2006). Associated with cross-shelf troughs, glacial debris-flow lobes
419 are found on the upper and mid- continental slope. Below 2000 m water depth turbidites are the

420 dominant sedimentary facies (Ó Cofaigh et al., 2004). The glacial debris-flows are dated >22.8 ka
421 BP (Wilken and Mienert, 2006). Turbidity current activity ceased by 13 ka BP (Fig. 7; Ó Cofaigh et al.,
422 2004). Prior to the cessation of turbidity current activity, deposition on this part of the margin was
423 characterised by laminated silt and mud layers associated with deglaciation. Sedimentation rates
424 peaked between 51 – 79 cm kyr⁻¹ between 15 and 13 ka BP before falling to <4 cm kyr⁻¹ after 13 ka
425 BP (Ó Cofaigh et al., 2004; Wilken and Mienert, 2006). An extensive submarine channel network is
426 also found along this part of the margin. The channels cross-cut the glacial debris-flow deposits
427 on the upper and mid-slope implying their formation post-dates the emplacement of these deposits
428 (Ó Cofaigh et al., 2004). The direct link between ice sheet delivery of meltwater and sediment, the
429 occurrence of turbidity currents and the cessation of activity within any of the channels following
430 the withdrawal of the ice sheet illustrates the role of the Greenland Ice Sheet in the sedimentary
431 evolution of the margin.

432 The northeast sector of the Greenland continental shelf is characterised by multiple mass wasting
433 processes during the Weichselian. Here, as in the previous sector, the upper and mid- continental
434 slopes are characterised by glacial debris-flows (Fig. 8; Evans et al., 2009). The lower continental
435 slope is characterised by turbidite deposition. These turbidites are inferred to be the result either of
436 downslope evolution of debris-flows sourced from higher up the slope or the triggering of turbidity
437 currents by other mass-wasting events (Dowdeswell et al., 1997; Evans et al., 2009). Swath
438 bathymetry showing prominent scarps also indicates that submarine landslides have occurred along
439 this part of the East Greenland Margin (Fig. 8c and 8d; Evans et al., 2009). There is little evidence of
440 submarine landslide occurrence along any other part of the East Greenland Margin.

441 The history of the Greenland Ice Sheet and the related sedimentation processes are summarised in
442 Table 1 and Fig. 9a.

443 **4. Barents Sea Ice Sheet**

444 The following section focusses on the evolution of the Barents Sea Ice Sheet and the Svalbard/south
445 west margin of the Barents Sea (Fig. 10). Compared to the East Greenland Margin, the
446 Svalbard/Barents Sea Margin has been much more intensively studied and this is shown by the
447 comparatively better understanding of this margin during the Quaternary.

448 **4.1.2.58 – 1.6 Ma**

449 The initial part of this period was characterised by the retreat of an extensive ice sheet based on
450 Svalbard and the northern Barents Sea (Myhre et al., 1995; Solheim et al., 1998; Knies et al., 2009).
451 The retreat is inferred from a substantial reduction in IRD at ODP sites on the Yermak Plateau (Wolf-
452 Welling et al., 1996; Winkler et al., 2002), and the presence of a regional seismic reflector (R7 in Fig.
453 11) on the continental shelf and slope that marks a distinctive change in sedimentation regime
454 (Faleide et al., 1996).

455 Following the initial ice sheet retreat, the period from 2.5 – 1.6 Ma was characterised by limited
456 advance and retreat of glaciers on Svalbard and in the northern Barents Sea (Fig. 12a; Sejrup et al.,
457 2005). The presence of ice in the northern Barents Sea is indicated by the reduction of specific clay
458 mineral groups (smectite) at ODP sites on the Yermak Plateau and the Fram Strait. Smectite in these
459 areas was previously sourced from the Mesozoic Siberian trap basalts on the Putorana Plateau and
460 transported by the Yenisey and Khatanga rivers and subsequently transported across the northern
461 Barents Sea (Vogt and Knies, 2008). A reduction in the amount of smectite is thought to be indicative
462 of ice blocking the transport path (Knies et al., 2009). The limited extent of ice expansion is inferred
463 from the lack of IRD at the same ODP sites and is thought to indicate that glaciers were too small to
464 calve large numbers of icebergs (Knies et al., 2009).

465 **4.1.1. Sedimentary records of ice sheet and submarine mass movement histories**

466 The average sedimentation rate on the continental shelf offshore Svalbard and in the southwest
467 Barents Sea from 2.5 – 1.6 Ma was higher than during the majority of the Pliocene (Solheim et al.,

468 1996). Using seismic data from the Storfjorden and Bear Island Trough-Mouth Fans, the average
469 sedimentation rate increased from 3.2 cm/kyr and 2.2 cm/kyr from 55 – 2.3 Ma to 62.5 cm/kyr and
470 37 cm/kyr respectively (Faleide et al., 1996; Fiedler and Faleide, 1996; Hjelstuen et al., 1996).
471 However, the limited nature of glacier expansion means that sediment was likely transported by
472 meltwater, either through fluvial action or in sediment-laden plumes and deposited in
473 fluvial/glacimarine sequences. These interpretations are supported by numerical modelling which
474 suggests that the continental shelf of the Barents Sea was still subaerial at this time (Butt et al.,
475 2002), and the presence of incised palaeo-channels in the stratigraphy of the present-day trough-
476 mouth fans which are filled with sand and gravel implying a strong meltwater influence (Sættem et
477 al., 1992; 1994; Vorren and Laberg, 1997; Vorren et al., 2011).

478 Beyond the shelf break offshore Svalbard, this period is also characterised by alternating deposition
479 of hemipelagite and emplacement of submarine mass movement deposits (Fig. 11). The submarine
480 mass movement deposits are characterised as massive, sandy units with soft sediment deformation
481 structures containing contorted and/or variably inclined beds (Jansen, 1996; Forsberg et al., 1999).
482 These deposits are not, however, characteristic of glaciogenic debris-flows. It is possible that the
483 hemipelagic sediments possibly acted as glide planes along which the mass movements occurred as
484 a consequence of the increased sedimentation rate. Glaciofluvial and submarine gravity flow deposit
485 emplacement during this period resulted in gradual aggradation and progradation of sedimentary
486 wedges at the continental shelf (Faleide et al., 1996; Hjelstuen et al., 1996; Dahlgren et al., 2005).

487 **4.2.1.6 – 1.3 Ma**

488 The period between 1.6 and 1.3 Ma, is characterised by greater expansion of the Barents Sea Ice
489 Sheet (Fig. 12b). Expansion is indicated by higher rates of IRD accumulation (Knies et al., 2009).
490 Stratigraphically, this expansion is marked regionally by the R6 seismic reflector (Fig. 11; Faleide et
491 al., 1996; Forsberg et al., 1999). During this period, glaciers sourced from Svalbard expanded
492 sufficiently to reach the shelf edge (Faleide et al., 1996; Solheim et al., 1998). Ice masses present in

493 the northern Barents Sea also expanded. However, their expansion southwards was relatively
494 limited. There is no evidence that the ice sheet expanded sufficiently in this sector to reach the shelf
495 edge, and thus the south western margin of the Barents Sea, i.e. the Bear Island Trough, remained
496 unglaciated during this period (Sættem et al., 1992; 1994; Solheim et al., 1998).

497 **4.2.1. Sedimentary records of ice sheet and submarine mass movement histories**

498 From 1.6 – 1.3 Ma the sedimentary processes along the Svalbard/Barents Sea margin can be divided
499 into two sectors. The southwestern margin of the Barents Sea continued to be dominated by
500 glaciofluvial and glaciomarine processes (Fig. 11; Sættem et al., 1994; Faleide et al., 1996; Hjelstuen et
501 al., 1996; Solheim et al., 1998). Around Svalbard, reflecting greater glacial expansion, continental
502 slope deposits are characterised by the onset of a period of major glacial debris-flow
503 emplacement and the acceleration of sedimentary wedge progradation (Solheim et al., 1998;
504 Dahlgren et al., 2005). These deposits are both thicker and seismically distinct from those associated
505 with the glaciofluvial/glaciomarine period of deposition from 2.5 – 1.6 Ma indicating the enhanced
506 efficiency of glacial sediment transportation and the contrasting character of submarine mass
507 movement deposit emplacement.

508 **4.3.1.3 – 0.7 Ma**

509 The largest change from 1.3 – 0.7 Ma in the Svalbard/Barents Sea sector was the greater expansion
510 of the Barents Sea Ice Sheet (Fig. 12c; Kristoffersen et al., 2004; Vorren et al., 2011). On the Svalbard
511 margin, glaciers originating on the archipelago continued to advance to, and retreat from, the shelf
512 edge (Solheim et al., 1996). Further south, the Barents Sea Ice Sheet expanded sufficiently to reach
513 the shelf edge along the southwestern margin of the Barents Sea for the first time (Andreassen et
514 al., 2004; 2007). Moreover, fast flowing ice has been inferred to have been present in the Bear Island
515 Trough from the presence of buried megascale glacial lineations (Andreassen et al., 2007; Vorren et
516 al., 2011). Further evidence of intensified glacial activity in the Barents Sea during this time comes

517 from IRD records at Site 908 and 909 which show large increases in accumulation during this period
518 (Knies et al., 2009).

519 **4.3.1. Sedimentary records of ice sheet and submarine mass movement histories**

520 The record of sedimentary processes along the Svalbard/Barents Sea Margin from 1.3 – 0.7 Ma is
521 best examined in two parts; the Svalbard and southwest Barents Sea margins. Continued glacial
522 sediment delivery from 1.3 – 0.7 Ma to the Svalbard continental shelf edge led to sustained
523 progradation of glacial wedges through glacial debris-flow emplacement (Faleide et al., 1996;
524 Solheim et al., 1998; Dahlgren et al., 2005). Between 1.0 and 0.78 Ma seismic stratigraphy also
525 indicates the presence of small scale slumps on a number of trough-mouth fans, e.g. Isfjorden
526 (Andersen et al., 1994). Although the volumes of these failures appears to be relatively limited, it is
527 important to note this is the first evidence of trough-mouth fan instability in this region beyond
528 those associated with the occurrence of glacial debris-flows. The occurrence of these slumps is
529 likely a consequence of either the enhanced sedimentation rate or increased seismicity resulting
530 from isostatic adjustment related to the presence of a larger Barents Sea Ice Sheet.

531 In contrast to the Svalbard margin, the expansion of the Barents Sea Ice Sheet to the shelf edge
532 along the southwestern sector of the margin resulted in a significant change of deposition style
533 marked by regional seismic reflector R5 (Fig. 11; Faleide et al., 1996; Fiedler and Faleide, 1996;
534 Hjelstuen et al., 1996; Solheim et al., 1998; Vorren et al., 2011). Ice sheet expansion to the shelf
535 edge increased the rate of sedimentation to 130 cm/kyr across the Bear Island Trough-Mouth Fan
536 from 1.3 – 1.0 Ma resulting in glacial debris-flow emplacement (Fig. 13; Hjelstuen et al., 2007).
537 This rate of sedimentation is nearly double that seen from 2.5 – 1.3 Ma and is attributed to ice sheet
538 expansion over readily erodible sediments on the continental shelf previously deposited by
539 glacial and fluvial processes (Fiedler and Faleide, 1996). From 1.0 – 0.78 Ma the rate of
540 sedimentation at the shelf edge of the Bear Island Trough halved to ~70 cm/kyr (Hjelstuen et al.,
541 2007). The reduced rate of sedimentation is thought to result from the drowning of the Barents Sea

542 and the transition from a subaerial ice sheet to a marine-based ice sheet (Butt et al., 2002). These
543 changing rates of erosion and deposition were also seen on the Storfjorden Trough-Mouth Fan
544 (Hjelstuen et al., 1996; Solheim et al., 1998; Butt et al., 2001b).

545 In addition to glacigenic debris-flow emplacement, this time period was also witness to submarine
546 landslide occurrence on the Storfjorden and Bear Island Trough-Mouth Fans. Submarine landslides
547 have affected the Storfjorden Trough-Mouth Fan between 1.0 and 0.8 Ma, with volumes up to ~45
548 km³ (Hjelstuen et al., 1996; Rebesco et al., 2012; Llopart et al., 2015). They are attributed to
549 instabilities resulting from increasing volumes of deposited sediment (Hjelstuen et al., 1996) being
550 delivered to the fan. On the Bear Island Trough-Mouth Fan seismic stratigraphy suggests that a large
551 submarine landslide occurred between 1.0 and 0.78 Ma (Fig. 13; Hjelstuen et al., 2007). The slide is
552 estimated to have mobilised in excess of 25,000 km³ of material and is the largest yet found on the
553 planet, nearly 10 times larger than Storegga (Table 2; Kuvaas and Kristoffersen, 1996; Hjelstuen et
554 al., 2007). The occurrence of this slide after 1.0 Ma suggests that its occurrence is related to the
555 increased delivery of sediment associated with glacial intensification associated with the Mid-
556 Pleistocene Transition (Fiedler and Faleide, 1996; Solheim et al., 1998). The expansion of the Barents
557 Sea Ice Sheet would also have led to an increase in regional seismicity as a consequence of isostatic
558 adjustment (Stewart et al., 2000). Increases to the rate of sedimentation and local levels of
559 seismicity would both increase the likelihood of slope failure (Masson et al., 2006; ten Brink et al.,
560 2009). The imprecise dating (Slide BFSC I has an age range of 0.21 Myr; Hjelstuen et al., 2007) makes
561 identification of a specific trigger difficult. However, it is interesting that the slide in fact occurred
562 after the average rate of sedimentation decreased implying that the earlier period of greatest
563 sedimentation was insufficient to reach a threshold whereby slope failure was triggered.

564 **4.4.0.7 – 0.13 Ma**

565 The adoption of the 100 kyr climate cycles was associated with regular expansion of the Barents Sea
566 Ice Sheet to the shelf edge along the Svalbard/Barents Sea Margin of the Barents Sea (Solheim et al.,

1996; Solheim et al., 1998). The ice sheet is interpreted to have reached the shelf edge during MIS 16 (676 – 621 ka BP), 12 (478 – 423 ka BP), 10 (374 – 337), 8 (303 – 245 ka BP) and 6 (186 – 128 ka BP) (Laberg and Vorren, 1996; Vorren and Laberg, 1997; Sejrup et al., 2005; Knies et al., 2009). An advance is also inferred to have occurred during MIS 14 (565 – 524 ka BP) but its extent is contentious. Evidence for each of these advances is present in stable isotope data from ODP Hole 910A (Knies et al., 2007) and buried mega-scale glacial lineations visible in seismic data (Andreassen et al., 2004). Each isotope stage could contain multiple advances to the shelf edge that are unresolvable in seismic data or in IRD records; five advances is therefore the minimum which occurred from 0.7 – 0.13 Ma (Vorren and Laberg, 1997). From ODP Sites around Svalbard, Knies et al. (2009) suggest ice reached the shelf edge, and interpretation of deposits on the Bear Island Trough-Mouth Fan confirms this (Sættem et al., 1994; Laberg and Vorren, 1996; Vorren and Laberg, 1997). It is, however, possible that the ice sheet reached the shelf edge of the Bear Island Trough but not around Svalbard. Of the identified advances, the Saalian (MIS 6) is interpreted to be of longest duration (Svendsen et al., 2004b; Ingólfsson and Landvik, 2013; Pope et al., 2016).

4.4.1. Sedimentary records of ice sheet and submarine mass movement histories

Here, we discuss sedimentary processes along specific sections of the margin, reflecting the large number of studies undertaken which cover this time period.

4.4.1.1. Western Svalbard Margin

Ice regularly reached the shelf edge of western Svalbard between 0.7 and 0.13 Ma (Solheim et al., 1998; Spielhagen et al., 2004; Knies et al., 2007; 2009). Each shelf edge advance was characterised by trough-mouth fan glacial debris-flow emplacement (Fig. 11; Andersen et al., 1994; Faleide et al., 1996; Fiedler and Faleide, 1996). During this period there was a shift from net-erosion of the continental shelf to net sediment accumulation on the outer continental shelf. As a consequence debris-flow deposit thickness declined compared with deposits before the onset of 100 kyr cyclicity

591 (Elverhøi et al., 1998; Solheim et al., 1998). The decline in glacial debris-flow thickness in
592 association with net sediment accumulation of the continental shelf is similar to the temporal
593 evolution of debris-flow characteristics on the Scoresby Sund Trough-Mouth Fan (see Section 3).

594 **4.4.1.2. Storfjorden Trough-Mouth Fan**

595 Seven distinct seismic units associated with ice stream advance to the shelf edge in the Storfjorden
596 Trough have been identified (Laberg and Vorren, 1996; Vorren and Laberg, 1997). These equate to
597 advances to the shelf edge during MIS 14, 12, 10, 8 and 6. Glacial debris-flows are thought to
598 dominate each unit reflecting direct input by the ice stream at the shelf edge (Solheim and
599 Kristoffersen, 1984; Vorren and Laberg, 1997). However, despite glacial debris-flows dominating
600 sedimentation across the fan throughout this period, the rate of sedimentation dramatically
601 decreased after 0.44 Ma (Faleide et al., 1996; Hjelstuen et al., 1996). Between 1.0 and 0.44 Ma, an
602 average of $2400 \text{ t km}^{-2}\text{a}^{-1}$ was deposited across the fan. This decreased to $420 \text{ t km}^{-2}\text{a}^{-1}$ between 0.44
603 and 0 Ma (Hjelstuen et al., 1996) showing that the adoption of the 'more' intense 100 kyr glacial
604 cycle does not necessarily increase the sediment supply to the shelf edge. Submarine landslides have
605 also been identified in seismic data during this period with volumes up to $\sim 128 \text{ km}^3$ (Llopart et al.,
606 2015).

607 **4.4.1.3. Bear Island Trough-Mouth Fan**

608 Ice sheet sedimentary processes dominated the Bear Island Trough-Mouth Fan from 0.7 – 0.13 Ma,
609 each advance being correlated to a specific seismic package (Fig. 14). Each of these units I – VI (Fig.
610 10) is dominated on the upper fan by a chaotic seismic facies (Sættem et al., 1992; 1994; Laberg and
611 Vorren, 1996). On the middle and lower fan they have a mounded geometry (Laberg and Vorren,
612 1996). The facies and their associated bounding seismic reflectors are interpreted to represent
613 glacial debris-flow lobes, interbedded with hemipelagic sediments (Vorren et al., 1990; Laberg
614 and Vorren, 1995; Vorren and Laberg, 1997). Distally, these sequences are characterised by fine-

615 grained turbidites, derived from the downslope evolution of glacigenic debris-flows, and hemipelagic
616 sediments (Laberg and Vorren, 1996; Pope et al., 2016).

617 Rates of sediment accumulation and debris-flow emplacement are not constant over either the fan
618 or between the different advances. The MIS 12 advance is estimated to have delivered the most
619 sediment at the highest rate to the fan. Represented by seismic unit III (Fig. 14b), 17,650 km³ of
620 sediment is estimated to have accumulated at a rate of 63 cm/ka during this glacial with the
621 depocentre on the central part of the fan (Laberg and Vorren, 1996). During the following two
622 glaciations (MIS 10 and 8) 7,266 km³ of sediment is estimated to have accumulated at a rate of 14
623 cm/ka with the depocentre situated on the southern end of the fan (Laberg and Vorren, 1996). The
624 MIS 6 advance depocentre was on the northern and southern parts of the fan. An estimated 4061
625 km³ of sediment accumulated at a rate of 19 cm/ka (Laberg and Vorren, 1996). Sedimentation rates
626 and depocentres could not be calculated for the oldest two units, although accumulation rates of
627 ~14 cm/ka have been hypothesised (Laberg and Vorren, 1996). These variations in depocentre and
628 sediment accumulation rate indicate the frequent nature of flow migration of the Bear Island Ice
629 Stream and possible range of sediment delivery rates (Dowdeswell and Siegert, 1999).

630 Five large submarine landslides are also believed to have affected the fan between 0.7 and 0.13 Ma
631 (see Table 2). These landslides range in size from 1.1 km³ to 24.5 km³ (Fig. 13; Hjelstuen et al., 2007).
632 The three oldest slides occurred between 0.78 and 0.5 Ma, indicating a period of large-scale
633 instability on the Bear Island Trough-Mouth Fan. Their age, and the unresolvable Units I and II, in
634 seismic profiles prevent a comparison between depocentres and landslide triggering (Laberg and
635 Vorren, 1996). Nevertheless, these are likely associated with the high sedimentation rates which had
636 occurred during this period and since the Mid-Pleistocene Transition and the intensification of
637 Barents Sea glaciation. The next youngest slide occurred between 0.5 and 0.2 Ma (Hjelstuen et al.,
638 2007). The headwall of this landslide occurred on the northern margin of the depocentre associated
639 with the MIS 10 and 8 advances (Fig. 14; Laberg and Vorren, 1996). The Bjørnøya Slide occurred

640 between 0.3 – 0.2 Ma, post-dating units IV and V and is located on the southern margin of the
641 depocentre of these units (Fig. 14; Laberg and Vorren, 1996). Better constraint of the dates of these
642 slides will be key to understanding their relationship with periods of enhanced sedimentation, sea
643 level change and earthquakes associated with glacio-isostatic adjustment.

644 **4.5.0.13 – 0 Ma (Weichselian – Present)**

645 Understanding of the Barents Sea Ice Sheet is most complete during the Weichselian period (Fig.
646 12d). Onshore and offshore records show that the ice sheet underwent multiple advance and retreat
647 cycles during this time (Mangerud et al., 1998; Svendsen et al., 1999; 2004a; 2004b; Patton et al.,
648 2015; Hughes et al., 2016).

649 The prevailing view of Barents Sea Ice Sheet history during the Weichselian is for four advances. The
650 earliest expansion occurred during MIS 5d from 115 – 105 ka (Patton et al., 2015). This advance is
651 believed to have been limited to Svalbard (Mangerud and Svendsen, 1992) but is envisaged to have
652 reached the shelf edge along the western margin (Knies et al., 1998). Evidence for this on Svalbard
653 comes from the dating of till units (Mangerud and Svendsen, 1992; Mangerud et al., 1996) and
654 offshore IRD records (Knies et al., 2001).

655 A second expansion is reconstructed from 100 – 70 ka BP (MIS 5b; Mangerud et al., 1998). On
656 Svalbard, this expansion is believed to be shorter (~90 – 80 ka BP) and less extensive, i.e. only
657 reaching the coastline, than in the Barents Sea (Svendsen et al., 1999). Ice sheet expansion in the
658 Barents Sea itself was limited to the eastern Barents and Kara Seas (Svendsen et al., 1999, 2004a, b;
659 Siegert et al., 2001). Evidence for the extent and timing of this glacial advance comes from OSL dates
660 on raised beach sediments from ice-dammed lakes (Mangerud et al., 2001; 2004), IRD records (Knies
661 et al., 2000) and till layers in the Barents Sea (Sættem et al., 1992).

662 During the Middle Weichselian (MIS 4 – 3/70 – 50 ka BP), the Barents Sea Ice Sheet advanced to the
663 shelf edge along the western Svalbard margin and in the southwestern Barents Sea (Mangerud and

664 Svendsen, 1992; Andersen et al., 1996; Knies et al., 2001). In the Bear Island Trough, ice is envisaged
665 to have been at the shelf edge between 68 – 60 ka BP (Pope et al., 2016). Reconstructions of glacier
666 extent on Svalbard from marine records suggest similar timings for maximum extension to the shelf
667 edge (Mangerud, 1991; Dowdeswell et al., 1995; Andersen et al., 1996; Knies et al., 2001). Evidence
668 for this advance includes dated till layers, IRD and glacial debris-flows beyond the shelf edge
669 (Mangerud and Svendsen, 1992; Mangerud et al., 1998; Houmark-Nielsen et al., 2001; Pope et al.,
670 2016).

671 The last advance to the shelf edge occurred during MIS 2. During this period ice began to build up at
672 ~32 cal ka BP (Andersen et al., 1996; Siegert et al., 2001). West of Svalbard, ice reached the shelf
673 break at ~24 cal ka BP (Elverhøi et al., 1995; Dowdeswell and Elverhøi, 2002; Andreassen et al.,
674 2004; Jessen et al., 2010; Hughes et al., 2016). Along the southwestern Barents Sea margin ice
675 reached the shelf edge at ~26 cal ka BP (Elverhøi et al., 1995; Laberg and Vorren, 1995; Vorren et al.,
676 2011; Pope et al., 2016). Ice retreated from the shelf edge in both areas as early as 20 cal ka BP (see
677 Hughes et al., 2016 for more detail).

678 In addition to these ice advances, a further advance has also been suggested during MIS 3. Pope et
679 al. (2016) suggest that ice advanced in the Bear Island Trough and was present at or close to the
680 shelf edge between 39.4 and 36 cal ka BP. Evidence for this advance came in the form of distal
681 debris-flow muds that were present on the distal Bear Island Trough-Mouth Fan. An ice advance
682 during this period is contrary to reconstructions made using terrestrial deposits on Svalbard
683 (Mangerud et al., 1998; Svendsen et al., 2004b). It is, however, consistent with offshore IRD records
684 (Dowdeswell et al., 1999; Dreger, 1999; Knies et al., 2001).

685 **4.5.1. Sedimentary records of ice sheet and submarine mass movement histories**

686 **4.5.1.1. Western Svalbard Margin**

687 The detailed offshore record of Svalbard glaciation begins at ~80 ka associated with the inferred
688 beginning of the shelf edge advance during MIS 4 (Mangerud et al., 1998; Svendsen et al., 2004b).
689 This period was characterised by the deposition of turbidites beyond the shelf edge (Andersen et al.,
690 1996) and the deposition of large amounts of IRD, especially following retreat of the ice after 60 ka
691 (Landvik et al., 1992; Dowdeswell et al., 1999).

692 Different sedimentary deposits are found offshore western Svalbard in conjunction with different
693 phases of ice advance during later periods. Ice began to build up ~32 cal ka BP, and reached the
694 shelf edge by ~24 cal ka BP (Elverhøi et al., 1995; Jessen et al., 2010). On Bellsund and Isfjorden
695 Trough-Mouth Fans (Fig. 10), deposition of laminated and massive muds and frequent turbidite
696 emplacement are thought to be reflective of periodic increases of meltwater and sediment delivery
697 associated with ice sheet advance (Andersen et al., 1996; Dowdeswell and Elverhøi, 2002; Landvik et
698 al., 2005). This was followed by the emplacement of glaciogenic debris-flow deposits reflecting the
699 arrival and 'switch-on' of ice streams at the shelf edge (Alley et al., 1989; Andersen et al., 1996;
700 Dowdeswell and Siegert, 1999; Dowdeswell and Elverhøi, 2002).

701 Initial retreat ~20 cal ka BP was characterised by a return to hemipelagic sedimentation and higher
702 IRD concentrations (Knies et al., 2001; Rasmussen et al., 2007; Jessen et al., 2010). Unlike other
703 regions (e.g. along the Norwegian slope or Storfjorden) there was no period of rapid sedimentation
704 associated with meltwater deposition. Between 15.7 and 14.65 cal ka BP, a second phase of retreat
705 associated with enhanced iceberg calving resulted in increased concentrations of IRD and
706 sedimentation rates offshore western Svalbard (Elverhøi et al., 1995; Andersen et al., 1996; Vogt et
707 al., 2001). Further accelerated retreat after 14.65 cal ka BP is linked to thick, fine-grained laminated
708 mud deposits on the continental slope indicative of meltwater processes (Elverhøi et al., 1995;
709 Rasmussen et al., 1997; Jessen et al., 2010). Sediment accumulation rates during this period were
710 between one and two orders of magnitude higher than they had been when the ice margin was at
711 the shelf edge (Dowdeswell and Siegert, 1999; Dowdeswell and Elverhøi, 2002; Jessen et al., 2010).

712 The record of Weichselian sedimentation shows that the West Svalbard Margin was dominated
713 primarily by meltwater delivery of sediment and subsequent downslope movement of this sediment
714 by turbidity currents. The emplacement of glacigenic debris-flows only occurred during limited
715 periods associated with an ice sheet grounded at the shelf edge.

716 **4.5.1.2. Storfjorden Trough-Mouth Fan**

717 Estimates of accumulated sediment volumes on the Storfjorden Trough-Mouth Fan during the
718 Weichselian glacial come from seismic stratigraphy. According to these calculations $422 \text{ t km}^{-2} \text{ yr}^{-1}$
719 were deposited during the Weichselian (Hjelstuen et al., 1996). This figure is part of an average
720 calculated for the last 440 ka (Hjelstuen et al., 1996). Dating of deposits on the Storfjorden Trough-
721 Mouth Fan associated with each of the Weichselian advances has not yet been achieved. This
722 section will therefore focus on the deposits associated with the Late Weichselian (MIS 2) advance.

723 Three depositional lobes can be seen on the Storfjorden Trough-Mouth Fan associated with the Late
724 Weichselian advance. Each of these lobes is inferred to be associated with different flow elements
725 of the larger Storfjorden palaeo-ice stream and has different depositional characteristics (Pedrosa et
726 al., 2011). The two northernmost lobes are characterised by diamictons and over 50 m of glacigenic
727 debris-flow deposits (Lucchi et al., 2013). Radiocarbon dating suggests that these deposits were
728 emplaced around $\sim 23.8 \text{ cal ka BP}$ (Lucchi et al., 2013). On the upper part of the fan these deposits
729 have subsequently been incised by gullies and a thin (2 – 3 m) drape of deglacial and Holocene
730 sediments (Pedrosa et al., 2011; Lucchi et al., 2013). These gullies disappear on the mid-slope.

731 The southern sector of the fan has markedly different sedimentary characteristics. The
732 southernmost lobe is characterised by $\sim 20 \text{ m}$ of glacigenic debris-flow deposits and multiple
733 submarine landslides with headwalls on the middle and upper slopes (Lucchi et al., 2012; Rebesco et
734 al., 2012; Llopart et al., 2015). The largest of these landslides covers an area of $>1,100 \text{ km}^2$ and
735 displaced a volume of $\sim 47 \text{ km}^3$ (Llopart et al., 2015). Stacked mass transport deposits can also be found

736 in the middle and lower slope subsurface (Rebesco et al., 2011; 2012). The nearby Kveithola Trough-
737 Mouth Fan exhibits similar characteristics (Lucchi et al., 2012). As on the northern sections of the
738 fan, gullies are also found on the upper slopes (Pedrosa et al., 2011).

739 The southern sector of the fan is also characterised by interlaminated sequences interbedded with
740 glacial debris-flow deposits. These facies are believed to relate to the Middle and Late
741 Weichselian advances and to be the result of subglacial meltwater plume deposition (Lucchi et al.,
742 2013). The thickness of the interlaminated sediments decreases from meter thicknesses on the
743 upper fan to only 15 cm 42 km downslope. Plumite deposits from previous deglaciations and
744 subsequent hemipelagic sediments have been identified as the glide planes along which many of the
745 submarine landslides occur (Pedrosa et al., 2011; Lucchi et al., 2012; 2013; Rebesco et al., 2012;
746 Llopart et al., 2015). The contrasting geotechnical properties of these sediment packages therefore
747 appear to have played a key role in the occurrence of the slope failures, in addition to rapid
748 sedimentation (Llopart et al., 2014; 2015). Submarine landslides are also common in the area
749 between the Storfjorden and Kveithola Trough-Mouth Fans due to the thickness of accumulations of
750 plumite deposits in this location (Llopart et al., 2015).

751 To the south of the Storfjorden and Kveithola Trough-Mouth Fans the continental slope is
752 characterised by a dendritic sediment drainage system comprising a number of canyons which
753 converge to form the INBIS Channel (Fig. 15; Taylor et al., 2002b; Laberg et al., 2010).

754 **4.5.1.3. Bear Island Trough-Mouth Fan**

755 Based on seismic stratigraphies, the estimated $\sim 2400 \text{ km}^3$ of accumulated sediment (13 cm/ka) on
756 the Bear Island Trough-Mouth Fan during the Weichselian is the lowest of any of the 100 kyr glacial
757 cycles (Laberg and Vorren, 1996). This is perceived to be a consequence of ice being stable at the
758 shelf edge for less time during the Weichselian compared to preceding glacials (Laberg and Vorren,
759 1995, 1996; Vorren et al., 2011; Pope et al., 2016).

760 The Weichselian sedimentary history of the Bear Island Trough-Mouth Fan is dominated by the
761 emplacement of glacial debris-flow deposits (Fig. 15; Taylor et al., 2002a; 2002b; Laberg and
762 Dowdeswell, 2016; Pope et al., 2016). Initial studies using side-scan sonar mapping showed the most
763 recently active (MIS 2) part of the fan was at its northern end and covered 125,000 km² where
764 debris-flow lobes radiated out from the top of the fan (Sættem et al., 1992; 1994; Taylor et al.,
765 2002a; 2002b; Laberg and Dowdeswell, 2016). These flows were shown to have run-out distances of
766 up to 490 km and contain between 10 and 35 km³ of sediment (Laberg and Vorren, 1995; Laberg and
767 Dowdeswell, 2016).

768 Dating of more distal deposits on the northern end of the Bear Island Trough-Mouth Fan has
769 subsequently shown that glacial debris-flows have been emplaced in four distinct clusters during
770 the Weichselian. Each cluster is proposed to be associated with an ice advance to the shelf edge of
771 the Bear Island Trough (Pope et al., 2016). The number and thickness of deposits also suggests that
772 the largest number of glacial debris-flows was in fact associated with advances during MIS 4 and
773 MIS 3 rather than the MIS 2 advance (Pope et al., 2016).

774 In addition to the glacial debris-flows, the northern end of the fan is characterised by the
775 presence of gullies (Vorren et al., 1989; Laberg and Vorren, 1995). Gullies are also present on the
776 southern margin of the fan (Bellec et al., 2016). Two hypotheses for gully formation exist. First, cold
777 and turbid dense water related to brine rejection during sea ice formation during the Holocene was
778 able to erode and transport sediment from the shelf and/or generate turbidity currents (Laberg and
779 Vorren, 1995). Second, hyperpycnal flows resulting from meltwater and sediment delivery when ice
780 was at or near to the shelf edge resulted in channel incision (Laberg and Vorren, 1995; Mulder et al.,
781 2003; Dowdeswell et al., 2006a; Bellec et al., 2016). This was, however, concentrated at the margins
782 of the trough-mouth fan.

783 Following retreat of the Bear Island Ice stream from the shelf edge, a relatively thin sequence (<10
784 m) of glacial marine sediments was left in the trough (Vorren et al., 1990). On the upper fan, less than

785 1 m of glacial marine sediments have been recovered above debris-flow deposits (Laberg and Vorren,
786 1995). On the lower part of the fan, no glacial marine sediments have been found (Laberg and Vorren,
787 1995; Pope et al., 2016). This supports the rapid rate of retreat of the Bear Island Ice stream which
788 has been inferred from seafloor geomorphology in the Barents Sea (Winsborrow et al., 2010; 2012).
789 The history of the Barents Sea Ice Sheet and the related sedimentation processes are summarised in
790 Table 3 and Fig. 9b.

791 **5. Scandinavian Ice Sheet**

792 The following section will focus on the evolution of the Scandinavian Ice Sheet (Fig. 16) during the
793 Quaternary.

794 **5.1.2.58 – 1.1 Ma**

795 Of the three major ice sheets, the Scandinavian Ice Sheet was the least extensive during this period
796 (Fig. 17a; Eidvin et al., 1998; Sejrup et al., 2000; Faleide et al., 2002; Henriksen et al., 2005; Ottesen
797 et al., 2009; Rise et al., 2010). The prevalent belief is that the ice sheet remained at an intermediate
798 size, rarely extending beyond the fjords of western Norway (Jansen and Sjøholm, 1991; Henrich and
799 Baumann, 1994; Dahlgren et al., 2002). Evidence for this comes from the limited IRD delivery to ODP
800 sites on the Vøring Plateau, the Norwegian Basin and cores bordering the Barents Sea as well as
801 seismic stratigraphy of the continental margin of Norway (Jansen et al., 1988; Henrich, 1989;
802 Hafliðason et al., 1991; Sejrup et al., 1996; Rise et al., 2010). Further evidence of a limited but
803 sufficiently large ice sheet to calve icebergs on the Norwegian coast as early as ~2 Ma comes from
804 iceberg ploughmarks observed in seismic data (Rise et al., 2006; Dowdeswell and Ottesen, 2013;
805 Newton et al., 2016).

806 An alternative view suggests that ice caps in northern and southern Scandinavia behaved differently
807 from 2.58 – 1.1 Ma (Fig. 17a). According to this interpretation, at latitudes higher than the Vøring
808 Plateau, the ice sheet regularly advanced to the palaeo-shelf edge between 2.7 and 1.1 Ma

809 (Rokoengen et al., 1995; Henriksen and Vorren, 1996). Meanwhile, south of the Vøring Plateau, the
810 ice sheet remained limited in size (Rise et al., 2005). Two hypotheses exist for the contrasting
811 response of the Scandinavian Ice Sheet. First, it may have been a consequence of the greater
812 influence of obliquity forcing at higher latitudes (Mangerud et al., 1996). Second, it may have been a
813 consequence of southern Norway being starved of sufficient moisture to build-up a large ice sheet as
814 a consequence of the presence of a British Irish Ice Sheet influencing atmospheric circulation
815 patterns (Thierens et al., 2012).

816 **5.1.1. Sedimentary records of ice sheet and submarine mass movement histories**

817 There is little direct evidence of Scandinavian Ice Sheet expansion from 2.58 – 1.1 Ma on the
818 continental shelf with the exception of iceberg ploughmarks and IRD records from more distal core
819 sites (Montelli et al., 2017a). There is no evidence of submarine mass movements in any ODP core
820 beyond the shelf break which are related to ice sheet sedimentation (Jansen and Raymo, 1996;
821 Jansen et al., 2000). It is therefore suggested that from 2.58 – 1.1 Ma sea level change and the
822 related continental shelf exposure was the dominant control on sedimentation along the West
823 Norwegian Margin (Eidvin et al., 2000; Faleide et al., 2002). In spite of the lack of rapid
824 sedimentation, a large submarine landslide (Slide W; Fig. 18) is inferred to have occurred in the same
825 area as the Storegga Slide complex between 2.7 and 1.7 Ma remobilising an estimated 24,600 km³ of
826 sediment (Hjelstuen and Andreassen, 2015). The occurrence of this slide does not appear to be
827 directly related to glacial processes although the imprecise dating makes this conclusion uncertain
828 (Solheim et al., 2005a).

829 The alternative model to explain differences in the development of the Scandinavian Ice Sheet
830 between northern and southern Scandinavia is based primarily on poorly constrained dating of
831 different seismic packages along the margin (Rise et al., 2005). According to this interpretation
832 limited ice advances in the south had little influence on sedimentary processes along this part of the
833 margin (Rise et al., 2005; 2010). However, in the north, ice is envisaged to have reached the shelf

834 edge on numerous occasions and to have contributed significantly to sediment wedge progradation,
835 particularly in the Trænabanken/Trænadjupet area (Fig. 19b; Henriksen and Vorren, 1996; Rise et al.,
836 2005; Ottesen et al., 2012; Montelli et al., 2017a).

837 **5.2.1.1 – 0.7 Ma**

838 Large scale intensification of glaciation in the Northern Hemisphere is believed to have started after
839 1.1 Ma (Fig. 17b; Mudelsee and Schulz, 1997; Mudelsee and Stattegger, 1997). The initial climate
840 step towards a longer glacial/interglacial periodicity is marked by the first definitive expansion of the
841 Scandinavian Ice Sheet to the shelf edge along the entire continental margin (Haflidason et al., 1991;
842 Sejrup et al., 1995; 2000; 2005). The extent of this advance is shown by dated till layers (Haflidason
843 et al., 1991) and IRD records on the Vøring Plateau and in the Norwegian Sea (Baumann and Huber,
844 1999; Helmke et al., 2003a; 2005). Following deglaciation the Scandinavian Ice Sheet appears to
845 have reverted to its relatively restricted dimensions exhibited from 2.58 – 1.1 Ma until the abrupt
846 adoption of the 100 kyr climatic cycles (Mudelsee and Schulz, 1997; Mudelsee and Stattegger, 1997).

847 **5.2.1. Sedimentary records of ice sheet and submarine mass movement histories**

848 The extent of the 1.1 Ma Scandinavian Ice Sheet advance is marked by the presence of a nearly
849 continuous till layer across the continental shelf (Sejrup et al., 2004). On the mid-Norwegian shelf
850 the rate of sedimentation increased by ~60% compared to the period from 2.58 – 1.1 Ma as a
851 consequence of the increased glacial influence (Montelli et al., 2017a). The shelf break also migrated
852 seaward by ~50 km from 1.3 – 0.8 Ma although the age of the top surface of this seismic unit is
853 uncertain (Montelli et al., 2017a).

854 On the southern margin of the Scandinavian Ice Sheet analysis of glacial tills in the Troll borehole
855 using amino acid, micropalaeontological and palaeomagnetic analysis has suggested that the 1.1 Ma
856 advance represents initiation of the Norwegian Channel Ice Stream (Haflidason et al., 1991; Sejrup et
857 al., 1995; Berg et al., 2005). The presence of the Norwegian Channel Ice Stream resulted in

858 significant delivery of glacial sediments to the location where the North Sea Trough-Mouth Fan
859 would develop (Fig. 19c; King et al., 1996). However, despite progradation of the proximal fan and
860 the inferred rapid delivery of glacial sediment, there are no recognisable debris-flow lobes
861 associated with this advance in the seismic stratigraphy (King et al., 1996; Faleide et al., 2002).
862 Moreover, the chronological control on the initiation of the Norwegian Channel Ice Stream has been
863 challenged, suggesting it may have initiated no earlier than ~0.5 Ma (Ottesen et al., 2014).

864 Despite uncertainty over the initiation of the Norwegian Channel Ice Stream, the presence of
865 Cretaceous chalk IRD at Site MD992277 (Fig. 3) associated with the 1.1 Ma advance indicates the
866 extension of the Scandinavian and British-Irish ice sheets into the North Sea (Helmke et al., 2005).
867 The nearest source of chalk extends from the Britain across the North Sea (Ziegler, 1990), thereby
868 implying a large number of icebergs originated from the North Sea region at this time (Helmke et al.,
869 2003b).

870 Marine sedimentation returned along the continental margin following the retreat of the ice sheet
871 from its maximum extent (Jansen et al., 1988; Hafliðason et al., 1991). The marine sediment package
872 is 40 m thick in the Norwegian Channel above the 1.1 Ma till (Sejrup et al., 1996). During subsequent
873 glaciations between 1.1 and 0.7 Ma, it does not appear that the Scandinavian Ice Sheet expanded
874 out onto the continental shelf and thus had little impact on sedimentary processes. Moreover, the
875 sporadic amount of IRD found in marine sequences from this period has been thought to suggest
876 that the ice sheet barely reached the coast (Sejrup et al., 2004; 2005).

877 **5.3.0.7 – 0.13 Ma**

878 The Scandinavian Ice Sheet remained restricted to alpine settings until ~600 ka (Sejrup et al., 2000;
879 Nygård et al., 2005) although there is evidence to suggest an eastward expansion during MIS 16
880 (Velichko et al., 2005; Gozhik et al., 2012; Šeirienė et al., 2015). IRD records from ODP Sites 643 and

881 644 show major increases in the amplitude of IRD peaks associated with the adoption of the 100 kyr
882 climatic cycle after ~600 ka (Henrich and Baumann, 1994; Mudelsee and Schulz, 1997).

883 From 0.7 – 0.13 Ma, 5 major advances are envisaged. Of these, four reached the shelf edge (Fig.
884 17c), while one is thought to have been restricted to the inner shelf (Dahlgren et al., 2002). The four
885 shelf-edge advances are attributed to MIS 14, MIS 12, MIS 10 and MIS 6. Disagreements exist as to
886 the extent of the MIS 8 advance. Some studies suggest that the ice sheet reached the shelf break
887 across most of the continental shelf (Sejrup et al., 2000; Berg et al., 2005; Nygård et al., 2005; Rise et
888 al., 2005; Montelli et al., 2017a). Others suggest that it only reached the mid-shelf (Dahlgren et al.,
889 2002).

890 The extent of retreat from these glacial maximum positions is equally varied. Reconstructions
891 suggest that Scandinavia was completely deglaciated during MIS 13 (524 – 478 ka BP), MIS 11 (423 –
892 362 ka BP) and MIS 5e (128 – 115 ka BP) (Henrich and Baumann, 1994; Hjelstuen et al., 2005; Sejrup
893 et al., 2005). This was a consequence of these interglacials being particularly warm (Helmke and
894 Bauch, 2003; Helmke et al., 2003a). In contrast, during MIS 9 (339 – 303 ka BP) and 7 (245 – 186 ka
895 BP) the Scandinavian Ice Sheet only retreated to fjord and alpine settings (Sejrup et al., 2000) as a
896 consequence of these interglacials being significantly cooler than other interglacials from 0.7 Ma to
897 the present (Helmke and Bauch, 2003). These interpretations have been based primarily on IRD,
898 stable isotope records and ocean temperature record reconstructions (Helmke and Bauch, 2003;
899 Helmke et al., 2003a; Kandiano and Bauch, 2003; 2007).

900 **5.3.1. Sedimentary records of ice sheet and submarine mass movement histories**

901 The six advances of the Scandinavian Ice Sheet from 0.7 – 0.13 Ma are reflected in the stratigraphic
902 record of the Norwegian continental shelf and its slope deposits (Figs 19 - 21; Dahlgren et al., 2002;
903 2005). Until the MIS 14 advance, the continental shelf and slope were dominated by deposition of
904 interbedded hemipelagic and glacimarine sediments reflecting the more restricted position of the

905 ice sheet at this time (Sejrup et al., 1989, 2004; King et al., 1996; Nygård et al., 2005). From MIS 14
906 onwards, continental shelf and slope deposition were dominated by glacial sediment delivery
907 (Dahlgren et al., 2005; Newton et al., 2016; Montelli et al., 2017a). The change in ice sheet extent at
908 this time is also reflected in the IRD records from the Vøring Plateau and in the Norwegian Basin;
909 larger amounts of IRD from the Scandinavian Ice Sheet penetrating further westward (Krissek, 1989;
910 Helmke et al., 2003b).

911 As far south as the Møre Shelf (Fig. 16), the MIS 14 advance is marked by the presence of a
912 structureless diamicton along the outer shelf (Fig. 20a; Dahlgren et al., 2002). Beyond the shelf edge,
913 seismic stratigraphy and ODP core records indicate that glacial debris-flows were the dominant
914 process by which sediment was re-worked (Talwani et al., 1976; Dahlgren et al., 2002). In contrast,
915 there is no evidence of an ice advance onto the continental shelf in southwestern Norway at this
916 time (Helmke et al., 2003a; Hjelstuen et al., 2005). This may be a consequence of later reworking of
917 sediment. However, it is unlikely that an advance in this area during MIS 14 was as significant for
918 sediment delivery as later advances.

919 The more extensive MIS 12 advance is marked by a diamicton on the shelf along most of the
920 Norwegian Margin (Fig. 20; Sejrup et al., 2000; Nygård et al., 2005). Beyond the continental shelf,
921 the sedimentation history is more varied. The outer Møre shelf and the continental slope beyond is
922 characterised by marine/glacimarine deposition (Fig 20; STRATAGEM, 2002; Nygård et al., 2005). In
923 the Møre shelf region, seismic stratigraphy suggests that this unit has primarily infilled the areas
924 between the MIS 14 advance depositional lobes and that the volume of deposited MIS 12
925 glacimarine sediment may have been greater than that deposited during MIS 14 (Dahlgren et al.,
926 2002). Further south, the North Sea Trough-Mouth Fan underwent a major constructional phase
927 (Fig. 21). It is estimated that the Norwegian Channel Ice Stream delivered as much as 3000 km³ of
928 sediment during this glacial, the majority of which was remobilised as glacial debris-flows (King et
929 al., 1996; Nygård et al., 2005). However, following deglaciation the Møre Submarine Landslide (400 –

930 380 ka BP) is estimated to have reworked 1200 km³ of this sediment (Figs 20b and 21; King et al.,
931 1996; Nygård et al., 2005; Hjelstuen et al., 2007). The coincidence of high sedimentation rates on the
932 North Sea Trough-Mouth Fan and the occurrence of the Møre Slide strongly implicates high
933 sedimentation as having a role in the triggering of the slide. Crucially, it has also been suggested that
934 the preceding period was dominated by meltwater and contourite deposition in the area of the fan
935 (Batchelor et al., 2017) thus allowing for the development of weak layers previously suggested to
936 have been responsible for mass failures on the Storfjorden Trough-Mouth Fan (Rebesco et al., 2012;
937 Lucchi et al., 2013; Llopart et al., 2015).

938 On the mid-Norwegian shelf MIS 10 and MIS 8 are characterised by diamicton on the shelf (Fig. 17a;
939 Rise et al., 2005). Beyond the shelf edge seismic data reveals large stacked glacigenic debris-flow
940 lobes and stacked glacigenic debris-flow lenses, related to strong glacial erosion of the shelf (Nygård
941 et al., 2003; Rise et al., 2005; Ottesen et al., 2009; Rydningen et al., 2016). As a consequence of
942 poorly constrained dating of different seismic facies, it is not clear what thickness of sediment is
943 related to the MIS 10 advance and what thickness is related to the MIS 8 advance (Dahlgren et al.,
944 2002; Rise et al., 2005).

945 In contrast to the mid-Norwegian shelf, MIS 10 and 8 can be clearly differentiated on the
946 southwestern part of the margin. Two distinct glacigenic till units were deposited on the South
947 Vøring Margin and North Sea Margin associated with these two glacials (Figs 20, 21b-d; King et al.,
948 1996; Hafliðason et al., 1998). The MIS 10 and 8 advances are estimated to have delivered
949 approximately 2600 and 3500 km³ of sediment to the North Sea Trough-Mouth Fan respectively
950 (Nygård et al., 2005). Once deposited by the ice at the shelf edge the MIS 10 glacigenic sediment was
951 remobilised and emplaced down the fan by glacigenic debris-flows (King et al., 1996; Sejrup et al.,
952 2004; 2005; Solheim et al., 2005a). In contrast, the initial phase of MIS 8 deposition (~2100 km³) was
953 characterised by a combination of glacimarine, marine and gravity-flow processes as a consequence
954 of ice terminating inshore of the shelf edge (Dahlgren et al., 2002; Sejrup et al., 2004). The second

955 phase of deposition ($\sim 1400 \text{ km}^3$) was dominated by glacigenic debris-flow emplacement and is
956 thought to represent the period when ice was at the shelf edge of the Norwegian Channel (Sejrup et
957 al., 2004; Nygård et al., 2005).

958 Two large submarine landslides also occurred during MIS 8. On the South Vøring Margin, the
959 Sklinnadjupet Landslide (Fig. 18) is inferred to have occurred $\sim 300 \text{ ka BP}$, the headwall of the slide
960 being based at the mouth of the Sklinnadjupet Trough (Dahlgren et al., 2002; Solheim et al., 2005a;
961 Hjelstuen et al., 2007). Further to the south at the mouth of Frøyabankhola Trough, the R Landslide
962 is also inferred to have occurred $\sim 300 \text{ ka BP}$ (Sejrup et al., 2005). The probable role of high sediment
963 delivery by ice streams in the triggering of large submarine landslides is shown by the close
964 association of the Sklinnadjupet and R Slides with cross-shelf troughs.

965 The sedimentary deposits from the mid-Norwegian shelf suggests that the Saalian ice sheet (MIS 6)
966 did not reach the shelf edge (Fig. 22b; Rokoengen et al., 1995; Rise et al., 2005). Glacigenic
967 sediments composed of laterally stacked 'till tongues', up to 200 m thick, were deposited on the
968 outer part of the shelf and are inferred to be the result of ice streams flowing out between
969 Haltenbanken and Trænabanken (Fig. 22b; Rise et al., 2005). Further south, the Saalian ice sheet did
970 reach the shelf edge. An extensive till layer is found from the South Vøring Margin to the northern
971 North Sea Margin (Fig. 20; Sejrup et al., 2004; 2005). Sediment deposited at the shelf edge along
972 these margins has been predominantly reworked by glacigenic debris-flows (Sejrup et al., 2004;
973 Batchelor et al., 2017). During this glacial, it is estimated that 2600 km^3 of sediment was deposited
974 on the North Sea Trough-Mouth Fan, the majority being reworked by glacigenic debris-flows (King et
975 al., 1996; Nygård et al., 2005). Large amounts of material were also supplied to the area where the
976 Storegga Slide subsequently occurred (Rise et al., 2005). Estimating the volume of sediment
977 delivered to this margin by the Saalian ice sheet is, however, problematic. This is a consequence of
978 the Tampen and Storegga Slides evacuating large volumes of material into the Norwegian Basin
979 (Haflidason et al., 2005; Paull et al., 2007). The Tampen Slide was originally thought to have occurred

980 on the North Sea Trough-Mouth Fan at ~130 ka BP, after the retreat of the Saalian ice sheet (Bryn et
981 al., 2003; Bryn et al., 2005; Solheim et al., 2005a), but this date has large uncertainties.

982 The ice sheet chronology and the associated sedimentary processes that have been described in this
983 section portray a simple pattern of advance, deposition and reworking of sediment, followed by
984 retreat of the ice sheet. This is, however, likely to be a simplification of the actual chronology.
985 Reconstructions of ice sheet histories in the Weichselian (see following section) show the ice sheet
986 to have undergone multiple advances and retreats during a single glaciation. It is therefore likely
987 that diamict and glacial debris-flow units which encompass a single glacial cycle could in the
988 future be subdivided to reflect multiple ice sheet fluctuations within one glacial (Dahlgren et al.,
989 2002). This will require higher resolution seismic stratigraphies of the continental shelf and slope
990 combined with higher resolution dating of marine sediments.

991 **5.4.0.13 – 0 Ma (Weichselian – Present)**

992 As was demonstrated for the Svalbard/Barents Sea region, the higher temporal resolution and more
993 complete records allow us to identify multiple advance and retreat cycles of the Scandinavian Ice
994 Sheet during the Weichselian (Sejrup et al., 2000; Svendsen et al., 2004a; Hughes et al., 2016).

995 Two advances are proposed during the Early Weichselian. Increased rates of IRD deposition around
996 the Norwegian Sea show the earliest advance to have occurred during MIS 5d (Baumann et al., 1995;
997 Fronval and Jansen, 1997; Rasmussen et al., 2003). From marine sediment records glacial ice is
998 believed to have expanded sufficiently to reach the coast and its fjords during this period (Sejrup et
999 al., 2004; Lekens et al., 2009). Ice retreated inland during MIS 5c before expanding to reach the
1000 outer coastline during MIS 5b. Ice again retreated inland during MIS 5a (Hjelstuen et al., 2005).

1001 The first ice sheet expansion to the shelf edge occurred during MIS 4. During this period ice is
1002 hypothesised to have reached the shelf edge between 70 and 60 ka BP (Mangerud, 1991). MIS 3 was
1003 predominantly characterised by ice sheet retreat into western Norwegian fjords (Baumann et al.,

1004 1995). A minor readvance, the Jæren-Skjonghelleren has been proposed at ~42 cal ka BP (Mangerud
1005 et al., 2003; Sejrup et al., 2003; Lambeck et al., 2010). This advance is tentatively proposed to have
1006 extended beyond the western Norwegian coastline before retreating by 37 cal ka BP (Sejrup et al.,
1007 2000). The exact extent of this retreat along the margin is uncertain; however, the minimum retreat
1008 scenario suggests that the ice sheet receded to the heads of the Norwegian fjords (Mangerud, 1991,
1009 2004; Svendsen et al., 2004a).

1010 Records of the MIS 2 Scandinavian Ice Sheet vary depending on location (Fig. 17d). In northern
1011 Norway, in the Andfjorden area, the ice sheet is hypothesised to have expanded from 34 cal ka BP
1012 (Vorren and Plassen, 2002), reaching the shelf edge from 24 – 23 cal ka BP. A retreat of up to 100 km
1013 occurred between 22 and 20 cal ka BP (Vorren and Plassen, 2002). It then readvanced and was
1014 present at the shelf edge from 16 – 14 cal ka BP before retreating. The remainder of the Late
1015 Weichselian was characterised by retreat, stillstands and minor readvances (Vorren and Plassen,
1016 2002; Dahlgren and Vorren, 2003).

1017 In mid-Norway reconstruction of the Late Weichselian ice sheet is highly dependent on the type of
1018 record used. Solely based on terrestrial data, the main expansion to the shelf edge is interpreted to
1019 have begun at ~24 cal ka BP, ice reaching the shelf edge at 23.5 cal ka BP (Olsen et al., 2001a;
1020 2001b). Limited advances had occurred previously between 34 – 32 and 30 – 28 cal ka BP (Olsen et
1021 al., 2001b). Terrestrial records suggest the ice retreated from the shelf edge after 23 cal ka BP, which
1022 was followed by a short re-advance after 18 cal ka BP until 16 cal ka BP (Olsen et al., 2001a; Dahlgren
1023 and Vorren, 2003). Using marine records (IRD and continental slope deposits) the ice sheet in mid-
1024 Norway is interpreted to have advanced to, and retreated from, the shelf edge four times between
1025 21 – 16 cal ka BP (Dahlgren and Vorren, 2003); a retreat occurring, on average, every 2 ka. The
1026 marine records suggest that the ice retreated from the shelf edge for the last time at ~16 cal ka BP
1027 (Dahlgren and Vorren, 2003).

1028 The glacial history of the Late Weichselian Scandinavian Ice Sheet in southwest Scandinavia is the
1029 best constrained in terms of chronology due to the numerous studies focussing on the Storegga Slide
1030 (Sejrup et al., 1996; 2000; Bryn et al., 2003; Hafliðason et al., 2005; Hjelstuen et al., 2005). The ice
1031 sheet is interpreted to have expanded from 30 ka BP in this sector and to have reached its first
1032 glacial maximum as early as 29 – 27 ka BP (Larsen et al., 2009; Svendsen et al., 2015), remaining on
1033 the shelf edge until 23 cal ka BP (Sejrup et al., 1994). Following a retreat from the shelf edge, the ice
1034 sheet subsequently readvanced to the shelf edge along the south western Norwegian margin from
1035 ~19 – ~15 ka BP after which it retreated. The ice sheet did not, however, advance to the shelf edge
1036 of the Norwegian Channel and thus the Norwegian Channel Ice Stream was not present at the shelf
1037 edge at this time (Sejrup et al., 2000; Sejrup et al., 2003; Hjelstuen et al., 2005; Svendsen et al.,
1038 2015). A more detailed history of the retreat is available from Hughes et al. (2016).

1039 **5.4.1. Sedimentary records of ice sheet and submarine mass movement histories**

1040 The record of associated ice sheet sedimentary processes is highly variable along the continental
1041 margin of Scandinavia. The completeness of the record and the precision with which it has been
1042 dated increases from north to south.

1043 **5.4.1.1. North Norwegian continental shelf**

1044 The record of Weichselian sedimentary deposits is least well understood along the northern margin
1045 (Lofoten – Vesterålen) of Norway and only extends back to MIS 3 (Fig. 16). Here, seismic and swath
1046 bathymetric mapping of the continental shelf and slope reveal mega-scale glacial lineations
1047 indicating the presence of former areas of fast flowing ice (Ottesen et al., 2005). However, the
1048 thickness of glaciogenic sediment deposited on the shelf and upper continental slope is limited
1049 (Brendryen et al., 2015; Rydningen et al., 2016). This is thought to be a consequence of relatively
1050 small ice stream catchment areas limiting sediment transport volumes (Brendryen et al., 2015;
1051 Rydningen et al., 2016) and effective downslope transport of sediment via gullies and canyons on

1052 the continental slope (Baeten et al., 2013; Rise et al., 2013). The number and size of submarine
1053 canyons in this sector is unique along the Norwegian Margin (Rise et al., 2012; 2013). Moreover, the
1054 Andøya Canyon and Lofoten Channel are the only canyon and channel systems of comparable size to
1055 the Greenland Submarine Channel system (Ó Cofaigh et al., 2006).

1056 The earliest dated sedimentary deposits on the Lofoten – Vesterålen margin correspond to the
1057 hypothesised 34 cal ka BP ice sheet expansion (Vorren and Plassen, 2002). Glacigenic debris-flow
1058 deposits and a plumite deposit (dated to 29.3 ± 0.095 cal ka BP) characterise this advance on the
1059 continental slope (Brendryen et al., 2015). The combination of these deposits suggest that the ice
1060 sheet was present at the shelf edge prior to 29.3 ± 0.095 cal ka BP before undergoing a major
1061 retreat. Subsequent glacigenic debris-flow deposits, indicative of ice at the shelf edge, are dated to
1062 18.5, 23 and between 25 and 25.7 cal ka BP (Baeten et al., 2014; Brendryen et al., 2015). Between
1063 these deposits, several laminated units interpreted as plumites were deposited (Brendryen et al.,
1064 2015). On top of the last glacigenic debris-flow deposits, finely-laminated units and finely-laminated
1065 dropstone muds were deposited; the former interpreted to be a plumite (Vorren and Plassen, 2002),
1066 the later, deposits beneath an ice shelf (Brendryen et al., 2015).

1067 Beyond the shelf edge, submarine landslide headscars are also visible on bathymetry. The largest is
1068 the Andøya Slide headwall. Located to the north of the Andøya Canyon, the Andøya Slide covers
1069 $\sim 9,700$ km² with a run-out distance of ~ 190 km (Laberg et al., 2000). Further south, slide scars from
1070 landslides containing between 0.061 and 8.7 km³ of sediment have also been mapped (Baeten et al.,
1071 2013). These landslides are interpreted to be of Holocene age due to a lack of sediment drape and
1072 rugged seafloor relief (Laberg et al., 2000; Baeten et al., 2013). However, more accurate dates are
1073 yet to be obtained. Baeten et al. (2013; 2014) postulate that earthquakes were the likely cause of
1074 these failures.

1075 *Mid-Norwegian Shelf*

1076 Studies of the mid-Norwegian Shelf and slope have identified two types of deposits associated with
1077 the Weichselian glacial. The MIS 5 and 4 advances are associated with two sets of laminated seismic
1078 facies on the continental slope (Henrich and Baumann, 1994; Dahlgren and Vorren, 2003). The MIS 5
1079 sediment package is thickest on the lower to mid-slope and is ~30 m thick (Dahlgren and Vorren,
1080 2003). The MIS 4 deposits are up to 70 m thick and thickest on the southern side of the
1081 Sklinnadjupet Slide scar (Dahlgren et al., 2002; Dahlgren and Vorren, 2003). Both deposits are
1082 thought to have been emplaced within 10 ka and correspond to marine and glacial marine deposition
1083 reflecting a more withdrawn ice sheet position.

1084 In contrast to earlier advances, the MIS 2 ice sheet is thought to have extended to the shelf edge
1085 along the entire mid-Norwegian Shelf (Ottesen et al., 2001; Taylor et al., 2002b). Two continental
1086 shelf till units can be recognised. These structureless grey diamictons terminate in sediment wedges
1087 at the shelf edge (Dahlgren and Vorren, 2003). According to conservative age estimates of ice sheet
1088 activity along this margin the till layers were deposited from 25.9 – 19.4 cal ka BP (Olsen et al.,
1089 2001b; Dahlgren and Vorren, 2003). This advance is associated with glacial debris-flow
1090 emplacement on the continental slope (Dahlgren et al., 2002). It has, however, been suggested from
1091 IRD records that these till layers may in fact represent up to four advances to the shelf edge between
1092 $\sim 27 \pm 0.1$ cal ka BP and $\sim 18.8 \pm 0.04$ cal ka BP (Dokken and Jansen, 1999; Dahlgren and Vorren,
1093 2003). In contrast to other parts of the Norwegian Margin, ice sheet retreat is not associated with
1094 plumite deposition (Hjelstuen et al., 2004; 2005).

1095 The preservation of these till layers and glacial debris-flows varies from north to south. In the
1096 north these sediments have been removed by successive submarine landslides (Fig. 22c; Laberg and
1097 Vorren, 2000; Laberg et al., 2003). Two large submarine landslides have been identified beyond the
1098 mouth of the Trænadjupet Trough. The Nyk Slide affects an area of 4,000 – 6,000 km² and contained
1099 an estimated 400 – 720 km³ of material (Lindberg et al., 2004; Allin et al., in review). The slide is
1100 dated from 21.8 – 19.3 cal ka BP (Allin et al., in review). The Trænadjupet Slide affected an area of

1101 4,000 – 5,000 km² and contained an estimated 500 – 700 km³ of material (Laberg and Vorren, 2000;
1102 Laberg et al., 2002a). The Trænadjupet Slide is dated from 3.5 – 2.8 cal ka BP (Allin et al., in review).
1103 The relationship between the timing of these slides and the local sedimentation patterns is
1104 significantly different. The Nyk Slide occurred after a period of glacigenic debris-flow emplacement
1105 on the continental slope beyond the Trænadjupet Trough when sedimentation rates were as high as
1106 4 m/ka showing the possible role that high sedimentation rates had in triggering the landslide
1107 (Baeten et al., 2014; Brendryen et al., 2015). The Trænadjupet Slide occurred ~10 ka after ice retreat
1108 from the shelf edge when sedimentation rates were reduced to only a few cm/ka (Baeten et al.,
1109 2014). Thus if high sedimentation rates had a role in triggering the Trænadjupet Slide, failure
1110 occurred after a substantial delay; eventual slope failure probably resulting from an additional
1111 triggering mechanism.

1112 *South Vøring Margin*

1113 Little evidence has yet been found that ice reached the shelf break along the South Vøring Margin
1114 before the MIS 2 glaciation (Hjelstuen et al., 2005; Hughes et al., 2016). Instead sedimentation is
1115 dominated by marine and glacial processes (King et al., 1996; Nygård et al., 2005). Three
1116 separate glacigenic units, envisaged to be glacigenic debris-flows, have been identified from MIS 2
1117 (Solheim et al., 2005a). These units are interpreted to have been deposited at $\sim 24.8 \pm 0.07$, $19 \pm$
1118 0.05 , 18.6 ± 0.06 cal ka BP (Hjelstuen et al., 2005). They are separated by laminated sequences
1119 reflecting a more restricted extent of the ice sheet.

1120 Thin and restricted to the uppermost continental slope, till and debris-flow units on the South Vøring
1121 Margin suggest slow rates of sediment delivery during MIS 2. In contrast, the rate of hemipelagic and
1122 glacial sedimentation which covered the limited glacial deposits was extremely rapid (Hjelstuen
1123 et al., 2005). Three periods of plumite deposition are hypothesised; 21.5 – 19.7 cal ka BP, 18.6 – 18.3
1124 cal ka BP and a less northerly extensive period from 18.3 – 18.0 cal ka BP (Fig. 23; Lekens et al., 2005;
1125 2009). During the deposition of these deposits it has been calculated that the sedimentation rate

1126 over this part of the margin was 1250 cm/ka and was as much as 1750 cm/ka (Lekens et al., 2005).
1127 The source of these sediments is inferred to be the Norwegian Channel Ice Stream (Hjelstuen et al.,
1128 2004). The greater rate of sediment accumulation in the Storegga Slide area and the South Vøring
1129 Margin is hypothesised to be related to slope parallel currents moving suspended sediment
1130 northwards from the North Sea Margin.

1131 *North Sea Margin*

1132 Weichselian sedimentation along the North Sea Margin is dominated by emplacement of diamict
1133 layers on the continental shelf and glacial debris-flow deposits beyond the shelf edge (Sejrup et
1134 al., 2003; Hjelstuen et al., 2005). With the exception of the MIS 2 advance of the Scandinavian Ice
1135 Sheet, there is a large amount of uncertainty concerning the extent of the earlier advances. Some
1136 authors suggest that there is little/no evidence of an ice advance to the shelf edge in the Norwegian
1137 Channel before 28 ka BP (Hjelstuen et al., 2005; Nygård et al., 2005; 2007). According to this
1138 interpretation sedimentation up until 28 ka BP was dominated by marine and glacial processes.
1139 Other studies have suggested that multiple till units exist and are linked to advances during the
1140 Karmøy Stadial (~85 to 70 ka BP) and the Skjonghelleren Stadial (~50 to 36 ka BP) (Sejrup et al.,
1141 1995; 2003; 2004). These till layers can be traced beyond the shelf break in the form of glacial
1142 debris-flow deposits on the upper slope (Sejrup et al., 2003).

1143 If it is assumed that ice only reached the shelf edge during MIS 2, 4 oscillations of the ice front are
1144 envisaged, although the Norwegian Channel Ice Stream was only present at the shelf edge during
1145 the earliest advance from after 30 cal ka BP to 23 cal ka BP (Sejrup et al., 1994; Nygård et al., 2005).
1146 Three sequences of glacial debris-flow deposits are associated with this advance on the North
1147 Sea Trough-Mouth Fan (Fig. 20). Each debris-flow sequence is separated by a phase of hemipelagic
1148 deposition (Lekens et al., 2009). Individual debris-flows from this period can be mapped out as far as
1149 500 km from the shelf edge (King et al., 1998). The volume of sediment accumulated on the fan

1150 during this period is estimated to be up to $\sim 5,300 \text{ km}^3$ (Nygård et al., 2005) out of a total of $\sim 5,800$
1151 km^3 deposited during the entire Weichselian (Nygård et al., 2005).

1152 Following the retreat of the Norwegian Channel Ice Stream at $\sim 23 \text{ cal ka BP}$, the North Sea Trough-
1153 Mouth Fan was dominated by marine and glacial-marine deposition (Fig. 23; Lekens et al., 2005).
1154 However, sedimentation rates were an order of magnitude lower compared to the Storegga and
1155 South Vøring areas. From $19 - 18 \text{ cal ka BP}$, plume sedimentation rates were $\sim 60 \text{ cm/ka}$. From $18 -$
1156 17 cal ka BP , plume sedimentation rates were $\sim 30 \text{ cm/ka}$. This rose to $\sim 40 \text{ cm/ka}$ until 14.5 cal ka
1157 BP before returning to normal sedimentation rates of $< 10 \text{ cm/ka}$ (Sejrup et al., 2000; Lekens et al.,
1158 2005; 2009).

1159 During the Weichselian two large submarine landslides are known to have occurred in this region
1160 (Fig. 18). The earlier slide, the Tampen Slide, has been dated to $\sim 130 \text{ ka BP}$ (Nygård et al., 2005), but
1161 this date is uncertain as it uses sedimentation rates. The headwall of this slide is found on the North
1162 Sea Trough-Mouth Fan (Figs 20b and 21j). The timing of this slide relative to Norwegian Channel Ice
1163 Stream activity is uncertain. If the ice stream is assumed to have reached the shelf edge repeatedly
1164 during the Weichselian then the slide occurred after the ice stream retreated from the shelf edge at
1165 the end of MIS 4. If correct a large volume of material was likely advected to the shelf edge and
1166 subsequently remobilised with large volumes of North Sea Trough-Mouth Fan Saalian deposits as
1167 part of this slide. If the ice stream is assumed not to have reached the shelf edge until MIS 2/3 then
1168 the slide occurred as a consequence of relatively little deposition of material on the trough-mouth
1169 fan. In this scenario, the majority of evacuated sediments were derived from the Saalian glaciation.

1170 The Storegga Slide occurred north of the North Sea Trough-Mouth Fan $\sim 8,200 \text{ BP}$ (Haflidason et al.,
1171 2005). The slide evacuated an estimated $3,000 \text{ km}^3$ of sediment and affected an area of $95,000 \text{ km}^2$
1172 (Haflidason et al., 2004). The Storegga Slide occurred significantly (6 ka) after the period of high
1173 sedimentation had finished. Within the Storegga Slide escarpment additional slides have been
1174 identified and dated to 5.7 cal ka BP and $2.8 - 2.2 \text{ cal ka BP}$ (Haflidason et al., 2005; Lekens et al.,

1175 2009). The Storegga Slide is thought to have been triggered by the sediment load from the preceding
1176 glaciation and an earthquake resulting from glacio-isostatic rebound initiating failure of marine clays
1177 (the Brygge Formation) (Bryn et al., 2005). Following this initial failure, the toe support for sediments
1178 further up the continental slope was removed resulting in a retrogressive failure propagating
1179 towards the continental shelf along the glide plane provided by marine clay layers (Bryn et al., 2003;
1180 2005; Hafliðason et al., 2003; 2004; Kvalstad et al., 2005).

1181 The history of the Scandinavian Ice Sheet and the related sedimentation processes are summarised
1182 in Table 4 and Fig. 9c.

1183 **6. How do the continental margins of the Nordic Seas compare with other glaciated margins?**

1184 The previous sections outlined the evolution of the continental margins of the Nordic Seas with
1185 respect to the histories of three ice sheets. The following section will discuss observed similarities
1186 and differences of processes observed on a range of other glaciated continental margins. The
1187 margins we have chosen to include in this comparison reflect the range of environments outlined in
1188 the continuum of glacier-influenced settings in Fig. 1.

1189 **6.1. Antarctic continental margin**

1190 The continental margins of Antarctica have the coldest climate and should therefore be the least
1191 influenced by meltwater processes. Many of the morphological features identified on the margins of
1192 the Nordic Seas are also present on the Antarctic continental margin. Bathymetric, seismic and
1193 sedimentological studies have all identified the presence of trough-mouth fans, submarine channels,
1194 gullies and landslides (Kuvaas and Leitchenkov, 1992; Dowdeswell et al., 2008; Amblas and Canals,
1195 2016; Canals et al., 2016; Gales et al., 2016; and references therein). However, there are significant
1196 differences in the morphologies of these features, their relative numbers and the relative timescales
1197 over which different sedimentation processes operate.

1198 **6.1.1. Antarctic trough-mouth fans**

1199 Antarctica has been glaciated for ~34 Ma (Zachos et al., 2001). However, despite the extended
1200 period over which glacial processes have operated compared with other regions and the number of
1201 cross-shelf troughs that have been identified there are relatively few trough-mouth fans (Ó Cofaigh
1202 et al., 2003). Nonetheless, three large trough-mouth fans have been recognised; the Crary Trough-
1203 Mouth Fan in the Weddell Sea (Kuvaas and Kristoffersen, 1991), the Prydz Bay Trough-Mouth Fan
1204 offshore of the Lambert-Amery glacial system in East Antarctica (Kuvaas and Leitchenkov, 1992), and
1205 the Belgica Trough-Mouth Fan in the Bellingshausen Sea (Dowdeswell et al., 2008).

1206 Of these trough-mouth fans, the morphology and inferred processes of the Belgica Trough-Mouth
1207 Fan most clearly resemble those outlined on Nordic Sea trough-mouth fans (Fig. 24a). It covers an
1208 estimated area of at least 22,000 km² and contains ~60,000 km³ of sediment that has accumulated
1209 over the past 5.3 Ma (Scheuer et al., 2006; Dowdeswell et al., 2008). Compared to the Nordic Sea
1210 trough-mouth fans it therefore falls between Storfjorden and Scoresby Sund (115,000 and 15,000
1211 km³ respectively) in terms of volume despite having a palaeo-drainage basin under full-glacial
1212 conditions an order of magnitude greater (200,000 km² vs 60,000 km²) than either of the Nordic Sea
1213 systems (Vorren et al., 1998; Ó Cofaigh et al., 2005; Håkansson et al., 2007). As seen in the Nordic
1214 Seas, seismic stratigraphic analysis of the Belgica Trough-Mouth Fan reveals semi-transparent lenses
1215 interpreted to be glacial debris-flow deposits (Ó Cofaigh et al., 2005; Hillenbrand et al., 2010).
1216 Gully and channel systems have been cut into the emplaced deposits (Fig. 24a; Dowdeswell et al.,
1217 2008). As seen on some trough-mouth fans in the Nordic Seas the density of these features is
1218 highest at the margins of the Belgica Trough-Mouth Fan. However, the depth of incision, downslope
1219 extent beyond the lower slope and presence across the entire width of the fan contrasts strongly
1220 with systems in the Nordic Seas whose gully systems are much less well developed and generally
1221 confined to the upper slopes (Dowdeswell et al., 2008; Pedrosa et al., 2011; Lucchi et al., 2013;
1222 Llopart et al., 2015). This may be a consequence of more sustained periods of brine rejection and
1223 cold water cascading off of the continental shelf (Ivanov et al., 2004). Also unlike the largest fans in
1224 the Nordic Seas, there is no evidence of major slides or other mass wasting (Nitsche et al., 1997;

1225 Dowdeswell et al., 2008). Unfortunately, no chronologic information is available to date the timing
1226 of debris-flow emplacement and channel incision.

1227 The Prydz Bay Trough-Mouth Fan is the best understood of the Antarctic trough-mouth fans (Fig.
1228 24c). Its development can be divided into three phases. Phase 1 lasted from the Late Miocene (ca. 7
1229 Ma) until 1.1 Ma. During this period the Lambert Glacier advanced to the shelf edge, depositing
1230 diamictons which were subsequently reworked by glacial debris-flows (Kuvaas and Leitchenkov,
1231 1992; O'Brien and Harris, 1996; Passchier et al., 2003; O'Brien et al., 2007). The volumes of these
1232 flows were much lower than those seen on the Bear Island and North Sea Trough-Mouth Fans
1233 (O'Brien and Harris, 1996). These deposits were interbedded with contouritic sediments and
1234 turbidites (Passchier et al., 2003). During Phase 2 (1.1 – 0.78 Ma), glacial sediment input decreased
1235 leading to a reduction in the number and thickness of glacial debris-flows (O'Brien et al., 2007).
1236 Phase 3 (0.78 Ma – present), coinciding with the adoption of 100 kyr climate cyclicity, was
1237 characterised by a cessation of debris-flow activity and a growing dominance of glacimarine
1238 deposition as the Lambert Glacier failed to reach the shelf edge (Passchier et al., 2003). No evidence
1239 has yet been found for large scale mass failures (Kuvaas and Leitchenkov, 1992). The volume of
1240 sediment which accumulated during the construction of the Prydz Bay Trough-Mouth Fan is
1241 comparatively small (27,740 km³) when the drainage area (3.5 x 10⁵ km²) of the Lambert Glacier
1242 under full glacial conditions is considered (Denton and Hughes, 2002).

1243 The Crary-Weddell Sea Fan system of which the Crary Trough-Mouth Fan is part covers an estimated
1244 area of 750,000 km² (Anderson et al., 1986). Initiation of the fan began ~34 Ma but unlike other
1245 trough-mouth fans has been dominated by the presence of large channel-levee complexes (Kuvaas
1246 and Kristoffersen, 1991). Three channel-levee complexes have existed during the last 34 Ma (Fig.
1247 24b). They are hypothesised as being a result of brine rejection eroding channels during interglacials
1248 and depositing winnowed fine sediments from the upper slope and shelf on the levees (Kuvaas and
1249 Kristoffersen, 1991). During glacials, glacial meltwater transport of sediment, turbidity currents and

1250 downslope evolving submarine slumps and debris-flows result in enhanced channel-levee activity
1251 and fan progradation (Kuvaas and Kristoffersen, 1991; Melles and Kuhn, 1993). Dating of material
1252 from the levee complexes supports this hypothesis; deposition on the levees in water depths of 2000
1253 – 3000 m ranged from 100 – 200 cm/kyr during the last glacial and has only been a few cm/kyr
1254 during the Holocene (Weber et al., 1994). Glacigenic debris-flows and submarine landslides have
1255 also been identified (Melles and Kuhn, 1993; Gales et al., 2016). Larger submarine landslides have
1256 also been suggested to have occurred on the Crary Trough-Mouth Fan during the Early Pleistocene
1257 during the drawdown of East Antarctica (Bart et al., 1999).

1258 **6.1.2. Antarctic gullies and submarine channels**

1259 A large proportion of the mapped Antarctic Margin is dominated by gullies and channel systems and
1260 therefore bears a greater similarity to the East Greenland Margin than the Norwegian Margin. The
1261 Antarctic gullies and channels are, however, more numerous and permanent features.

1262 Gullies have been found incised into trough-mouth fans (e.g. the Crary Trough-Mouth Fan) and the
1263 continental slope in front and between cross-shelf troughs (Ó Cofaigh et al., 2003; Dowdeswell et al.,
1264 2004; 2006a; Heroy and Anderson, 2005; Wellner et al., 2006; Gales et al., 2013; 2014). Depending
1265 on their location, gully formation has been linked to different processes. Along parts of the Antarctic
1266 Margin, gully formation is hypothesised to be a consequence of cold-dense water cascading down
1267 the continental slope through brine rejection (Noormets et al., 2009). Many, however, are
1268 hypothesised to be a consequence of turbidity current activity, sediment-laden subglacial meltwater
1269 discharge or small-scale mass failures (Dowdeswell et al., 2006a; Gales et al., 2016). In many cases
1270 gullies feed channel systems or coalesce to form channels themselves further down the continental
1271 slope.

1272 Extensive channel networks have been found offshore of the continental shelf around most of the
1273 Antarctic Margin (Rebesco et al., 1996; 2002; De Santis et al., 2003; Dowdeswell et al., 2006a;

1274 Hillenbrand et al., 2008). Offshore of the Antarctic Peninsula, dendritic canyon-channel systems are
1275 found at the mouths of cross-shelf troughs (Amblas et al., 2006; Amblas and Canals, 2016). These
1276 systems are a consequence of intense turbidity current activity which occurs due to ice at the shelf
1277 edge delivering large amounts of sediment and, subglacial meltwater, as well as the relatively steep
1278 continental slope favouring turbidity current formation (Pudsey and Camerlenghi, 1998; Dowdeswell
1279 et al., 2004). Sediment mounds are found between these channels as a consequence of bottom
1280 current reworking and deposition of sediment (Amblas et al., 2006).

1281 Other extensive channel/submarine canyon and related submarine fan systems have been found on
1282 the Wilkes Land Margin (130 – 145°E) and Queen Maud Land (12 – 18°W) (Escutia et al., 2000;
1283 Buseti et al., 2003; De Santis et al., 2003; Ó Cofaigh et al., 2003). The presence and morphology of
1284 these systems are thought to be the result of multiple factors and reflect the dynamic evolution of
1285 the Antarctic Ice Sheet with changing climate in this sector (Donda et al., 2007). During the Early –
1286 Late Miocene (23.03 – 5.333 Ma), the meltwater derived from a highly dynamic temperate Antarctic
1287 Ice Sheet delivered large amounts of sediment to the shelf edge. The high sedimentation rate led to
1288 the triggering of submarine mass movements (probably turbidity currents) which led in turn to the
1289 development of high-relief channel-levee complexes (Donda et al., 2007). Since the end of the
1290 Miocene, climatic deterioration has led to a less dynamic ice sheet (Rebesco and Camerlenghi,
1291 2008). As a result the ice streams feeding these systems are relatively small, frequently migrate and
1292 deliver insufficient volumes of sediment when at the shelf edge to build a trough-mouth fan (Cooper
1293 et al., 1991; Escutia et al., 2000; 2005). The proportionally larger volumes of coarse sediment
1294 delivered to the top of these systems by ice streams is also thought to be partially responsible for
1295 their steep upper and mid- slopes when compared to similar fluvial systems (Escutia et al., 2000;
1296 2003).

1297 **6.1.3. Antarctic submarine landslides**

1298 When compared to the margins of the Nordic Seas, the Antarctic continental margin is notable for its
1299 lack of submarine landslides. Exceptions exist, the Gebra Slide on the Antarctic Peninsula margin
1300 contains $\sim 21 \text{ km}^3$ of sediment (Imbo et al., 2003; Canals et al., 2004; 2016) and slides have been
1301 identified on the Crary Trough-Mouth Fan (Gales et al., 2014; 2016). The Gebra Slide and the
1302 recurrence of large mass movements in this area are thought to result from enhanced sediment
1303 delivery associated with the onset of 100 kyr climate cyclicity and the extension of the Laclavere,
1304 Mott Snowfield and D'Urville ice streams to the shelf edge (García et al., 2008; 2009). The failure of
1305 deposited glacial sediments is thought to result from a strong earthquake associated with tectonic
1306 activity of a half-graben and related structures, or volcanic activity and changes in the slope profile
1307 related to the opening of the Central Bransfield Basin (Casas et al., 2013). It is thought that
1308 interglacial sediments, muddy turbidites and hemipelagites, acted as weak layers and glide planes
1309 (García et al., 2011; Casas et al., 2013). The Crary Trough-Mouth Fan slides are also thought to be a
1310 consequence of the presence of weak layers which are susceptible to liquefaction under loading
1311 (Long et al., 2003). These layers are thought to result from dense bottom water formation on the
1312 Southern Weddell Sea Shelf which deposits winnowed fines on the continental slope as it forms
1313 cascading bottom flows (Melles and Kuhn, 1993; Weber et al., 2011). Actual slope failure may result
1314 from rapid sedimentation or an earthquake.

1315 There is as yet little evidence of frequent mass wasting events around Antarctica with volumes
1316 comparable to the Storegga or Trænadjupet Slides, despite the clear contrasts in sediment package
1317 characteristics that would be deposited by glacial and contouritic processes that operate around
1318 Antarctica (Kuvaas et al., 2005; Gales et al., 2014).

1319 **6.2. East Canadian Margin**

1320 The continental margin of East Canada was the location of the furthest eastern extension of the
1321 Laurentide Ice Sheet (Fig. 25). Running from $\sim 40 - 76^\circ \text{N}$, the East Canadian Margin has features
1322 similar to those seen on other glaciated margins but also exhibits features indicative of greater

1323 meltwater influence. This could be a consequence of either the lower latitude of the southern part
1324 of the margin or of the internal dynamics of the Laurentide Ice Sheet (Bond et al., 1992; Piper, 2005).

1325 **6.2.1. East Canadian trough-mouth fans**

1326 Trough-mouth fans have been identified along the entire East Canadian Margin (Aksu and Hiscott,
1327 1989; Piper, 2005; Tripsanas and Piper, 2008a; Li et al., 2011). However, their morphology changes
1328 with latitude. At the northern end of the East Canadian Margin, trough-mouth fans have similar
1329 architectures and sedimentation regimes to those described on the Svalbard/Barents Sea
1330 continental margin. For example, the depositional systems operating on Lancaster Sound and Trinity
1331 Trough-Mouth Fan are dominated by the emplacement of glacial debris-flow units (Fig. 26; Piper
1332 and McCall, 2003; Tripsanas and Piper, 2008a; Li et al., 2011). Originating from till wedges higher on
1333 the continental slope, glacial debris-flow emplacement is responsible for the majority of
1334 progradation of these fans during glacial periods (Piper, 2005).

1335 Further south, the Laurentian and Northeast Trough-Mouth Fans have very different morphologies
1336 and thus different sedimentation histories (Mosher et al., 2017). Both trough-mouth fans are
1337 dominated by large channel-levee systems (Hughes Clarke et al., 1992; Piper et al., 2016). Seismic
1338 profiles across both fans shows that similar channel systems have previously existed on these fans
1339 throughout the Quaternary (Campbell and Mosher, 2014; Piper et al., 2016). These channel systems
1340 and the growth of these fans is hypothesised to have been the result of exceptionally large
1341 discharges of sediment-laden meltwater to the slope from the Laurentide Ice Sheet leading to the
1342 formation of hyperpycnal flows or turbidity currents which re-work the rapidly deposited plume
1343 deposits (Hughes Clarke et al., 1990; Piper et al., 2007; Clare et al., 2016b). Submarine slump and
1344 debris avalanche reworking of deposited material is also thought to play a role in the sedimentation
1345 history of these fans (Piper et al., 2012). Critically, there is little evidence of glacial debris-flows
1346 being important to the development of these trough-mouth fans.

1347 **6.2.2. East Canadian gullies and submarine channels**

1348 Much of the East Canadian Margin is characterised by alternating regions of high and low density
1349 gullies and channels (Hesse et al., 1999; Mosher et al., 2004; Jenner et al., 2007; Campbell and
1350 Mosher, 2014). Where cross-shelf troughs are found, sedimentation is dominated by glacigenic
1351 debris-flow emplacement (Hesse et al., 2001; Piper, 2005). Gullies and channels have, however,
1352 been incised into the emplaced debris-flow units by sediment-laden meltwater being discharged
1353 from the ice margin and the downslope evolution of glacigenic debris-flows into turbidity currents
1354 (Piper, 2005; Dowdeswell et al., 2016a; 2016c; Piper et al., 2016). Between the cross-shelf troughs,
1355 meltwater processes dominate resulting in the formation of dendritic gully and canyon systems.
1356 These systems are hypothesised to be a consequence of hyperpycnal and hypopycnal flow formation
1357 (Piper and Hundert, 2002; Piper and Normark, 2009), the re-working of sediment by turbidity
1358 currents which has settled out from meltwater plumes that have been entrained southward by the
1359 Labrador Current and mass-wasting processes (Fig. 26; Hesse et al., 1997; 2001; 2004; Ó Cofaigh et
1360 al., 2003). Many of the channel and canyon systems subsequently coalesce to feed deep-sea
1361 channels such as the North Atlantic Mid-Ocean Channel (Piper, 2005).

1362 **6.2.3. East Canadian submarine landslides**

1363 The first identified submarine landslide was the Grand Banks Slide in 1929 (Heezen and Ewing, 1952;
1364 Piper and Aksu, 1987). Like the Storegga region, these events appear to be relatively common along
1365 the East Canadian Margin. Landslide headscarps have been identified on the upper continental
1366 slope, in gullies, on canyon flanks, and at the base of the continental slope (Mosher et al., 1994;
1367 2004; Piper, 2005; Dowdeswell et al., 2016a). These landslides are therefore likely to play an
1368 important role in the maintenance and morphology of the channel and gully systems which exist
1369 along much of the margin (Piper, 2005; Dowdeswell et al., 2016a; 2016c).

1370 The majority of the landslides within the gully and channel systems north of Orphan Basin have been
1371 interpreted to have contained relatively small volumes of sediment. As a consequence these
1372 landslides are unlikely to have the geohazard potential of the large submarine landslides seen during
1373 the Holocene in the Nordic Seas. They do, however, still represent a significant hazard to offshore
1374 infrastructure development (Pickrill et al., 2001). In contrast, the south eastern part of the Canadian
1375 Margin from the Flemish Cap to Georges Banks has experienced large numbers of large mass failures
1376 during the Quaternary (Piper et al., 2003; Piper, 2005; Bennett et al., 2014). Here, failures with
1377 volumes up to $\sim 800 \text{ km}^3$ have been identified (Piper and Ingram, 2003). 10 Quaternary landslides
1378 with volumes $>10 \text{ km}^3$ have been identified on this part of the margin suggesting a mean recurrence
1379 interval of 0.25 Ma (Piper and Ingram, 2003; Piper et al., 2003). However, the recurrence times vary
1380 between individual basins (Piper et al., 2003) and there are large dating uncertainties on most
1381 landslides. The recurrence of smaller, but still $>1 \text{ km}^3$, landslides is shorter. For example, 9 turbidite
1382 deposits, interpreted to originate from landslides on the Flemish Cap occurred during the last 150 ka
1383 (Huppertz and Piper, 2009).

1384 The identified large submarine landslides on the south eastern part of the Canadian Margin are
1385 thought to be directly linked to glaciation of the continental slope and delivery of large volumes of
1386 glacial sediment. Glacial and pro-glacial sediment packages have been shown to fail
1387 retrogressively along their bedding plane on this section of the margin (Piper et al., 1999; Mosher et
1388 al., 2004). Moreover, the most recent failures identified on the Scotian Slope and Grand Banks
1389 occurred at or immediately after the Laurentide Ice Sheet reached its local maximum extent during
1390 the last glaciation of the shelf (Piper and Campbell, 2005). Extrapolating further back into the
1391 Quaternary, the Laurentide Ice Sheet is interpreted to have reached the shelf edge in this area
1392 repeatedly from MIS 12 (0.45 Ma) onwards (Piper et al., 1994). However, the poorly constrained
1393 dating of the large mass transport deposits which pre- and post- date MIS 12 prevents any further
1394 understanding of the influence that shelf edge glaciations have had on the frequency of large
1395 submarine landslides. Based on the distribution of failures (Piper et al., 1985) and sediment strength

1396 estimates (Baltzer et al., 1994; Mosher et al., 1994; 2004) the majority of slope failures identified are
1397 thought to result from large passive margin earthquakes, the frequency of which are increased as a
1398 consequence of glacial loading and unloading associated with Laurentide Ice Sheet growth and decay
1399 (Stewart et al., 2000).

1400 **7. Glaciated margin systems – a new conceptual model**

1401 In the following section we develop a new conceptual model of sedimentation on glaciated margins
1402 based on the ice sheet histories around the Nordic Seas outlined in Sections 2 – 5 and the
1403 comparisons made in Section 6 with other margins.

1404 **7.1. How has ice sheet history and sedimentation changed with climate?**

1405 We first address the influence that climate has had in the Nordic Seas on ice sheet and
1406 sedimentation histories in reference to the variables outlined in Section 1.1 and in Figs. 1 and 2. Two
1407 key questions have to be addressed. First, do cooler climates result in increased glacial sediment
1408 delivery to the continental margin? Second, has the transition between the 41 and 100 kyr climate
1409 cycles enhanced glacial delivery of sediment?

1410 If the history of ice sheets and sedimentation around the Nordic Seas is considered as a whole then
1411 no clear relationship exists between climate and delivery of glacial sediment. For example, a
1412 fundamental contrast exists between the East Greenland and southern Norwegian margins. The
1413 delivery of sediment by the Greenland Ice Sheet appears to increase as climate cools until the
1414 adoption of the 100 kyr climate cycles at which point it decreases (Table 1). In contrast, glacial
1415 sedimentation dramatically increases on the southern Norwegian Margin as climate cools and the
1416 100 kyr climatic cycles are adopted (Table 4). It is therefore prudent to instead consider the
1417 evolution of ice sheet sediment delivery on individual margins of the Nordic Seas related to their
1418 climatic setting.

1419 The Nordic Seas margins can be considered to exist within a climatic range. The southern Norwegian
1420 section of the margin is the warmest and wettest (Patton et al., 2016). Both the temperature and
1421 volume of precipitation are believed to reduce with increasing latitude along this margin; Svalbard
1422 therefore having the coolest and driest climate (Patton et al., 2016). The Greenland Margin is the
1423 coolest of the margins (Fig. 1). For each of these margins the climatic deterioration seen during the
1424 Quaternary therefore represents a shift towards a cooler climate (Fronval and Jansen, 1996; Thiede
1425 et al., 1998; Jansen et al., 2000). Assuming that this is correct, it therefore appears that a threshold
1426 exists, at which point continued cooling of the climate serves to reduce the efficiency of ice sheet
1427 sedimentation. This threshold is likely controlled by the comparative areas of cold-based ice and the
1428 extent and area of fast flowing ice streams. The sedimentation history offshore Svalbard most clearly
1429 illustrates such a relationship (Table 3). As climate deteriorated from 2.8 Ma to 1.0 Ma, ice sheet
1430 driven sedimentation through glacimarine processes and glacigenic debris-flow emplacement on the
1431 continental shelf increased. However, since 1.0 Ma the rate of sedimentation and the thickness of
1432 glacigenic debris-flow deposits have decreased (Sættem et al., 1994; Solheim et al., 1998; Knies et
1433 al., 2009). Despite the extent and drainage area of the ice sheet being similar it therefore appears
1434 that the efficiency of glacial sedimentation decreased following a cooling of the climate and
1435 adoption of the 100 kyr climate cycles. Further support for this suggestion is found on the
1436 Norwegian Margin where the location of maximum volume of deposited sediment has progressively
1437 moved southwards as climate has cooled (Fig. 19; Rise et al., 2005).

1438 Analysis of the history of sedimentation offshore Antarctica (Section 6.1) supports the idea of a
1439 tipping point in glacigenic sediment delivery across a continental margin. Since the inception of the
1440 Antarctic Ice Sheet, glacigenic sedimentation has occurred on the continental margin (Kuvaas and
1441 Kristoffersen, 1991). Dating of sediment packages beyond the continental shelf has, however, shown
1442 the volume of sediment transported to have decreased in line with cooling climates. For example,
1443 sedimentation on the Prydz Bay Trough-Mouth Fan from the Late Miocene to 1.1 Ma was dominated
1444 by glacigenic debris-flows (Passchier et al., 2003). As climate continued to cool, the temperature of

1445 the East Antarctic interior and precipitation received there were reduced. This led to a hypothesised
1446 reduction in the area of fast flowing warm-based ice (Passchier et al., 2003; O'Brien et al., 2004). The
1447 reduced sediment transport manifest itself in reduced numbers and thickness of glacigenic debris-
1448 flow deposits; emplacement of these deposits eventually ceasing after 0.78 Ma with the adoption of
1449 100 kyr climate cycles.

1450 **7.2. Trough-mouth fans**

1451 The largest sedimentary features on glaciated margins are trough-mouth fans which are of
1452 comparable size to deep-sea fans formed offshore the World's largest rivers. They form
1453 preferentially in front of cross-shelf troughs as a consequence of fast-flowing ice streams delivering
1454 large volumes of sediment to the shelf edge over repeated glacial cycles (Ó Cofaigh et al., 2003;
1455 Dowdeswell et al., 2010b). The classical trough-mouth fan model was developed from observations
1456 in the Nordic Seas (Laberg and Vorren, 1995; Dowdeswell et al., 1996; Vorren and Laberg, 1997). This
1457 model was further developed by Ó Cofaigh et al. (2003) recognising the importance of slope setting
1458 and hypothetical cases of low sedimentation. Here, we attempt to improve the model of trough-
1459 mouth fan processes using the observations outlined in previous sections.

1460 **7.2.1. Characterisation of trough-mouth fans**

1461 Our analysis of trough-mouth fans around the Nordic Seas and on other continental margins
1462 identifies four variants of trough-mouth fan depending on the dominant sediment/meltwater
1463 environment present in each location (Fig. 27). Type 1 trough-mouth fans are dominated almost
1464 entirely by glacigenic debris-flow emplacement. During full-glacial conditions, the rate of sediment
1465 delivery to the shelf edge is sufficient to trigger multiple glacigenic debris-flows which dominate the
1466 upper slope (Vorren and Laberg, 1997; Laberg and Dowdeswell, 2016). Sufficient numbers of flows
1467 can occur, that form an apron radiating out from the top of the fan to the mid/lower slope (Fig. 27;
1468 King et al., 1998; Taylor et al., 2002a). The lower slope is dominated by interbedded hemipelagic

1469 sediments and distal debris-flow muds and turbidites from the downslope evolution of glacigenic
1470 debris-flows (Laberg and Vorren, 1995). The volume and rate of sediment delivery to type 1 trough-
1471 mouth fans by ice streams is sufficiently large to dampen any influence that meltwater
1472 sedimentation may have on trough-mouth fan evolution. The Bear Island Trough-Mouth Fan
1473 represents a type 1 trough-mouth fan. During full-glacial conditions, sedimentation has been
1474 dominated by the emplacement of glacigenic debris-flow deposits on the upper and mid-fan, and on
1475 the lower fan by distal debris-flow muds, turbidites and hemipelagic sediments (Vorren et al., 1989;
1476 Sættem et al., 1994; Laberg and Vorren, 1996; Vorren et al., 1998; Pope et al., 2016). No large
1477 submarine landslide is thought to have originated from the Bear Island Trough-Mouth Fan for >200
1478 ka, a period which includes two full glacial cycles. However, prior to that seismic data suggests that
1479 the fan may have experienced 'relatively' frequent large submarine landslides (Figs 13 and 14) and
1480 would therefore have been categorised differently during these periods. A further example of a type
1481 1 trough-mouth fan can be found in the Gulf of Alaska. Here, sedimentation dominated by glacigenic
1482 debris-flow emplacement has resulted in the construction of the Bering Trough-Mouth Fan (Montelli
1483 et al., 2017b).

1484 Type 2 trough-mouth fans are dominated by a range of submarine mass movement processes (Fig.
1485 27). In the Nordic Seas, the North Sea and Storfjorden Trough-Mouth Fans are the type examples of
1486 type 2 trough-mouth fans. As on type 1 trough-mouth fans, these fans are dominated by the
1487 emplacement of glacigenic debris-flow deposits. Where these fans differ to type 1 fans is that the
1488 rate of sedimentation and the emplacement of the debris-flow apron leads to further instabilities
1489 within the trough-mouth fan. These instabilities can culminate in submarine slumping and large
1490 submarine landslides. Although other processes may play a role in the evolution of these trough-
1491 mouth fans (e.g. gully formation, plumite or contourite deposition which are key to landslide
1492 occurrence), their sedimentary architecture is dominated by different types of submarine mass
1493 movement deposit.

1494 Type 3 trough-mouth fans are characterised by medium rates of sediment delivery but meltwater
1495 processes also have a greater influence (Fig. 27). Kveithola is an example of a type 3 trough-mouth
1496 fan. As was the case for type 1 and type 2 trough-mouth fans, a significant volume of a type 3
1497 trough-mouth fan may still be made up of glacial-debris flow deposits which are emplaced when
1498 ice is at the shelf edge. However, the number and volume of these deposits is limited compared to
1499 type 1 and type 2 trough-mouth fans. Instead the defining characteristic of these fans is the
1500 presence of gullies, channel systems and plumites deposits. Gully incision in the upper slope has
1501 been hypothesised as a consequence of sediment-laden subglacial meltwater flow (Lowe and
1502 Anderson, 2002; Noormets et al., 2009; Bellec et al., 2016; Ó Cofaigh et al., in review). Alternatively
1503 they may be the result of dense water formation related to sea ice production on the shelf which
1504 subsequently cascades down the face of the trough-mouth fan. Although relatively rare, in some
1505 settings, e.g. Laurentian, Northeast and Crary Trough-Mouth Fans (Fig. 24b), channel-levee
1506 complexes have also been observed (Aksu and Piper, 1987; Piper, 1988; Kuvaas and Kristoffersen,
1507 1991). It is interesting to note the contrasting latitudes where these trough-mouth fans are found;
1508 the channel-levee systems perhaps being initiated by different processes. Channel formation is
1509 thought to be characteristic of warm-based ice at the shelf edge delivering large amounts of
1510 meltwater and sediment. Where sufficient meltwater and sediment is present, turbidity currents
1511 and hyperpycnal flows are able to produce channel systems (Aksu and Piper, 1987; Piper and
1512 Normark, 2009). It has also been speculated that some of these systems may be associated with
1513 catastrophic meltwater discharge; in some cases from subglacial lake drainage. Plumites meanwhile
1514 are deposited as a consequence of sediment-laden meltwater plumes (Lucchi et al., 2013). The
1515 extent and influence of these processes may, however, be controlled by the rate of retreat of the ice
1516 stream from the trough-mouth fan during deglaciation.

1517 Type 4 trough-mouth fans are characterised by low rates of sedimentation (Fig. 27). Scoresby Sund
1518 and Prydz Bay Trough-Mouth Fan represent type 4 trough-mouth fans. These fans are comparatively
1519 sediment starved, even during full-glacials. This reflects a number of factors, either individually or in

1520 combination. It can be a consequence of ice delivering little sediment to the fan due to it rarely
1521 extending to the shelf edge or to being present at the shelf edge for only a limited period of time,
1522 or to supplying relatively little sediment. Importantly, meltwater processes associated with ice
1523 stream advance and retreat also deliver little sediment to the shelf edge. The lack of sediment
1524 delivery means that glaciogenic debris-flows are infrequent with small volumes and do not produce
1525 the apron of deposits seen on type 1 and 2 trough-mouth fans (Dowdeswell et al., 1997). It is
1526 perhaps unlikely that a trough-mouth fan would form under type 4 conditions alone. These systems
1527 therefore probably reflect rates of sediment delivery associated with glacial maxima where different
1528 ice sheet regimes existed or where margins have evolved and which no longer favour progradation
1529 of the trough-mouth fan.

1530 **7.2.1.1. Can trough-mouth fan characteristics change?**

1531 To understand glaciated continental margin evolution it is important to understand whether trough-
1532 mouth fans can switch their type characteristics. Fundamental to this question is whether location,
1533 e.g. continental shelf geology and catchment area, or climate/ice sheet characteristics control the
1534 type of trough-mouth fan which develops. It is clear from the compilation of sedimentary records
1535 from the Nordic Seas that location can play a significant role in the type of trough-mouth fan which
1536 develops or whether a trough-mouth fan is able to develop at all (Wellner et al., 2001; Ó Cofaigh et
1537 al., 2003). For example, there is a clear contrast between the East Greenland and Svalbard/Barents
1538 Sea margin trough-mouth fans as a consequence of ice streams overriding sediments and bedrock
1539 with contrasting erodibilities (Solheim et al., 1996; 1998; Ó Cofaigh et al., 2003). The position and
1540 flow of ice streams is not, however, static. Analysis of buried mega-scale glacial lineations has shown
1541 that ice streams frequently migrate between glaciations (Dowdeswell et al., 2006b; Graham et al.,
1542 2009). Flow migration may result in the ice stream flowing over a substrate with contrasting
1543 properties and thus changing the input of sediment to a trough-mouth fan. Flow migration of the
1544 Lambert-Amery Ice Stream, from an area of readily erodible sediment to hard bedrock, has been

1545 cited as one of the main contributing factors for the initial reduction in sediment transport to the
1546 Prydz Bay Trough-Mouth Fan (Passchier et al., 2003; O'Brien et al., 2007).

1547 The compilation of ice sheet and sedimentation histories does, however, suggest that climate and its
1548 associated impacts on ice sheet characteristics may have a larger impact on controlling temporal
1549 switches between trough-mouth fan types. Climatic deterioration can clearly be seen as a driving
1550 factor behind the transition of the Scoresby Sund Trough-Mouth Fan from a type 1 to a type 4 fan. It
1551 is also responsible for the cessation of sediment supply to the Prydz Bay Trough-Mouth Fan after the
1552 adoption of 100 kyr climatic cyclicity. Further evidence can also be found in the changing
1553 sedimentation regimes seen on trough-mouth fans on the Svalbard margin (Table 3) and the
1554 transition in fan type associated with latitudinal change along the east Canadian margin.
1555 Interestingly, it could also be suggested that the Bear Island Trough-Mouth Fan has transitioned
1556 between type characteristics. Between 1.3 and 0.2 Ma the Bear Island Trough-Mouth Fan was
1557 dominated by glacigenic debris-flow emplacement and large submarine landslide occurrence (i.e. a
1558 type 2 trough-mouth fan). However, since at least 0.2 Ma (a consequence of poor age constraints),
1559 there is no evidence of large submarine landslide occurrence on the fan itself (Fig. 14). It is therefore
1560 possible that the Bear Island Trough-Mouth Fan has transitioned to type 1, characterised
1561 predominantly by glacigenic debris-flow emplacement. A possible explanation for this is the
1562 continued subsidence of the Barents Sea continental shelf and deepening of the Bear Island Trough
1563 which may have reduced the sediment supply (see Fig. 14). It may also have led to a reduction in the
1564 volume of glacimarine sediment deposition on the fan as the Bear Island Ice stream became more
1565 susceptible to rapid retreat due to its deeper water setting. This may have reduced the volume of
1566 contrasting sediment packages on the fan hypothesised to be required for large submarine landslide
1567 occurrence (Bryn et al., 2005).

1568 **7.2.1.2. Do trough-mouth fans have characteristic depositional sequences?**

1569 The sedimentary sequence of the Late Weichselian advance and retreat has been described on a
1570 number of trough-mouth fans around the Nordic Seas, e.g. Isfjorden (Elverhøi et al., 1995;
1571 Dowdeswell and Elverhøi, 2002). However, the setting of, and sedimentary processes operating on
1572 trough-mouth fans are highly variable. For example, depositional characteristics vary across and
1573 between the Storfjorden and Bear Island trough-mouth fans during the Late Weichselian (Laberg and
1574 Vorren, 1995; Pedrosa et al., 2011; Lucchi et al., 2013). It is therefore difficult if not problematic to
1575 describe a characteristic depositional sequence for a trough-mouth fan type.

1576 **7.2.2. How can we better understand controls on trough-mouth fans?**

1577 Understanding the controls on trough-mouth fan morphologies and processes remains challenging.
1578 Fundamentally this stems from there being very few/no direct observations of sediment transport
1579 by ice streams and submarine mass movements on trough-mouth fans and thus estimating sediment
1580 accumulation across a single trough-mouth fan during a full glacial period is very difficult. This is the
1581 case even when using the sedimentary record; there are very few studies which have been able to
1582 produce estimates of sediment accumulation (Laberg and Vorren, 1996; Nygård et al., 2005).
1583 Crucially, the precise timing of sediment delivery is usually uncertain in these studies. Fewer studies
1584 still have been able to model the delivery of sediment by ice streams to trough-mouth fans
1585 (Dowdeswell et al., 1999; Dowdeswell et al., 2010b). Future efforts to understand trough-mouth fans
1586 should therefore follow two separate lines. First, understanding of ice stream transfer of sediment
1587 needs to be improved and how this can be impacted by meltwater drainage system evolution.
1588 Achieving this will likely require observations from currently deforming glacier beds and proglacial
1589 environments in marine settings (e.g., Hart et al., 2011; Dowdeswell et al., 2015). Second, additional
1590 high resolution seismic and sedimentary records are needed on trough-mouth fans in order to
1591 precisely constrain the timing and volume of sediment delivery by ice streams.

1592 **7.3. Glaciated continental margins**

1593 In addition to the multiple types of trough-mouth fan that have been identified, our records also
1594 indicate that there are multiple types of glaciated margins (Fig. 28). We recognise three
1595 characteristic margin types. The first is characterised by high sediment inputs by ice streams and by
1596 the formation of trough-mouth fans (Dowdeswell et al., 1996). Along these margins, ice stream
1597 sedimentation is sufficiently high or has been sufficiently high in the past to allow trough-mouth fans
1598 to form even when conditions appear unfavourable such as seismically active or steep margins, e.g.
1599 the Bering Trough-Mouth Fan formation over the Aleutian Trench (Montelli et al., 2017b).

1600 The second margin type is characterised by high sediment inputs but which are insufficient to lead to
1601 the formation of trough-mouth fans. Along these margins, large volumes of sediment are delivered
1602 by a range of mechanisms. First, ice sheet flow delivers sediment at an enhanced rate compared to
1603 rates of interglacial sedimentation (Dowdeswell and Elverhøi, 2002). Second, ice streams may still be
1604 present and deliver large volumes of sediment. Third, sediment is delivered by glacial meltwater in
1605 addition to glacigenic debris-flows (Lekens et al., 2005; 2006). Fourth, ocean currents may deposit
1606 significant contourite deposits. The interbedding of the multiple types of sediment and the
1607 contrasting properties of these packages can lead to instabilities within the sediment stack (Baeten
1608 et al., 2013; 2014). As a consequence these margin types are often characterised by the occurrence
1609 of submarine slumps and landslides. The Storegga region is the type example for this margin type.

1610 The third margin type is characterised by low sediment input (Dowdeswell et al., 1996; Ó Cofaigh et
1611 al., 2003). Here, ice may not always reach the shelf edge during full glacials and thus direct delivery
1612 of sediment by ice is temporally limited. Alternatively, where ice regularly reaches the shelf edge, it
1613 may not transport large volumes of sediment. As a consequence the number and extent of glacigenic
1614 debris-flows is limited, as is the progradation of glacigenic structures. The development of these
1615 features will be further hindered if the continental slope is steep or the margin is tectonically active.
1616 The continental shelf and slope are, thus dominated by glacimarine and marine processes. As a

1617 result the dominant sediment transport process which dominates margin characteristics is turbidity
1618 currents which often result in the formation of channels.

1619 **8. Submarine mass movements on glaciated margins: geohazard assessment**

1620 Submarine mass movements are a common feature of glaciated margins and are considered
1621 significant geohazards. Poleward migration of human activity as a consequence of climate change
1622 increases exposure to these hazards necessitating hazard mitigation (Øverland, 2010; Boswell and
1623 Collett, 2011; Bennett, 2016). Hazard assessment requires us to understand the impact of past
1624 events, likely triggering mechanisms and their frequency. In the following section we discuss; (1) the
1625 potential hazard associated with these events using historical examples; (2) the potential triggers for
1626 submarine mass movements on glaciated margins; (3) the history of submarine landslides, their
1627 connection to ice sheet histories and conceptual models of flow preconditioning and triggering.

1628 **8.1. Submarine mass movements and societal impacts**

1629 Submarine mass movements have the potential to generate very damaging and far travelling
1630 tsunamis and damage seafloor infrastructure and they can therefore have significant societal impacts.
1631 The following section will briefly outline the geohazard potential based on two events; the Storegga
1632 Slide and the Grand Banks Slide.

1633 **8.1.1. Landslide-generated tsunami**

1634 The Storegga Slide (>3000 km³) and the Grand Banks Slide (~200 km³) both triggered tsunamis which
1635 impacted surrounding coastlines. The 1929 Grand Banks generated tsunami had runup heights of 13
1636 m along the Burin Peninsula, Canada, killing 27 people and leaving >1000 homeless (Fine et al.,
1637 2005). The 8.2 ka Storegga Slide generated a tsunami which impacted the coastlines of Greenland,
1638 Norway, the Shetland Islands, the Faroe Islands, Scotland, Eastern England and Doggerland with
1639 runup heights in excess of 20 m (see Fig. 29; Dawson et al., 1988; Long et al., 1989; Bondevik et al.,
1640 1997; 2003; 2005; 2012; Grauert et al., 2001; Bondevik et al., 2003; Smith et al., 2004; Fruergaard et

1641 al., 2015). In addition to fatalities directly caused by the tsunami, the Storegga tsunami is also
1642 thought to have had significant impacts on Mesolithic societies. Occurring contemporaneously with
1643 climatic deterioration associated with the 8.2 ka neoglacial, the tsunami is thought to have had
1644 significant long term impacts on Mesolithic populations around the coasts of the North Sea due to
1645 the combined stress caused by multiple hazards (Wicks and Mithen, 2014; Ballin, 2017; Waddington
1646 and Wicks, 2017). In addition, archaeological evidence has also suggested shifting settlement
1647 patterns following the tsunami with the abandonment of sites affected by the tsunami (Bondevik,
1648 2003; Weninger et al., 2008; Waddington and Wicks, 2017). Recurrence of an event of this scale
1649 today would also have significant impacts due to the increase in population inhabiting areas affected
1650 by the Storegga tsunami and the location of critical infrastructure on these coastlines such as power
1651 stations.

1652 Despite clear evidence of tsunami generation by large submarine landslides, there is evidence to
1653 suggest that not all large submarine landslides generate damaging tsunami. The Trænadjupet Slide
1654 contained 500 – 700 km³ of material, at least double that of the Grand Banks Slide, but no significant
1655 tsunami deposit has yet been linked with the slide (Løvholt et al., 2017). Landslide-tsunami
1656 generation is dependent on; (1) landslide volume, whether it is emplaced in one or multiple stages;
1657 (2) initial acceleration and speed of the mass movement; (3) the length and thickness of the slide
1658 and; (4) the water depth (Geist, 2000; Tappin et al., 2001; Waythomas and Watts, 2003; Harbitz et
1659 al., 2006; Masson et al., 2006; Waythomas et al., 2006; Hunt et al., 2011; Hunt et al., 2013; Harbitz et
1660 al., 2014; Løvholt et al., 2016). If the mass movement is of sufficient volume and accelerates quickly
1661 enough, it can generate a tsunami. The clear contrasts between the tsunami generated by the
1662 Storegga Slide and the Trænadjupet Slide shows that further work is needed in order to understand
1663 the likelihood of different potential failure mechanisms for submarine landslides around these
1664 margins.

1665 **8.1.2. Damage to seafloor infrastructure**

1666 Submarine mass movement damage to seafloor infrastructure has the potential to cause significant
1667 environmental and economic impacts. They represent a threat to seafloor infrastructure used for
1668 seafloor resource extraction which can be worth many millions of dollars including infrastructure
1669 used by the hydrocarbon industry (Thomas et al., 2010). For example, the Ormen Lange gas field,
1670 which currently supplies ~20% of the UK's supply of natural gas is located directly below the
1671 headwall of the Storegga Slide (Talling et al., 2014). They can also break seafloor
1672 telecommunications cables which currently carry >99% of intercontinental data traffic, including the
1673 internet and financial markets (Carter et al., 2014). Damage to cables at pinch points, i.e. areas
1674 where multiple cables transfer extremely high proportions of data traffic between specific regions,
1675 by turbidity currents has been shown to have significant impacts on local and regional economies
1676 (Rauscher, 2010; Carter et al., 2012; Gavey et al., 2017). The Grand Banks represents one such pinch
1677 point (Clare et al., 2016a). The 1929 slide and its associated turbidity current broke 11 telegraph
1678 cables (Heezen and Ewing, 1952). Today, >20 submarine fibre optic cables exist in the same area
1679 (Clare et al., 2016a). A similar event could therefore have a significant impact on the global
1680 economy.

1681 **8.2. Submarine mass movement triggers on glaciated margins**

1682 This section serves to summarise the processes that precondition and trigger submarine mass
1683 movements on glaciated margins. Numerous mechanisms by which submarine mass movements can
1684 be triggered have been proposed. On non-glaciated margins individual triggers have been identified
1685 using submarine cable breaks (Heezen and Ewing, 1952; 1955; Heezen et al., 1964; El-Robrini et al.,
1686 1985; Piper et al., 1999; Hsu et al., 2008; Carter et al., 2012; 2014; Cattaneo et al., 2012; Pope et al.,
1687 2017a; 2017b), repeat bathymetric surveys (Clare et al., 2016b), acoustic Doppler current profilers
1688 (Shepard et al., 1979; Ikehara, 2012; Liu et al., 2012; Azpiroz-Zabala et al., 2017) and damage to
1689 marine platforms (Prior et al., 1982; Bea et al., 1983; Alvarado, 2006). However, on glaciated
1690 margins, evidence for most submarine mass movements comes from their deposits. It is therefore

1691 often difficult to definitively link a specific flow deposit to a specific triggering mechanism. It must
1692 also be recognised that many individual triggering mechanisms, such as rapid sedimentation, can
1693 also act as preconditioning factors; the actual failure resulting from a subsequent trigger.

1694 **8.2.1. Earthquakes**

1695 Submarine mass movements on all margins are commonly attributed to earthquakes (ten Brink et
1696 al., 2009; Stigall and Dugan, 2010; Masson et al., 2011). In addition to earthquakes related to plate
1697 tectonics, glaciated margins are also subject to pronounced increases in seismic activity associated
1698 with glacio-isostatic adjustment (Fjeldskaar et al., 2000; Stewart et al., 2000; Bryn et al., 2003;
1699 Bungum et al., 2005; Steffen and Wu, 2011). Establishing a direct causal link between a mass
1700 movement and an earthquake from the geological record alone is challenging. Previous attempts
1701 include the use of contemporaneous mass movement deposits to infer periods of enhanced
1702 seismicity or large regional earthquakes (Goldfinger, 2011; Goldfinger et al., 2012; Bellwald et al.,
1703 2016). Alternatively, isostatic rebound models have been used to assess peaks in earthquake
1704 numbers and magnitudes related to glacio-isostatic adjustment (see Steffen and Wu, 2011 for full
1705 details), the outputs of which are then compared to known dated mass movement deposits (Bryn et
1706 al., 2003; 2005). Most submarine landslides are suggested to have an earthquake trigger, however,
1707 the Grand Banks Slide is known to have been triggered by a M_w 7.2 earthquake (Heezen and Ewing,
1708 1952), whilst a strong earthquake is believed to have played some role in triggering the Storegga
1709 Slide (Bryn et al., 2005). Both earthquakes are thought to be the result of isostatic adjustment.

1710 Earthquakes mainly trigger submarine mass movements in two ways. First, acceleration-induced
1711 sliding occurs when strong seismic motions subject sediments to horizontal and vertical
1712 accelerations that exceed their yield strength (Owen et al., 2007; 2008). Second, liquefaction-
1713 induced sliding can occur as a consequence of reduced sediment strength due to accumulated
1714 deformation from cyclic shearing. Cyclic loading can also result in the generation of excess pore
1715 pressures due to the upward migration of pore fluid. The migration of this fluid can generate

1716 instability if the migrating fluid encounters a sediment layer or region with a lower dissipation rate
1717 thereby allowing pore pressures to build up and eventually cause a failure to occur (Biscontin et al.,
1718 2004; Biscontin and Pestana, 2006; Özener et al., 2009; L'Heureux et al., 2013). The timing of the
1719 subsequent slope failure may occur several months after the seismic event that has triggered it as
1720 the time required to reach critical conditions for different sediment profiles ranges from minutes to
1721 months according to consolidation profiles, sediment types and dissipation rates (Biscontin and
1722 Pestana, 2006; Leynaud et al., 2009).

1723 **8.2.2. High sedimentation rates**

1724 The importance of high sedimentation rates for triggering submarine mass movements on glaciated
1725 margins has been emphasised throughout this review. Extension of a grounded ice sheet to the shelf
1726 edge has commonly been shown to be associated with enhanced rates of deposition and the
1727 occurrence of greater numbers of mass movements. High sedimentation rates are linked to slope
1728 failure in two ways. First, rapid sedimentation can lead to oversteepening of a slope resulting in
1729 eventual failure of the sediment (Powell and Domack, 1995; Powell and Alley, 1997; Dugan and
1730 Flemings, 2000; Clare et al., 2016b). Second, rapid sediment deposition can lead to progressively
1731 increasing pore pressures by preventing dewatering of the deposited sediment (Leynaud et al., 2007;
1732 Flemings et al., 2008; Stigall and Dugan, 2010). This can lead to the build-up of excess pore pressure
1733 (overpressure) and eventually lead to failure (Dugan and Sheahan, 2012). In addition to these
1734 mechanisms, glacigenic debris-flows have been interpreted to have been triggered in a third way.
1735 From observations on the Newfoundland continental slope, glacigenic debris-flows have been
1736 attributed to the continuous (or near continuous) input of sediment at the shelf break (Aksu and
1737 Hiscott, 1989, 1992). When triggered by this mechanism, downslope transport of sediment in
1738 glacigenic debris-flows has been likened to a 'lava flow' (Vorren and Laberg, 1997).

1739 **8.2.3. Hydrate dissociation**

1740 Gas hydrate dissociation has been suggested to be a preconditioning or triggering mechanism for
1741 submarine mass movements on glaciated margins (Best et al., 2003; Kennett et al., 2003). Seabed
1742 and subsurface fluid escape features have been identified along the Norwegian continental shelf, the
1743 Barents Sea and other glaciated margins indicating the presence of overpressure and pressure
1744 release in continental shelf sediments in these environments (Solheim and Elverhøi, 1985; Mienert
1745 et al., 1998; Gravdal et al., 2003; Hovland et al., 2005; Mienert et al., 2005; Chand et al., 2012;
1746 Andreassen et al., 2017). Hydrates form where there is a sufficient supply of gas, water at moderate
1747 pressure and relatively low temperatures (Berndt, 2005; Mienert et al., 2005). Dissociation of these
1748 hydrates can occur as a consequence of changes to pressure or temperature regimes in the
1749 substrate (Vanoudheusden et al., 2004; Hornbach et al., 2007; Berndt et al., 2014). Hydrate
1750 dissociation can provide overpressure through the expulsion of gas leading to the generation of a
1751 potential failure plane as a consequence of the reduction of yield strength. This can either cause
1752 failure to occur or increase the susceptibility of sediment to fail as a consequence of a further trigger
1753 (Prior et al., 1982; Kayen and Lee, 1991; Mienert et al., 1998; Sultan et al., 2004a). Alternatively
1754 submarine mass movements can cause dissociation themselves by exposing new horizons in the
1755 headwall and slide scar or by de-weighting deeper sediments (Sultan et al., 2004b). This alternative
1756 mechanism for dissociation greatly complicates identifying the exact role that dissociation may have
1757 had in triggering a mass movement (Maslin et al., 2004).

1758 **8.2.4. Sea level change**

1759 Sea level change is commonly invoked as being linked to changes in submarine mass movement
1760 frequency on all margins (Vail et al., 1977; Piper and Savoye, 1993; Owen et al., 2007; Lebreiro et al.,
1761 2009; Covault and Graham, 2010; Brothers et al., 2013; Smith et al., 2013). Sea level change itself is
1762 thought to be capable of causing slope failure as it can alter seafloor stress regimes due to changes
1763 in hydrostatic water pressure (Weaver and Kuijpers, 1983; Lee et al., 1996; Urlaub et al., 2012).
1764 These pressure changes are thought to also have the potential to cause hydrate dissociation (Maslin

1765 et al., 1998; 2004; Sultan et al., 2004a; Vanoudheusden et al., 2004; Leynaud et al., 2007; Owen et
1766 al., 2007). Modelling studies have also suggested that particularly rapid changes in sea level can also
1767 lead to increased seismicity (Brothers et al., 2013). However, it is the change to the location and rate
1768 of deposition that results from sea level change that is most commonly associated with changes in
1769 submarine mass movement frequency (Lee, 2009; Covault and Graham, 2010; Urlaub et al., 2012).

1770 Isolating the direct role of sea level change on submarine mass movement triggering on glaciated
1771 margins is challenging. This is a consequence of (1) the difficulty in precisely dating deposits (Urlaub
1772 et al., 2014; Pope et al., 2015); (2) needing to constrain local isostatic adjustment resulting from local
1773 ice sheet growth/decay (Shennan et al., 2002); (3) precisely dating and quantifying the local effects
1774 of rapid sea level change (Clark et al., 2002; Weaver et al., 2003; Brothers et al., 2013; Smith et al.,
1775 2013) and; (4) understanding the relative roles of other preconditioning and triggering mechanisms.
1776 Nonetheless, slope failures on glaciated margins have been recognised to be associated with rising
1777 sea levels and highstand (Owen et al., 2007; Lebreiro et al., 2009; Lee, 2009).

1778 **8.2.5. Hyperpycnal and hypopycnal flows**

1779 Hyperpycnal and hypopycnal flows are both known to have triggered submarine mass movements
1780 on glaciated margins. Hyperpycnal flows occur as a consequence of water discharged into the ocean
1781 having a sufficiently high sediment concentration to overcome the density difference between fresh
1782 water and sea water (Mulder and Moran, 1995; Parsons et al., 2001; Mulder et al., 2003; Felix et al.,
1783 2006). Once sediment-laden water is able to plunge it may then continue downslope under gravity
1784 and entrain water and sediments leading to the formation of a turbidity current (Carter et al., 2012).
1785 In contrast, hypopycnal flows initially maintain their sediment loads in suspension. Fallout from the
1786 plume can then trigger a subsequent submarine mass movement (Parsons et al., 2001; Curran et al.,
1787 2004; Zajaczkowski, 2008; Piper and Normark, 2009). Examples of deposits from submarine mass
1788 movements triggered by these flows can be found on the East Canadian Margin, dating from the

1789 Weichselian and as during ice sheet retreat (Hesse et al., 2001; Piper and Hundert, 2002; Piper et al.,
1790 2007; Tripsanas and Piper, 2008b).

1791 **8.3.Submarine landslides on glaciated margins**

1792 Submarine landslides are considered to be one of the main morphological features of glaciated
1793 margins and a common feature of trough-mouth fans. In the following section we will therefore
1794 discuss the connection between ice sheets and landslides and conceptual models of these flows on
1795 glaciated margins.

1796 **8.3.1. The distribution of large submarine landslides**

1797 The global distribution of known large submarine landslides on glaciated margins is very uneven.
1798 Where large submarine landslides have been identified, their locations appear to favour recurrent
1799 mass-failures of this scale. In other areas they are extremely rare or have yet to be identified as a
1800 consequence of globally uneven data coverage. The frequency of these events in two regions
1801 stand out; they are especially common on the Norwegian/Barents Sea Margin and the South East
1802 Canadian Margin (e.g. Hjelstuen et al., 2005; Urlaub et al., 2013). They are conspicuously absent
1803 from several other glaciated margins. The following section will discuss the likely causes of this
1804 distribution.

1805 **8.3.1.1. Sediment supply and the presence of weak layers**

1806 Sediment supply appears to be crucial for submarine landslide occurrence on glaciated margins.
1807 Models based on the Storegga Slide suggested that ice stream driven rapid sedimentation could
1808 generate overpressure or increased pore pressures (Bryn et al., 2003; Hafliðason et al., 2003).
1809 Sedimentary evidence from this part of the Norwegian Margin suggests that sedimentation rates
1810 were as high as 1750 cm/ka during deglaciation (Lekens et al., 2005; 2009). However, slope failure
1811 was not caused by the rate of sedimentation alone but by the contrasting strength and porosity
1812 profiles of soft marine clays and glacial sediments (Bryn et al., 2003; 2005; Kvalstad et al., 2005;

1813 Leynaud et al., 2007). The boundary between the two sediment packages provided the plane along
1814 which slope failure occurred. Geotechnical investigations of other sections of the Norwegian margin
1815 where submarine landslides are common have revealed similar site characteristics (Lucchi et al.,
1816 2013; Baeten et al., 2014; Llopart et al., 2014; Madhusudhan et al., 2017). In the Trænadjupet
1817 region, the contrast is provided by glacial sediments, contouritic and marine clays (Laberg et al.,
1818 2003; Baeten et al., 2014). Failures on the Storfjorden Trough-Mouth Fan are thought to relate to
1819 the contrasting properties of glacial sediments and water-rich, clayey sediments with low shear
1820 strength deposited by meltwater plumes and contour currents (Hjelstuen et al., 1996; Rebesco et al.,
1821 2012; Lucchi et al., 2013). The South East Canadian Margin also experiences similarly rapid
1822 sedimentation (4 m/ka) from meltwater plumes (Mosher et al., 1989; Piper and Ingram, 2003).

1823 We therefore suggest that the Bryn et al. (2005) model for triggering/preconditioning of large
1824 submarine landslides where rapid deposition of sediment by ice sheets onto pre-existing 'weak'
1825 layers is applicable to large sections of glaciated continental margins not just the Storegga section of
1826 the Norwegian Margin (Fig. 30).

1827 **8.3.1.2. Passive vs. active margins**

1828 Earthquakes are often cited as the triggering mechanisms for submarine mass movements (see
1829 previous section). Indeed, the Grand Banks submarine landslide is evidence that large earthquakes
1830 can trigger large submarine landslides on glaciated margins (Heezen and Ewing, 1952; Piper et al.,
1831 1999). However, as has been identified on non-glaciated margins there is a significant contrast
1832 between submarine landslide occurrence on passive and active margins. The multiple large
1833 submarine landslides on the South East Canadian and Norwegian margins are thought to have been
1834 triggered by earthquakes related to isostatic adjustment following ice sheet retreat (Laberg and
1835 Vorren, 2000; Piper and Ingram, 2003; Bryn et al., 2005; Piper, 2005). The passive nature of both
1836 these margins means that sediments deposited by the ice sheets were rarely subject to seismic
1837 shaking sufficient to generate large surface motions. Sufficient sediment was therefore able to

1838 accumulate in both regions before failure was triggered by the increased seismicity associated with
1839 deglaciation. In contrast, no large submarine landslides have been identified on the South Alaskan
1840 Margin during the Quaternary. Here, ice sheet deposited sediments as well as those deposited more
1841 recently by rivers are exposed to repeated strong ground-shaking. Observations from large historical
1842 earthquakes, i.e. the 1964 Alaskan Earthquake, have shown that smaller scale submarine mass
1843 movements regularly remove weaker sediments (Brothers et al., 2016), while subduction zone
1844 shaking has been shown to lead to enhanced consolidation and strengthening of seafloor sediment
1845 (Sultan et al., 2004a; Völker et al., 2011; Sawyer and DeVore, 2015; Pope et al., 2017a; Sawyer et al.,
1846 2017). The combination of enhanced consolidation and the regular removal of weaker sediments
1847 therefore likely prevents large submarine landslides occurring on active glaciated margins.

1848 **8.3.2. An integrated model of submarine landslides on glaciated margins?**

1849 The Bryn et al. (2005) model of large submarine landslide occurrence was used in geohazard
1850 assessment for the development of the Ormen Lange gas field (Solheim et al., 2005b) and has since
1851 been used to inform tsunami hazard assessment on the margins of the Nordic Seas (e.g. Tsunami risk
1852 and strategies for the European Region Project). Hazard assessment for submarine landslides
1853 requires the likely triggering mechanisms, failure dynamics and frequency of events to be identified
1854 (Talling et al., 2014; Pope et al., 2015). However, our increasing understanding of landslides along
1855 the Norwegian Margin has shown significant differences between landslides on different parts of the
1856 margins.

1857 In terms of frequency, the Bryn et al. (2005) model suggests that each submarine landslide requires
1858 a separate ice stream advance to the shelf edge; each advance delivering sediment to fill the slide
1859 scar from the previous event and recharge the slope for failure (Fig. 30). However, dating of other
1860 landslides along this margin shows that landslide recurrence does not correlate simply with each ice
1861 advance. The Nyk and Trænadjupet Slides were separated by about 14 ka. A short lived glacial
1862 advance occurred between the two events but did not reach the shelf edge nor did it result in a large

1863 increase in sedimentation (Olsen et al., 2001b). Even in the Storegga area the recurrence rate for the
1864 three submarine landslides that occurred here (Storegga, R and S) was 200 kyr representing multiple
1865 ice stream advances to the shelf edge (Hjelstuen et al., 2005).

1866 A contrast between the failure dynamics also exists. Analysis of the Storegga Slide deposits has led
1867 to the interpretation that the slide was a retrogressive failure during which the slide mass
1868 disintegrated rapidly forming a large turbidite (Haflidason et al., 2004; Bondevik et al., 2005; Masson
1869 et al., 2006). The initial acceleration of the slide mass was key to the generation of the associated
1870 tsunami (Løvholt et al., 2005; Harbitz et al., 2006). In contrast, detailed analysis of the Trænadjupet
1871 Slide has led to the hypothesis that the Trænadjupet Slide occurred top-down due to the presence of
1872 three progressively deeper headwalls and that the slide mass largely failed to disintegrate as shown
1873 by the presence of large block fields (Laberg et al., 2002b). Progressive subaerial landslides have
1874 been recognised in a number of locations, notably Norway and Quebec (Locat et al., 2008; Quinn et
1875 al., 2012). These landslides are generally a consequence of strain induced loss of structure in clays
1876 resulting in slope failure (Urciuoli et al., 2007). In the submarine environment, top-down slope
1877 failure would likely have been initiated as a consequence of pore pressure build-up along a 'weak'
1878 layer. This is likely to have been a contouritic deposit in the Trænadjupet case (Sultan et al., 2004a;
1879 Baeten et al., 2014). Failure of the initial sediment package and its downslope progression resulted
1880 in the subsequent failure of deeper 'weak' layers due to shearing or rapid increases in overburden
1881 pressure. It is possible that the occurrence of the Nyk Slide played a significant role in the triggering
1882 of the Trænadjupet Slide either through unloading of the seafloor or as a consequence of
1883 deformation of seafloor sediments due to overriding slide material (Fig. 30). The different failure
1884 dynamics means that the tsunamigenic potential of landslides from the two regions is probably
1885 different (Løvholt et al., 2005; 2016; 2017).

1886 Despite the clear similarities identified in terms of preconditioning and triggering mechanisms in the
1887 Storegga and Trænadjupet regions clear differences exist which are important for understanding

1888 landslide processes on glaciated margins. This suggests that a single model of landslide occurrence
1889 may not be appropriate. Further work is therefore needed in order to understand whether the close
1890 temporal association of the Nyk and Trænadjupet Slides is unique or whether this can be a common
1891 feature on these margins.

1892 **9. Conclusions**

1893 Our understanding of glaciated continental margin processes and evolution has come predominantly
1894 from studies of the Nordic Seas during the last glacial period. Using a combination of geophysical
1895 and sedimentological records, these studies have produced conceptual models for processes
1896 associated with different morphological features, continental slope architecture and the primary
1897 drivers (e.g. climate) behind these observations. Here, we have reviewed the current understanding
1898 of ice sheet growth and decay around the Nordic Seas and how this is related to the history of
1899 sedimentation and margin architecture. These histories have then been compared with other
1900 glaciated margins in order to identify unified models of glaciated continental margin evolution. This
1901 contribution achieves the following:

- 1902 1) A comprehensive record of Greenland, Barents Sea and Scandinavian Ice Sheet growth and
1903 decay on the margins of the Nordic Seas over the last 2.58 Ma is provided.
- 1904 2) The record of sedimentation and submarine mass movements which have occurred as a
1905 consequence of the growth and decay of the reconstructed ice sheets has been compiled.
- 1906 3) However, the completeness of ice sheet growth and decay records and the record of
1907 sedimentary processes is shown to be temporally and spatially highly variable.
- 1908 4) From the records of ice sheet growth and decay and the associated sedimentation, we have
1909 been able to review the first order controls on sediment delivery to the continental margin
1910 at the scale of an ice sheet.
- 1911 5) We have identified a new conceptual model of trough-mouth fans and glaciated margins
1912 worldwide according to the driving factors behind their associated sedimentary processes.

1913 6) We have provided a review of the relationship between ice sheets and large submarine
1914 landslides on glaciated margins. We have tested previous models of submarine landslide
1915 occurrence on glaciated margins using this information and hence proposed an additional
1916 model to explain some large submarine landslides.

1917

1918

1919

1920 **Acknowledgements**

1921 This contribution is based on the previous work by numerous individuals worldwide whose efforts
1922 we greatly appreciate. This research was supported by the UK NERC Arctic Research Programme
1923 under the project on whether climate change increases the landslide-tsunami risk to the UK
1924 (NE/K00008K/1). E. Pope was supported by grant NE/K00008K/1. We thank the editor Ian Candy,
1925 Jonathan Lee and an anonymous reviewer; their comments greatly improved the manuscript.

1926

1927 **References**

- 1928 Adrielsson, L., Alexanderson, H., 2005. Interactions between the Greenland Ice Sheet and the
1929 Liverpool Land coastal ice cap during the last two glaciation cycles. *Journal of Quaternary Science* 20,
1930 269-283.
- 1931
- 1932 Aksu, A.E., Hiscott, R.N., 1989. Slides and debris flows on the high-latitude continental slopes of
1933 Baffin Bay. *Geology* 17, 885-888.
- 1934
- 1935 Aksu, A.E., Hiscott, R.N., 1992. Shingled Quaternary debris flow lenses on the north-east
1936 Newfoundland Slope. *Sedimentology* 39, 193-206.
- 1937
- 1938 Aksu, A.E., Piper, D.J.W., 1987. Late Quaternary sedimentation in Baffin Bay. *Canadian Journal of*
1939 *Earth Sciences* 24, 1833-1846.
- 1940
- 1941 Alley, R.B., Blankenship, D.D., Rooney, S.T., Bentley, C.R., 1989. Sedimentation beneath ice shelves—
1942 the view from ice stream B. *Mar Geol* 85, 101-120.
- 1943
- 1944 Alvarado, A., 2006. Updates on MMS (Minerals Management Service) regulatory issues for offshore
1945 operators. Uniform Resource Locator (URL):
1946 <http://www.southernngas.org/EVENTS/documents/SGAOGO06Alvarado.pdf> (accessed 13 March,
1947 2007).
- 1948
- 1949 Amblas, D., Canals, M., 2016. Contourite drifts and canyon-channel systems on the Northern
1950 Antarctic Peninsula Pacific margin. *Geological Society, London, Memoirs* 46, 393-394.
- 1951
- 1952 Amblas, D., Urgeles, R., Canals, M., Calafat, A.M., Rebesco, M., Camerlenghi, A., Estrada, F., De
1953 Batist, M., Hughes-Clarke, J.E., 2006. Relationship between continental rise development and
1954 palaeo-ice sheet dynamics, Northern Antarctic Peninsula Pacific margin. *Quaternary Sci Rev* 25, 933-
1955 944.
- 1956
- 1957 Andersen, E.S., Dokken, T.M., Elverhoi, A., Solheim, A., Fossen, I., 1996. Late Quaternary
1958 sedimentation and glacial history of the western Svalbard continental margin. *Mar Geol* 133, 123-
1959 156.
- 1960
- 1961 Andersen, E.S., Solheim, A., Elverhøi, A., 1994. Development of a high Arctic margin, exemplified by
1962 the western margin of Svalbard, *International Conference on Arctic Margins, Alaska*, pp. 155 - 160.
- 1963
- 1964 Anderson, J.B., Wright, R., Andrews, B., 1986. Weddell Fan and associated abyssal plain, Antarctica:
1965 morphology, sediment processes, and factors influencing sediment supply. *Geo-Mar Lett* 6, 121-129.
- 1966
- 1967 Andreassen, K., Hubbard, A., Winsborrow, M., Patton, H., Vadakkepuliambatta, S., Plaza-Faverola,
1968 A., Gudlaugsson, E., Serov, P., Deryabin, A., Mattingsdal, R., 2017. Massive blow-out craters formed
1969 by hydrate-controlled methane expulsion from the Arctic seafloor. *Science* 356, 948-953.
- 1970
- 1971 Andreassen, K., Nilssen, L.C., Rafaelsen, B., Kuilman, L., 2004. Three-dimensional seismic data from
1972 the Barents Sea margin reveal evidence of past ice streams and their dynamics. *Geology* 32, 729-732.
- 1973
- 1974 Andreassen, K., Ødegaard, C.M., Rafaelsen, B., 2007. Imprints of former ice streams, imaged and
1975 interpreted using industry three-dimensional seismic data from the south-western Barents Sea.
1976 *Geological Society, London, Special Publications* 277, 151-169.

1977
1978 Andrews, J.T., 2008. The role of the Iceland Ice Sheet in the North Atlantic during the late
1979 Quaternary: a review and evidence from Denmark Strait. *Journal of Quaternary Science* 23, 3-20.
1980
1981 Azpiroz-Zabala, M., Cartigny, M.J.B., Talling, P.J., Parsons, D.R., Sumner, E.J., Clare, M.A., Simmons,
1982 S.M., Cooper, C., Pope, E.L., 2017. Newly recognised turbidity current structure can explain
1983 prolonged flushing of submarine canyons. *Science Advances* 3, e1700200.
1984
1985 Baeten, N.J., Laberg, J.S., Forwick, M., Vorren, T.O., Vanneste, M., Forsberg, C.F., Kvalstad, T.J.,
1986 Ivanov, M., 2013. Morphology and origin of smaller-scale mass movements on the continental slope
1987 off northern Norway. *Geomorphology* 187, 122-134.
1988
1989 Baeten, N.J., Laberg, J.S., Vanneste, M., Forsberg, C.F., Kvalstad, T.J., Forwick, M., Vorren, T.O.,
1990 Hafliðason, H., 2014. Origin of shallow submarine mass movements and their glide planes—
1991 Sedimentological and geotechnical analyses from the continental slope off northern Norway. *Journal*
1992 *of Geophysical Research: Earth Surface* 119, 2335-2360.
1993
1994 Ballin, T.B., 2017. Rising waters and processes of diversification and unification in material culture:
1995 the flooding of Doggerland and its effect on north-west European prehistoric populations between
1996 ca. 13 000 and 1500 cal BC. *Journal of Quaternary Science* 32, 329-339.
1997
1998 Baltzer, A., Cochonat, P., Piper, D.J.W., 1994. In situ geotechnical characterization of sediments on
1999 the Nova Scotian Slope, eastern Canadian continental margin. *Mar Geol* 120, 291-308.
2000
2001 Bart, P.J., De Batist, M., Jokat, W., 1999. Interglacial collapse of Cray Trough-mouth fan, Weddell
2002 Sea, Antarctica: implications for Antarctic glacial history. *Journal of Sedimentary Research* 69.
2003
2004 Batchelor, C.L., Ottesen, D., Dowdeswell, J.A., 2017. Quaternary evolution of the northern North Sea
2005 margin through glacial debris-flow and contourite deposition. *Journal of Quaternary Science* 32,
2006 416-426.
2007
2008 Baumann, K.-H., Lackschewitz, K.S., Mangerud, J., Spielhagen, R.F., Wolf-Welling, T.C.W., Henrich, R.,
2009 Kassens, H., 1995. Reflection of Scandinavian ice sheet fluctuations in Norwegian Sea sediments
2010 during the past 150,000 years. *Quaternary Res* 43, 185-197.
2011
2012 Baumann, K.H., Huber, R., 1999. 12. Sea-surface gradients between the North Atlantic and the
2013 Norwegian Sea during the last 3.1 MY: Comparison of Sites 982 and 985, *Proceedings of the Ocean*
2014 *Drilling Program: Scientific Results. The Program*, p. 179.
2015
2016 Bea, R.G., Wright, S.G., Sircar, P., Niedoroda, A.W., 1983. Wave-Induced Slides in South Pass Block
2017 70, Mississippi Delta. *J Geotech Eng-Asce* 109, 619-644.
2018
2019 Bellec, V.K., Rise, L., Bøe, R., Dowdeswell, J.A., 2016. Glacially related gullies on the upper
2020 continental slope, SW Barents Sea margin. *Geological Society, London, Memoirs* 46, 381-382.
2021
2022 Bellwald, B., Hjelstuen, B.O., Sejrup, H.P., Hafliðason, H., 2016. Postglacial Mass Failures in the Inner
2023 Hardangerfjorden System, Western Norway, *Adv Nat Tech Haz Res. Springer*, pp. 73-82.
2024
2025 Bennett, M.M., 2016. Discursive, material, vertical, and extensive dimensions of post-Cold War Arctic
2026 resource extraction. *Polar Geography* 39, 258-273.
2027

2028 Bennett, M.R., 2003. Ice streams as the arteries of an ice sheet: their mechanics, stability and
2029 significance. *Earth-Sci Rev* 61, 309-339.
2030
2031 Bennett, R., Campbell, D.C., Furze, M.F.A., 2014. The shallow stratigraphy and geohazards of the
2032 Northeast Baffin Shelf and Lancaster Sound. *Bulletin of Canadian Petroleum Geology* 62, 217-231.
2033
2034 Berg, K., Solheim, A., Bryn, P., 2005. The Pleistocene to recent geological development of the Ormen
2035 Lange area. *Mar Petrol Geol* 22, 45-56.
2036
2037 Berndt, C., 2005. Focused fluid flow in passive continental margins. *Philosophical Transactions of the*
2038 *Royal Society of London A: Mathematical, Physical and Engineering Sciences* 363, 2855-2871.
2039
2040 Berndt, C., Feseker, T., Treude, T., Krastel, S., Liebetrau, V., Niemann, H., Bertics, V.J., Dumke, I.,
2041 Dünnbier, K., Ferré, B., Graves, C., Gross, F., Hissmann, K., Hühnerbach, V., Krause, S., Lieser, K.,
2042 Schauer, J., Steinle, L., 2014. Temporal Constraints on Hydrate-Controlled Methane Seepage off
2043 Svalbard. *Science* 343, 284-287.
2044
2045 Best, A.I., Clayton, C.R.I., Longva, O., Szuman, M., 2003. The role of free gas in the activation of
2046 submarine slides in Finneidfjord, Adv Nat Tech Haz Res. Springer, pp. 491-498.
2047
2048 Biscontin, G., Pestana, J.M., 2006. Factors affecting seismic response of submarine slopes. *Natural*
2049 *Hazards and Earth System Science* 6, 97-107.
2050
2051 Biscontin, G., Pestana, J.M., Nadim, F., 2004. Seismic triggering of submarine slides in soft cohesive
2052 soil deposits. *Mar Geol* 203, 341-354.
2053
2054 Björck, S., Bennike, O., Ingólfsson, Ó., Barnekow, L., Penney, D.N., 1994a. Lake Boksehandsken's
2055 earliest postglacial sediments and their palaeoenvironmental implications, Jameson Land, East
2056 Greenland. *Boreas* 23, 459-472.
2057
2058 Björck, S., Wohlfarth, B., Bennike, O., Hjort, C., Persson, T., 1994b. Revision of the early Holocene
2059 lake sediment based chronology and event stratigraphy on Hochstetter Forland, NE Greenland.
2060 *Boreas* 23, 513-523.
2061
2062 Bond, G., Heinrich, H., Broecker, W., Labeyrie, L., McManus, J.F., Andrews, J., Huon, S., Jantschik, R.,
2063 Clasen, S., Simet, C., 1992. Evidence for massive discharges of icebergs into the North Atlantic ocean
2064 during the last glacial period.
2065
2066 Bond, G.C., Showers, W., Elliot, M., Evans, M., Lotti, R., Hajdas, I., Bonani, G., Johnson, S., 1999. The
2067 North Atlantic's 1-2 Kyr Climate Rhythm: Relation to Heinrich Events, Dansgaard/Oeschger Cycles
2068 and the Little Ice Age. *Mechanisms of global climate change at millennial time scales*, 35-58.
2069
2070 Bondevik, S., 2003. Storegga tsunami sand in peat below the Tapes beach ridge at Harøy, western
2071 Norway, and its possible relation to an early Stone Age settlement. *Boreas* 32, 476-483.
2072
2073 Bondevik, S., Løvholt, F., Harbitz, C.B., Mangerud, J., Dawson, A., Inge Svendsen, J., 2005. The
2074 Storegga Slide tsunami—comparing field observations with numerical simulations. *Mar Petrol Geol*
2075 22, 195-208.
2076

2077 Bondevik, S., Mangerud, J., Dawson, S., Dawson, A., Lohne, Ø., 2003. Record-breaking height for
2078 8000-year-old tsunami in the North Atlantic. *Eos, Transactions American Geophysical Union* 84, 289-
2079 293.
2080
2081 Bondevik, S., Stormo, S.K., Skjerdal, G., 2012. Green mosses date the Storegga tsunami to the
2082 chilliest decades of the 8.2 ka cold event. *Quaternary Sci Rev* 45, 1-6.
2083
2084 Bondevik, S., Svendsen, J.I., Johnson, G., Mangerud, J., Kaland, P.E., 1997. The Storegga tsunami
2085 along the Norwegian coast, its age and run up. *Boreas* 26, 29-53.
2086
2087 Böse, M., Lüthgens, C., Lee, J.R., Rose, J., 2012. Quaternary glaciations of northern Europe.
2088 *Quaternary Sci Rev* 44, 1-25.
2089
2090 Boswell, R., Collett, T.S., 2011. Current perspectives on gas hydrate resources. *Energy &*
2091 *environmental science* 4, 1206-1215.
2092
2093 Boulton, G.S., 1978. Boulder shapes and grain-size distributions of debris as indicators of transport
2094 paths through a glacier and till genesis. *Sedimentology* 25, 773-799.
2095
2096 Brendryen, J., Hafliðason, H., Rise, L., Chand, S., Vanneste, M., Longva, O., L'Heureux, J.S., Forsberg,
2097 C.F., 2015. Ice sheet dynamics on the Lofoten–Vesterålen shelf, north Norway, from Late MIS-3 to
2098 Heinrich Stadial 1. *Quaternary Sci Rev* 119, 136-156.
2099
2100 Broecker, W.S., Denton, G.H., 1990. The role of ocean-atmosphere reorganizations in glacial cycles.
2101 *Quaternary Sci Rev* 9, 305-341.
2102
2103 Brothers, D.S., Haeussler, P.J., Liberty, L., Finlayson, D., Geist, E.L., Labay, K., Byerly, M., 2016. A
2104 submarine landslide source for the devastating 1964 Chenega tsunami, southern Alaska. *Earth and*
2105 *Planetary Science Letters* 438, 112-121.
2106
2107 Brothers, D.S., Luttrell, K.M., Chaytor, J.D., 2013. Sea-level-induced seismicity and submarine
2108 landslide occurrence. *Geology* 41, 979-982.
2109
2110 Bryn, P., Berg, K., Forsberg, C.F., Solheim, A., Kvalstad, T.J., 2005. Explaining the Storegga slide. *Mar*
2111 *Petrol Geol* 22, 11-19.
2112
2113 Bryn, P., Solheim, A., Berg, K., Lien, R., Forsberg, C.F., Hafliðason, H., Ottesen, D., Rise, L., 2003. The
2114 Storegga Slide complex; repeated large scale sliding in response to climatic cyclicality, *Adv Nat Tech*
2115 *Haz Res*. Springer, pp. 215-222.
2116
2117 Bugge, T., 1983. Submarine slides on the Norwegian continental margin, with special emphasis on
2118 the Storegga area, vol. 110. Trondheim, Norway: Continental Shelf and Petroleum Technology
2119 Research Institute, A/S publication.
2120
2121 Bugge, T., Befring, S., Belderson, R.H., Eidvin, T., Jansen, E., Kenyon, N.H., Holtedahl, H., Sejrup, H.P.,
2122 1987. A giant three-stage submarine slide off Norway. *Geo-Mar Lett* 7, 191-198.
2123
2124 Bungum, H., Lindholm, C., Faleide, J.I., 2005. Postglacial seismicity offshore mid-Norway with
2125 emphasis on spatio-temporal–magnitudal variations. *Mar Petrol Geol* 22, 137-148.
2126

2127 Busetti, M., Caburlotto, A., Armand, L., Damiani, D., Giorgetti, G., Lucchi, R.G., Quilty, P.G., Villa, G.,
2128 2003. Plio-Quaternary sedimentation on the Wilkes Land continental rise: preliminary results. *Deep*
2129 *Sea Research Part II: Topical Studies in Oceanography* 50, 1529-1562.

2130

2131 Butt, F.A., Drange, H., Elverhøi, A., Otterå, O.H., Solheim, A., 2002. Modelling Late Cenozoic isostatic
2132 elevation changes in the Barents Sea and their implications for oceanic and climatic regimes:
2133 preliminary results. *Quaternary Sci Rev* 21, 1643-1660.

2134

2135 Butt, F.A., Elverhøi, A., Forsberg, C.F., Solheim, A., 2001a. Evolution of the Scoresby Sund Fan, central
2136 East Greenland-evidence from ODP Site 987. *NORSK GEOLOGISK TIDSSKRIFT* 81, 3-15.

2137

2138 Butt, F.A., Elverhøi, A., Hjelstuen, B.O., Dimakis, P., Solheim, A., 2001b. Modelling late Cenozoic
2139 isostatic elevation changes in Storfjorden, NW Barents Sea: an indication of varying erosional
2140 regimes. *Sediment Geol* 143, 71-89.

2141

2142 Campbell, D.C., Mosher, D.C., 2014. Detailed geomorphology and surficial geology of the outer Nova
2143 Scotia margin. *Atlantic Geology* 50.

2144

2145 Canals, M., Amblas, D., Casamor, J.L., Lastras, G., 2016. Gebra Slide: glacial and tectonic controls on
2146 recurrent submarine landsliding off the northern tip of the Antarctic Peninsula. *Geological Society,*
2147 *London, Memoirs* 46, 417-418.

2148

2149 Canals, M., Calafat, A., Camerlenghi, A., De Batist, M., Urgeles, R., Farran, M., Geletti, R., Versteeg,
2150 W., Amblas, D., Rebesco, M., 2003. Uncovering the footprint of former ice streams off Antarctica.
2151 *EOS: TRANSACTIONS AMERICAN GEOPHYSICAL UNION* 84, 97-103.

2152

2153 Canals, M., Lastras, G., Urgeles, R., Casamor, J.L., Mienert, J., Cattaneo, A., De Batist, M., Haflidason,
2154 H., Imbo, Y., Laberg, J.S., Locat, J., Long, D., Longva, O., Masson, D.G., Sultan, N., Trincardi, F., Bryn,
2155 P., 2004. Slope failure dynamics and impacts from seafloor and shallow sub-seafloor geophysical
2156 data: case studies from the COSTA project. *Mar Geol* 213, 9-72.

2157

2158 Carter, L., Gavey, R., Talling, P.J., Liu, J.T., 2014. Insights into submarine geohazards from breaks in
2159 subsea telecommunication cables. *Oceanography* 27, 58-67.

2160

2161 Carter, L., Milliman, J.D., Talling, P.J., Gavey, R., Wynn, R.B., 2012. Near-synchronous and delayed
2162 initiation of long run-out submarine sediment flows from a record-breaking river flood, offshore
2163 Taiwan. *Geophys Res Lett* 39.

2164

2165 Casas, D., Ercilla, G., García, M., Yenes, M., Estrada, F., 2013. Post-rift sedimentary evolution of the
2166 Gebra Debris Valley. A submarine slope failure system in the Central Bransfield Basin (Antarctica).
2167 *Mar Geol* 340, 16-29.

2168

2169 Catania, G.A., Scambos, T.A., Conway, H., Raymond, C.F., 2006. Sequential stagnation of Kamb ice
2170 stream, West Antarctica. *Geophys Res Lett* 33.

2171

2172 Cattaneo, A., Babonneau, N., Ratzov, G., Dan-Unterseh, G., Yelles, K., Bracene, R., De Lepinay, B.M.,
2173 Boudiaf, A., Déverchère, J., 2012. Searching for the seafloor signature of the 21 May 2003
2174 Boumerdes earthquake offshore central Algeria. *Nat Hazard Earth Sys* 12, 2159-2172.

2175

2176 Chand, S., Thorsnes, T., Rise, L., Brunstad, H., Stoddart, D., Bøe, R., Lågstad, P., Svolsbru, T., 2012.
2177 Multiple episodes of fluid flow in the SW Barents Sea (Loppa High) evidenced by gas flares,
2178 pockmarks and gas hydrate accumulation. *Earth and Planetary Science Letters* 331, 305-314.
2179

2180 Channell, J.E.T., Smelror, M., Jansen, E., Higgins, S.M., Lehman, B., Eidvin, T., Solheim, A., 1999. 10.
2181 Age models for glacial fan deposits off East Greenland and Svalbard (Sites 986 and 987), *Proceedings*
2182 *of the Ocean Drilling Program: Scientific results. The Program*, p. 149.
2183

2184 Christoffersen, P., Tulaczyk, S., Behar, A., 2010. Basal ice sequences in Antarctic ice stream: Exposure
2185 of past hydrologic conditions and a principal mode of sediment transfer. *Journal of Geophysical*
2186 *Research: Earth Surface (2003–2012)* 115.
2187

2188 Clare, M., Pope, E., Talling, P., Hunt, J., Carter, L., 2016a. What threat do turbidity currents and
2189 submarine landslides pose to submarine telecommunications cable infrastructure?, *EGU General*
2190 *Assembly Conference Abstracts*, p. 4347.
2191

2192 Clare, M.A., Hughes Clarke, J.E., Talling, P.J., Cartigny, M.J.B., Pratomo, D.G., 2016b. Preconditioning
2193 and triggering of offshore slope failures and turbidity currents revealed by most detailed monitoring
2194 yet at a fjord-head delta. *Earth and Planetary Science Letters* 450, 208-220.
2195

2196 Clark, C.D., 1993. Mega-scale glacial lineations and cross-cutting ice-flow landforms. *Earth Surf Proc*
2197 *Land* 18, 1-29.
2198

2199 Clark, P.U., Mitrovica, J.X., Milne, G.A., Tamisiea, M.E., 2002. Sea-level fingerprinting as a direct test
2200 for the source of global meltwater pulse 1A. *Science* 295, 2438-2441.
2201

2202 Cooper, A.K., Barrett, P.J., Hinz, K., Traube, V., Letichenkov, G., Stagg, H.M.J., 1991. Cenozoic
2203 prograding sequences of the Antarctic continental margin: a record of glacio-eustatic and tectonic
2204 events. *Mar Geol* 102, 175-213.
2205

2206 Covault, J.A., Graham, S.A., 2010. Submarine fans at all sea-level stands: Tectono-morphologic and
2207 climatic controls on terrigenous sediment delivery to the deep sea. *Geology* 38, 939-942.
2208

2209 Cuffey, K.M., Paterson, W.S.B., 2010. *The physics of glaciers*. Academic Press.
2210

2211 Curran, K.J., Hill, P.S., Milligan, T.G., Cowan, E.A., Syvitski, J.P.M., Konings, S.M., 2004. Fine-grained
2212 sediment flocculation below the Hubbard Glacier meltwater plume, Disenchantment Bay, Alaska.
2213 *Mar Geol* 203, 83-94.
2214

2215 Dahlgren, K.I.T., Vorren, T.O., 2003. Sedimentary environment and glacial history during the last 40
2216 ka of the Vøring continental margin, mid-Norway. *Mar Geol* 193, 93-127.
2217

2218 Dahlgren, K.I.T., Vorren, T.O., Laberg, J.S., 2002. Late Quaternary glacial development of the mid-
2219 Norwegian margin—65 to 68 N. *Mar Petrol Geol* 19, 1089-1113.
2220

2221 Dahlgren, K.I.T., Vorren, T.O., Stoker, M.S., Nielsen, T., Nygård, A., Sejrup, H.P., 2005. Late Cenozoic
2222 prograding wedges on the NW European continental margin: their formation and relationship to
2223 tectonics and climate. *Mar Petrol Geol* 22, 1089-1110.
2224

2225 Dawson, A., Long, D., Smith, D., 1988. The Storegga slides: evidence from eastern Scotland for a
2226 possible tsunami. *Mar Geol* 82, 271-276.

2227
2228 De Santis, L., Brancolini, G., Donda, F., 2003. Seismo-stratigraphic analysis of the Wilkes Land
2229 continental margin (East Antarctica): influence of glacially driven processes on the Cenozoic
2230 deposition. *Deep Sea Research Part II: Topical Studies in Oceanography* 50, 1563-1594.
2231
2232 Denton, G.H., Hughes, T.J., 2002. Reconstructing the Antarctic Ice Sheet at the Last Glacial
2233 Maximum. *Quaternary Sci Rev* 21, 193-202.
2234
2235 Dokken, T.M., Jansen, E., 1999. Rapid changes in the mechanism of ocean convection during the last
2236 glacial period. *Nature* 401, 458-461.
2237
2238 Donda, F., Brancolini, G., O'Brien, P.E., De Santis, L., Escutia, C., 2007. Sedimentary processes in the
2239 Wilkes Land margin: a record of the Cenozoic East Antarctic Ice Sheet evolution. *Journal of the
2240 Geological Society* 164, 243-256.
2241
2242 Doré, A.G., Corcoran, D.V., Scotchman, I.C., 2002. Prediction of the hydrocarbon system in exhumed
2243 basins, and application to the NW European margin. *Geological Society, London, Special Publications*
2244 196, 401-429.
2245
2246 Doré, A.G., Jensen, L.N., 1996. The impact of late Cenozoic uplift and erosion on hydrocarbon
2247 exploration: offshore Norway and some other uplifted basins. *Global and Planetary Change* 12, 415-
2248 436.
2249
2250 Dowdeswell, E.K., Todd, B.J., Dowdeswell, J.A., 2016a. Canyons and slides on the continental slope
2251 seaward of a shallow bank, Labrador margin, eastern Canada. *Geological Society, London, Memoirs*
2252 46, 405-406.
2253
2254 Dowdeswell, J.A., Canals, M., Jakobsson, M., Todd, B.J., Dowdeswell, E.K., Hogan, K.A., 2016b.
2255 Introduction: an Atlas of Submarine Glacial Landforms. *Geological Society, London, Memoirs* 46, 3-
2256 14.
2257
2258 Dowdeswell, J.A., Dowdeswell, E.K., Todd, B.J., Saint-Ange, F., Piper, D.J.W., 2016c. Channels and
2259 gullies on the continental slope seaward of a cross-shelf trough, Labrador margin, eastern Canada.
2260 *Geological Society, London, Memoirs* 46, 385-386.
2261
2262 Dowdeswell, J.A., Elverhøi, A., 2002. The timing of initiation of fast-flowing ice streams during a
2263 glacial cycle inferred from glacial marine sedimentation. *Mar Geol* 188, 3-14.
2264
2265 Dowdeswell, J.A., Elverhøi, A., Andrews, J.T., Hebbeln, D., 1999. Asynchronous deposition of ice-
2266 rafted layers in the Nordic seas and North Atlantic Ocean. *Nature* 400, 348-351.
2267
2268 Dowdeswell, J.A., Elverhøi, A., Spielhagen, R., 1998. Glacial marine sedimentary processes and facies
2269 on the Polar North Atlantic margins. *Quaternary Sci Rev* 17, 243-272.
2270
2271 Dowdeswell, J.A., Evans, J., Ó Cofaigh, C., 2010a. Submarine landforms and shallow acoustic
2272 stratigraphy of a 400 km-long fjord-shelf-slope transect, Kangerlussuaq margin, East Greenland.
2273 *Quaternary Sci Rev* 29, 3359-3369.
2274
2275 Dowdeswell, J.A., Evans, J., Ó Cofaigh, C., Anderson, J.B., 2006a. Morphology and sedimentary
2276 processes on the continental slope off Pine Island Bay, Amundsen Sea, West Antarctica. *Geological
2277 Society of America Bulletin* 118, 606-619.

2278
2279 Dowdeswell, J.A., Hogan, K.A., Arnold, N.S., Mugford, R.I., Wells, M., Hirst, J.P.P., Decalf, C., 2015.
2280 Sediment-rich meltwater plumes and ice-proximal fans at the margins of modern and ancient
2281 tidewater glaciers: Observations and modelling. *Sedimentology* 62, 1665-1692.
2282
2283 Dowdeswell, J.A., Kenyon, N.H., Elverhøi, A., Laberg, J.S., Hollender, F.J., Mienert, J., Siegert, M.J.,
2284 1996. Large-scale sedimentation on the glacier-influenced polar North Atlantic Margins: Long-range
2285 side-scan sonar evidence. *Geophys Res Lett* 23, 3535-3538.
2286
2287 Dowdeswell, J.A., Kenyon, N.H., Laberg, J.S., 1997. The glacier-influenced Scoresby Sund Fan, East
2288 Greenland continental margin: evidence from GLORIA and 3.5 kHz records. *Mar Geol* 143, 207-221.
2289
2290 Dowdeswell, J.A., Maslin, M.A., Andrews, J.T., McCave, I.N., 1995. Iceberg production, debris rafting,
2291 and the extent and thickness of Heinrich layers (H-1, H-2) in North Atlantic sediments. *Geology* 23,
2292 301-304.
2293
2294 Dowdeswell, J.A., Ó Cofaigh, C., Noormets, R., Larter, R.D., Hillenbrand, C.-D., Benetti, S., Evans, J.,
2295 Pudsey, C.J., 2008. A major trough-mouth fan on the continental margin of the Bellingshausen Sea,
2296 West Antarctica: the Belgica Fan. *Mar Geol* 252, 129-140.
2297
2298 Dowdeswell, J.A., Ó Cofaigh, C., Pudsey, C.J., 2004. Continental slope morphology and sedimentary
2299 processes at the mouth of an Antarctic palaeo-ice stream. *Mar Geol* 204, 203-214.
2300
2301 Dowdeswell, J.A., Ottesen, D., 2013. Buried iceberg ploughmarks in the early Quaternary sediments
2302 of the central North Sea: a two-million year record of glacial influence from 3D seismic data. *Mar*
2303 *Geol* 344, 1-9.
2304
2305 Dowdeswell, J.A., Ottesen, D., Rise, L., 2006b. Flow switching and large-scale deposition by ice
2306 streams draining former ice sheets. *Geology* 34, 313-316.
2307
2308 Dowdeswell, J.A., Ottesen, D., Rise, L., 2010b. Rates of sediment delivery from the Fennoscandian Ice
2309 Sheet through an ice age. *Geology* 38, 3-6.
2310
2311 Dowdeswell, J.A., Siegert, M.J., 1999. Ice-sheet numerical modeling and marine geophysical
2312 measurements of glacier-derived sedimentation on the Eurasian Arctic continental margins.
2313 *Geological Society of America Bulletin* 111, 1080-1097.
2314
2315 Dreger, D., 1999. Decadal to Centennial Scale Sediment Records of Ice Advance on the Barents Shelf
2316 and Meltwater Discharge Into the Northeastern Norwegian Sea Over the Last 40 Kyr: Dekadische Bis
2317 Jahrhundert-Variabilität Von Eisvorstößen Auf Dem Barentsschelf und Schmelzwasserschüben in Die
2318 Nordöstliche Norwegensee Während Der Letzten 40 Ka. *Inst. für Geowiss.*, pp. 1 - 79.
2319
2320 Dugan, B., Flemings, P.B., 2000. Overpressure and fluid flow in the New Jersey continental slope:
2321 implications for slope failure and cold seeps. *Science* 289, 288-291.
2322
2323 Dugan, B., Sheahan, T.C., 2012. Offshore sediment overpressures of passive margins: Mechanisms,
2324 measurement, and models. *Rev Geophys* 50.
2325
2326 Egholm, D.L., Pedersen, V.K., Knudsen, M.F., Larsen, N.K., 2012. Coupling the flow of ice, water, and
2327 sediment in a glacial landscape evolution model. *Geomorphology* 141, 47-66.
2328

2329 Ehlers, J., Gibbard, P.L., 2004. Quaternary Glaciations-Extent and Chronology: Part I: Europe. Elsevier.
2330 Eidvin, T., Brekke, H., Riis, F., Renshaw, D.K., 1998. Cenozoic stratigraphy of the Norwegian Sea
2331 continental shelf, 64 N-68 N. Norsk Geologisk Tidsskrift 78, 125-152.
2332
2333 Eidvin, T., Jansen, E., Rundberg, Y., Brekke, H., Grogan, P., 2000. The upper Cainozoic of the
2334 Norwegian continental shelf correlated with the deep sea record of the Norwegian Sea and the
2335 North Atlantic. Mar Petrol Geol 17, 579-600.
2336
2337 El-Robrini, M., Gennesseaux, M., Mauffret, A., 1985. Consequences of the El-Asnam earthquakes:
2338 Turbidity currents and slumps on the Algerian margin (Western Mediterranean). Geo-Mar Lett 5,
2339 171-176.
2340
2341 Elverhøi, A., Andersen, E.S., Dokken, T., Hebbeln, D., Spielhagen, R., Svendsen, J.I., Sorflaten, M.,
2342 Rornes, A., Hald, M., Forsberg, C.F., 1995. The growth and decay of the late weichselian ice sheet in
2343 western Svalbard and adjacent areas based on provenance studies of marine sediments. Quaternary
2344 Res 44, 303-316.
2345
2346 Elverhøi, A., Hooke, R.L.B., Solheim, A., 1998. Late Cenozoic erosion and sediment yield from the
2347 Svalbard-Barents Sea region: Implications for understanding erosion of glacierized basins.
2348 Quaternary Sci Rev 17, 209-241.
2349
2350 Escutia, C., De Santis, L., Donda, F., Dunbar, R.B., Cooper, A.K., Brancolini, G., Eittrheim, S.L., 2005.
2351 Cenozoic ice sheet history from East Antarctic Wilkes Land continental margin sediments. Global and
2352 Planetary Change 45, 51-81.
2353
2354 Escutia, C., Eittrheim, S.L., Cooper, A.K., Nelson, C.H., 2000. Morphology and acoustic character of the
2355 Antarctic Wilkes Land turbidite systems: ice-sheet-sourced versus river-sourced fans. Journal of
2356 Sedimentary Research 70, 84-93.
2357
2358 Escutia, C., Warnke, D., Acton, G.D., Barcena, A., Burckle, L., Canals, M., Frazee, C.S., 2003. Sediment
2359 distribution and sedimentary processes across the Antarctic Wilkes Land margin during the
2360 Quaternary. Deep Sea Research Part II: Topical Studies in Oceanography 50, 1481-1508.
2361
2362 Evans, J., Ó Cofaigh, C., Dowdeswell, J.A., Wadhams, P., 2009. Marine geophysical evidence for
2363 former expansion and flow of the Greenland Ice Sheet across the north-east Greenland continental
2364 shelf. Journal of Quaternary Science 24, 279-293.
2365
2366 Faleide, J.I., Kyrkjebø, R., Kjennerud, T., Gabrielsen, R.H., Jordt, H., Fanavoll, S., Bjerke, M.D., 2002.
2367 Tectonic impact on sedimentary processes during Cenozoic evolution of the northern North Sea and
2368 surrounding areas. Geological Society, London, Special Publications 196, 235-269.
2369
2370 Faleide, J.I., Solheim, A., Fiedler, A., Hjelstuen, B.O., Andersen, E.S., Vanneste, K., 1996. Late
2371 Cenozoic evolution of the western Barents Sea-Svalbard continental margin. Global and Planetary
2372 Change 12, 53-74.
2373
2374 Felix, M., Peakall, J., McCaffrey, W.D., 2006. Relative importance of processes that govern the
2375 generation of particulate hyperpycnal flows. Journal of Sedimentary Research 76, 382-387.
2376
2377 Fiedler, A., Faleide, J.I., 1996. Cenozoic sedimentation along the southwestern Barents Sea margin in
2378 relation to uplift and erosion of the shelf. Global and Planetary Change 12, 75-93.
2379

2380 Fine, I.V., Rabinovich, A.B., Bornhold, B.D., Thomson, R.E., Kulikov, E.A., 2005. The Grand Banks
2381 landslide-generated tsunami of November 18, 1929: preliminary analysis and numerical modeling.
2382 *Mar Geol* 215, 45-57.
2383
2384 Fjeldskaar, W., Amantov, A., 2017. Effects of glaciations on sedimentary basins. *J Geodyn.*
2385 Fjeldskaar, W., Lindholm, C., Dehls, J.F., Fjeldskaar, I., 2000. Postglacial uplift, neotectonics and
2386 seismicity in Fennoscandia. *Quaternary Sci Rev* 19, 1413-1422.
2387
2388 Flemings, P.B., Long, H., Dugan, B., Germaine, J., John, C.M., Behrmann, J.H., Sawyer, D., Scientists,
2389 I.E., 2008. Erratum to "Pore pressure penetrometers document high overpressure near the seafloor
2390 where multiple submarine landslides have occurred on the continental slope, offshore Louisiana,
2391 Gulf of Mexico" (vol 269, pg 309, 2008). *Earth and Planetary Science Letters* 274, 269-283.
2392
2393 Forsberg, C.F., Solheim, A., Elverhøi, A., Jansen, E., Channell, J.E.T., Andersen, E.S., 1999. 17. The
2394 depositional environment of the Western Svalbard margin during the Late Pliocene and the
2395 Pleistocene: Sedimentary facies changes at Site 986, Proceedings of the Ocean Drilling Program:
2396 Scientific results. The Program, p. 233.
2397
2398 Fronval, T., Jansen, E., 1996. Late Neogene paleoclimates and paleoceanography in the Iceland-
2399 Norwegian Sea: evidence from the Iceland and Vøring Plateaus, Proceedings of the Ocean Drilling
2400 Program. Scientific Results. Ocean Drilling Program, pp. 455-468.
2401
2402 Fronval, T., Jansen, E., 1997. Eemian and early Weichselian (140–60 ka) paleoceanography and
2403 paleoclimate in the Nordic seas with comparisons to Holocene conditions. *Paleoceanography* 12,
2404 443-462.
2405
2406 Fruergaard, M., Piasecki, S., Johannessen, P.N., Noe-Nygaard, N., Andersen, T.J., Pejrup, M., Nielsen,
2407 L.H., 2015. Tsunami propagation over a wide, shallow continental shelf caused by the Storegga slide,
2408 southeastern North Sea, Denmark. *Geology* 43, 1047-1050.
2409
2410 Funder, S., Hansen, L., 1996. The Greenland ice sheet—a model for its culmination and decay during
2411 and after the last glacial maximum. Geological Society of Denmark.
2412
2413 Funder, S., Hjort, C., Landvik, J.Y., 1994. The last glacial cycles in East Greenland, an overview. *Boreas*
2414 23, 283-293.
2415
2416 Funder, S., Hjort, C., Landvik, J.Y., Nam, S.-I., Reeh, N., Stein, R., 1998. History of a stable ice margin—
2417 East Greenland during the middle and upper Pleistocene. *Quaternary Sci Rev* 17, 77-123.
2418
2419 Funder, S., Kjeldsen, K.K., Kjær, K.H., Ó Cofaigh, C., 2011. The Greenland Ice Sheet during the past
2420 300,000 years: A review. *Developments in Quaternary Science* 15, 699-713.
2421
2422 Gales, J.A., Forwick, M., Laberg, J.S., Vorren, T.O., Larter, R.D., Graham, A.G.C., Baeten, N.J.,
2423 Amundsen, H.B., 2013. Arctic and Antarctic submarine gullies—A comparison of high latitude
2424 continental margins. *Geomorphology* 201, 449-461.
2425
2426 Gales, J.A., Larter, R.D., Leat, P.T., Jokat, W., 2016. Components of an Antarctic trough-mouth fan:
2427 examples from the Crary Fan, Weddell Sea. Geological Society, London, *Memoirs* 46, 377-378.
2428

2429 Gales, J.A., Leat, P.T., Larter, R.D., Kuhn, G., Hillenbrand, C.-D., Graham, A.G.C., Mitchell, N.C., Tate,
2430 A.J., Buys, G.B., Jokat, W., 2014. Large-scale submarine landslides, channel and gully systems on the
2431 southern Weddell Sea margin, Antarctica. *Mar Geol* 348, 73-87.
2432
2433 García, M., Ercilla, G., Alonso, B., 2009. Morphology and sedimentary systems in the Central
2434 Bransfield Basin, Antarctic Peninsula: sedimentary dynamics from shelf to basin. *Basin Research* 21,
2435 295-314.
2436
2437 García, M., Ercilla, G., Alonso, B., Casas, D., Dowdeswell, J.A., 2011. Sediment lithofacies, processes
2438 and sedimentary models in the Central Bransfield Basin, Antarctic Peninsula, since the Last Glacial
2439 Maximum. *Mar Geol* 290, 1-16.
2440
2441 García, M., Ercilla, G., Anderson, J.B., Alonso, B., 2008. New insights on the post-rift seismic
2442 stratigraphic architecture and sedimentary evolution of the Antarctic Peninsula margin (Central
2443 Bransfield Basin). *Mar Geol* 251, 167-182.
2444
2445 Gard, G., Backman, J., 1990. Synthesis of Arctic and Sub-Arctic Coccolith Biochronology and History
2446 of North Atlantic Drift Water Influx during the Last 500.000 Years, in: Bleil, U., Thiede, J. (Eds.),
2447 Geological History of the Polar Oceans: Arctic versus Antarctic. Springer Netherlands, Dordrecht, pp.
2448 417-436.
2449
2450 Gavey, R., Carter, L., Liu, J.T., Talling, P.J., Hsu, R.T., Pope, E.L., Evans, G., 2017. Frequent sediment
2451 density flows during 2006 to 2015, triggered by competing seismic and weather events:
2452 Observations from subsea cable breaks off southern Taiwan. *Mar Geol* 384, 147-158.
2453
2454 Geist, E.L., 2000. Origin of the 17 July 1998 Papua New Guinea tsunami: earthquake or landslide.
2455 *Seismological Research Letters* 71, 344-351.
2456
2457 Goldfinger, C., 2011. Submarine Paleoseismology Based on Turbidite Records. *Annu Rev Mar Sci* 3,
2458 35-66.
2459
2460 Goldfinger, C., Nelson, C.H., Morey, A.E., Johnson, J.E., Patton, J.R., Karabanov, E., Gutierrez-Pastor,
2461 J., Eriksson, A.T., Gracia, E., Dunhill, G., 2012. Turbidite event history: Methods and implications for
2462 Holocene paleoseismicity of the Cascadia subduction zone. US Department of the Interior, US
2463 Geological Survey.
2464
2465 Gozhik, P., Lindner, L., Marks, L., 2012. Late Early and early Middle Pleistocene limits of Scandinavian
2466 glaciations in Poland and Ukraine. *Quatern Int* 271, 31-37.
2467
2468 Graham, A.G.C., Larter, R.D., Gohl, K., Hillenbrand, C.-D., Smith, J.A., Kuhn, G., 2009. Bedform
2469 signature of a West Antarctic palaeo-ice stream reveals a multi-temporal record of flow and
2470 substrate control. *Quaternary Sci Rev* 28, 2774-2793.
2471
2472 Grauert, M., BJÖRCK, S., Bondevik, S., 2001. Storegga tsunami deposits in a coastal lake on Suouroy,
2473 the Faroe Islands. *Boreas* 30, 263-271.
2474
2475 Gravdal, A., Hafliðason, H., Evans, D., 2003. Seabed and subsurface features on the southern Vøring
2476 Plateau and northern Storegga slide escarpment, in: Mienert, J., Weaver, P.E. (Eds.), *European*
2477 *Margin Sediment Dynamics: Side-Scan Sonar and Seismic Images*. Springer, Berlin, pp. 111-117.
2478

2479 Greenwood, S.L., Clark, C.D., 2009. Reconstructing the last Irish Ice Sheet 1: changing flow
2480 geometries and ice flow dynamics deciphered from the glacial landform record. *Quaternary Sci Rev*
2481 28, 3085-3100.

2482

2483 Greenwood, S.L., Clason, C.C., Jakobsson, M., 2016. Ice-flow and meltwater landform assemblages in
2484 the Gulf of Bothnia, in: Dowdeswell, J.A., Canals, M., Jakobsson, M., Todd, B.J., Dowdeswell, E.K.,
2485 Hogan, K.A. (Eds.), *Geological Society, London, Memoirs. Geological Society, London*, pp. 321-324.

2486

2487 Gulick, S.P.S., Jaeger, J.M., Mix, A.C., Asahi, H., Bahlburg, H., Belanger, C.L., Berbel, G.B.B., Childress,
2488 L., Cowan, E., Drab, L., Forwick, M., Fukumura, A., Ge, S., Gupta, S., Kioka, A., Konno, S., LeVay, L.J.,
2489 März, C., Matsuzaki, K.M., McClymont, E.L., Moy, C., Müller, J., Nakamura, A., Ojima, T., Ribeiro, F.R.,
2490 Ridgway, K.D., Romero, O.E., Slagle, A.L., Stoner, J.S., St-Onge, G., Suto, I., Walczak, M.D.,
2491 Worthington, L.L., Bailey, I., Enkelmann, E., Reece, R., Swartz, J.M., 2015. Mid-Pleistocene climate
2492 transition drives net mass loss from rapidly uplifting St. Elias Mountains, Alaska. *Proceedings of the*
2493 *National Academy of Sciences* 112, 15042-15047.

2494

2495 Hafliðason, H., Aarseth, I., Haugen, J.-E., Sejrup, H.P., Løvlie, R., Reither, E., 1991. Quaternary
2496 stratigraphy of the Draugen area, mid-Norwegian shelf. *Mar Geol* 101, 125-146.

2497

2498 Hafliðason, H., Iversen, M., Løvlie, R., 1998. Møre and Vøring Basin Geological Investigation:
2499 lithological and chronological analyses of the geotechnical borings. Unpublished Report, Department
2500 of Geology, University of Bergen, Norway, 50pp.

2501

2502 Hafliðason, H., Lien, R., Sejrup, H.P., Forsberg, C.F., Bryn, P., 2005. The dating and morphometry of
2503 the Storegga Slide. *Mar Petrol Geol* 22, 123-136.

2504

2505 Hafliðason, H., Sejrup, H.P., Berstad, I.M., Nygård, A., Richter, T.O., Bryn, P., Lien, R., Berg, K., 2003. A
2506 weak layer feature on the Northern Storegga Slide escarpment, European Margin Sediment
2507 Dynamics. Springer, pp. 55-62.

2508

2509 Hafliðason, H., Sejrup, H.P., Nygard, A., Mienert, J., Bryn, P., Lien, R., Forsberg, C.F., Berg, K., Masson,
2510 D., 2004. The Storegga Slide: architecture, geometry and slide development. *Mar Geol* 213, 201-234.

2511

2512 Håkansson, L., Alexanderson, H., Hjort, C., Möller, P., Briner, J.P., Aldahan, A., Possnert, G., 2009.
2513 Late Pleistocene glacial history of Jameson Land, central East Greenland, derived from cosmogenic
2514 ^{10}Be and ^{26}Al exposure dating. *Boreas* 38, 244-260.

2515

2516 Håkansson, L., Briner, J., Alexanderson, H., Aldahan, A., Possnert, G., 2007. ^{10}Be ages from central
2517 east Greenland constrain the extent of the Greenland ice sheet during the Last Glacial Maximum.
2518 *Quaternary Sci Rev* 26, 2316-2321.

2519

2520 Hallam, A., 1989. *Great geological controversies*. Oxford University Press.

2521

2522 Hallet, B., Hunter, L., Bogen, J., 1996. Rates of erosion and sediment evacuation by glaciers: A review
2523 of field data and their implications. *Global and Planetary Change* 12, 213-235.

2524

2525 Hansen, L., Funder, S., Murray, A.S., Mejdahl, V., 1999. Luminescence dating of the last Weichselian
2526 glacier advance in East Greenland. *Quaternary Sci Rev* 18, 179-190.

2527

2528 Harbitz, C.B., Løvholt, F., Bungum, H., 2014. Submarine landslide tsunamis: how extreme and how
2529 likely? *Nat Hazards* 72, 1341-1374.

2530
2531 Harbitz, C.B., Løvholt, F., Pedersen, G., Masson, D.G., 2006. Mechanisms of tsunami generation by
2532 submarine landslides: a short review. *Norsk Geologisk Tidsskrift* 86, 255.
2533
2534 Hart, J.K., Rose, K.C., Martinez, K., 2011. Subglacial till behaviour derived from in situ wireless multi-
2535 sensor subglacial probes: Rheology, hydro-mechanical interactions and till formation. *Quaternary Sci*
2536 *Rev* 30, 234-247.
2537
2538 Heezen, B.C., Ewing, M., 1955. Orleansville earthquake and turbidity currents. *AAPG Bulletin* 39,
2539 2505-2514.
2540
2541 Heezen, B.C., Ewing, W.M., 1952. Turbidity currents and submarine slumps, and the 1929 Grand
2542 Banks [Newfoundland] earthquake. *American Journal of Science* 250, 849-873.
2543
2544 Heezen, B.C., Menzies, R.J., Schneider, E.D., Ewing, W.M., Granelli, N.C.L., 1964. Congo submarine
2545 canyon. *AAPG Bulletin* 48, 1126-1149.
2546
2547 Helmke, J.P., Bauch, H.A., 2003. Comparison of glacial and interglacial conditions between the polar
2548 and subpolar North Atlantic region over the last five climatic cycles. *Paleoceanography* 18.
2549
2550 Helmke, J.P., Bauch, H.A., Erlenkeuser, H., 2003a. Development of glacial and interglacial conditions
2551 in the Nordic seas between 1.5 and 0.35 Ma. *Quaternary Sci Rev* 22, 1717-1728.
2552
2553 Helmke, J.P., Bauch, H.A., Mazaud, A., 2003b. Evidence for a mid-Pleistocene shift of ice-drift pattern
2554 in the Nordic seas. *Journal of Quaternary Science* 18, 183-191.
2555
2556 Helmke, J.P., Bauch, H.A., Röhl, U., Mazaud, A., 2005. Changes in sedimentation patterns of the
2557 Nordic seas region across the mid-Pleistocene. *Mar Geol* 215, 107-122.
2558
2559 Henrich, R., 1989. Glacial/interglacial cycles in the Norwegian Sea: sedimentology,
2560 paleoceanography, and evolution of Late Pliocene to Quaternary northern hemisphere climate,
2561 *Proceedings of the Ocean Drilling Program, scientific results*, pp. 189-232.
2562
2563 Henrich, R., Baumann, K.-H., 1994. Evolution of the Norwegian Current and the Scandinavian Ice
2564 Sheets during the past 2.6 my: evidence from ODP Leg 104 biogenic carbonate and terrigenous
2565 records. *Palaeogeography, Palaeoclimatology, Palaeoecology* 108, 75-94.
2566
2567 Henriksen, S., Fichler, C., Grønlie, A., Henningsen, T., Laursen, I., Løseth, H., Ottesen, D., Prince, I.,
2568 2005. The Norwegian Sea during the Cenozoic, in: Wandås, B.T.G., Nystuen, J.P., Eide, E., Gradstein,
2569 F. (Eds.), *Norwegian Petroleum Society Special Publications*. Elsevier, pp. 111-133.
2570
2571 Henriksen, S., Vorren, T.O., 1996. Late Cenozoic sedimentation and uplift history on the mid-
2572 Norwegian continental shelf. *Global and Planetary Change* 12, 171-199.
2573
2574 Herman, F., Beaud, F., Champagnac, J.-D., Lemieux, J.-M., Sternai, P., 2011. Glacial hydrology and
2575 erosion patterns: a mechanism for carving glacial valleys. *Earth and Planetary Science Letters* 310,
2576 498-508.
2577
2578 Heroy, D.C., Anderson, J.B., 2005. Ice-sheet extent of the Antarctic Peninsula region during the Last
2579 Glacial Maximum (LGM)—Insights from glacial geomorphology. *Geological Society of America*
2580 *Bulletin* 117, 1497-1512.

2581
2582 Hesse, R., Klauck, I., Khodabakhsh, S., Piper, D., 1999. Continental slope sedimentation adjacent to
2583 an ice margin. III. The upper Labrador Slope. *Mar Geol* 155, 249-276.
2584
2585 Hesse, R., Klaucke, I., Khodabakhsh, S., Piper, D.J.W., Ryan, W.B.F., Group, N.S., 2001. Sandy
2586 submarine braid plains: potential deep-water reservoirs. *AAPG bulletin* 85, 1499-1521.
2587
2588 Hesse, R., Klaucke, I., Khodabakhsh, S., Ryan, W.B.F., 1997. Glacimarine Drainage Systems in Deep-
2589 sea: The NAMOC System of the Labrador Sea and its Sibling, in: Davies, T.A., al., e. (Eds.), *Glaciated*
2590 *Continental Margins*. Springer, pp. 286-289.
2591
2592 Hesse, R., Rashid, H., Khodabakhsh, S., 2004. Fine-grained sediment lofting from meltwater-
2593 generated turbidity currents during Heinrich events. *Geology* 32, 449-452.
2594
2595 Hibbert, F.D., Austin, W.E.N., Leng, M.J., Gatliff, R.W., 2010. British Ice Sheet dynamics inferred from
2596 North Atlantic ice-rafted debris records spanning the last 175 000 years. *Journal of Quaternary*
2597 *Science* 25, 461-482.
2598
2599 Hillenbrand, C.-D., Camerlenghi, A., Cowan, E.A., Hernández-Molina, F.J., Lucchi, R.G., Rebesco, M.,
2600 Uenzelmann-Neben, G., 2008. The present and past bottom-current flow regime around the
2601 sediment drifts on the continental rise west of the Antarctic Peninsula. *Mar Geol* 255, 55-63.
2602
2603 Hillenbrand, C.-D., Larter, R.D., Dowdeswell, J.A., Ehrmann, W., Ó Cofaigh, C., Benetti, S., Graham,
2604 A.G.C., Grobe, H., 2010. The sedimentary legacy of a palaeo-ice stream on the shelf of the southern
2605 Bellingshausen Sea: Clues to West Antarctic glacial history during the Late Quaternary. *Quaternary*
2606 *Sci Rev* 29, 2741-2763.
2607
2608 Hjelstuen, B.O., Andreassen, E.V., 2015. North Atlantic Ocean deep-water processes and
2609 depositional environments: A study of the Cenozoic Norway Basin. *Mar Petrol Geol* 59, 429-441.
2610
2611 Hjelstuen, B.O., Eldholm, O., Faleide, J.I., 2007. Recurrent Pleistocene mega-failures on the SW
2612 Barents Sea margin. *Earth and Planetary Science Letters* 258, 605-618.
2613
2614 Hjelstuen, B.O., Elverhøi, A., Faleide, J.I., 1996. Cenozoic erosion and sediment yield in the drainage
2615 area of the Storfjorden Fan. *Global and Planetary Change* 12, 95-117.
2616
2617 Hjelstuen, B.O., Sejrup, H.P., Hafliðason, H., Nygård, A., Berstad, I.M., Knorr, G., 2004. Late
2618 Quaternary seismic stratigraphy and geological development of the south Vøring margin, Norwegian
2619 Sea. *Quaternary Sci Rev* 23, 1847-1865.
2620
2621 Hjelstuen, B.O., Sejrup, H.P., Hafliðason, H., Nygard, A., Ceramicola, S., Bryn, P., 2005. Late Cenozoic
2622 glacial history and evolution of the Storegga Slide area and adjacent slide flank regions, Norwegian
2623 continental margin. *Mar Petrol Geol* 22, 57-69.
2624
2625 Hogan, K.A., Dowdeswell, J.A., Mienert, J., 2013. New insights into slide processes and seafloor
2626 geology revealed by side-scan imagery of the massive Hinlopen Slide, Arctic Ocean margin. *Geo-Mar*
2627 *Lett* 33, 325-343.
2628
2629 Hogan, K.A., Ó Cofaigh, C., Jennings, A.E., Dowdeswell, J.A., Hiemstra, J.F., 2016. Deglaciation of a
2630 major palaeo-ice stream in Disko Trough, West Greenland. *Quaternary Sci Rev* 147, 5-26.
2631

2632 Hornbach, M.J., Lavier, L.L., Ruppel, C.D., 2007. Triggering mechanism and tsunamogenic potential of
2633 the Cape Fear Slide complex, US Atlantic margin. *Geochemistry, Geophysics, Geosystems* 8.
2634
2635 Houmark-Nielsen, M., Demidov, I., Funder, S., Grøsfjeld, K., Kjær, K.H., Larsen, E., Lavrova, N., Lyså,
2636 A., Nielsen, J.K., 2001. Early and Middle Valdaian glaciations, ice-dammed lakes and periglacial
2637 interstadials in northwest Russia: new evidence from the Pyoza River area. *Global and Planetary*
2638 *Change* 31, 215-237.
2639
2640 Hovland, M., Svensen, H., Forsberg, C.F., Johansen, H., Fichler, C., Fosså, J.H., Jonsson, R., Rueslåtten,
2641 H., 2005. Complex pockmarks with carbonate-ridges off mid-Norway: products of sediment
2642 degassing. *Mar Geol* 218, 191-206.
2643
2644 Hsu, S.K., Kuo, J., Lo, C.L., Tsai, C.H., Doo, W.B., Ku, C.Y., Sibuet, J.C., 2008. Turbidity Currents,
2645 Submarine Landslides and the 2006 Pingtung Earthquake off SW Taiwan. *Terr Atmos Ocean Sci* 19,
2646 767-772.
2647
2648 Hughes, A.L.C., Gyllencreutz, R., Lohne, Ø.S., Mangerud, J., Svendsen, J.I., 2016. The last Eurasian ice
2649 sheets—a chronological database and time-slice reconstruction, DATED-1. *Boreas* 45, 1-45.
2650
2651 Hughes Clarke, J.E., O'Leary, D., Piper, D.J.W., 1992. The relative importance of mass wasting and
2652 deep boundary current activity on the continental rise off western Nova Scotia, in: W., P.C., de
2653 Graniansky, P.C. (Eds.), *Geologic evolution of Atlantic continental rises*. Edited by CW Poag and PC de
2654 Graciansky. van Nostrand Reinhold, New York. van Nostrand Reinhold, New York, pp. 266-281.
2655
2656 Hughes Clarke, J.E., Shor, A.N., Piper, D.J.W., Mayer, L.A., 1990. Large-scale current-induced erosion
2657 and deposition in the path of the 1929 Grand Banks turbidity current. *Sedimentology* 37, 613-629.
2658
2659 Hunt, J.E., Wynn, R.B., Masson, D.G., Talling, P.J., Teagle, D.A.H., 2011. Sedimentological and
2660 geochemical evidence for multistage failure of volcanic island landslides: A case study from Icod
2661 landslide on north Tenerife, Canary Islands. *Geochemistry, Geophysics, Geosystems* 12, n/a-n/a.
2662
2663 Hunt, J.E., Wynn, R.B., Talling, P.J., Masson, D.G., 2013. Multistage collapse of eight western Canary
2664 Island landslides in the last 1.5 Ma: Sedimentological and geochemical evidence from subunits in
2665 submarine flow deposits. *Geochemistry, Geophysics, Geosystems* 14, 2159-2181.
2666
2667 Huppertz, T.J., Piper, D.J.W., 2009. The influence of shelf-crossing glaciation on continental slope
2668 sedimentation, Flemish Pass, eastern Canadian continental margin. *Mar Geol* 265, 67-85.
2669
2670 Ikehara, K., 2012. Offshore earthquake-and/or tsunami-induced sediment transports and their
2671 deposits: Importance of marine sediment study for understanding past earthquakes and tsunami.
2672 *Journal of the Sedimentological Society of Japan* 71, 141-147.
2673
2674 Imbo, Y., De Batist, M., Canals, M., Prieto, M.J., Baraza, J., 2003. The Gebra slide: a submarine slide
2675 on the Trinity Peninsula Margin, Antarctica. *Mar Geol* 193, 235-252.
2676
2677 Ingólfsson, Ó., Landvik, J.Y., 2013. The Svalbard–Barents Sea ice-sheet—Historical, current and future
2678 perspectives. *Quaternary Sci Rev* 64, 33-60.
2679 Ingólfsson, Ó., Lyså, A., Funder, S., Møller, P., Björck, S., 1994. Late Quaternary glacial history of the
2680 central west coast of Jameson Land, East Greenland. *Boreas* 23, 447-458.
2681

2682 Ivanov, V.V., Shapiro, G.I., Huthnance, J.M., Aleynik, D.L., Golovin, P.N., 2004. Cascades of dense
2683 water around the world ocean. *Progress in Oceanography* 60, 47-98.
2684
2685 Jakobsson, M., Andreassen, K., Bjarnadóttir, L.R., Dove, D., Dowdeswell, J.A., England, J.H., Funder,
2686 S., Hogan, K.A., Ingólfsson, Ó., Jennings, A., 2014. Arctic Ocean glacial history. *Quaternary Sci Rev* 92,
2687 40-67.
2688
2689 Jansen, E., Bleil, U., Henrich, R., Kringstad, L., Slettemark, B., 1988. Paleoenvironmental changes in
2690 the Norwegian Sea and the northeast Atlantic during the last 2.8 my: Deep Sea Drilling
2691 Project/Ocean Drilling Program sites 610, 642, 643 and 644. *Paleoceanography* 3, 563-581.
2692
2693 Jansen, E., et al., 1996. 8. Site 985, Proc. Ocean Drill. Program Initial Rep, pp. 253-283.
2694
2695 Jansen, E., Fronval, T., Rack, F., Channell, J.E.T., 2000. Pliocene-Pleistocene ice rafting history and
2696 cyclicity in the Nordic Seas during the last 3.5 Myr. *Paleoceanography* 15, 709-721.
2697
2698 Jansen, E., Raymo, M.E., 1996. 1. Leg 162: New Frontiers on Past Climates, in: Jansen, E., Raymo,
2699 M.E., Blum, P., et al. (Eds.), *Proceedings Ocean Drilling Program Initial Reports*, vol. 162.
2700
2701 Jansen, E., Sjøholm, J., 1991. Reconstruction of glaciation over the past 6 Myr from ice-borne
2702 deposits in the Norwegian Sea. *Nature* 349, 600-603.
2703
2704 Jenner, K.A., Piper, D.J.W., Campbell, D.C., Mosher, D.C., 2007. Lithofacies and origin of late
2705 Quaternary mass transport deposits in submarine canyons, central Scotian Slope, Canada.
2706 *Sedimentology* 54, 19-38.
2707
2708 Jennings, A.E., Grönvold, K., Hilberman, R., Smith, M., Hald, M., 2002. High-resolution study of
2709 Icelandic tephras in the Kangerlussuaq Trough, southeast Greenland, during the last deglaciation.
2710 *Journal of Quaternary Science* 17, 747-757.
2711
2712 Jennings, A.E., Hald, M., Smith, M., Andrews, J.T., 2006. Freshwater forcing from the Greenland Ice
2713 Sheet during the Younger Dryas: evidence from southeastern Greenland shelf cores. *Quaternary Sci*
2714 *Rev* 25, 282-298.
2715
2716 Jessen, S.P., Rasmussen, T.L., Nielsen, T., Solheim, A., 2010. A new Late Weichselian and Holocene
2717 marine chronology for the western Svalbard slope 30,000–0 cal years BP. *Quaternary Sci Rev* 29,
2718 1301-1312.
2719
2720 Kandiano, E.S., Bauch, H.A., 2003. Surface ocean temperatures in the north-east Atlantic during the
2721 last 500 000 years: evidence from foraminiferal census data. *Terra Nova* 15, 265-271.
2722
2723 Kandiano, E.S., Bauch, H.A., 2007. Phase relationship and surface water mass change in the
2724 Northeast Atlantic during Marine Isotope Stage 11 (MIS 11). *Quaternary Res* 68, 445-455.
2725
2726 Kayen, R.E., Lee, H.J., 1991. Pleistocene slope instability of gas hydrate-laden sediment on the
2727 Beaufort sea margin. *Marine Georesources & Geotechnology* 10, 125-141.
2728
2729 Kennett, J.P., Cannariato, K.G., Hendy, I.L., Behl, R.J., 2003. Methane hydrates in Quaternary climate
2730 change: The clathrate gun hypothesis. *American Geophysical Union*.
2731

2732 King, E.L., Hafliðason, H., Sejrup, H.P., Løvlie, R., 1998. Glacigenic debris flows on the North Sea
2733 Trough Mouth Fan during ice stream maxima. *Mar Geol* 152, 217-246.
2734
2735 King, E.L., Sejrup, H.P., Hafliðason, H., Elverhøi, A., Aarseth, I., 1996. Quaternary seismic stratigraphy
2736 of the North Sea Fan: glacially-fed gravity flow aprons, hemipelagic sediments, and large submarine
2737 slides. *Mar Geol* 130, 293-315.
2738
2739 Kjemperud, A.T., Fjeldskaar, W., 1992. Pleistocene glacial isostasy—implications for petroleum
2740 geology. Tectonic modelling and its application to petroleum geology. Norwegian Petroleum Society
2741 Spec Publ 1, 187-195.
2742
2743 Kleiven, H.F., Jansen, E., Fronval, T., Smith, T.M., 2002. Intensification of Northern Hemisphere
2744 glaciations in the circum Atlantic region (3.5–2.4 Ma)—ice-rafted detritus evidence. *Palaeogeography,*
2745 *Palaeoclimatology, Palaeoecology* 184, 213-223.
2746
2747 Kleman, J., Hättestrand, C., Borgström, I., Stroeven, A., 1997. Fennoscandian palaeoglaciology
2748 reconstructed using a glacial geological inversion model. *J Glaciol* 43, 283-299.
2749
2750 Knies, J., Kleiber, H.-P., Matthiessen, J., Müller, C., Nowaczyk, N., 2001. Marine ice-rafted debris
2751 records constrain maximum extent of Saalian and Weichselian ice-sheets along the northern
2752 Eurasian margin. *Global and Planetary Change* 31, 45-64.
2753
2754 Knies, J., Matthiessen, J., Mackensen, A., Stein, R., Vogt, C., Frederichs, T., Nam, S.-I., 2007. Effects of
2755 Arctic freshwater forcing on thermohaline circulation during the Pleistocene. *Geology* 35, 1075-
2756 1078.
2757
2758 Knies, J., Matthiessen, J., Vogt, C., Laberg, J.S., Hjelstuen, B.O., Smelror, M., Larsen, E., Andreassen,
2759 K., Eidvin, T., Vorren, T.O., 2009. The Plio-Pleistocene glaciation of the Barents Sea–Svalbard region:
2760 a new model based on revised chronostratigraphy. *Quaternary Sci Rev* 28, 812-829.
2761
2762 Knies, J., Nowaczyk, N., Müller, C., Vogt, C., Stein, R., 2000. A multiproxy approach to reconstruct the
2763 environmental changes along the Eurasian continental margin over the last 150 000 years. *Mar Geol*
2764 163, 317-344.
2765
2766 Knies, J., Vogt, C., Stein, R., 1998. Late Quaternary growth and decay of the Svalbard/Barents Sea ice
2767 sheet and paleoceanographic evolution in the adjacent Arctic Ocean. *Geo-Mar Lett* 18, 195-202.
2768
2769 Koppes, M., Hallet, B., Rignot, E., Mougnot, J., Wellner, J.S., Boldt, K., 2015. Observed latitudinal
2770 variations in erosion as a function of glacier dynamics. *Nature* 526, 100-103.
2771
2772 Krissek, L.A., 1989. Late Cenozoic records of ice-rafting at ODP Sites 642, 643, and 644, Norwegian
2773 Sea: onset, chronology, and characteristics of glacial/interglacial fluctuations, Proceedings of the
2774 Ocean Drilling Project. Scientific Results. Texas A&M University College Station, TX, pp. 61-69.
2775
2776 Kristoffersen, Y., Coakley, B., Jokat, W., Edwards, M., Brekke, H., Gjengedal, J., 2004. Seabed erosion
2777 on the Lomonosov Ridge, central Arctic Ocean: A tale of deep draft icebergs in the Eurasia Basin and
2778 the influence of Atlantic water inflow on iceberg motion? *Paleoceanography* 19, n/a-n/a.
2779
2780 Kuvaas, B., Kristoffersen, Y., 1991. The Crary Fan: a trough-mouth fan on the Weddell Sea
2781 continental margin, Antarctica. *Mar Geol* 97, 345-362.
2782

2783 Kuvaas, B., Kristoffersen, Y., 1996. Mass movements in glaciomarine sediments on the Barents Sea
2784 continental slope. *Global and Planetary Change* 12, 287-307.
2785
2786 Kuvaas, B., Kristoffersen, Y., Guseva, J., Leitchenkov, G., Gandjukhin, V., Løvås, O., Sand, M., Brekke,
2787 H., 2005. Interplay of turbidite and contourite deposition along the Cosmonaut Sea/Enderby Land
2788 margin, East Antarctica. *Mar Geol* 217, 143-159.
2789
2790 Kuvaas, B., Leitchenkov, G., 1992. Glaciomarine turbidite and current controlled deposits in Prydz
2791 Bay, Antarctica. *Mar Geol* 108, 365-381.
2792
2793 Kvalstad, T.J., Andresen, L., Forsberg, C.F., Berg, K., Bryn, P., Wangen, M., 2005. The Storegga slide:
2794 evaluation of triggering sources and slide mechanics. *Mar Petrol Geol* 22, 245-256.
2795
2796 L'Heureux, J.S., Vanneste, M., Rise, L., Brendryen, J., Forsberg, C.F., Nadim, F., Longva, O., Chand, S.,
2797 Kvalstad, T.J., Hafliðason, H., 2013. Stability, mobility and failure mechanism for landslides at the
2798 upper continental slope off Vesterålen, Norway. *Mar Geol* 346, 192-207.
2799
2800 Laberg, J.S., Andreassen, K., Knies, J., Vorren, T.O., Winsborrow, M., 2010. Late Pliocene–Pleistocene
2801 development of the Barents Sea ice sheet. *Geology* 38, 107-110.
2802
2803 Laberg, J.S., Dowdeswell, J.A., 2016. Glacigenic debris-flows on the Bear Island Trough-Mouth Fan,
2804 Barents Sea margin, in: Dowdeswell, J.A., Canals, M., Jakobsson, M., Todd, B.J., Dowdeswell, E.K.,
2805 Hogan, K.A. (Eds.), *Atlas of Submarine Glacial Landforms: Modern, Quaternary and Ancient*.
2806 Geological Society, Geological Society, London, *Memoirs*, v. 46.
2807
2808 Laberg, J.S., Forwick, M., Husum, K., Nielsen, T., 2013. A re-evaluation of the Pleistocene behavior of
2809 the Scoresby Sund sector of the Greenland Ice Sheet. *Geology* 41, 1231-1234.
2810
2811 Laberg, J.S., Vorren, T.O., 1995. Late Weichselian submarine debris flow deposits on the Bear Island
2812 Trough mouth fan. *Mar Geol* 127, 45-72.
2813
2814 Laberg, J.S., Vorren, T.O., 1996. The Middle and Late Pleistocene evolution and the Bear Island
2815 Trough Mouth Fan. *Global and Planetary Change* 12, 309-330.
2816
2817 Laberg, J.S., Vorren, T.O., 2000. The Trænadjupet Slide, offshore Norway—morphology, evacuation
2818 and triggering mechanisms. *Mar Geol* 171, 95-114.
2819
2820 Laberg, J.S., Vorren, T.O., Dowdeswell, J.A., Kenyon, N.H., Taylor, J., 2000. The Andoya Slide and the
2821 Andoya Canyon, north-eastern Norwegian-Greenland Sea. *Mar Geol* 162, 259-275.
2822
2823 Laberg, J.S., Vorren, T.O., Mienert, J., Bryn, P., Lien, R., 2002a. The Trænadjupet Slide: a large slope
2824 failure affecting the continental margin of Norway 4,000 years ago. *Geo-Mar Lett* 22, 19-24.
2825
2826 Laberg, J.S., Vorren, T.O., Mienert, J., Evans, D., Lindberg, B., Ottesen, D., Kenyon, N.H., Henriksen, S.,
2827 2002b. Late Quaternary palaeoenvironment and chronology in the Trænadjupet Slide area offshore
2828 Norway. *Mar Geol* 188, 35-60.
2829
2830 Laberg, J.S., Vorren, T.O., Mienert, J., Hafliðason, H., Bryn, P., Lien, R., 2003. Preconditions Leading to
2831 the Holocene Trænadjupet Slide Offshore Norway, in: Locat, J., Mienert, J., Boisvert, L. (Eds.), *Adv*
2832 *Nat Tech Haz Res*. Springer Netherlands, pp. 247-254.
2833

2834 Lambeck, K., Purcell, A., Zhao, J., Svensson, N.O., 2010. The Scandinavian ice sheet: from MIS 4 to the
2835 end of the Last Glacial Maximum. *Boreas* 39, 410-435.
2836
2837 Landvik, J.Y., 1994. The last glaciation of Germania Land and adjacent areas, northeast Greenland.
2838 *Journal of Quaternary Science* 9, 81-92.
2839
2840 Landvik, J.Y., Bolstad, M., Lycke, A.K., Mangerud, J., Sejrup, H.P., 1992. Weichselian stratigraphy and
2841 palaeoenvironments at Bellsund, western Svalbard. *Boreas* 21, 335-358.
2842
2843 Landvik, J.Y., Ingolfsson, O., Mienert, J., Lehman, S.J., Solheim, A., Elverhøi, A., Ottesen, D., 2005.
2844 Rethinking Late Weichselian ice-sheet dynamics in coastal NW Svalbard. *Boreas* 34, 7-24.
2845
2846 Landvik, J.Y., Lyså, A., Funder, S., Kelly, M., 1994. The Eemian and Weichselian stratigraphy of the
2847 Langelandselv area, Jameson Land, East Greenland. *Boreas* 23, 412-423.
2848
2849 Larsen, H., Saunders, A., Clift, P., Beget, J., Wei, W., Spezzaferri, S., Party, a.O.L.S., 1994. Seven
2850 million years of glaciation in Greenland. *Science* 264, 952 - 955.
2851
2852 Larsen, H.C., 1990. The East Greenland shelf. *The Geology of North America* 50, 185-210.
2853
2854 Larsen, N.K., Knudsen, K.L., Krohn, C.F., Kronborg, C., Murray, A.S., Nielsen, O.B., 2009. Late
2855 Quaternary ice sheet, lake and sea history of southwest Scandinavia—a synthesis. *Boreas* 38, 732-
2856 761.
2857
2858 Lebreiro, S.M., Voelker, A.H.L., Vizcaino, A., Abrantes, F.G., Alt-Epping, U., Jung, S., Thouveny, N.,
2859 Gracia, E., 2009. Sediment instability on the Portuguese continental margin under abrupt glacial
2860 climate changes (last 60 kyr). *Quaternary Sci Rev* 28, 3211-3223.
2861
2862 Lee, H.J., 2009. Timing of occurrence of large submarine landslides on the Atlantic Ocean margin.
2863 *Mar Geol* 264, 53-64.
2864
2865 Lee, H.J., Chough, S.K., Yoon, S.H., 1996. Slope-stability change from late pleistocene to holocene in
2866 the Ulleung Basin, East Sea (Japan Sea). *Sediment Geol* 104, 39-51.
2867
2868 Lee, J.R., Busschers, F.S., Sejrup, H.P., 2012. Pre-Weichselian Quaternary glaciations of the British
2869 Isles, The Netherlands, Norway and adjacent marine areas south of 68 N: implications for long-term
2870 ice sheet development in northern Europe. *Quaternary Sci Rev* 44, 213-228.
2871
2872 Lekens, W.A.H., Hafliðason, H., Sejrup, H.P., Nygård, A., Richter, T., Vogt, C., Frederichs, T., 2009.
2873 Sedimentation history of the northern North Sea Margin during the last 150 ka. *Quaternary Sci Rev*
2874 28, 469-483.
2875
2876 Lekens, W.A.H., Sejrup, H.P., Hafliðason, H., Knies, J., Richter, T., 2006. Meltwater and ice rafting in
2877 the southern Norwegian Sea between 20 and 40 calendar kyr BP: Implications for Fennoscandian
2878 Heinrich events. *Paleoceanography* 21.
2879
2880 Lekens, W.A.H., Sejrup, H.P., Hafliðason, H., Petersen, G.Ø., Hjelstuen, B.O., Knorr, G., 2005.
2881 Laminated sediments preceding Heinrich event 1 in the Northern North Sea and Southern
2882 Norwegian Sea: origin, processes and regional linkage. *Mar Geol* 216, 27-50.
2883

2884 Leynaud, D., Mienert, J., Vanneste, M., 2009. Submarine mass movements on glaciated and non-
2885 glaciated European continental margins: A review of triggering mechanisms and preconditions to
2886 failure. *Mar Petrol Geol* 26, 618-632.
2887
2888 Leynaud, D., Sultan, N., Mienert, J., 2007. The role of sedimentation rate and permeability in the
2889 slope stability of the formerly glaciated Norwegian continental margin: the Storegga slide model.
2890 *Landslides* 4, 297-309.
2891
2892 Li, G., Piper, D.J.W., Calvin Campbell, D., 2011. The Quaternary Lancaster Sound trough-mouth fan,
2893 NW Baffin Bay. *Journal of Quaternary Science* 26, 511-522.
2894
2895 Lindberg, B., Laberg, J.S., Vorren, T.O., 2004. The Nyk Slide—morphology, progression, and age of a
2896 partly buried submarine slide offshore northern Norway. *Mar Geol* 213, 277-289.
2897
2898 Lisiecki, L.E., Raymo, M.E., 2007. Plio–Pleistocene climate evolution: trends and transitions in glacial
2899 cycle dynamics. *Quaternary Sci Rev* 26, 56-69.
2900
2901 Liu, J.T., Wang, Y.H., Yang, R.J., Hsu, R.T., Kao, S.J., Lin, H.L., Kuo, F.H., 2012. Cyclone-induced
2902 hyperpycnal turbidity currents in a submarine canyon. *Journal of Geophysical Research: Oceans* 117.
2903
2904 Llopart, J., Urgeles, R., Camerlenghi, A., Lucchi, R.G., Mol, B., Rebesco, M., Pedrosa, M.T., 2014. Slope
2905 Instability of Glaciated Continental Margins: Constraints from Permeability-Compressibility Tests and
2906 Hydrogeological Modeling Off Storfjorden, NW Barents Sea, in: Krastel, S., Behrmann, J.-H., Völker,
2907 D., Stipp, M., Berndt, C., Urgeles, R., Chaytor, J., Huhn, K., Strasser, M., Harbitz, C.B. (Eds.), *Adv Nat*
2908 *Tech Haz Res*. Springer International Publishing, pp. 95-104.
2909
2910 Llopart, J., Urgeles, R., Camerlenghi, A., Lucchi, R.G., Rebesco, M., De Mol, B., 2015. Late Quaternary
2911 development of the Storfjorden and Kveithola Trough Mouth Fans, northwestern Barents Sea.
2912 *Quaternary Sci Rev* 129, 68-84.
2913
2914 Locat, A., Leroueil, S., Bernander, S., Demers, D., Locat, J., Ouehb, L., 2008. Study of a lateral spread
2915 failure in an eastern Canada clay deposit in relation with progressive failure: the Saint-Barnabé-Nord
2916 slide, *Proceedings of the 4th Canadian conference on geohazards: from causes to management*, pp.
2917 20-24.
2918
2919 Long, D., Smith, D.E., Dawson, A.G., 1989. A Holocene tsunami deposit in eastern Scotland. *Journal of*
2920 *Quaternary Science* 4, 61-66.
2921
2922 Long, D., Stevenson, A.G., Wilson, C.K., Bulat, J., 2003. Slope Failures in the Faroe — Shetland
2923 Channel, in: Locat, J., Mienert, J., Boisvert, L. (Eds.), *Submarine Mass Movements and Their*
2924 *Consequences: 1st International Symposium*. Springer Netherlands, Dordrecht, pp. 281-289.
2925
2926 Løvholt, F., Bondevik, S., Laberg, J.S., Kim, J., Boylan, N., 2017. Some giant submarine landslides do
2927 not produce large tsunamis. *Geophys Res Lett* 44, 8463-8472.
2928
2929 Løvholt, F., Harbitz, C.B., Haugen, K.B., 2005. A parametric study of tsunamis generated by
2930 submarine slides in the Ormen Lange/Storegga area off western Norway. *Mar Petrol Geol* 22, 219-
2931 231.
2932

2933 Løvholt, F., Pedersen, G., Harbitz, C.B., 2016. Tsunami-Genesis Due to Retrogressive Landslides on an
2934 Inclined Seabed, in: Lamarche, G., Mountjoy, J., Bull, S., Hubble, T., Krastel, S., Lane, E., Micallef, A.,
2935 Moscardelli, L., Mueller, C., Pecher, I., Woelz, S. (Eds.), *Adv Nat Tech Haz Res*. Springer, pp. 569-578.
2936
2937 Lowe, A.L., Anderson, J.B., 2002. Reconstruction of the West Antarctic ice sheet in Pine Island Bay
2938 during the Last Glacial Maximum and its subsequent retreat history. *Quaternary Sci Rev* 21, 1879-
2939 1897.
2940
2941 Lucchi, R.G., Camerlenghi, A., Rebesco, M., Colmenero-Hidalgo, E., Sierro, F.J., Sagnotti, L., Urgeles,
2942 R., Melis, R., Morigi, C., Bárcena, M.-A., 2013. Postglacial sedimentary processes on the Storfjorden
2943 and Kveithola trough mouth fans: Significance of extreme glacial marine sedimentation. *Global and*
2944 *planetary change* 111, 309-326.
2945
2946 Lucchi, R.G., Pedrosa, M.T., Camerlenghi, A., Urgeles, R., De Mol, B., Rebesco, M., 2012. Recent
2947 submarine landslides on the continental slope of Storfjorden and Kveithola Trough-Mouth Fans
2948 (north west Barents Sea), *Adv Nat Tech Haz Res*. Springer, pp. 735-745.
2949
2950 Lykke-Andersen, H., 1998. Neogene-Quaternary depositional history of the East Greenland shelf in
2951 the vicinity of the Leg 152 shelf sites, in: Larsen, H.C., Saunders, A.D., Clift, P.D. (Eds.), *Proceedings,*
2952 *Ocean Drilling Program, Scientific Results*. National Science Foundation, Texas, pp. 29-38.
2953
2954 Madhusudhan, B.N., Clare, M.A., Clayton, C.R.I., Hunt, J.E., 2017. Geotechnical profiling of deep-
2955 ocean sediments at the AFEN submarine slide complex. *Quarterly Journal of Engineering Geology*
2956 *and Hydrogeology* 50, 148-157.
2957
2958 Mangerud, J., 1991. The last interglacial/glacial cycle in northern Europe. *Quaternary landscapes* 38,
2959 75.
2960
2961 Mangerud, J., 2004. Ice sheet limits in Norway and on the Norwegian continental shelf.
2962 *Developments in Quaternary Sciences* 2, 271-294.
2963
2964 Mangerud, J., Astakhov, V.I., Murray, A., Svendsen, J.I., 2001. The chronology of a large ice-dammed
2965 lake and the Barents–Kara Ice Sheet advances, Northern Russia. *Global and Planetary Change* 31,
2966 321-336.
2967
2968 Mangerud, J., Dokken, T., Hebbeln, D., Heggen, B., Ingolfsson, O., Landvik, J.Y., Mejdahl, V.,
2969 Svendsen, J.I., Vorren, T.O., 1998. Fluctuations of the Svalbard–Barents Sea Ice Sheet during the last
2970 150 000 years. *Quaternary Sci Rev* 17, 11-42.
2971
2972 Mangerud, J., Jakobsson, M., Alexanderson, H., Astakhov, V., Clarke, G.K.C., Henriksen, M., Hjort, C.,
2973 Krinner, G., Lunkka, J.-P., Möller, P., 2004. Ice-dammed lakes and rerouting of the drainage of
2974 northern Eurasia during the Last Glaciation. *Quaternary Sci Rev* 23, 1313-1332.
2975
2976 Mangerud, J., Jansen, E., Landvik, J.Y., 1996. Late Cenozoic history of the Scandinavian and Barents
2977 Sea ice sheets. *Global and Planetary Change* 12, 11-26.
2978
2979 Mangerud, J., Løvlie, R., Gulliksen, S., Hufthammer, A.-K., Larsen, E., Valen, V., 2003. Paleomagnetic
2980 correlations between scandinavian ice-sheet fluctuations and greenland dansgaard–oeschger
2981 events, 45,000–25,000 yr BP. *Quaternary Res* 59, 213-222.
2982

2983 Mangerud, J., Svendsen, J.I., 1992. The last interglacial-glacial period on Spitsbergen, Svalbard.
2984 Quaternary Sci Rev 11, 633-664.
2985
2986 Maslin, M., Mikkelsen, N., Vilela, C., Haq, B., 1998. Sea-level- and gas-hydrate-controlled
2987 catastrophic sediment failures of the Amazon Fan. *Geology* 26, 1107-1110.
2988
2989 Maslin, M., Owen, M., Day, S., Long, D., 2004. Linking continental-slope failures and climate change:
2990 Testing the clathrate gun hypothesis. *Geology* 32, 53-56.
2991
2992 Masson, D.G., Arzola, R.G., Wynn, R.B., Hunt, J.E., Weaver, P.P.E., 2011. Seismic triggering of
2993 landslides and turbidity currents offshore Portugal. *Geochem Geophys Geosy* 12.
2994
2995 Masson, D.G., Harbitz, C.B., Wynn, R.B., Pedersen, G., Lovholt, F., 2006. Submarine landslides:
2996 processes, triggers and hazard prediction. *Philos T R Soc A* 364, 2009-2039.
2997
2998 Melles, M., Kuhn, G., 1993. Sub-bottom profiling and sedimentological studies in the southern
2999 Weddell Sea, Antarctica: evidence for large-scale erosional/depositional processes. *Deep Sea*
3000 *Research Part I: Oceanographic Research Papers* 40, 739-760.
3001
3002 Mienert, J., Posewang, J., Baumann, M., 1998. Gas hydrates along the northeastern Atlantic margin:
3003 possible hydrate-bound margin instabilities and possible release of methane. *Geological Society,*
3004 *London, Special Publications* 137, 275-291.
3005
3006 Mienert, J., Vanneste, M., Bunz, S., Andreassen, K., Hafliðason, H., Sejrup, H.P., 2005. Ocean
3007 warming and gas hydrate stability on the mid-Norwegian margin at the Storegga Slide. *Mar Petrol*
3008 *Geol* 22, 233-244.
3009
3010 Milliman, J.D., Meade, R.H., 1983. World-wide delivery of river sediment to the oceans. *The Journal*
3011 *of Geology,* 1-21.
3012
3013 Montelli, A., Dowdeswell, J.A., Ottesen, D., Johansen, S.E., 2017a. Ice-sheet dynamics through the
3014 Quaternary on the mid-Norwegian continental margin inferred from 3D seismic data. *Mar Petrol*
3015 *Geol* 80, 228-242.
3016
3017 Montelli, A., Gulick, S.P.S., Worthington, L.L., Mix, A., Davies-Walczak, M., Zellers, S.D., Jaeger, J.M.,
3018 2017b. Late Quaternary glacial dynamics and sedimentation variability in the Bering Trough, Gulf of
3019 Alaska. *Geology,* G38836. 38831.
3020
3021 Mosher, D.C., Campbell, D.C., Gardner, J.V., Piper, D.J.W., Chaytor, J.D., Rebesco, M., 2017. The role
3022 of deep-water sedimentary processes in shaping a continental margin: The Northwest Atlantic. *Mar*
3023 *Geol* 393, 245-259.
3024
3025 Mosher, D.C., Moran, K., Hiscott, R.N., 1994. Late Quaternary Sediment, Sediment Mass-Flow
3026 Processes and Slope Stability on the Scotian Slope, Canada. *Sedimentology* 41, 1039-1061.
3027
3028 Mosher, D.C., Piper, D.J.W., Campbell, D.C., Jenner, K.A., 2004. Near-surface geology and sediment-
3029 failure geohazards of the central Scotian Slope. *AAPG bulletin* 88, 703-723.
3030
3031 Mosher, D.C., Piper, D.J.W., Vilks, G.V., Aksu, A.E., Fader, G.B., 1989. Evidence for Wisconsinan
3032 glaciations in the Verrill Canyon area, Scotian Slope. *Quaternary Res* 31, 27-40.
3033

3034 Mudelsee, M., Schulz, M., 1997. The Mid-Pleistocene climate transition: onset of 100 ka cycle lags
3035 ice volume build-up by 280 ka. *Earth and Planetary Science Letters* 151, 117-123.
3036

3037 Mudelsee, M., Stattegger, K., 1997. Exploring the structure of the mid-Pleistocene revolution with
3038 advanced methods of time-series analysis. *Geologische Rundschau* 86, 499-511.
3039

3040 Mugford, R.I., Dowdeswell, J.A., 2010. Modeling iceberg-rafted sedimentation in high-latitude fjord
3041 environments. *Journal of Geophysical Research: Earth Surface* 115.
3042

3043 Mulder, T., Moran, K., 1995. Relationship among Submarine Instabilities, Sea-Level Variations, and
3044 the Presence of an Ice-Sheet on the Continental-Shelf - an Example from the Verrill Canyon Area,
3045 Scotian Shelf. *Paleoceanography* 10, 137-154.
3046

3047 Mulder, T., Syvitski, J.P.M., Migeon, S., Faugeres, J.-C., Savoye, B., 2003. Marine hyperpycnal flows:
3048 initiation, behavior and related deposits. A review. *Mar Petrol Geol* 20, 861-882.
3049

3050 Myhre, A.M., Thiede, J., Firth, J.V., 1995. 1. North Atlantic-Arctic Gateways, in: Myhre, A.M., Thiede,
3051 J., Firth, J.V., et al. (Eds.), *Proceedings Ocean Drilling Program Initial Reports*, vol. 151.
3052

3053 Nam, S.-I., Stein, R., Grobe, H., Hubberten, H., 1995. Late Quaternary glacial-interglacial changes in
3054 sediment composition at the East Greenland continental margin and their paleoceanographic
3055 implications. *Mar Geol* 122, 243-262.
3056

3057 Nam, S.I., Stein, R.A., 1999. Late Quaternary variations in sediment accumulation rates and their
3058 paleoenvironmental implications: a case study from the East Greenland continental margin,
3059 Retrospective Collection. *Trans Tech Publ*, p. 223.
3060

3061 Newton, A.M.W., Huuse, M., Brocklehurst, S.H., 2016. Buried iceberg scours reveal reduced North
3062 Atlantic Current during the stage 12 deglacial. *Nature communications* 7, 10927.
3063

3064 Nitsche, F.O., Gohl, K., Vanneste, K., Miller, H., 1997. Seismic expression of glacially deposited
3065 sequences in the Bellingshausen and Amundsen Seas, West Antarctica, in: Barker, P.F., Cooper, A.K.
3066 (Eds.), *Geology and Seismic Stratigraphy of the Antarctic Margin*, pp. 95-108.
3067

3068 Noormets, R., Dowdeswell, J.A., Larter, R.D., Ó Cofaigh, C., Evans, J., 2009. Morphology of the upper
3069 continental slope in the Bellingshausen and Amundsen Seas—Implications for sedimentary processes
3070 at the shelf edge of West Antarctica. *Mar Geol* 258, 100-114.
3071

3072 Nothold, H., 1998. Die Auswirkungen der "NorthEastWater"-Polynya auf die Sedimentation vor NO-
3073 Grönland und Untersuchungen zur Paläo-Ozeanographie seit dem Mittelweichsel= The implication of
3074 the "NorthEastWater"-Polynya on the sedimentation by NE-Greenland and Late Quaternary Paleo-
3075 oceanic investigations. *Berichte zur Polarforschung (Reports on Polar Research)* 275.
3076

3077 Nygård, A., Hafliðason, H., Sejrup, H.P., 2003. Morphology of a non-glacigenic debris flow lobe in the
3078 Helland Hansen area investigated with 3D seismic data, *European Margin Sediment Dynamics*.
3079 Springer, pp. 63-65.
3080

3081 Nygård, A., Sejrup, H.P., Hafliðason, H., Bryn, P., 2005. The glacial North Sea Fan, southern
3082 Norwegian Margin: architecture and evolution from the upper continental slope to the deep-sea
3083 basin. *Mar Petrol Geol* 22, 71-84.
3084

3085 Nygård, A., Sejrup, H.P., Hafliðason, H., Lekens, W.A.H., Clark, C.D., Bigg, G.R., 2007. Extreme
3086 sediment and ice discharge from marine-based ice streams: New evidence from the North Sea.
3087 *Geology* 35, 395-398.
3088

3089 O'Brien, P.E., Cooper, A.K., Florindo, F., Handwerger, D.A., Lavelle, M., Passchier, S., Pospichal, J.J.,
3090 Quilty, P.G., Richter, C., Theissen, K.M., 2004. Prydz Channel Fan and the history of extreme ice
3091 advances in Prydz Bay, *Proceedings of the Ocean Drilling Program, Scientific Results*, pp. 1-32.
3092

3093 O'Brien, P.E., Goodwin, I., Forsberg, C.-F., Cooper, A.K., Whitehead, J., 2007. Late Neogene ice
3094 drainage changes in Prydz Bay, East Antarctica and the interaction of Antarctic ice sheet evolution
3095 and climate. *Palaeogeography, Palaeoclimatology, Palaeoecology* 245, 390-410.
3096

3097 O'Brien, P.E., Harris, P.T., 1996. Patterns of glacial erosion and deposition in Prydz Bay and the past
3098 behaviour of the Lambert Glacier, *Papers and Proceedings of the Royal Society of Tasmania*, pp. 79-
3099 85.
3100

3101 Ó Cofaigh, C., Hogan, K. A., Jennings, A. E., Callard, S. L., Dowdeswell, J. A., Noormets, R., Evans, J., in
3102 review. The role of meltwater in high-latitude trough-mouth fan development: the Disko Trough-
3103 Mouth Fan, West Greenland. *Marine Geology*.
3104

3105 Ó Cofaigh, C., Dowdeswell, J. A., Jennings, A. E., Hogan, K., Kilfeather, A., Hiemstra, J. F., Noormets,
3106 R., Evans, J., McCarthy, D. J., Andrews, J. T., Lloyd, J. M., Moros, M. (2013a). An extensive and
3107 dynamic ice sheet on the West Greenland shelf during the last glacial cycle. *Geology* 41, 219-222.
3108

3109 Ó Cofaigh, C., Andrews, J.T., Jennings, A.E., Dowdeswell, J.A., Hogan, K.A., Kilfeather, A.A., Sheldon,
3110 C., 2013b. Glacimarine lithofacies, provenance and depositional processes on a West Greenland
3111 trough-mouth fan. *Journal of Quaternary Science* 28, 13-26.
3112

3113 Ó Cofaigh, C., Dowdeswell, J.A., Evans, J., Kenyon, N.H., Taylor, J., Mienert, J., Wilken, M., 2004.
3114 Timing and significance of glacially influenced mass-wasting in the submarine channels of the
3115 Greenland Basin. *Mar Geol* 207, 39-54.
3116

3117 Ó Cofaigh, C., Dowdeswell, J.A., Evans, J., Larter, R.D., 2008. Geological constraints on Antarctic
3118 palaeo-ice-stream retreat. *Earth Surf Proc Land* 33, 513-525.
3119

3120 Ó Cofaigh, C., Dowdeswell, J.A., Kenyon, N.H., 2006. Geophysical investigations of a high-latitude
3121 submarine channel system and associated channel-mouth lobe in the Lofoten Basin, polar North
3122 Atlantic. *Mar Geol* 226, 41-50.
3123

3124 Ó Cofaigh, C., Larter, R.D., Dowdeswell, J.A., Hillenbrand, C.D., Pudsey, C.J., Evans, J., Morris, P.,
3125 2005. Flow of the West Antarctic Ice Sheet on the continental margin of the Bellingshausen Sea at
3126 the Last Glacial Maximum. *Journal of Geophysical Research: Solid Earth* 110.
3127

3128 Ó Cofaigh, C., Taylor, J., Dowdeswell, J.A., Pudsey, C.J., 2003. Palaeo-ice streams, trough mouth fans
3129 and high-latitude continental slope sedimentation. *Boreas* 32, 37-55.
3130

3131 Olsen, J., van der Borg, K., Bergstrøm, B., Sveian, H., Lauritzen, S.-E., Hansen, G., 2001a. AMS
3132 radiocarbon dating of glacial sediments with low organic carbon content - an important tool for
3133 reconstructing the glacial variations in Norway. *Norwegian Journal of Geology* 2, 59-92.
3134

3135 Olsen, L., Sveian, H., Bergstrøm, B., 2001b. Rapid adjustments of the western part of the
3136 Scandinavian lee Sheet during the Mid and late Weichselian. *Norwegian Journal of Geology* 2, 93-
3137 117.
3138
3139 Ottesen, D., Dowdeswell, J.A., 2006. Assemblages of submarine landforms produced by tidewater
3140 glaciers in Svalbard. *Journal of Geophysical Research: Earth Surface* (2003–2012) 111.
3141
3142 Ottesen, D., Dowdeswell, J.A., Bugge, T., 2014. Morphology, sedimentary infill and depositional
3143 environments of the Early Quaternary North Sea Basin (56°–62°N). *Mar Petrol Geol* 56, 123-146.
3144
3145 Ottesen, D., Dowdeswell, J.A., Rise, L., 2005. Submarine landforms and the reconstruction of fast-
3146 flowing ice streams within a large Quaternary ice sheet: The 2500-km-long Norwegian-Svalbard
3147 margin (57–80 N). *Geological Society of America Bulletin* 117, 1033-1050.
3148
3149 Ottesen, D., Dowdeswell, J.A., Rise, L., Bugge, T., 2012. Large-scale development of the mid-
3150 Norwegian shelf over the last three million years and potential for hydrocarbon reservoirs in glacial
3151 sediments. *Geological Society, London, Special Publications* 368, 53-73.
3152
3153 Ottesen, D., Rise, L., Rokoengen, K., 2001. Glacial processes and large-scale morphology on the mid-
3154 Norwegian continental shelf. *Norwegian Petroleum Society Special Publications* 10, 441-449.
3155
3156 Ottesen, D., Rise, L., Sletten Andersen, E., Bugge, T., Eidvin, T., 2009. Geological evolution of the
3157 Norwegian continental shelf between 61° N and 68° N during the last 3 million years. *Norwegian*
3158 *Journal of Geology* 89, 251-265.
3159
3160 Øverland, I., 2010. Russia's Arctic energy policy. *International Journal* 65, 865-878.
3161
3162 Owen, L.A., Kamp, U., Khattak, G.A., Harp, E.L., Keefer, D.K., Bauer, M.A., 2008. Landslides triggered
3163 by the 8 October 2005 Kashmir earthquake. *Geomorphology* 94, 1-9.
3164
3165 Owen, M., Day, S., Maslin, M., 2007. Late Pleistocene submarine mass movements: occurrence and
3166 causes. *Quaternary Sci Rev* 26, 958-978.
3167
3168 Özener, P.T., Özyaydin, K., Berilgen, M.M., 2009. Investigation of liquefaction and pore water pressure
3169 development in layered sands. *Bulletin of Earthquake Engineering* 7, 199-219.
3170
3171 Parsons, J.D., Bush, J.W.M., Syvitski, J.P.M., 2001. Hyperpycnal plume formation from riverine
3172 outflows with small sediment concentrations. *Sedimentology* 48, 465-478.
3173
3174 Passchier, S., O'Brien, P.E., Damuth, J.E., Januszczak, N., Handwerger, D.A., Whitehead, J.M., 2003.
3175 Pliocene–Pleistocene glaciomarine sedimentation in eastern Prydz Bay and development of the
3176 Prydz trough-mouth fan, ODP Sites 1166 and 1167, East Antarctica. *Mar Geol* 199, 279-305.
3177
3178 Patton, H., Andreassen, K., Bjarnadóttir, L.R., Dowdeswell, J.A., Winsborrow, M.C.M., Noormets, R.,
3179 Polyak, L., Auriac, A., Hubbard, A., 2015. Geophysical constraints on the dynamics and retreat of the
3180 Barents Sea Ice Sheet as a palaeo-benchmark for models of marine ice-sheet deglaciation. *Rev*
3181 *Geophys* 53, 1051-1098.
3182
3183 Patton, H., Hubbard, A., Andreassen, K., Winsborrow, M., Stroeven, A.P., 2016. The build-up,
3184 configuration, and dynamical sensitivity of the Eurasian ice-sheet complex to Late Weichselian
3185 climatic and oceanic forcing. *Quaternary Sci Rev* 153, 97-121.

3186
3187 Paull, C.K., Ussler, W., Holbrook, W.S., 2007. Assessing methane release from the colossal Storegga
3188 submarine landslide. *Geophys Res Lett* 34.
3189
3190 Pedrosa, M.T., Camerlenghi, A., De Mol, B., Urgeles, R., Rebesco, M., Lucchi, R.G., 2011. Seabed
3191 morphology and shallow sedimentary structure of the Storfjorden and Kveithola trough-mouth fans
3192 (north west Barents Sea). *Mar Geol* 286, 65-81.
3193
3194 Pickrill, R., Piper, D.J.W., Collins, J., Kleiner, A., Gee, L., 2001. Scotian Slope mapping project: the
3195 benefits of an integrated regional high-resolution multibeam survey, Offshore Technology
3196 Conference. Offshore Technology Conference.
3197
3198 Piper, D.J., Hundert, T., 2002. Provenance of distal Sohm Abyssal Plain sediments: history of supply
3199 from the Wisconsinan glaciation in eastern Canada. *Geo-Mar Lett* 22, 75-85.
3200
3201 Piper, D.J.W., 1988. Glaciomarine sedimentation on the continental slope off eastern Canada.
3202 *Geoscience Canada* 15.
3203
3204 Piper, D.J.W., 2005. Late Cenozoic evolution of the continental margin of eastern Canada. *Norsk*
3205 *geologisk tidsskrift* 85, 305.
3206
3207 Piper, D.J.W., Aksu, A.E., 1987. The source and origin of the 1929 grand banks turbidity current
3208 inferred from sediment budgets. *Geo-Mar Lett* 7, 177-182.
3209
3210 Piper, D.J.W., Campbell, D.C., 2005. Quaternary geology of Flemish Pass and its application to
3211 geohazard evaluation for hydrocarbon development. *GAC Special Paper* 43, 29-43.
3212
3213 Piper, D.J.W., Campbell, D.C., Mosher, D.C., 2016. Mid-latitude complex trough-mouth fans,
3214 Laurentian and Northeast fans, eastern Canada. *Geological Society, London, Memoirs* 46, 363-364.
3215
3216 Piper, D.J.W., Cochonat, P., Morrison, M.L., 1999. The sequence of events around the epicentre of
3217 the 1929 Grand Banks earthquake: initiation of debris flows and turbidity current inferred from
3218 sidescan sonar. *Sedimentology* 46, 79-97.
3219
3220 Piper, D.J.W., Deptuck, M.E., Mosher, D.C., Hughes Clarke, J.E., Migeon, S., 2012. Erosional and
3221 depositional features of glacial meltwater discharges on the eastern Canadian continental margin.
3222 *Applications of the Principles of Seismic Geomorphology to Continental Slope and Base-of-slope*
3223 *Systems: Case Studies from Seafloor and Near-Seafloor Analogues*. Edited by BE Prather, ME
3224 Deptuck, D. Mohrig, B. van Hoorn, and R. Wynn. *Society for Sedimentary Geology (SEPM), Special*
3225 *Publications* 99, 61-80.
3226
3227 Piper, D.J.W., Farre, J.A., Shor, A., 1985. Late Quaternary slumps and debris flows on the Scotian
3228 Slope. *Geological Society of America Bulletin* 96, 1508-1517.
3229
3230 Piper, D.J.W., Ingram, S., 2003. Major Quaternary sediment failures on the east Scotian Rise, eastern
3231 Canada. *Natural Resources Canada, Geological Survey of Canada*.
3232
3233 Piper, D.J.W., McCall, C., 2003. A Synthesis of the Distribution of Submarine Mass Movements on the
3234 Eastern Canadian Margin, in: Locat, J., Mienert, J., Boisvert, L. (Eds.), *Submarine Mass Movements*
3235 *and Their Consequences: 1st International Symposium*. Springer Netherlands, Dordrecht, pp. 291-
3236 298.

3237
3238 Piper, D.J.W., Mosher, D.C., Gauley, B.-J., Jenner, K., Campbell, D.C., 2003. The chronology and
3239 recurrence of submarine mass movements on the continental slope off southeastern Canada, *Adv*
3240 *Nat Tech Haz Res.* Springer, pp. 299-306.
3241
3242 Piper, D.J.W., Mudie, P.J., Aksu, A.E., Skene, K.I., 1994. A 1 Ma record of sediment flux south of the
3243 Grand Banks used to infer the development of glaciation in southeastern Canada. *Quaternary Sci Rev*
3244 *13*, 23-37.
3245
3246 Piper, D.J.W., Normark, W.R., 2009. Processes that initiate turbidity currents and their influence on
3247 turbidites: a marine geology perspective. *Journal of Sedimentary Research* *79*, 347-362.
3248
3249 Piper, D.J.W., Savoye, B., 1993. Processes of late Quaternary turbidity current flow and deposition on
3250 the Var deep-sea fan, north-west Mediterranean Sea. *Sedimentology* *40*, 557-582.
3251
3252 Piper, D.J.W., Shaw, J., Skene, K.I., 2007. Stratigraphic and sedimentological evidence for late
3253 Wisconsinan sub-glacial outburst floods to Laurentian Fan. *Palaeogeography, Palaeoclimatology,*
3254 *Palaeoecology* *246*, 101-119.
3255
3256 Pope, E.L., Talling, P.J., Carter, L., 2017a. Which earthquakes trigger damaging submarine mass
3257 movements: Insights from a global record of submarine cable breaks? *Mar Geol* *348*, 131-146.
3258
3259 Pope, E.L., Talling, P.J., Carter, L., Clare, M.A., Hunt, J.E., 2017b. Damaging sediment density flows
3260 triggered by tropical cyclones. *Earth and Planetary Science Letters* *458*, 161-169.
3261
3262 Pope, E.L., Talling, P.J., Hunt, J.E., Dowdeswell, J.A., Allin, J.R., Cartigny, M.J.B., Long, D., Mozzato, A.,
3263 Stanford, J.D., Tappin, D.R., Watts, M., 2016. Long-term record of Barents Sea Ice Sheet advance to
3264 the shelf edge from a 140,000 year record. *Quaternary Sci Rev* *150*, 55-66.
3265
3266 Pope, E.L., Talling, P.J., Urlaub, M., Hunt, J.E., Clare, M.A., Challenor, P., 2015. Are large submarine
3267 landslides temporally random or do uncertainties in available age constraints make it impossible to
3268 tell? *Mar Geol* *369*, 19-33.
3269
3270 Powell, R.D., Alley, R.B., 1997. Grounding-Line Systems: Processes, Glaciological Inferences and the
3271 Stratigraphic Record. *Geology and seismic stratigraphy of the Antarctic Margin*, *2*, 169-187.
3272
3273 Powell, R.D., Domack, E., 1995. Modern glaciomarine environments. *Glacial environments* *1*, 445-
3274 486.
3275
3276 Prior, D.B., Coleman, J.M., Bornhold, B.D., 1982. Results of a known seafloor instability event. *Geo-*
3277 *Mar Lett* *2*, 117-122.
3278
3279 Pudsey, C.J., Camerlenghi, A., 1998. Glacial–interglacial deposition on a sediment drift on the Pacific
3280 margin of the Antarctic Peninsula. *Antarctic Science* *10*, 286-308.
3281
3282 Quinn, P.E., Diederichs, M.S., Rowe, R.K., Hutchinson, D.J., 2012. Development of progressive failure
3283 in sensitive clay slopes. *Canadian Geotechnical Journal* *49*, 782-795.
3284
3285 Rasmussen, E., Fjeldskaar, W., 1996. Quantification of the Pliocene-Pleistocene erosion of the
3286 Barents Sea from present-day bathymetry. *Global and Planetary Change* *12*, 119-133.
3287

3288 Rasmussen, T.L., Thomsen, E., Kuijpers, A., Wastegård, S., 2003. Late warming and early cooling of
3289 the sea surface in the Nordic seas during MIS 5e (Eemian Interglacial). *Quaternary Sci Rev* 22, 809-
3290 821.
3291
3292 Rasmussen, T.L., Thomsen, E., Ślubowska, M.A., Jessen, S., Solheim, A., Koç, N., 2007.
3293 Paleoceanographic evolution of the SW Svalbard margin (76 N) since 20,000 14 C yr BP. *Quaternary*
3294 *Res* 67, 100-114.
3295
3296 Rasmussen, T.L., Van Weering, T.C.E., Labeyrie, L., 1997. Climatic instability, ice sheets and ocean
3297 dynamics at high northern latitudes during the last glacial period (58-10 KA BP). *Quaternary Sci Rev*
3298 16, 71-80.
3299
3300 Rauscher, K.F., 2010. The Reliability of Global Undersea Communications Cable Infrastructure
3301 (ROGUCCI) Report. IEEE.
3302
3303 Raymo, M.E., Nisancioglu, K.H., 2003. The 41 kyr world: Milankovitch's other unsolved mystery.
3304 *Paleoceanography* 18.
3305
3306 Raymo, M.E., Ruddiman, W.F., 1992. Tectonic forcing of late Cenozoic climate. *Nature* 359, 117-122.
3307
3308 Rebesco, M., Camerlenghi, A., 2008. Late Pliocene margin development and mega debris flow
3309 deposits on the Antarctic continental margins: Evidence of the onset of the modern Antarctic Ice
3310 Sheet? *Palaeogeography, Palaeoclimatology, Palaeoecology* 260, 149-167.
3311
3312 Rebesco, M., Larter, R.D., Camerlenghi, A., Barker, P.F., 1996. Giant sediment drifts on the
3313 continental rise west of the Antarctic Peninsula. *Geo-Mar Lett* 16, 65-75.
3314
3315 Rebesco, M., Liu, Y., Camerlenghi, A., Winsborrow, M., Laberg, J.S., Caburlotto, A., Diviaco, P.,
3316 Accettella, D., Sauli, C., Wardell, N., 2011. Deglaciation of the western margin of the Barents Sea Ice
3317 Sheet—a swath bathymetric and sub-bottom seismic study from the Kveithola Trough. *Mar Geol*
3318 279, 141-147.
3319
3320 Rebesco, M., Pedrosa, M.T., Camerlenghi, A., Lucchi, R.G., Sauli, C., De Mol, B., Madrussani, G.,
3321 Urgeles, R., Rossi, G., Böhm, G., 2012. One million years of climatic generated landslide events on
3322 the northwestern Barents Sea continental margin, *Adv Nat Tech Haz Res*. Springer, pp. 747-756.
3323
3324 Rebesco, M., Pudsey, C.J., Canals, M., Camerlenghi, A., Barker, P.F., Estrada, F., Giorgetti, A., 2002.
3325 Sediment drifts and deep-sea channel systems, Antarctic Peninsula Pacific Margin. *Geological*
3326 *Society, London, Memoirs* 22, 353-371.
3327
3328 Rise, L., Bøe, R., Riis, F., Bellec, V.K., Laberg, J.S., Eidvin, T., Elvenes, S., Thorsnes, T., 2013. The
3329 Lofoten-Vesterålen continental margin, North Norway: Canyons and mass-movement activity. *Mar*
3330 *Petrol Geol* 45, 134-149.
3331
3332 Rise, L., Chand, S., Hafliðason, H., L'Heureux, J.S., Hjelstuen, B.O., Bellec, V., Longva, O., Brendryen,
3333 J., Vanneste, M., Bøe, R., 2012. Investigations of Slides at the Upper Continental Slope Off
3334 Vesterålen, North Norway, in: Yamada, Y., Kawamura, K., Ikehara, K., Ogawa, Y., Urgeles, R., Mosher,
3335 D., Chaytor, J., Strasser, M. (Eds.), *Adv Nat Tech Haz Res*. Springer Netherlands, pp. 167-176.
3336
3337 Rise, L., Chand, S., Hjelstuen, B.O., Hafliðason, H., Bøe, R., 2010. Late Cenozoic geological
3338 development of the south Vøring margin, mid-Norway. *Mar Petrol Geol* 27, 1789-1803.

3339
3340 Rise, L., Ottesen, D., Berg, K., Lundin, E., 2005. Large-scale development of the mid-Norwegian
3341 margin during the last 3 million years. *Mar Petrol Geol* 22, 33-44.
3342
3343 Rise, L., Ottesen, D., Longva, O., Solheim, A., Andersen, E.S., Ayers, S., 2006. The Sklinnadjupet slide
3344 and its relation to the Elsterian glaciation on the mid-Norwegian margin. *Mar Petrol Geol* 23, 569-
3345 583.
3346
3347 Rokoengen, K., Rise, L., Bryn, P., Frengstad, B., Gustavsen, B., Nygaard, E., Sættem, J., 1995. Upper
3348 Cenozoic stratigraphy on the mid-Norwegian continental shelf. *Norsk Geologisk Tidsskrift* 75, 88-104.
3349
3350 Rydningen, T.A., Laberg, J.S., Kolstad, V., 2016. Late Cenozoic evolution of high-gradient trough
3351 mouth fans and canyons on the glaciated continental margin offshore Troms, northern Norway—
3352 Paleoclimatic implications and sediment yield. *Geological Society of America Bulletin* 128, 576-596.
3353
3354 Sættem, J., Bugge, T., Fanavoll, S., Goll, R.M., Mørk, A., Mørk, M.B.E., Smelror, M., Verdenius, J.G.,
3355 1994. Cenozoic margin development and erosion of the Barents Sea: Core evidence from southwest
3356 of Bjørnøya. *Mar Geol* 118, 257-281.
3357
3358 Sættem, J., Poole, D.A.R., Ellingsen, L., Sejrup, H.P., 1992. Glacial geology of outer Bjørnøyrenna,
3359 southwestern Barents Sea. *Mar Geol* 103, 15-51.
3360
3361 Sawyer, D.E., DeVore, J.R., 2015. Elevated shear strength of sediments on active margins: Evidence
3362 for seismic strengthening. *Geophys Res Lett* 42.
3363
3364 Sawyer, D.E., Reece, R.S., Gulick, S.P.S., Lenz, B.L., 2017. Submarine landslide and tsunami hazards
3365 offshore southern Alaska: Seismic strengthening versus rapid sedimentation. *Geophys Res Lett*.
3366
3367 Scheuer, C., Gohl, K., Larter, R.D., Rebesco, M., Udintsev, G., 2006. Variability in Cenozoic
3368 sedimentation along the continental rise of the Bellingshausen Sea, West Antarctica. *Mar Geol* 227,
3369 279-298.
3370
3371 Šeirienė, V., Karabanov, A., Rylova, T., Baltrūnas, V., Savchenko, I., 2015. The Pleistocene
3372 stratigraphy of the south-eastern sector of the Scandinavian glaciation (Belarus and Lithuania): a
3373 review. *Baltica* 28.
3374
3375 Sejrup, H.P., Aarseth, I., Hafliðason, H., Løvlie, R., Bratten, Å., Tjøstheim, G., Forsberg, C.F., Ellingsen,
3376 K.L., 1995. Quaternary of the Norwegian Channel: glaciation history and palaeoceanography.
3377 *Norwegian Journal of Geology* 75, 65-87.
3378
3379 Sejrup, H.P., Hafliðason, H., Aarseth, I., King, E.L., Forsberg, C.F., Long, D., Rokoengen, K., 1994. Late
3380 Weichselian glaciation history of the northern North Sea. *Boreas-International Journal of Quaternary*
3381 *Research* 23, 1-13.
3382
3383 Sejrup, H.P., Hafliðason, H., Hjelstuen, B.I., Nygard, A., Bryn, P., Lien, R., 2004. Pleistocene
3384 development of the SE Nordic seas margin. *Mar Geol* 213, 169-200.
3385
3386 Sejrup, H.P., Hjelstuen, B.O., Dahlgren, K.I.T., Hafliðason, H., Kuijpers, A., Nygård, A., Praeg, D.,
3387 Stoker, M.S., Vorren, T.O., 2005. Pleistocene glacial history of the NW European continental margin.
3388 *Mar Petrol Geol* 22, 1111-1129.
3389

3390 Sejrup, H.P., King, E.L., Aarseth, I., Hafliðason, H., Elverhøi, A., 1996. Quaternary erosion and
3391 depositional processes: western Norwegian fjords, Norwegian Channel and North Sea Fan.
3392 Geological Society, London, Special Publications 117, 187-202.
3393
3394 Sejrup, H.P., Larsen, E., Hafliðason, H., Berstad, I.M., Hjelstuen, B.O., Jonsdottir, H.E., King, E.L.,
3395 Landvik, J., Longva, O., Nygård, A., Ottesen, D., Raunholm, S., Rise, L., Stalsberg, K., 2003.
3396 Configuration, history and impact of the Norwegian Channel Ice Stream. *Boreas* 32, 18-36.
3397
3398 Sejrup, H.P., Larsen, E., Landvik, J., King, E.L., Hafliðason, H., Nesje, A., 2000. Quaternary glaciations
3399 in southern Fennoscandia: evidence from southwestern Norway and the northern North Sea region.
3400 *Quaternary Sci Rev* 19, 667-685.
3401
3402 Sejrup, H.P., Nagy, J., Brigham-Grette, J., 1989. Foraminiferal stratigraphy and amino acid
3403 geochronology of Quaternary sediments in the Norwegian Channel, northern North Sea. *Norsk*
3404 *geologisk tidsskrift* 69, 111-124.
3405
3406 Shennan, I., Peltier, W.R., Drummond, R., Horton, B., 2002. Global to local scale parameters
3407 determining relative sea-level changes and the post-glacial isostatic adjustment of Great Britain.
3408 *Quaternary Sci Rev* 21, 397-408.
3409
3410 Shepard, F.P., Marshall, N.F., McLoughlin, P.A., Sullivan, G.G., 1979. Currents in submarine canyons
3411 and other seavalleys.
3412
3413 Siebert, M.J., Dowdeswell, J.A., Hald, M., Svendsen, J.-I., 2001. Modelling the Eurasian Ice Sheet
3414 through a full (Weichselian) glacial cycle. *Global and Planetary Change* 31, 367-385.
3415
3416 Smith, D.E., Harrison, S., Jordan, J.T., 2013. Sea level rise and submarine mass failures on open
3417 continental margins. *Quaternary Sci Rev* 82, 93-103.
3418
3419 Smith, D.E., Shi, S., Cullingford, R.A., Dawson, A.G., Dawson, S., Firth, C.R., Foster, I.D.L., Fretwell,
3420 P.T., Haggart, B.A., Holloway, L.K., 2004. The holocene storegga slide tsunami in the United Kingdom.
3421 *Quaternary Sci Rev* 23, 2291-2321.
3422
3423 Solheim, A., Andersen, E.S., Elverhøi, A., Fiedler, A., 1996. Late Cenozoic depositional history of the
3424 western Svalbard continental shelf, controlled by subsidence and climate. *Global and Planetary*
3425 *Change* 12, 135-148.
3426
3427 Solheim, A., Berg, K., Forsberg, C.F., Bryn, P., 2005a. The Storegga Slide complex: repetitive large
3428 scale sliding with similar cause and development. *Mar Petrol Geol* 22, 97-107.
3429
3430 Solheim, A., Bryn, P., Sejrup, H.P., Mienert, J., Berg, K., 2005b. Ormen Lange—an integrated study for
3431 the safe development of a deep-water gas field within the Storegga Slide Complex, NE Atlantic
3432 continental margin; executive summary. *Mar Petrol Geol* 22, 1-9.
3433
3434 Solheim, A., Elverhøi, A., 1985. A pockmark field in the Central Barents Sea; gas from a petrogenic
3435 source? *Polar research* 3, 11-19.
3436
3437 Solheim, A., Faleide, J.I., Andersen, E.S., Elverhøi, A., Forsberg, C.F., Vanneste, K., Uenzelmann-
3438 Neben, G., Channell, J.E.T., 1998. Late Cenozoic seismic stratigraphy and glacial geological
3439 development of the East Greenland and Svalbard–Barents Sea continental margins. *Quaternary Sci*
3440 *Rev* 17, 155-184.

3441
3442 Solheim, A., Kristoffersen, Y., 1984. Sediments above the upper regional unconformity: thickness,
3443 seismic stratigraphy and outline of the glacial history. Norsk Polarinstitut.
3444
3445 Spiegler, D., Jansen, E., 1989. Planktonic foraminifer biostratigraphy of Norwegian Sea sediments:
3446 ODP Leg 104, Proceedings of the Ocean Drilling Program, Scientific Results. TX (Ocean Drilling
3447 Program) College Station, pp. 681-696.
3448
3449 Spielhagen, R.F., Baumann, K.-H., Erlenkeuser, H., Nowaczyk, N.R., Nørgaard-Pedersen, N., Vogt, C.,
3450 Weiel, D., 2004. Arctic Ocean deep-sea record of northern Eurasian ice sheet history. *Quaternary Sci*
3451 *Rev* 23, 1455-1483.
3452
3453 St. John, K.E., Krissek, L.A., 2002. The late Miocene to Pleistocene ice-rafting history of southeast
3454 Greenland. *Boreas* 31, 28-35.
3455
3456 Steffen, H., Wu, P., 2011. Glacial isostatic adjustment in Fennoscandia—a review of data and
3457 modeling. *J Geodyn* 52, 169-204.
3458
3459 Stein, R., Grobe, H., Hubberten, H., Marienfeld, P., Nam, S., 1993. Latest Pleistocene to Holocene
3460 changes in glaciomarine sedimentation in Scoresby Sund and along the adjacent East Greenland
3461 Continental Margin: Preliminary results. *Geo-Mar Lett* 13, 9-16.
3462
3463 Stein, R., Nam, S.-I., Grobe, H., Hubberten, H., 1996. Late Quaternary glacial history and short-term
3464 ice-rafted debris fluctuations along the East Greenland continental margin. *Geological Society,*
3465 *London, Special Publications* 111, 135-151.
3466
3467 Stewart, I.S., Sauber, J., Rose, J., 2000. Glacio-seismotectonics: ice sheets, crustal deformation and
3468 seismicity. *Quaternary Sci Rev* 19, 1367-1389.
3469
3470 Stewart, M.A., Lonergan, L., Hampson, G., 2013. 3D seismic analysis of buried tunnel valleys in the
3471 central North Sea: morphology, cross-cutting generations and glacial history. *Quaternary Sci Rev* 72,
3472 1-17.
3473
3474 Stigall, J., Dugan, B., 2010. Overpressure and earthquake initiated slope failure in the Ursa region,
3475 northern Gulf of Mexico. *J Geophys Res-Sol Ea* 115.
3476
3477 Stoker, M.S., Leslie, A.B., Scott, W.D., Briden, J.C., Hine, N.M., Harland, R., Wilkinson, I.P., Evans, D.,
3478 Ardu, D.A., 1994. A record of late Cenozoic stratigraphy, sedimentation and climate change from
3479 the Hebrides Slope, NE Atlantic Ocean. *Journal of the Geological Society* 151, 235-249.
3480
3481 STRATAGEM, P., 2002. The Neogene stratigraphy of the glaciated European margin from Lofoten to
3482 Porcupine. A product of the EC-supported STRATAGEM project, p. 75.
3483
3484 Sultan, N., Cochonat, P., Canals, M., Cattaneo, A., Dennielou, B., Hafliðason, H., Laberg, J.S., Long, D.,
3485 Mienert, J., Trincardi, F., Urgeles, R., Vorren, T.O., Wilson, C., 2004a. Triggering mechanisms of slope
3486 instability processes and sediment failures on continental margins: a geotechnical approach. *Mar*
3487 *Geol* 213, 291-321.
3488
3489 Sultan, N., Cochonat, P., Foucher, J.-P., Mienert, J., 2004b. Effect of gas hydrates melting on seafloor
3490 slope instability. *Mar Geol* 213, 379-401.
3491

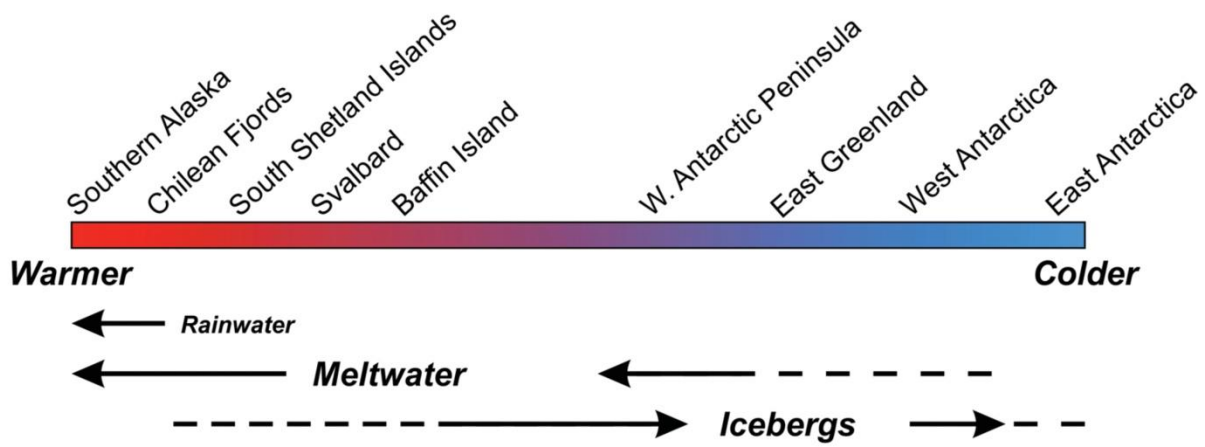
3492 Svendsen, J.I., Alexanderson, H., Astakhov, V.I., Demidov, I., Dowdeswell, J.A., Funder, S., Gataullin,
3493 V., Henriksen, M., Hjort, C., Houmark-Nielsen, M., 2004a. Late Quaternary ice sheet history of
3494 northern Eurasia. *Quaternary Sci Rev* 23, 1229-1271.
3495
3496 Svendsen, J.I., Astakhov, V.I., Bolshiyakov, D.Y., Demidov, I., Dowdeswell, J.A., Gataullin, V., Hjort, C.,
3497 Hubberten, H.W., Larsen, E., Mangerud, J., 1999. Maximum extent of the Eurasian ice sheets in the
3498 Barents and Kara Sea region during the Weichselian. *Boreas* 28, 234-242.
3499
3500 Svendsen, J.I., Briner, J.P., Mangerud, J., Young, N.E., 2015. Early break-up of the norwegian channel
3501 ice stream during the last glacial maximum. *Quaternary Sci Rev* 107, 231-242.
3502
3503 Svendsen, J.I., Gataullin, V., Mangerud, J., Polyak, L., 2004b. The glacial history of the Barents and
3504 Kara Sea region. *Developments in Quaternary Sciences* 2, 369-378.
3505
3506 Talling, P.J., Clare, M.A., Urlaub, M., Pope, E., Hunt, J.E., Watt, S.F.L., 2014. Large Submarine
3507 Landslides on Continental Slopes. *Oceanography* 27, 32.
3508
3509 Talwani, M., Udintsev, G.B., White, S.M., 1976. Introduction and explanatory notes, leg 38, deep sea
3510 drilling project. Initial Reports DSDP 38.
3511
3512 Tappin, D.R., Watts, P., McMurtry, G.M., Lafoy, Y., Matsumoto, T., 2001. The Sissano, Papua New
3513 Guinea tsunami of July 1998 - offshore evidence on the source mechanism. *Mar Geol* 175, 1-23.
3514
3515 Tasianias, A., Martens, I., Bünz, S., Mienert, J., 2016. Mechanisms initiating fluid migration at Snøhvit
3516 and Albatross fields, Barents Sea. *arktos* 2, 26.
3517
3518 Taylor, J., Dowdeswell, J.A., Kenyon, N.H., Ó Cofaigh, C., 2002a. Late Quaternary architecture of
3519 trough-mouth fans: debris flows and suspended sediments on the Norwegian margin. *Geological*
3520 *Society, London, Special Publications* 203, 55-71.
3521
3522 Taylor, J., Dowdeswell, J.A., Siegert, M.J., 2002b. Late Weichselian depositional processes, fluxes,
3523 and sediment volumes on the margins of the Norwegian Sea (62–75 N). *Mar Geol* 188, 61-77.
3524
3525 ten Brink, U.S., Lee, H.J., Geist, E.L., Twichell, D., 2009. Assessment of tsunami hazard to the US East
3526 Coast using relationships between submarine landslides and earthquakes. *Mar Geol* 264, 65-73.
3527
3528 ten Brink, U.S., Schneider, C., Johnson, A.H., 1995. Morphology and Stratal Geometry of the Antarctic
3529 Continental Shelf: Insights from Models, in: Cooper, A.K., Barker, P.F., Brancolini, G. (Eds.), *Geology*
3530 *and Seismic Stratigraphy of the Antarctic Margin*. American Geophysical Union, pp. 1-24.
3531
3532 Thiede, J., Eldholm, O., Taylor, E., 1989. Variability of Cenozoic Norwegian-Greenland Sea
3533 paleoceanography and northern hemisphere paleoclimate, *Proceedings of the Ocean Drilling*
3534 *Program, Scientific Results*, pp. 1067-1118.
3535
3536 Thiede, J., Winkler, A., Wolf-Welling, T.C.W., Eldholm, O., Myhre, A.M., Baumann, K.-H., Henrich, R.,
3537 Stein, R., 1998. Late Cenozoic history of the polar North Atlantic: results from ocean drilling.
3538 *Quaternary Sci Rev* 17, 185-208.
3539
3540 Thierens, M., Pirlet, H., Colin, C., Latruwe, K., Vanhaecke, F., Lee, J.R., Stuut, J.-B., Titschack, J.,
3541 Huvenne, V.A.I., Dorschel, B., 2012. Ice-rafting from the British–Irish ice sheet since the earliest

3542 Pleistocene (2.6 million years ago): implications for long-term mid-latitudinal ice-sheet growth in the
3543 North Atlantic region. *Quaternary Sci Rev* 44, 229-240.
3544
3545 Thomas, S., Hooper, J., Clare, M.A., 2010. Constraining geohazards to the past: Impact assessment of
3546 submarine mass movements on seabed developments, *Adv Nat Tech Haz Res*. Springer, pp. 387-398.
3547
3548 Tripsanas, E.K., Piper, D.J.W., 2008a. Glaciogenic debris-flow deposits of Orphan Basin, offshore
3549 eastern Canada: sedimentological and rheological properties, origin, and relationship to meltwater
3550 discharge. *Journal of Sedimentary Research* 78, 724-744.
3551
3552 Tripsanas, E.K., Piper, D.J.W., 2008b. Late Quaternary stratigraphy and sedimentology of Orphan
3553 Basin: implications for meltwater dispersal in the southern Labrador Sea. *Palaeogeography,*
3554 *Palaeoclimatology, Palaeoecology* 260, 521-539.
3555
3556 Trofimuk, A., Cherskiy, N., Tsarev, V., 1977. The role of continental glaciation and hydrate formation
3557 on petroleum occurrences, *Future supply of nature made petroleum and gas*. Pergamon, New York,
3558 pp. 919-926.
3559
3560 Tveranger, J., Houmark-Nielsen, M., Løvberg, K., Mangerud, J., 1994. Eemian-Weichselian
3561 stratigraphy of the Flakkerhuk ridge, southern Jameson Land, East Greenland. *Boreas* 23, 359-384.
3562
3563 Tziperman, E., Gildor, H., 2003. On the mid-Pleistocene transition to 100-kyr glacial cycles and the
3564 asymmetry between glaciation and deglaciation times. *Paleoceanography* 18.
3565
3566 Urciuoli, G., Picarelli, L., Leroueil, S., 2007. Local soil failure before general slope failure. *Geotechnical*
3567 *and Geological Engineering* 25, 103-122.
3568
3569 Urlaub, M., Talling, P.J., Clare, M.A., 2014. Sea-level-induced seismicity and submarine landslide
3570 occurrence: Comment. *Geology* 42, e337.
3571
3572 Urlaub, M., Zervos, A., Talling, P.J., Masson, D.G., Clayton, C.I., 2012. How Do ~2° Slopes Fail in Areas
3573 of Slow Sedimentation? A Sensitivity Study on the Influence of Accumulation Rate and Permeability
3574 on Submarine Slope Stability, in: Yamada, Y., Kawamura, K., Ikehara, K., Ogawa, Y., Urgeles, R.,
3575 Mosher, D., Chaytor, J., Strasser, M. (Eds.), *Adv Nat Tech Haz Res*. Springer Netherlands, pp. 277-287.
3576
3577 Vadakkepuliymbatta, S., Bünz, S., Mienert, J., Chand, S., 2013. Distribution of subsurface fluid-flow
3578 systems in the SW Barents Sea. *Mar Petrol Geol* 43, 208-221.
3579
3580 Vail, P.R., Mitchum Jr, R.M., Thompson III, S., 1977. Seismic stratigraphy and global changes of sea
3581 level: Part 4. Global cycles of relative sea level change., in: Payton, C.E. (Ed.), *Seismic stratigraphy -*
3582 *Applications to hydrocarbon exploration: American Association of Petroleum Geologists Memoir* 26,
3583 pp. 83-97.
3584
3585 Vanneste, K., Uenzelmann-Neben, G., Miller, H., 1995. Seismic evidence for long-term history of
3586 glaciation on central East Greenland shelf south of Scoresby Sund. *Geo-Mar Lett* 15, 63-70.
3587
3588 Vanoudheusden, E., Sultan, N., Cochonat, P., 2004. Mechanical behaviour of unsaturated marine
3589 sediments: experimental and theoretical approaches. *Mar Geol* 213, 323-342.
3590
3591 Velichko, A.A., Pisareva, V.V., Faustova, M.A., 2005. Glaciations and interglacials of East European
3592 plain in the Early and Middle Pleistocene. *Stratigr. Geol. Correl* 13, 195-211.

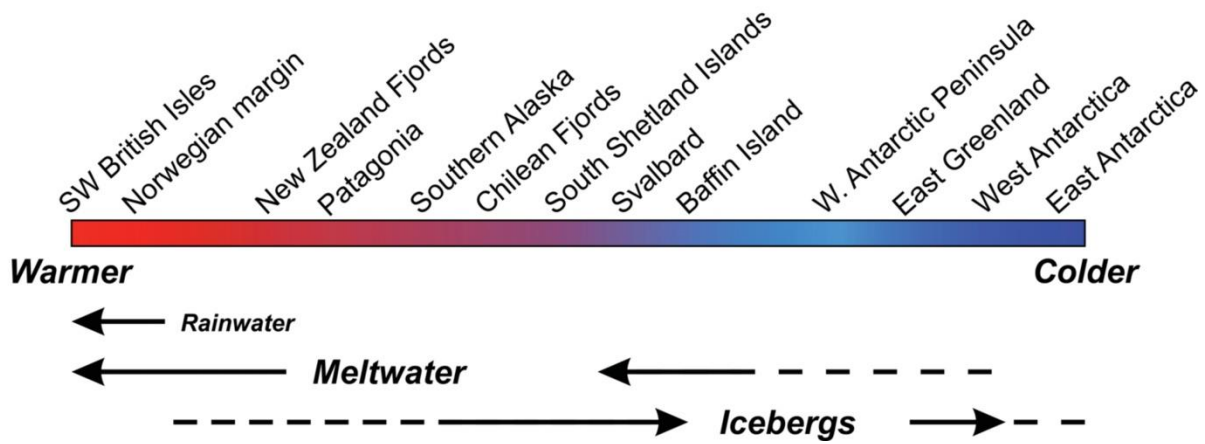
3593
3594 Vogt, C., Knies, J., 2008. Sediment dynamics in the Eurasian Arctic Ocean during the last
3595 deglaciation—the clay mineral group smectite perspective. *Mar Geol* 250, 211-222.
3596
3597 Vogt, C., Knies, J., Spielhagen, R.F., Stein, R., 2001. Detailed mineralogical evidence for two nearly
3598 identical glacial/deglacial cycles and Atlantic water advection to the Arctic Ocean during the last
3599 90,000 years. *Global and Planetary Change* 31, 23-44.
3600
3601 Völker, D., Scholz, F., Geersen, J., 2011. Analysis of submarine landsliding in the rupture area of the
3602 27 February 2010 Maule earthquake, Central Chile. *Mar Geol* 288, 79-89.
3603
3604 Vorren, T.O., Laberg, J.S., 1997. Trough mouth fans—palaeoclimate and ice-sheet monitors.
3605 *Quaternary Sci Rev* 16, 865-881.
3606
3607 Vorren, T.O., Laberg, J.S., Blaume, F., Dowdeswell, J.A., Kenyon, N.H., Mienert, J., Rumohr, J.,
3608 Werner, F., 1998. The Norwegian Greenland Sea continental margins: Morphology and late
3609 Quaternary sedimentary processes and environment. *Quaternary Sci Rev* 17, 273-302.
3610
3611 Vorren, T.O., Landvik, J.Y., Andreassen, K., Laberg, J.S., 2011. Glacial history of the Barents Sea
3612 region. *Quaternary Glaciations—Extent and Chronology—A Closer Look*, *Dev. in Quat. Sci.* 361-372.
3613
3614 Vorren, T.O., Lebesbye, E., Andreassen, K., Larsen, K.-B., 1989. Glacigenic sediments on a passive
3615 continental margin as exemplified by the Barents Sea. *Mar Geol* 85, 251-272.
3616
3617 Vorren, T.O., Lebesbye, E., Larsen, K.B., 1990. Geometry and genesis of the glacigenic sediments in
3618 the southern Barents Sea. *Geological Society, London, Special Publications* 53, 269-288.
3619
3620 Vorren, T.O., Plassen, L.I.V., 2002. Deglaciation and palaeoclimate of the Andfjord-Vågsfjord area,
3621 North Norway. *Boreas* 31, 97-125.
3622
3623 Waddington, C., Wicks, K., 2017. Resilience or wipe out? Evaluating the convergent impacts of the
3624 8.2 ka event and Storegga tsunami on the Mesolithic of northeast Britain. *Journal of Archaeological*
3625 *Science: Reports* 14, 692-714.
3626
3627 Waythomas, C.F., Watts, P., 2003. Numerical simulation of tsunami generation by pyroclastic flow at
3628 Aniakchak Volcano, Alaska. *Geophys Res Lett* 30.
3629
3630 Waythomas, C.F., Watts, P., Walder, J.S., 2006. Numerical simulation of tsunami generation by cold
3631 volcanic mass flows at Augustine Volcano, Alaska. *Natural Hazards & Earth System Sciences* 6.
3632
3633 Weaver, A.J., Saenko, O.A., Clark, P.U., Mitrovica, J.X., 2003. Meltwater pulse 1A from Antarctica as a
3634 trigger of the Bølling-Allerød warm interval. *Science* 299, 1709-1713.
3635
3636 Weaver, P.P.E., Kuijpers, A., 1983. Climatic control of turbidite deposition on the Madeira Abyssal
3637 Plain.
3638
3639 Weber, M.E., Bonani, G., Fütterer, K.D., 1994. Sedimentation processes within channel-ridge
3640 systems, southeastern Weddell Sea, Antarctica. *Paleoceanography* 9, 1027-1048.
3641
3642 Weber, M.E., Clark, P.U., Ricken, W., Mitrovica, J.X., Hostetler, S.W., Kuhn, G., 2011.
3643 Interhemispheric ice-sheet synchronicity during the Last Glacial Maximum. *Science* 334, 1265-1269.

3644
3645 Wellner, J.S., Heroy, D.C., Anderson, J.B., 2006. The death mask of the Antarctic ice sheet:
3646 comparison of glacial geomorphic features across the continental shelf. *Geomorphology* 75, 157-
3647 171.
3648
3649 Wellner, J.S., Lowe, A.L., Shipp, S.S., Anderson, J.B., 2001. Distribution of glacial geomorphic features
3650 on the Antarctic continental shelf and correlation with substrate: implications for ice behavior. *J*
3651 *Glaciol* 47, 397-411.
3652
3653 Weninger, B., Schulting, R., Bradtmöller, M., Lee, C., Collard, M., Edinborough, K., Hilpert, J., Jöris, O.,
3654 Niekus, M., Rohling, E.J., 2008. The catastrophic final flooding of Doggerland by the Storegga Slide
3655 tsunami. *Documenta Praehistorica* 35, 1.
3656
3657 Wicks, K., Mithen, S., 2014. The impact of the abrupt 8.2 ka cold event on the Mesolithic population
3658 of western Scotland: a Bayesian chronological analysis using 'activity events' as a population proxy.
3659 *Journal of Archaeological Science* 45, 240-269.
3660
3661 Wilken, M., Mienert, J., 2006. Submarine glacial debris flows, deep-sea channels and past ice-
3662 stream behaviour of the East Greenland continental margin. *Quaternary Sci Rev* 25, 784-810.
3663
3664 Winkelmann, D., Jokat, W., Jensen, L., Schenke, H.-W., 2010. Submarine end moraines on the
3665 continental shelf off NE Greenland—Implications for Lateglacial dynamics. *Quaternary Sci Rev* 29,
3666 1069-1077.
3667
3668 Winkler, A., Wolf-Welling, T., Stattegger, K., Thiede, J., 2002. Clay mineral sedimentation in high
3669 northern latitude deep-sea basins since the Middle Miocene (ODP Leg 151, NAAG). *International*
3670 *Journal of Earth Sciences* 91, 133-148.
3671
3672 Winsborrow, M.C.M., Andreassen, K., Corner, G.D., Laberg, J.S., 2010. Deglaciation of a marine-
3673 based ice sheet: Late Weichselian palaeo-ice dynamics and retreat in the southern Barents Sea
3674 reconstructed from onshore and offshore glacial geomorphology. *Quaternary Sci Rev* 29, 424-442.
3675
3676 Winsborrow, M.C.M., Stokes, C.R., Andreassen, K., 2012. Ice-stream flow switching during
3677 deglaciation of the southwestern Barents Sea. *Geological Society of America Bulletin* 124, 275-290.
3678
3679 Wolf-Welling, T.C.W., Cremer, M., O'Connell, S., Winkler, A., Thiede, J., 1996. Cenozoic Arctic
3680 gateway paleoclimate variability: Indications from changes in coarse-fraction composition,
3681 *Proceedings of the Ocean Drilling Program. Scientific Results. Ocean Drilling Program*, pp. 515-567.
3682
3683 Zachos, J., Pagani, M., Sloan, L., Thomas, E., Billups, K., 2001. Trends, rhythms, and aberrations in
3684 global climate 65 Ma to present. *Science* 292, 686-693.
3685
3686 Zajaczkowski, M., 2008. Sediment supply and fluxes in glacial and outwash fjords, Kongsfjorden and
3687 Adventfjorden, Svalbard. *Polish Polar Research* 29, 59-72.
3688
3689 Zieba, K.J., Grøver, A., 2016. Isostatic response to glacial erosion, deposition and ice loading. Impact
3690 on hydrocarbon traps of the southwestern Barents Sea. *Mar Petrol Geol* 78, 168-183.
3691
3692 Ziegler, P.A., 1990. *Geological atlas of western and central Europe*. Geological Society of London.
3693

a) Modern, Quaternary interglacial



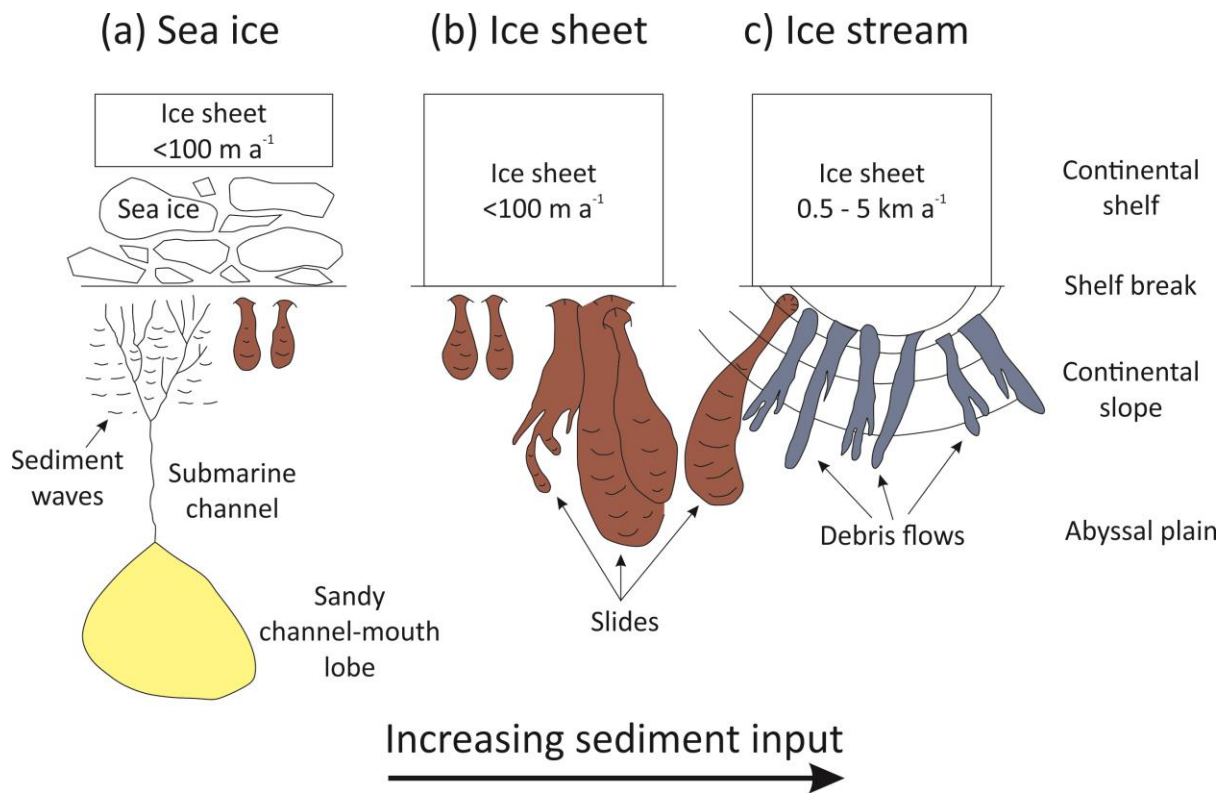
b) Quaternary full-glacial



3696

3697 Fig. 1. The climatic continuum of glacier-influenced marine settings for (a) the modern, or
 3698 Quaternary interglacial Earth, and (b) Quaternary full-glacial conditions. Adapted from Dowdeswell
 3699 et al. (2006b).

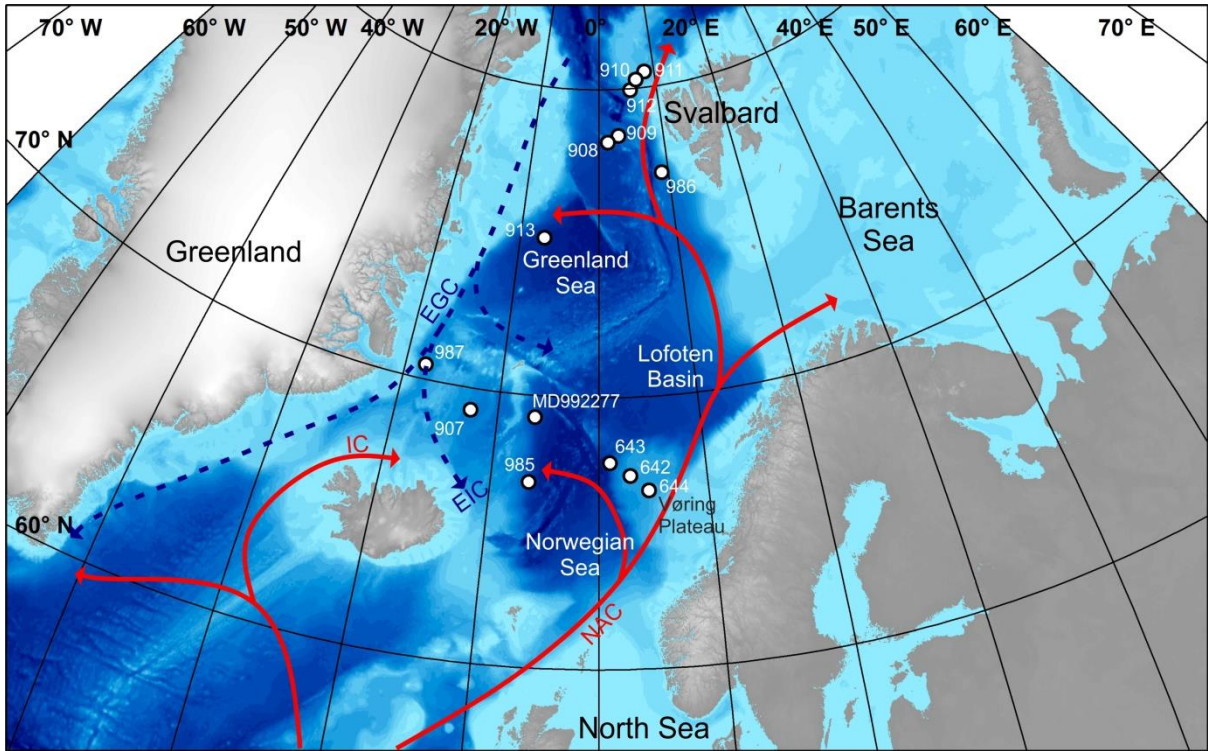
3700



3701

3702 Fig. 2. Conceptual model of sedimentation on glacier-influenced continental margins. a) Sediment
 3703 starved margin with an ice sheet terminating inshore of the shelf edge. b) Inter-ice stream areas with
 3704 ice at the shelf edge. c) Continental margin dominated by ice stream delivery of sediment and the
 3705 resulting formation of a trough-mouth fan (adapted from Dowdeswell et al., 1996).

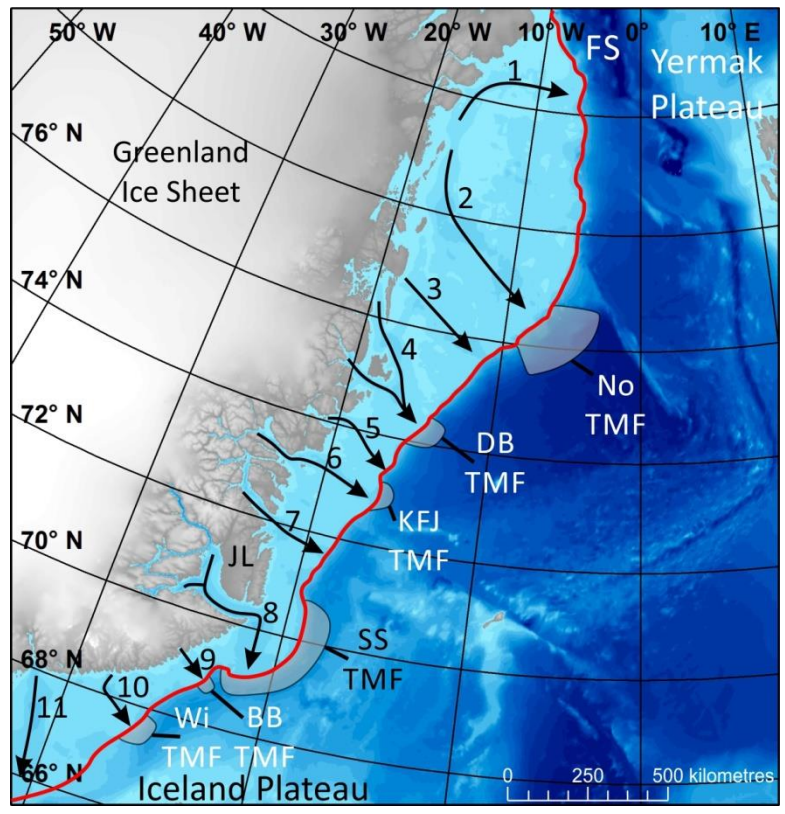
3706



3707

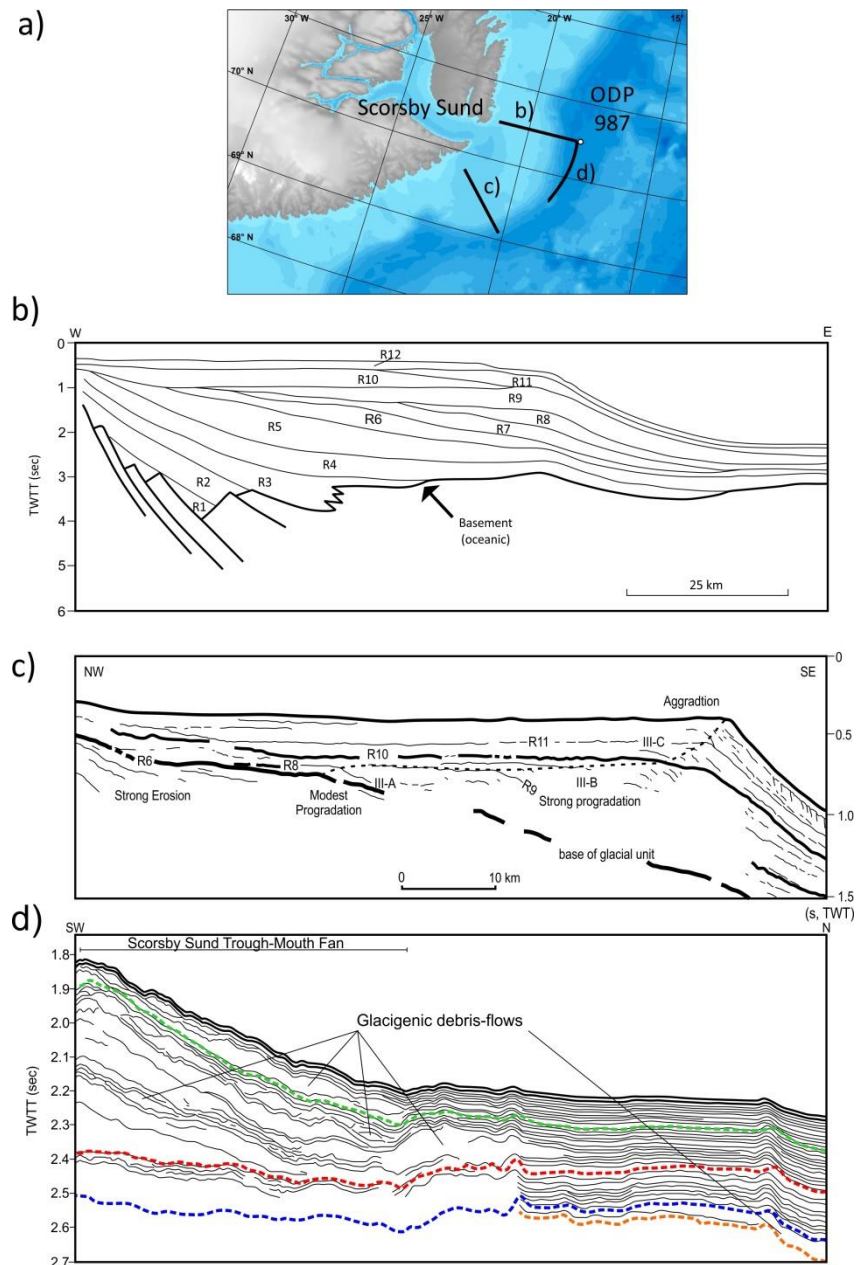
3708 Fig. 3. Map of the Nordic Seas and the ODP sites used in this study. General ocean circulation during
 3709 the present interglacial is also shown (red – warm; blue – cold). NAC – Norwegian Atlantic Current;
 3710 EGC – East Greenland Current; EIC – East Iceland Current; IC – Irminger Current.

3711



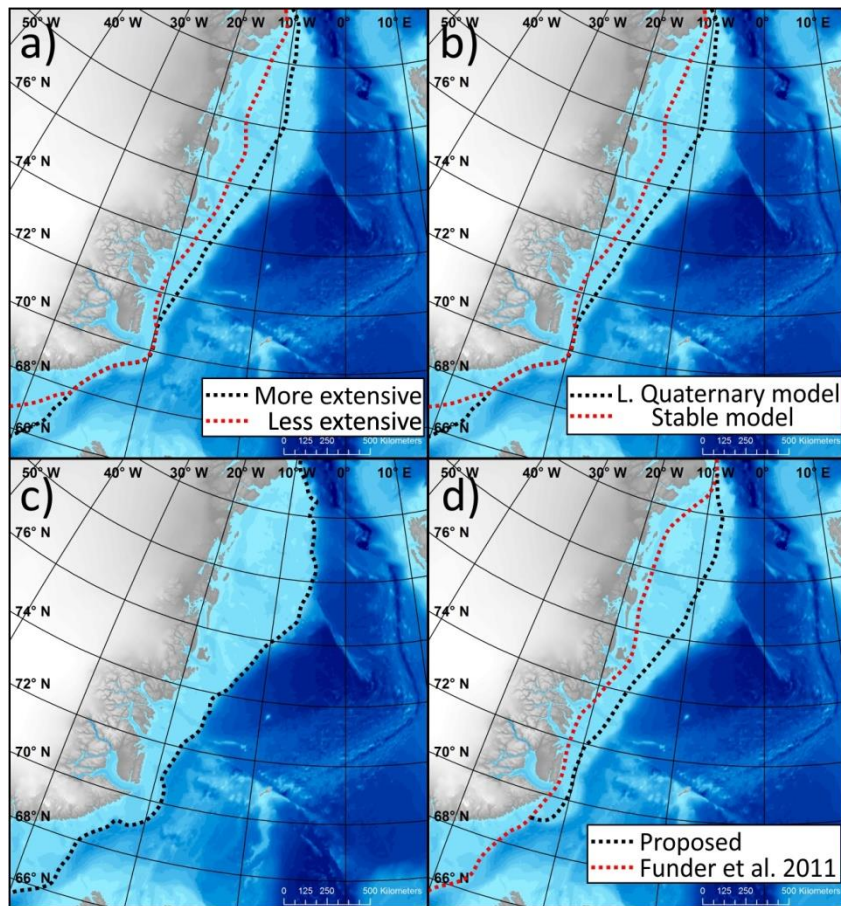
3712

3713 Fig. 4. Maximum Quaternary extent of the Greenland Ice Sheet in East Greenland (red line) with
 3714 notable cross-shelf troughs and trough-mouth fans displayed on IBCAO bathymetric data (Jakobsson
 3715 et al., 2012). Arrows indicate cross-shelf troughs thought to have previously contained ice streams. 1
 3716 = Westwind. 2 = Norske. 3 = Store Koldewey. 4 = Dove Bugt. 5 = Unnamed. 6 = Kaiser Franz Josef. 7 =
 3717 Kong Oscar. 8 = Scorsby Sund. 9 = Barclay Bugt. 10 = Wiedemann. 11 = Kangerdlussuaq. Trough-
 3718 mouth fans/bulges in bathymetry indicated by grey shading (Batchelor et al., 2014). No TMF =
 3719 Norske Trough-Mouth Fan. DB TMF = Dove Bugt Trough-Mouth Fan. KFJ TMF = Kaiser Franz Josef
 3720 Trough-Mouth Fan. SS TMF = Scorseby Sund Trough-Mouth Fan. BB TMF = Barclay Bugt Trough
 3721 Mouth Fan. Wi TMF = Wiedemann Trough Mouth Fan. FS = Fram Strait. JL = Jameson Land.



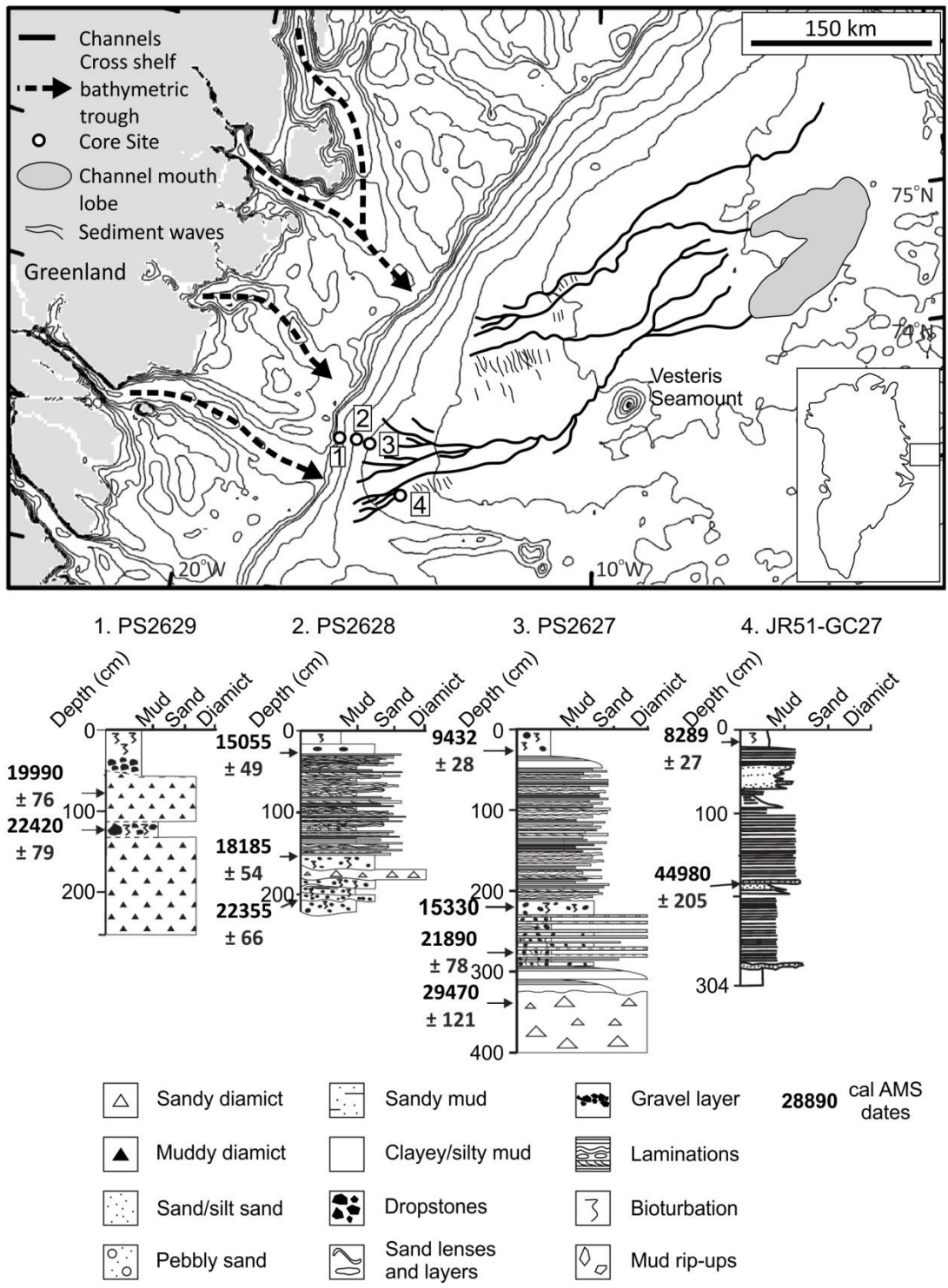
3722

3723 Fig. 5. Multichannel seismic lines on the Scoresby Sund Trough-Mouth Fan (modified from Vanneste
 3724 et al., 1995; Solheim et al., 1998; Laberg et al., 2013). a) Location map showing seismic lines GGU 82-
 3725 12 and 90600 and the line of Laberg et al. (2013), and the relative position of ODP Site 987. b)
 3726 Seismic line GGU 82-12. According to Larson's (1990) original interpretation sequences 9 – 11
 3727 represent Late Miocene to Pliocene and 12 represents the Pleistocene. c) Interpretation of the
 3728 stratal geometry in the continental shelf part of line 90600. Based on variations in the aggradation
 3729 and progradation components, the glacial unit, Unit III, has been divided into subunits A (2.6 – 1.2
 3730 Ma), B (1.2 – 0.5 Ma), and C (0.5 – 0 Ma). d) Single channel seismic profile extending from ODP Site
 3731 987 southward. Lithological units, age model and seismic reflections according to Shipboard
 3732 Scientific Party (1996) are reflected by dashed lines. Green – 0.78 Ma; Red – R1 reflector at 1.77 Ma;
 3733 Blue – R2 reflector; Orange – 2.58 Ma.



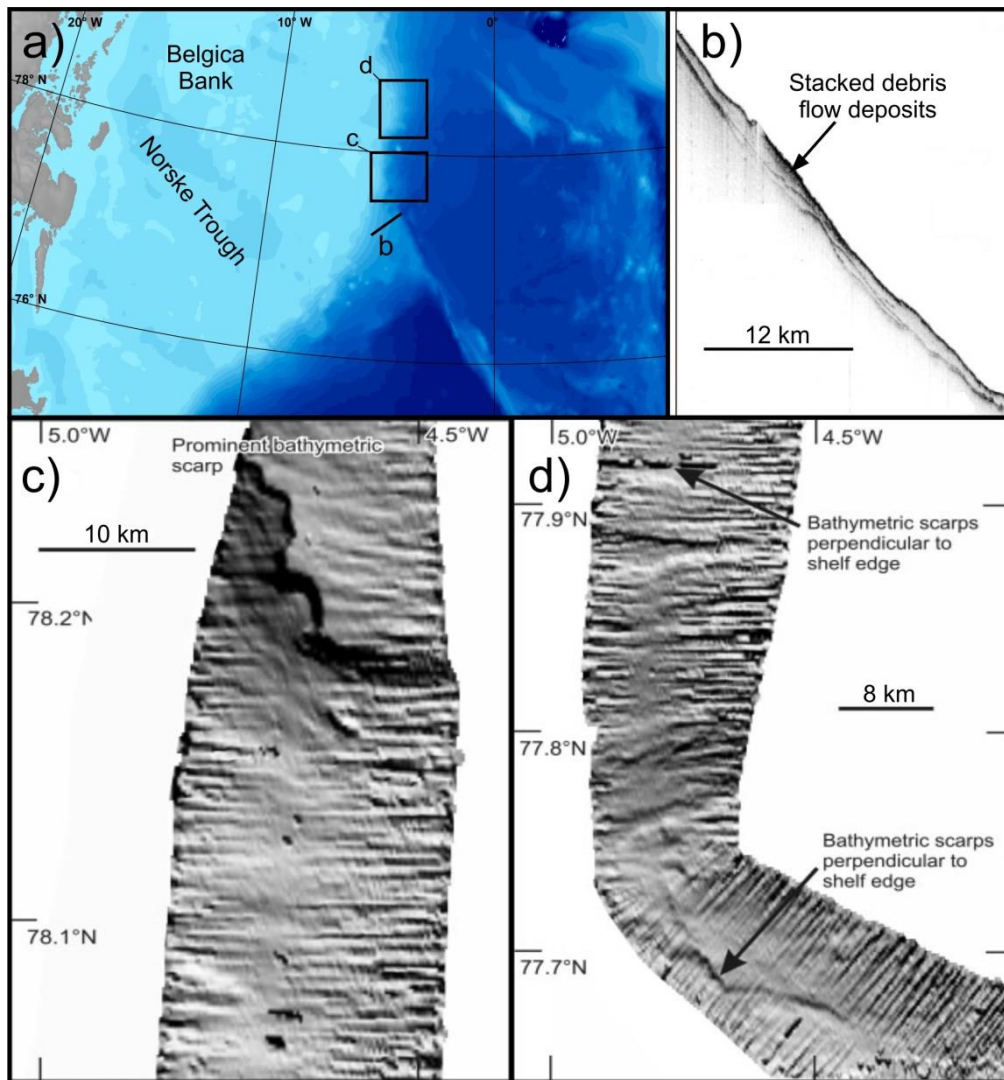
3734

3735 Fig. 6. Maximum extents of the Greenland Ice Sheet on the East Greenland Margin. a) 2.58 – 1.3 Ma.
 3736 Two regimes of advance and retreat are envisaged for this period; an extensive advance regime (2.5
 3737 – 2.4 and ~2.1 Ma) and a less extensive advance regime. The ice sheet appears not to have
 3738 undergone widespread collapses (Solheim et al., 1998). b) 1.3 – 0.7 Ma. Two regimes are again
 3739 envisaged, a stable confined ice sheet or a dynamic ice sheet akin to the Late Quaternary Greenland
 3740 Ice Sheet (Winkelmann et al., 2010). c) 0.7 – 0.13 Ma. Maximum extent of the Saalian Greenland Ice
 3741 Sheet; the margin position of other advances between 0.7 and 0.13 are uncertain. d) 0.13 – 0 Ma.
 3742 Maximum ice sheet extent according to Funder et al. (2011) and a revised limit based on shelf
 3743 geomorphology. A large degree of uncertainty exists regarding the shown ice sheet margins. Even
 3744 the Weichselian reconstruction is largely inferred.



3745

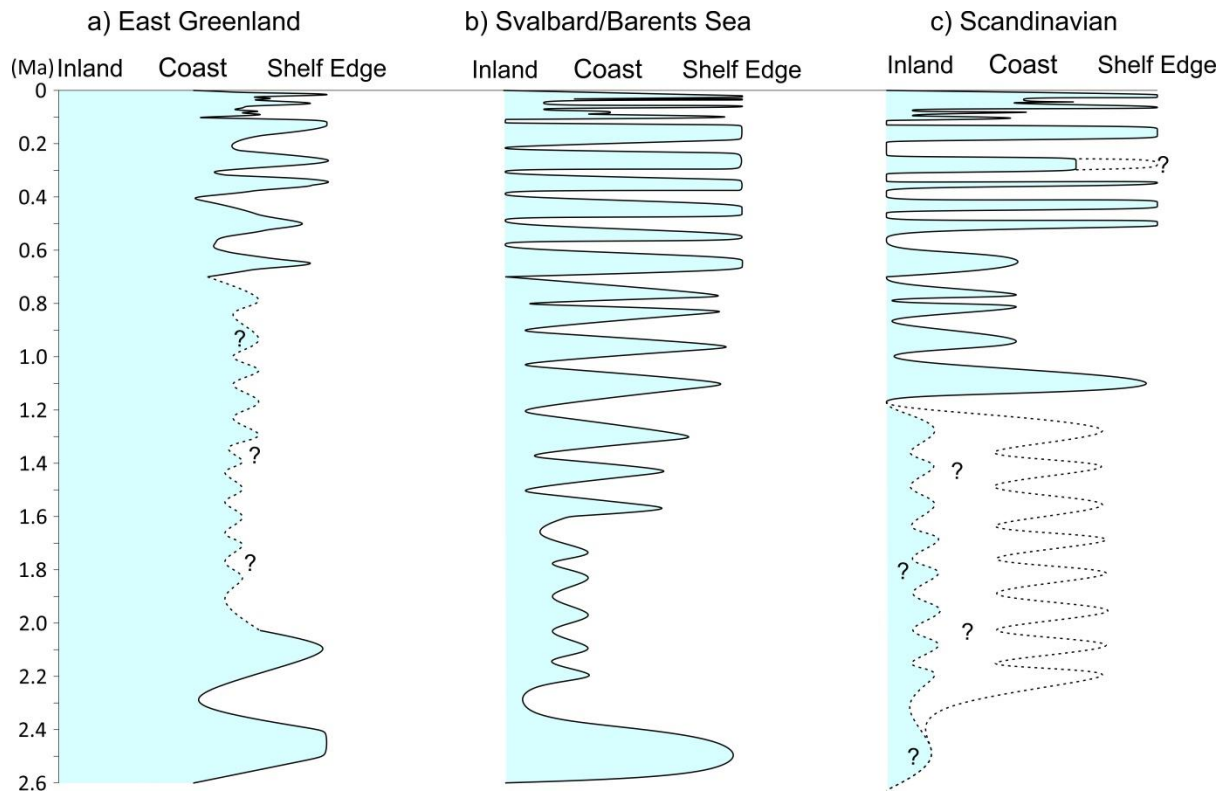
3746 Fig. 7. Bathymetry of the Greenland Basin and the adjoining continental shelf, northeast Greenland
 3747 and major submarine geological features (channel systems, sediment waves and channel-mouth
 3748 lobes). Major cross-shelf troughs on the continental shelf are highlighted by arrows. Core sites are
 3749 numbered 1 to 4. Sediment logs of gravity cores identified on the bathymetric map are included with
 3750 calibrated AMS radiocarbon dates. Bathymetric data on continental shelf are derived from the
 3751 IBCAO Arctic bathymetry database (Jakobsson et al., 2000). Figure is adapted from Ó Cofaigh et al.
 3752 (2004).



3753

3754 Fig. 8. a) Location map of the northeast Greenland continental margin. b) TOPAS sub-bottom
 3755 acoustic profile. Along slope profile from the upper-middle slope showing acoustically transparent
 3756 sediment lenses interpreted as stacked debris-flow deposits. c) and d) EM120 shaded swath
 3757 bathymetry from the northeast Greenland continental slope showing prominent and sinuous
 3758 bathymetric scarps consistent with slide scars produced during the process of sediment failure and
 3759 sliding (adapted from Evans et al., 2009).

3760



3761

3762 Fig. 9. Schematic glaciation curves for the general behaviour of the Greenland, Barents Sea and
 3763 Scandinavian Ice Sheets. Dashed lines and question marks represent time periods where there is a
 3764 lack of data from various margins or conflicting interpretations of ice sheet extent.

3765

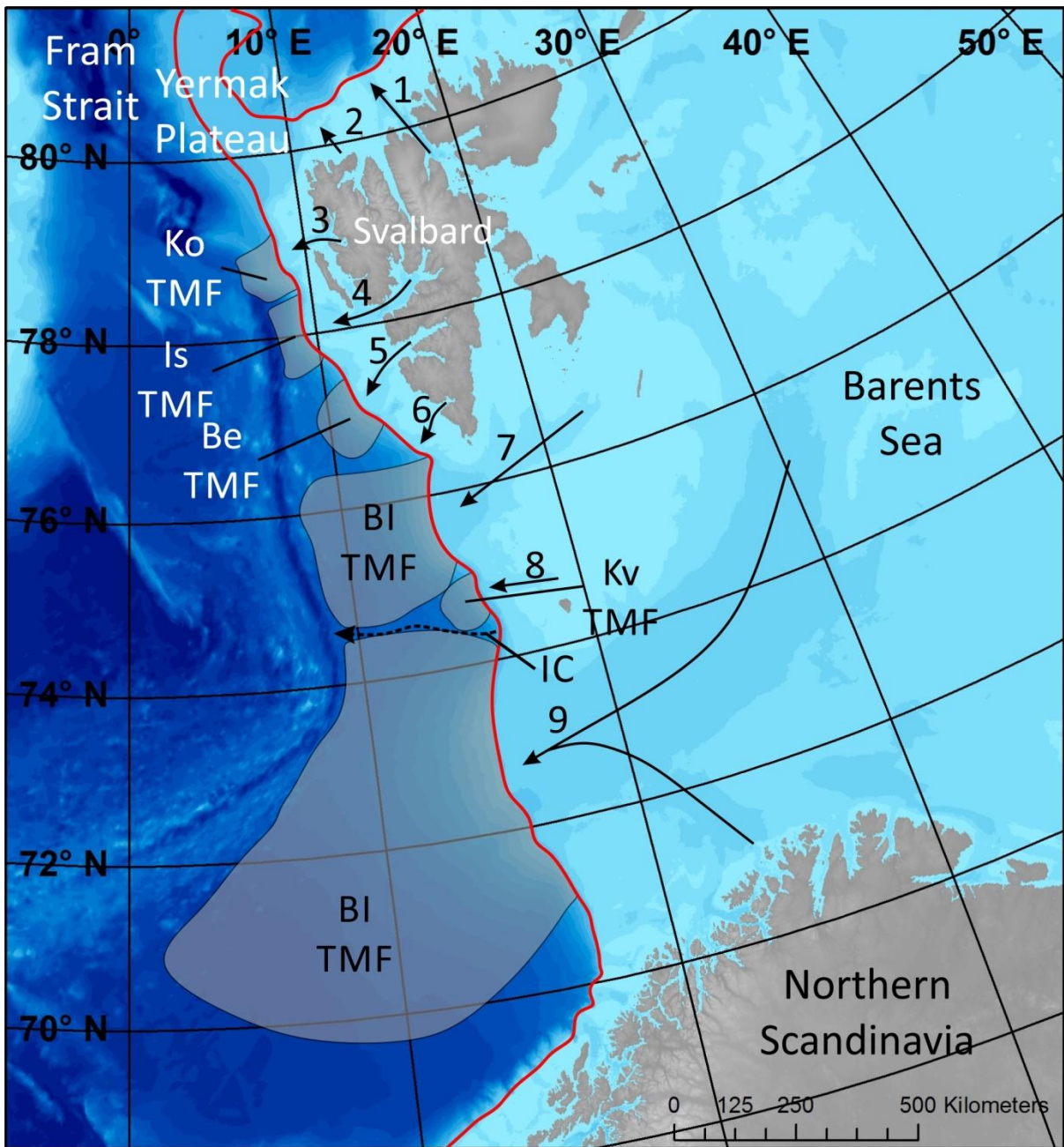
3766

3767

3768

3769

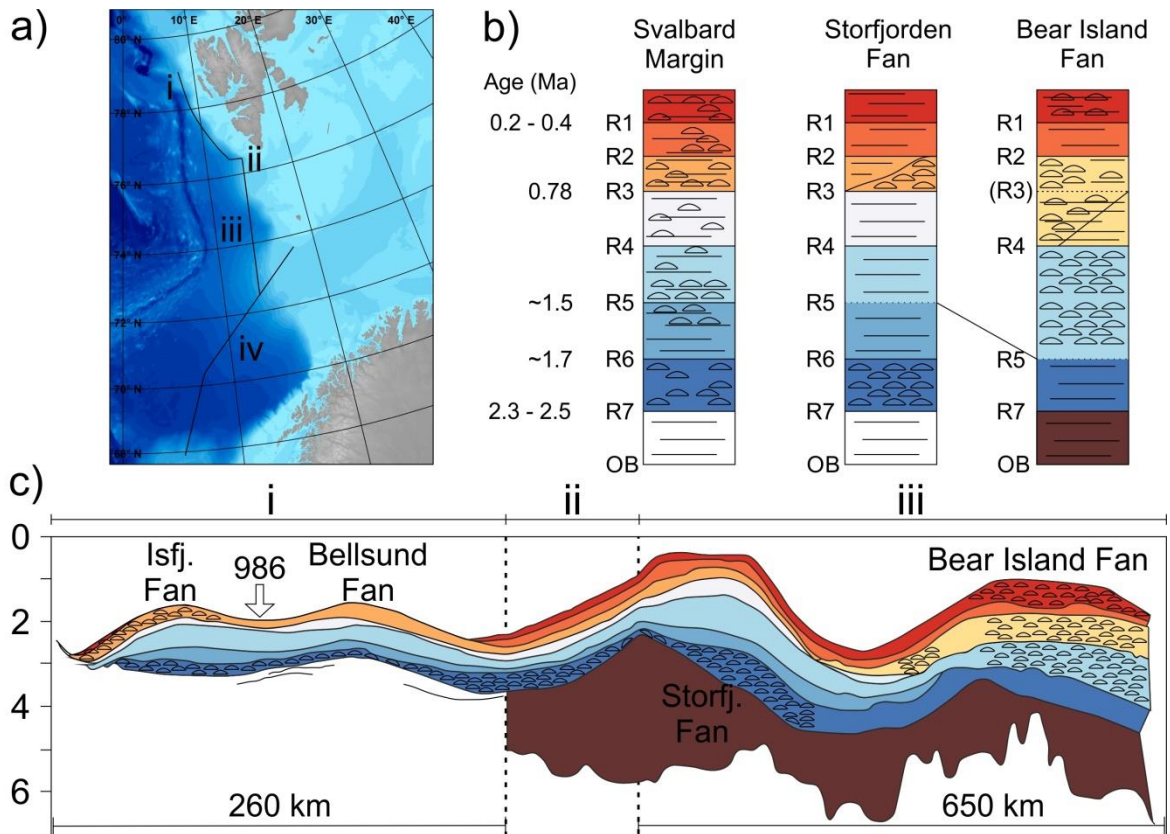
3770



3771

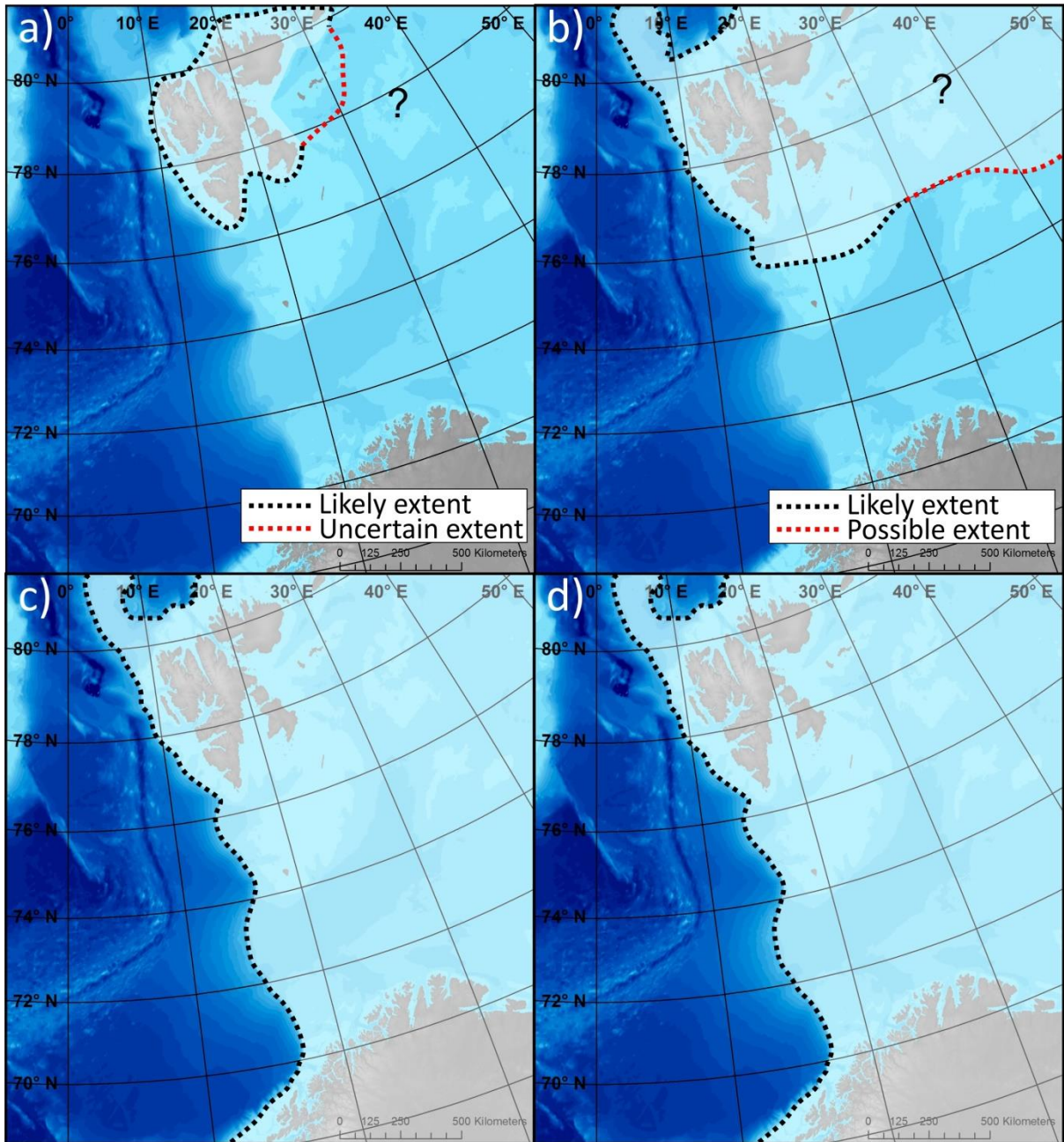
3772 Fig. 10. Maximum westward Quaternary extent of the Barents Sea Ice Sheet (red line) with notable
 3773 gross-shelf troughs and trough-mouth fans displayed on IBCAO bathymetric data (Jakobsson et al.,
 3774 2012). Arrows indicate cross-shelf troughs thought to have previously contained ice streams. 1 =
 3775 Hinlopen. 2 = Woodfjorden. 3 = Kongsfjorden. 4 = Isfjorden. 5 = Bellsund. 6 = Hornsund. 7 =
 3776 Storfjorden. 8 = Kveithola. 9 = Bear Island. Trough-Mouth Fans on the Svalbard/Barents Sea
 3777 southwest margin shown by grey shaded regions (Ottesen et al., 2006). Ko TMF = Kongsfjorden
 3778 Trough-Mouth Fan. Is TMF = Trough-Mouth Fan. Be TMF = Bellsund Trough-Mouth Fan. Kv TMF =
 3779 Kveithola Trough-Mouth Fan. BI TMF = Bear Island Trough-Mouth Fan. IC = INBIS Channel.

3780



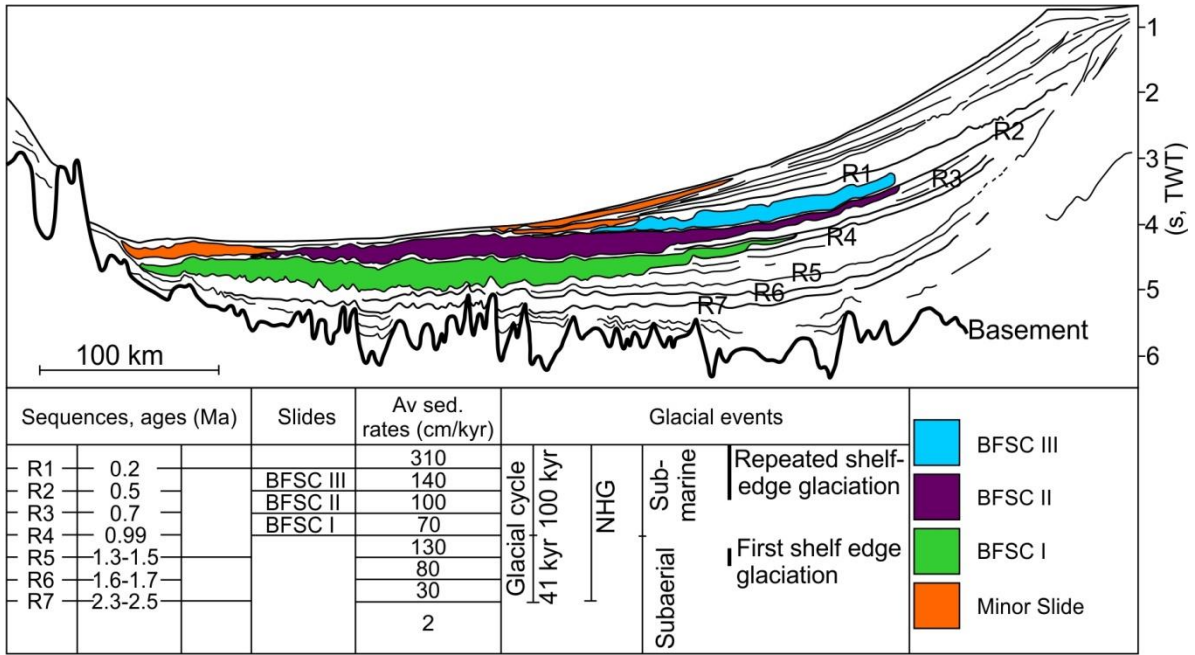
3781 (s, TWT)

3782 Fig. 11. a) Location map of seismic profiles along the Svalbard/Barents Sea continental margin. b)
 3783 Seismic stratigraphic framework for the Svalbard/Barents Sea Margin, with correlation of the main
 3784 sequence boundaries between the Svalbard Margin (Isfjorden), Storfjorden and Bear Island Trough-
 3785 Mouth Fans. c) Composite regional seismic strike-line covering Isfjorden, Bellsund, Storfjorden and
 3786 Bear Island Trough-Mouth Fans. Internal reflection pattern in b) and c) is indicated with changes
 3787 between stratified (parallel lines) and chaotic with mass movement structures (half circle pattern).
 3788 Regional reflectors based on chronology from ODP Site 986 are indicated. Modified from Faleide et
 3789 al. (1996), Jansen et al. (1996) and Solheim et al. (1998).



3790

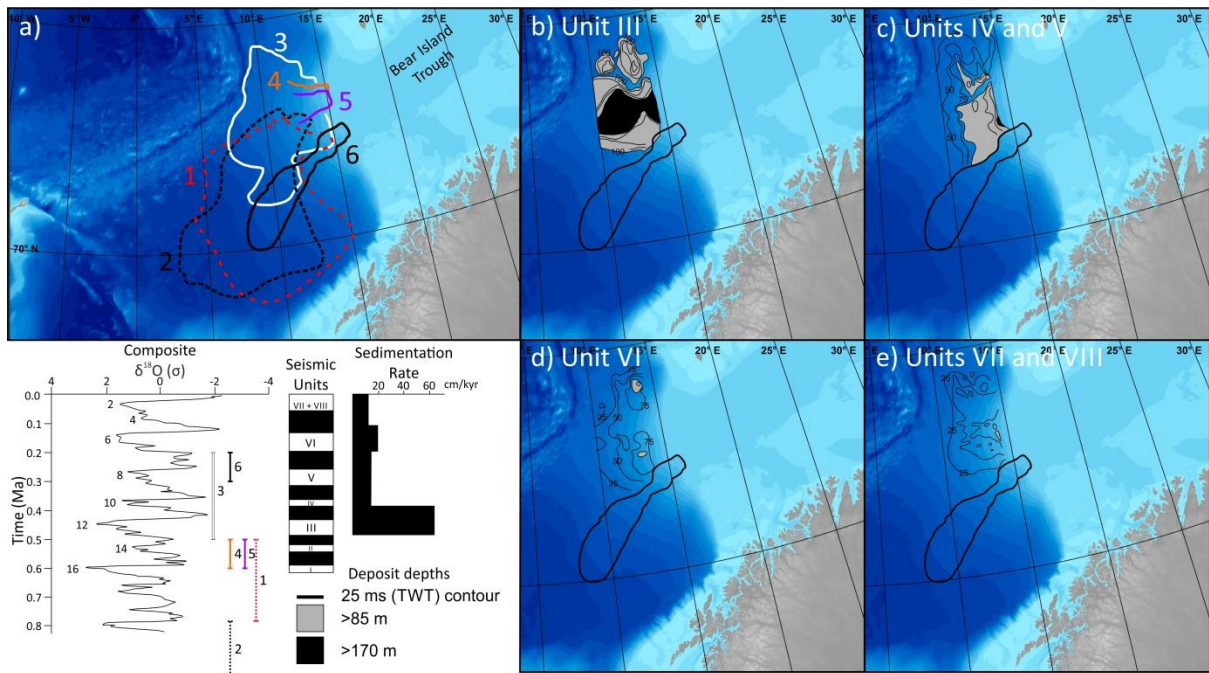
3791 Fig. 12. Maximum extents of the Barents Sea Ice Sheet. a) 2.58 – 1.6 Ma. Limited advance and
 3792 retreat of glaciers on Svalbard. The eastward extent of ice is uncertain (Knies et al., 2009). b) 1.6 –
 3793 1.3 Ma. Glaciers sourced from Svalbard expand sufficiently to reach the shelf edge. Ice masses are
 3794 present in the Northern Barents Sea but southward expansion was limited (Solheim et al., 1998). c)
 3795 1.3 – 0.13 Ma. Glaciers on Svalbard continued to expand sufficiently to reach to shelf edge. Further
 3796 south, the Barents Sea Ice Sheet expanded sufficiently to repeatedly reach the shelf edge along the
 3797 southwestern margin of the Barents Sea (Andreassen et al., 2004; 2007). d) 0.13 – 0 Ma. Maximum
 3798 ice extent of the Weichselian Ice Sheet (Svendsen et al., 2004).



3799

3800 Fig. 13. Seismic transect across the Lofoten Basin from the Bear Island Trough-Mouth Fan to the
 3801 Vøring Plateau (see Fig. 11a). Sequence boundaries (R1 – R7) and submarine landslides (BFSC
 3802 I – III) are indicated. GDF = Glacigenic Debris-Flow deposits. Summary of chronology, average
 3803 depositional rates and main glacial events are shown in the lower panel. Modified from Hjelstuen et
 3804 al. (2007).

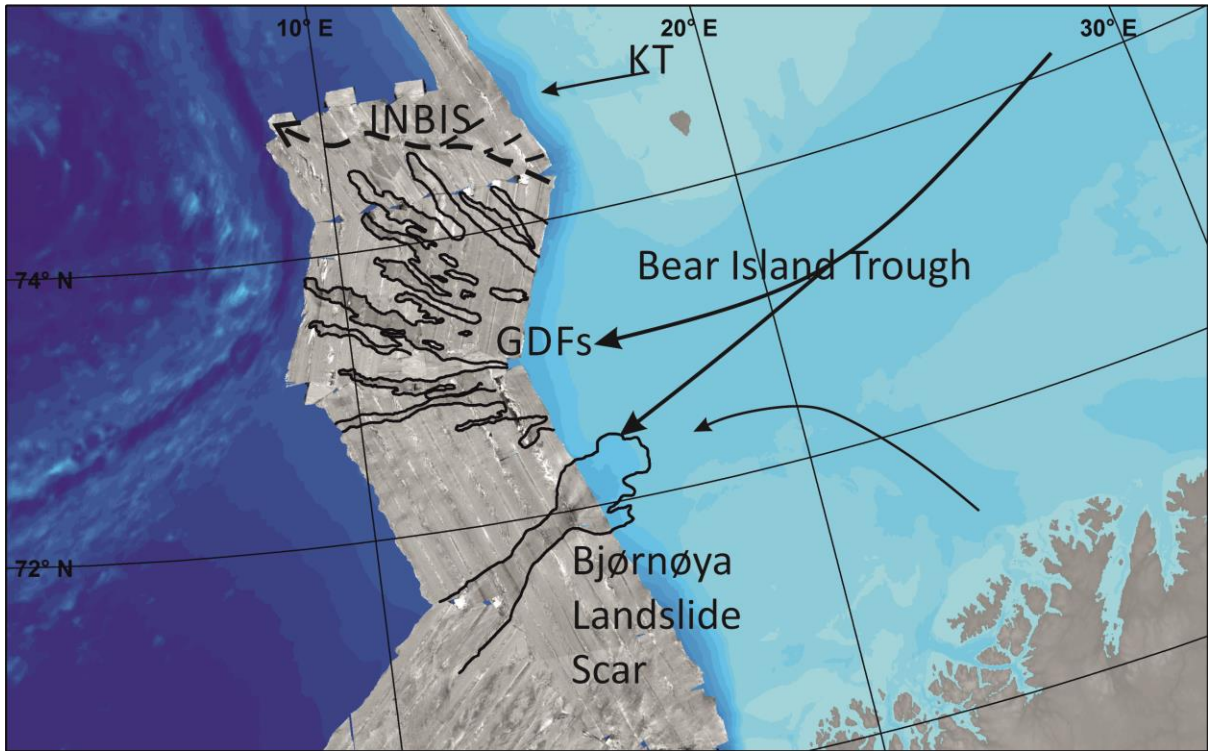
3805



3806

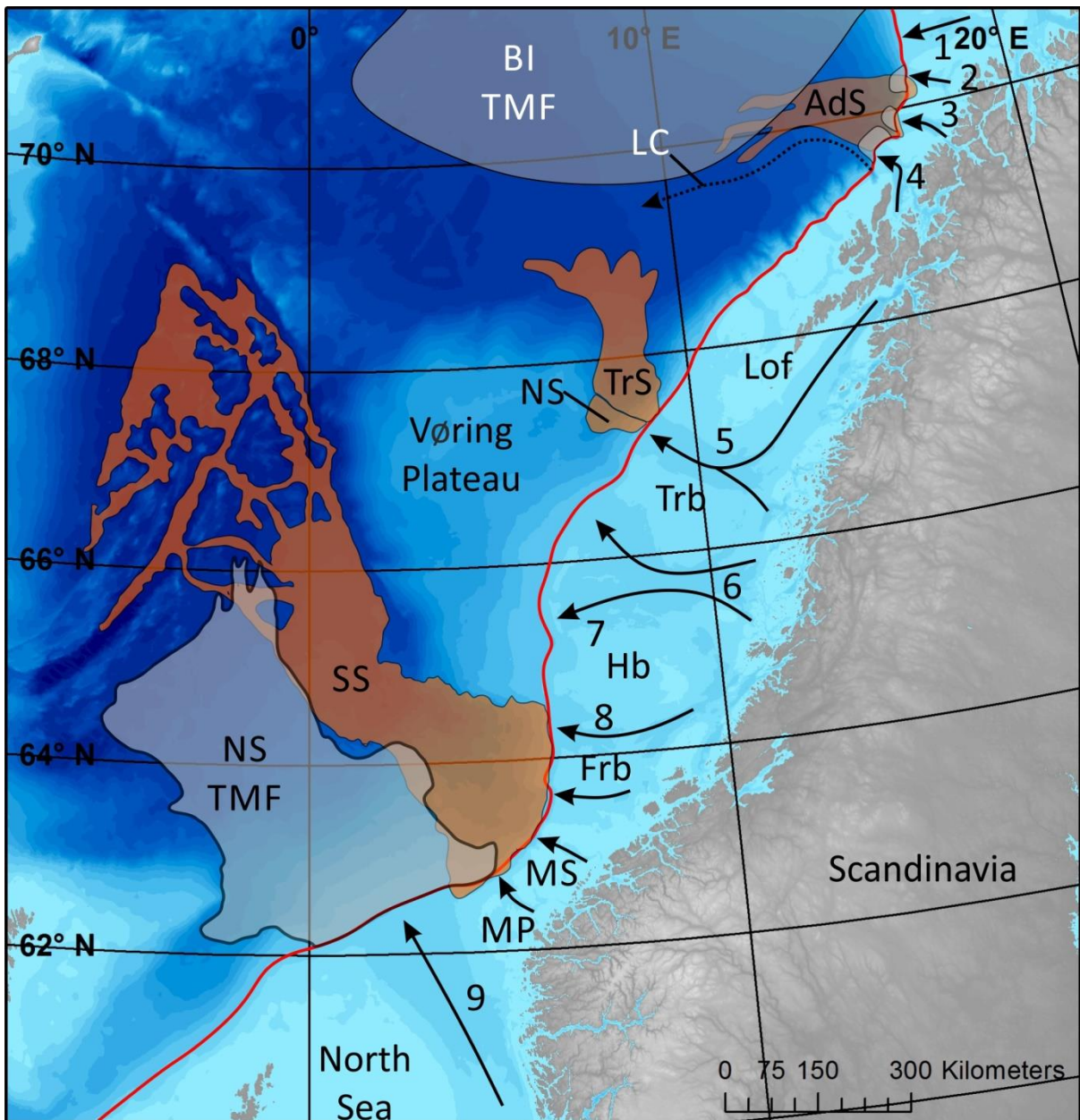
3807 Fig. 14. a) Location of large submarine landslides sourced from the Bear Island Trough-Mouth Fan. 1)
 3808 BFSC II; 2) BFSC I; 3) BFSC III; 4) Slide B; 5) Slide A; 6) Bjørnøya Slide. b) – e) Isopach maps of units
 3809 deposited on the Bear Island Trough-Mouth Fan. Each isopach map is correlated to a given time
 3810 period which can be compared to a composite $\delta^{18}O$ curve and the relative timings of the large
 3811 submarine landslides outlined in a). b) = Unit III; c) = Unit IV and V; d) = Unit VI; e) = Units VII and VIII.
 3812 Contour interval 25 ms (TWT). For depth conversion an internal velocity of 1700 m/s was used.
 3813 Modified from Laberg and Vorren (1996) and Hjelstuen et al. (2007).

3814



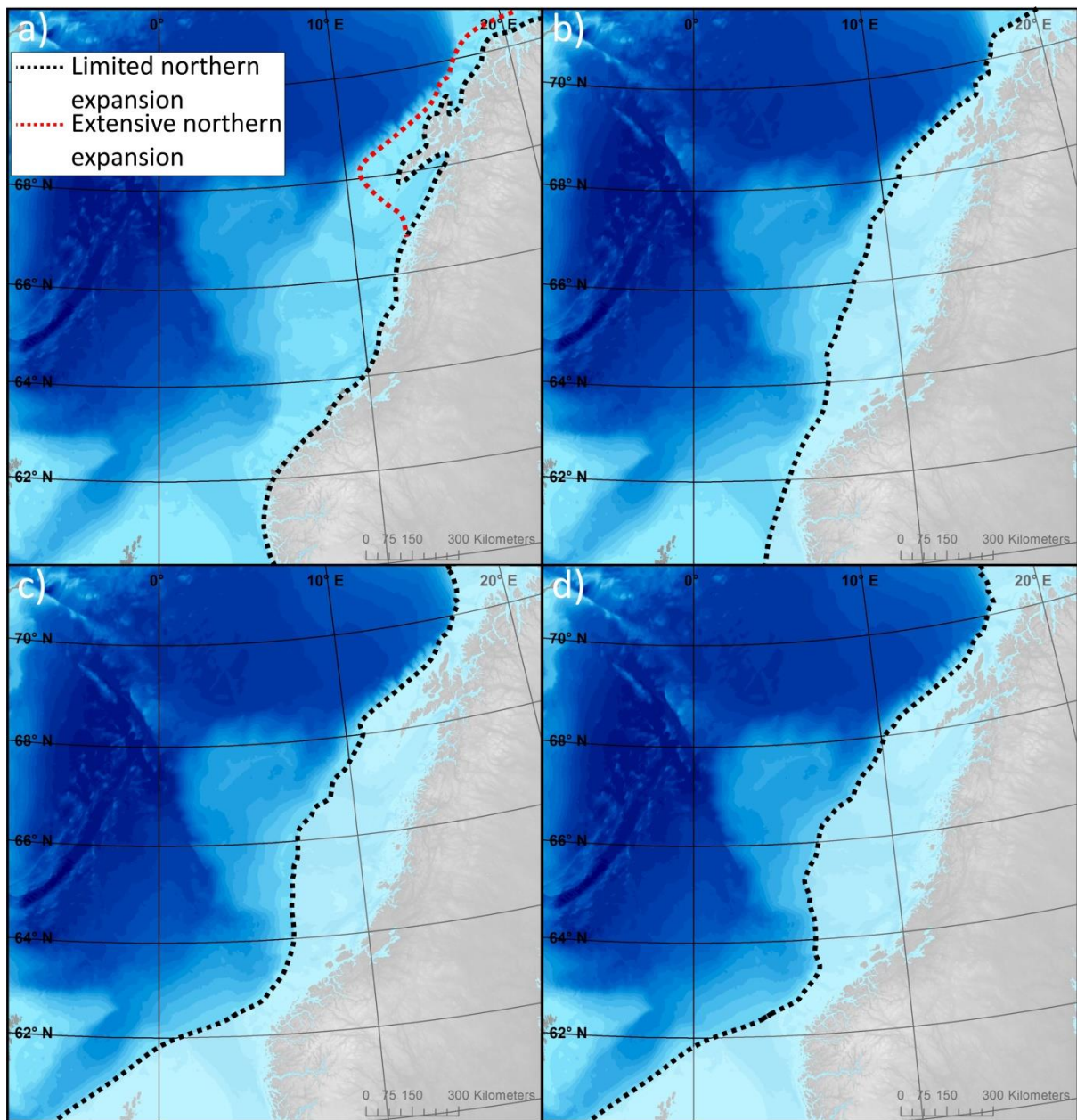
3815

3816 Fig. 15. GLORIA long range side-scan sonar imagery superimposed on the Bear Island Trough-Mouth
 3817 Fan. Glacigenic Debris-Flows (GDF), the INBIS Submarine Channel system and the Bjørnøya
 3818 submarine landslide are identified using the GLORIA imagery. Palaeo-ice flow directions are
 3819 indicated by arrows. KT = Kveithola. Glacigenic debris-flows visible in the GLORIA imagery are
 3820 thought to relate to the Late Weichselian (MIS 2) glacial advance.



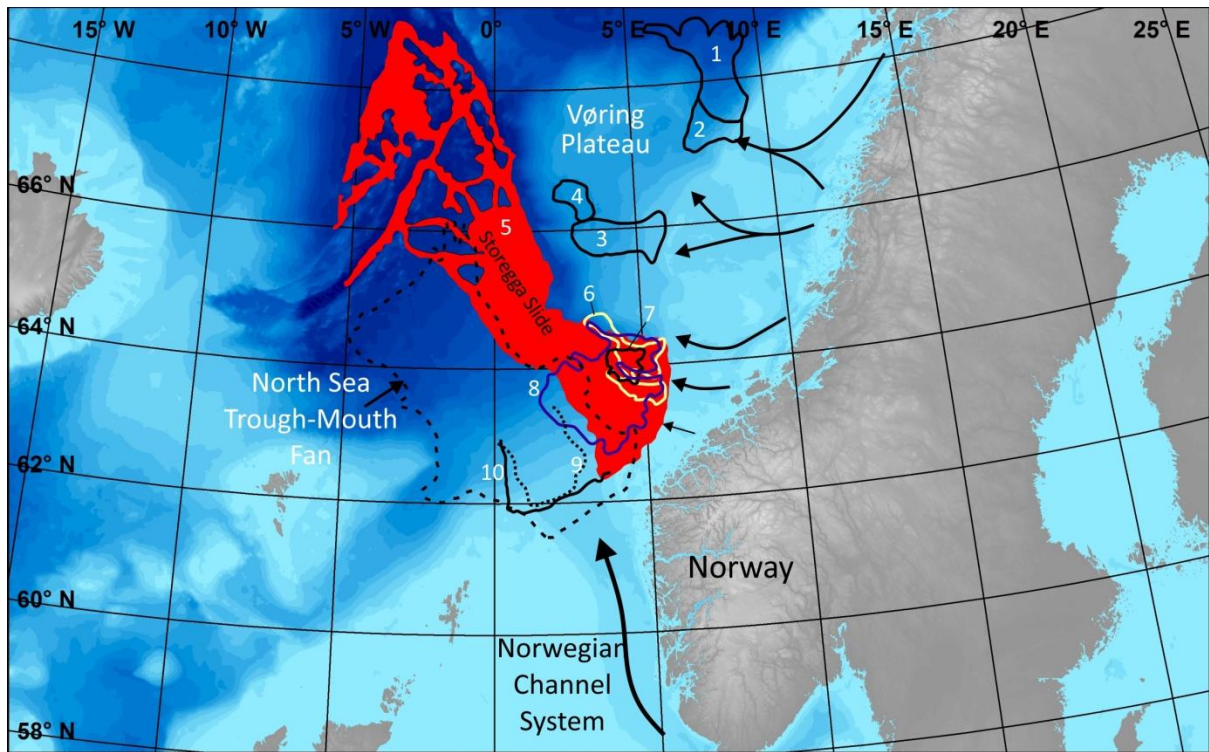
3821

3822 Fig. 16. Maximum westward Quaternary extent of the Scandinavian Ice Sheet (red line) with notable
 3823 cross-shelf troughs, trough-mouth fans and landslides displayed on IBCAO bathymetric data
 3824 (Jakobsson et al., 2012). Arrows indicate cross-shelf troughs thought to have previously contained ice
 3825 streams. Grey shaded areas represent trough-mouth fans. 1 = Håkjerringdjupet 2 = Rebbenedjupet.
 3826 3 = Malangsdjupet. 4 = Andfjord. 5 = Trænadjupet. 6 = Sklinnadjupet. 7 = Suladjupet. 8 = Buadjupet.
 3827 9 = Norwegian Channel. Lof = Lofoten. Trb = Trænabanken. Hb = Haltenbanken. Frb = Frøyabanken.
 3828 MS = Møre Shelf. MP = Måløy Plateau. BI TMF = Bear Island Trough-Mouth Fan. NS = North Sea
 3829 Trough-Mouth Fan. AdS = Andøya Slide. TrS = Trænadjupet Slide. NS = Nyk Slide. SS = Storegga Slide.
 3830 LC = Lofoten Channel.



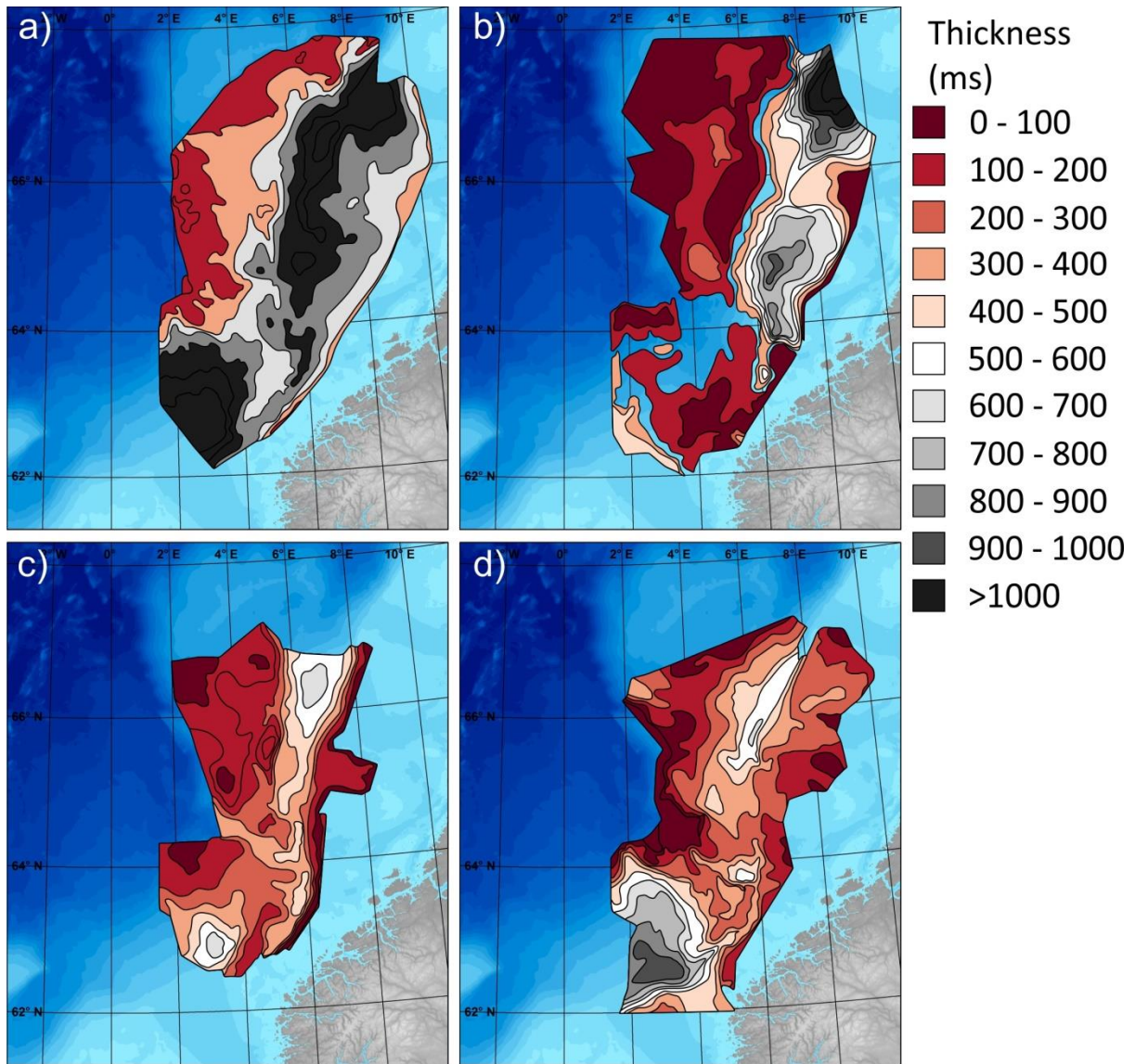
3831

3832 Fig. 17. Maximum extents of the Scandinavian Ice Sheet. a) 2.58 – 1.1 Ma. Two models of
 3833 Scandinavian Ice Sheet extent during the Early Quaternary are envisaged. 1) Black-dashed line: An
 3834 intermediate sized ice sheet rarely extending beyond the fjords of western Norway (Sejrup et al.,
 3835 1996; Dowdeswell et al., 2013; Newton et al., 2016). 2) Red-dashed line: A limited southern extent
 3836 but regular expansion to the shelf edge north of the Vøring Plateau (Rokoengen et al., 1995;
 3837 Henriksen and Vorren, 1996). b) 1.1 – 0.7 Ma. Definitive first expansion of the ice sheet at 1.1 Ma
 3838 followed by a retreat to dimensions more akin with outlined in a) (Helmke et al. 2005; Sejrup et al.,
 3839 2005). c) 0.7 – 0.13 Ma. Extent of the Saalian Scandinavian Ice Sheet. Other glaciations have been
 3840 reconstructed as delivering sediment to the mid-Norwegian Margin resulting in progressive
 3841 westward movement of the shelf edge (Montelli et al., 2017a). d) 0.13 – 0 Ma. Maximum extent of
 3842 the Weichelian ice sheet (Hughes et al., 2016).



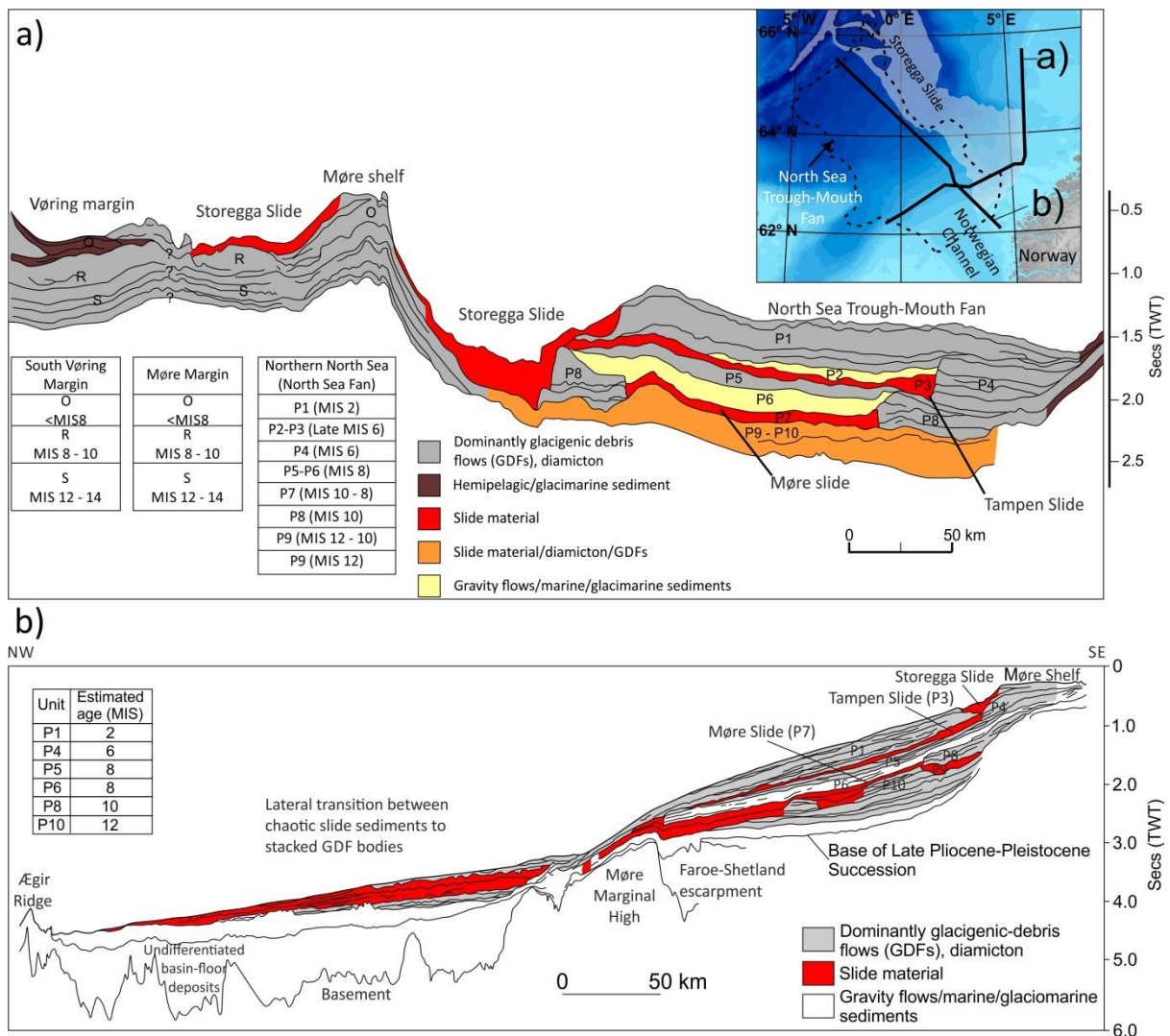
3843

3844 Fig. 18. Large submarine landslides identified on the Norwegian Continental Margin. 1) Trænadjupet
 3845 Slide; 2) Nyk Slide; 3) Vigrid Slide; 4) Sklinnadjupet Slide; 5) Storegga Slide; 6) R Slide; 7) W Slide; 8) S
 3846 Slide; 9) Tampen Slide; 10) Møre Slide. Palaeo-ice stream flow directions are indicated by arrows.



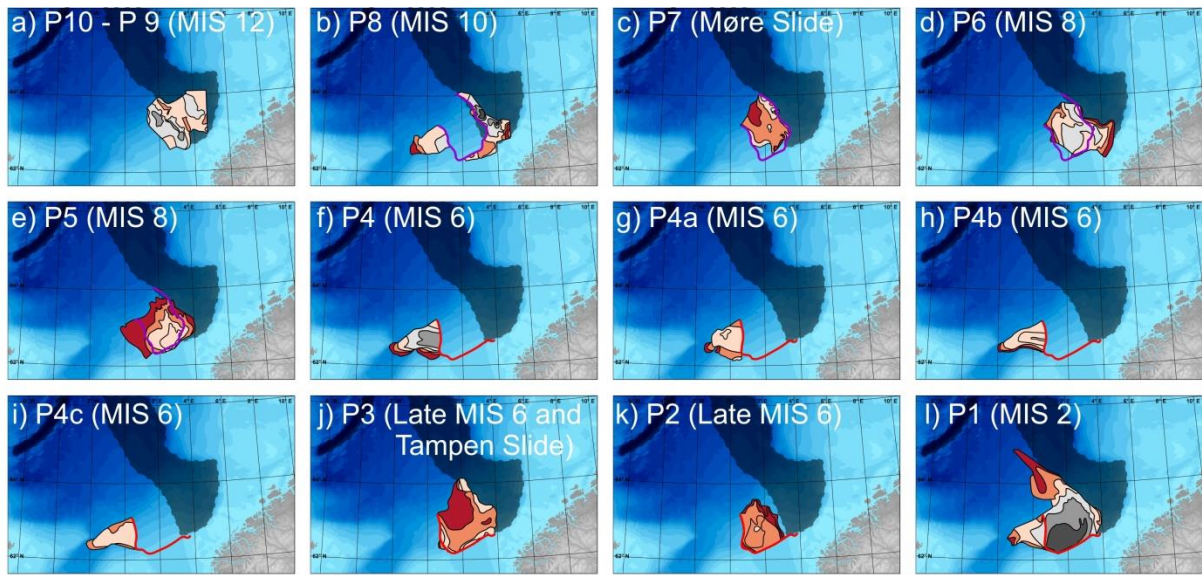
3847

3848 Fig. 19. Isopach maps of: a) Naust Formation; b) Naust W (deposited from 2.7 – 1.7 Ma);
 3849 Naust U (deposited from 1.7 – 1.1 Ma) and Naust S (deposited from (1.1 – 0.4 Ma); d) Naust R (deposited
 3850 from 0.4 – 0.2 Ma) and O (deposited from 0.2 – 0 Ma). Note that the thickness of the deposited
 3851 material increases to the south with younger ages. Modified from Rise et al. (2005).



3852

3853 Fig. 20. Seismic profiles across the Storegga Slide and North Sea Trough-Mouth Fan; location of
 3854 seismic lines shown in inset. a) Seismic profile crossing the southern Vøring Margin, the Storegga
 3855 Slide and the North Sea Trough-Mouth Fan showing the distribution and correlation of identified
 3856 Pleistocene units along the Norwegian Sea Margin. b) Seismic profile down the North Sea Trough-
 3857 Mouth Fan. P1 – P10: identified Late Plio-Pleistocene seismic sequences on the proximal North Sea
 3858 Trough-Mouth Fan. GDFs = glaciogenic debris-flows. Adapted from Sejrup et al. 2004.



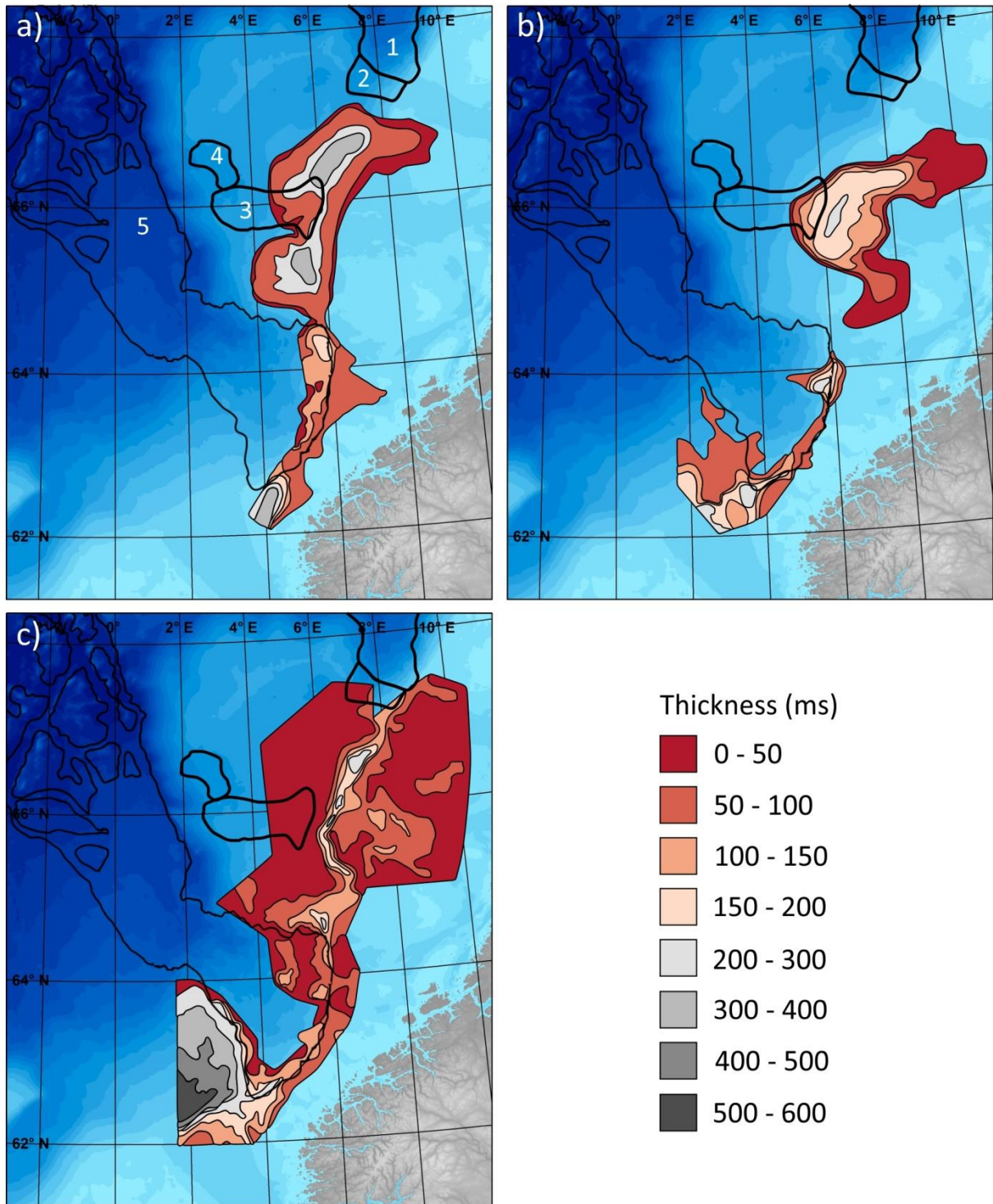
twt (ms)

■ 0 - 50 ■ 50 - 100 ■ 100 - 200 ■ 200 - 300 ■ 300 - 400 ■ >400

3859 — Møre Slide headwall

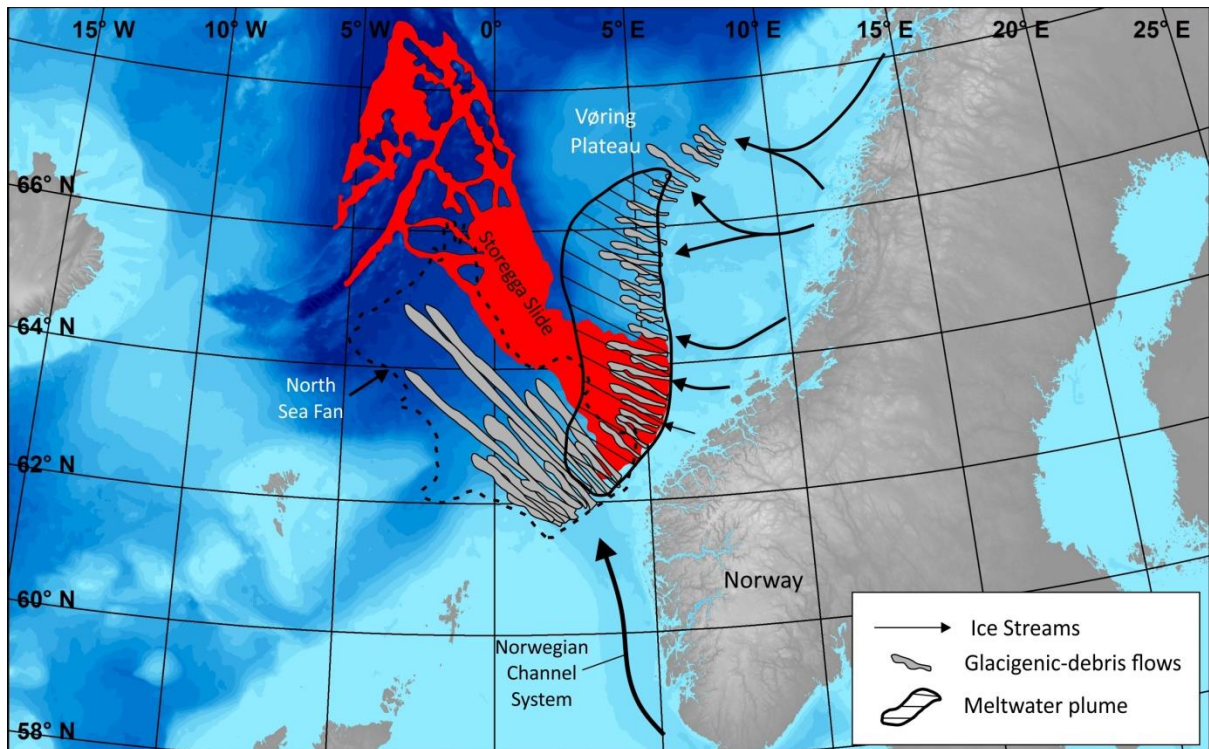
— Tampen Slide headwall

3860 Fig. 21. Isopach maps for units P1 – P10 identified in Fig. 20. a) P10 – P9; b) P8; c) P7; d) P6; e) P5; f)
 3861 P4; g) P4a; h) P4b; i) P4c; j) P3 and Tampen Slide; k) P2; l) P1.



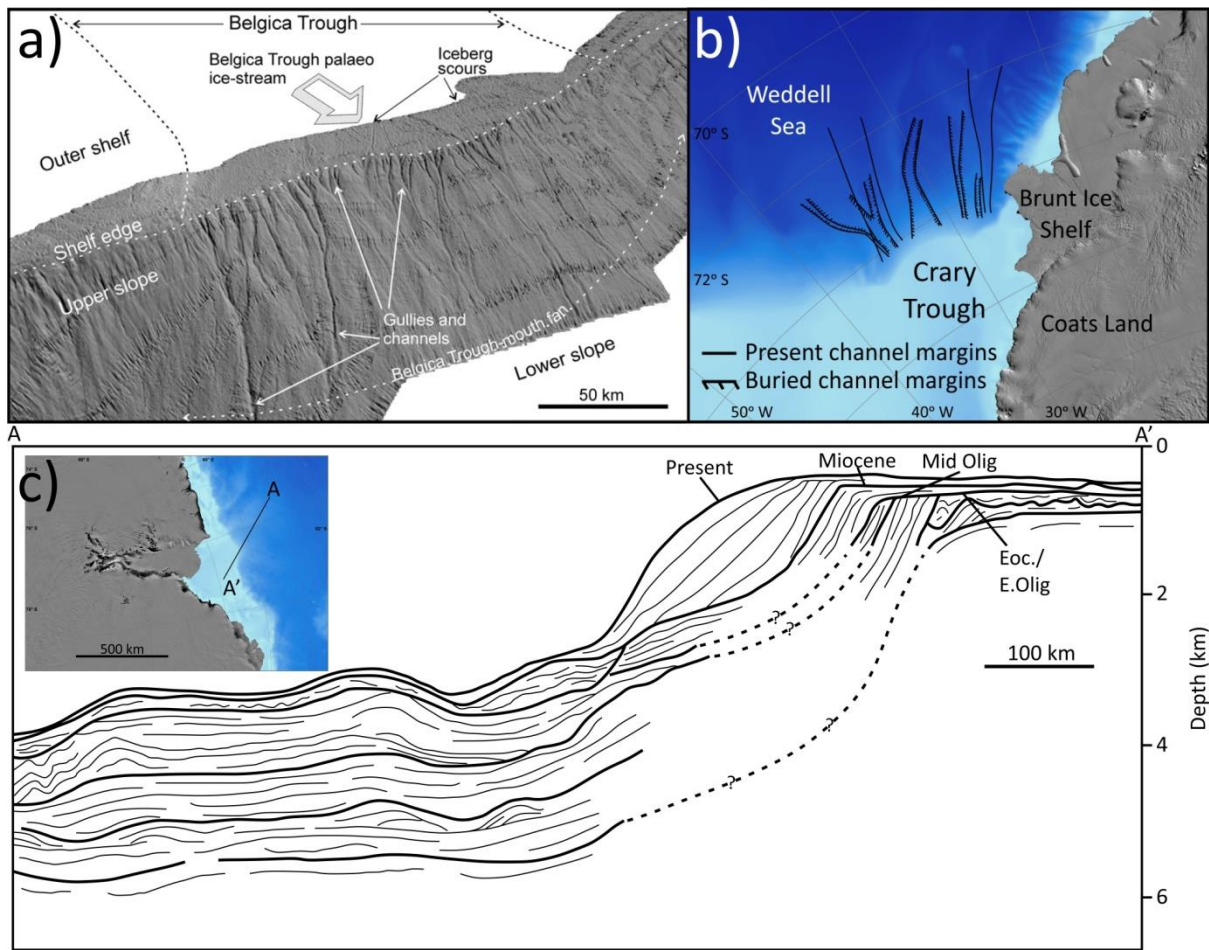
3862

3863 Fig. 22. Isopach maps of glacial deposits along the mid- and southern Norwegian margins from a)
 3864 the Elsterian (MIS 10 – 8), b) the Saalian (MIS 6) and c) the Weichselian (MIS 5d – 2). 1 – 7:
 3865 Submarine landslide outlines. 1) Trænadjupet Slide; 2) Nyk Slide; 3) Vigrid Slide; 4) Sklinnadjupet
 3866 Slide; 5) Storegga Slide.



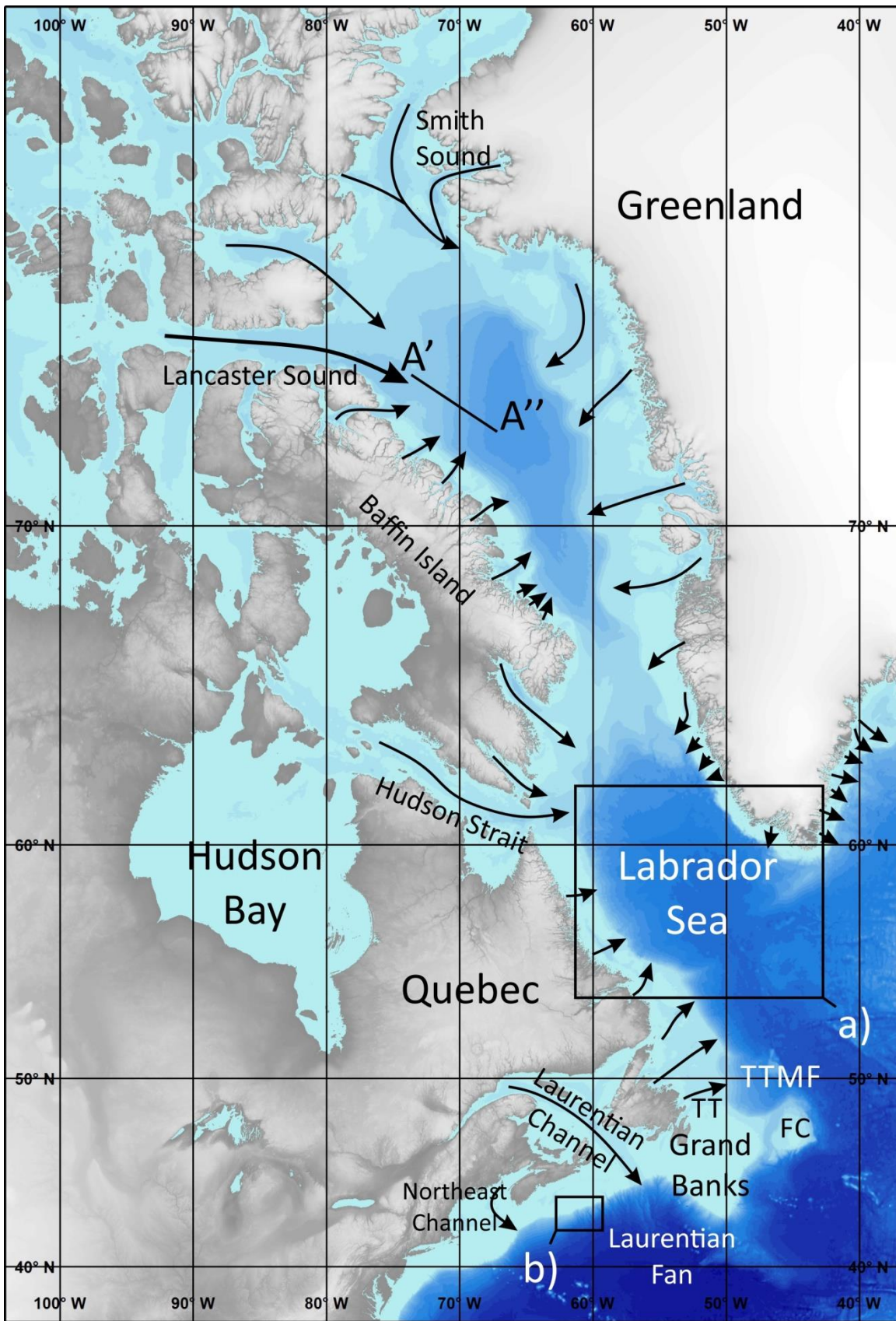
3867

3868 Fig. 23. Schematic model showing Late Weichselian ice sheet related deposition across the North Sea
 3869 and South Vøring Margins. The continental slope is characterised by glacigenic debris-flow
 3870 emplacement. The disintegration of the Norwegian Channel Ice Stream resulted in the release of a
 3871 meltwater plume which transported fine-grained material to the Storegga Slide region and the south
 3872 Voring margin. Palaeo-ice stream flow directions are indicated by arrows. Adapted from Lekens et al.
 3873 (2005) and Hjelstuen et al. (2005).



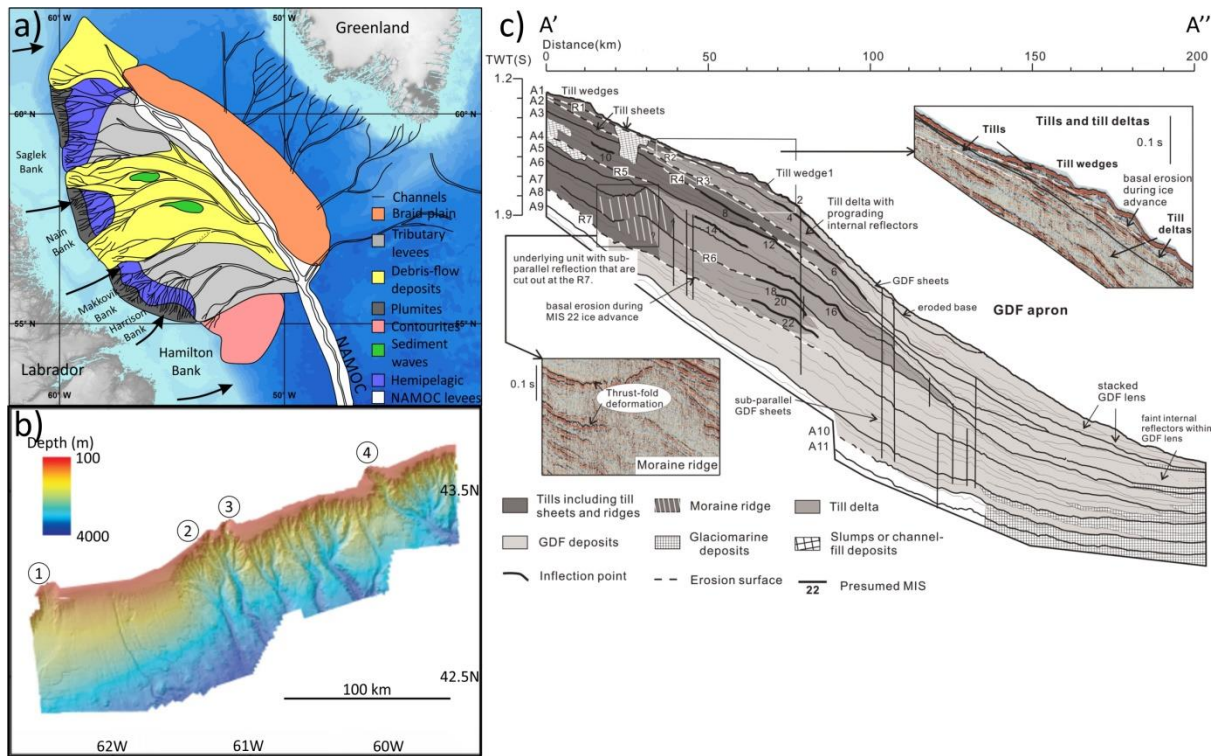
3874

3875 Fig. 24. Examples of trough-mouth fans from Antarctica with varying morphologies. a) Oblique view
 3876 (from the North) of sun-illuminated swath bathymetry of the Belgica Trough-Mouth Fan and the
 3877 major sedimentary features. b) Present and buried channels identified on the Crary Trough-Mouth
 3878 Fan. c) Bathymetric map and seismic interpretation of the Prydz Bay Trough-Mouth Fan. Modified
 3879 from Dowdeswell et al. (2008), Kuvaas and Kristoffersen (1991) and Passchier et al., (2003).



3880

3881 Fig. 25. Location map of the East Canadian Margin. Cross-shelf troughs inferred to have contained
 3882 ice streams during the last glacial are illustrated with arrows.

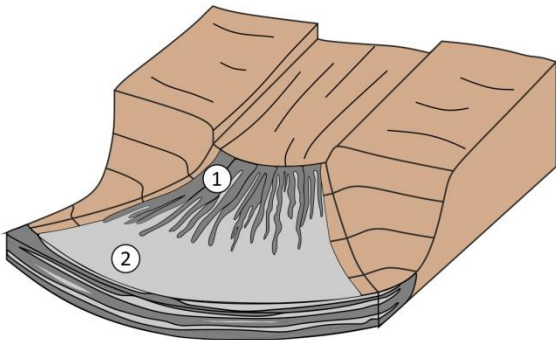


3883

3884 Fig. 26. Examples of ice sheet influenced sedimentary features on the East Canadian Margin. a) Map
 3885 of the Labrador Sea showing the upslope branching of tributary channels on the slope and the
 3886 distribution of major sediment facies (redrawn from Hesse et al. (1997) and Ó Cofaigh et al. (2003)).
 3887 Inferred ice stream positions are marked with arrows. NAMOC = North Atlantic Mid-Ocean Channel.
 3888 b) Multibeam bathymetry sonar data showing the morphology of the central Scotian Slope. 1 =
 3889 Mohican Channel; 2) Verrill Canyon; 3) Dawson Canyon; 4) Logan Channel. Modified from Mosher et
 3890 al. (2004). c) Seismic interpretation of the Lancaster Sound Trough-Mouth Fan from an airgun
 3891 profile. Detail of stacked structure of till and till data are shown in the upper inset. A close-up of two
 3892 moraine ridges is shown in the lower inset. Presumed MIS stages are labelled along their
 3893 corresponding seismic reflector. Modified from Li et al. (2011).

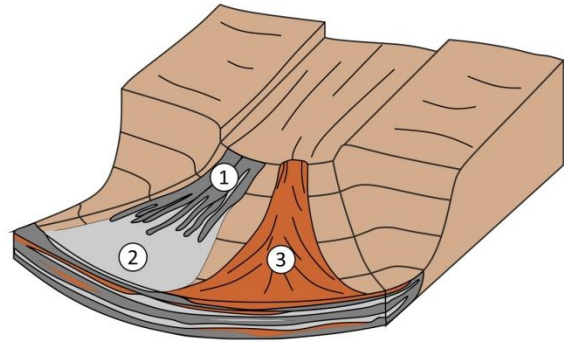
Type 1 - High sedimentation

- ① Glacigenic debris-flows
- ② Distal debris-flow muds/
Turbidites



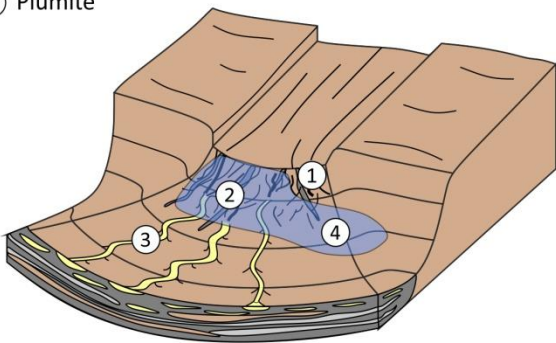
Type 2 - High sedimentation

- ① Glacigenic debris-flows
- ② Distal debris-flow muds/
Turbidites
- ③ Large submarine landslides



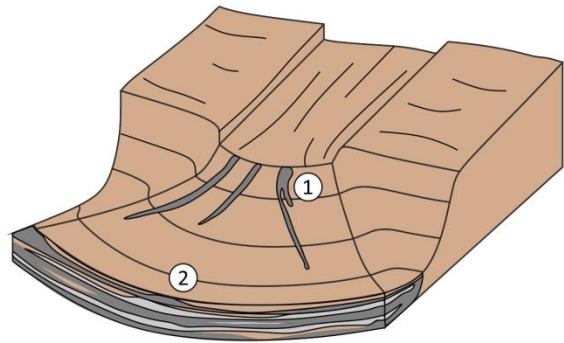
Type 3 - Medium sedimentation/High water

- ① Glacigenic debris-flows
- ② Meltwater/Dense water gullies
- ③ Channel-levee system
- ④ Plumite



Type 4 - Low sedimentation

- ① Glacigenic debris-flows
- ② Sediment-starved lower fan

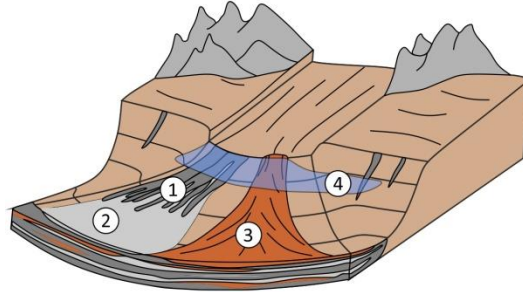


3894

3895 Fig. 27. Schematic model of trough-mouth fan classification from analysis of glaciated continental
3896 margins in this study.

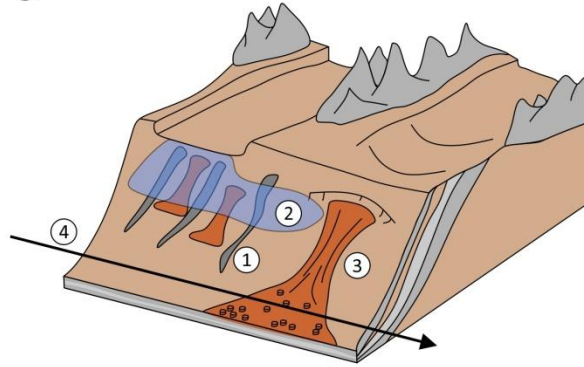
Margin 1 - Trough-mouth fans

- ① Glacigenic debris-flows
- ② Distal debris-flow muds/
Turbidites
- ③ Large submarine landslides
- ④ Plumite



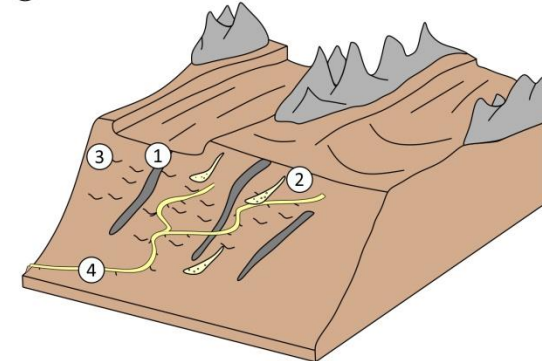
Margin 2 - High sediment/High meltwater input

- ① Glacigenic debris-flows
- ② Plumite
- ③ Submarine landslides
- ④ Contourrite



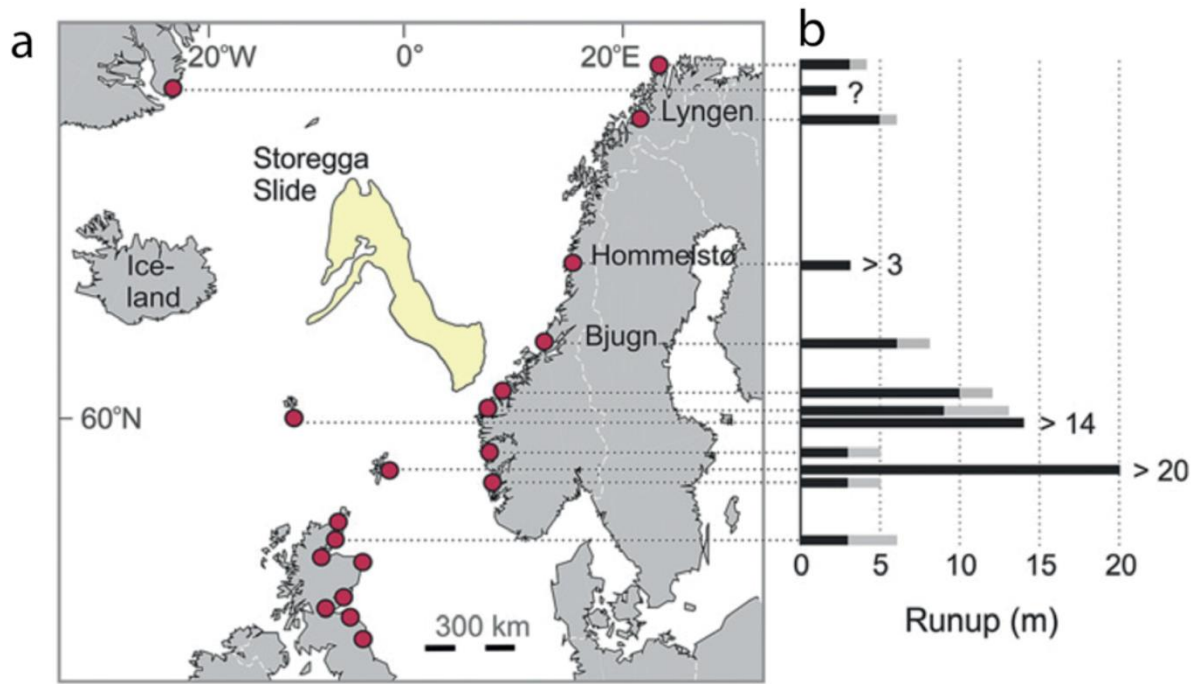
Margin 3 - Low sediment input

- ① Glacigenic debris-flows
- ② Turbidity currents
- ③ Sediment waves
- ④ Channel-levee system



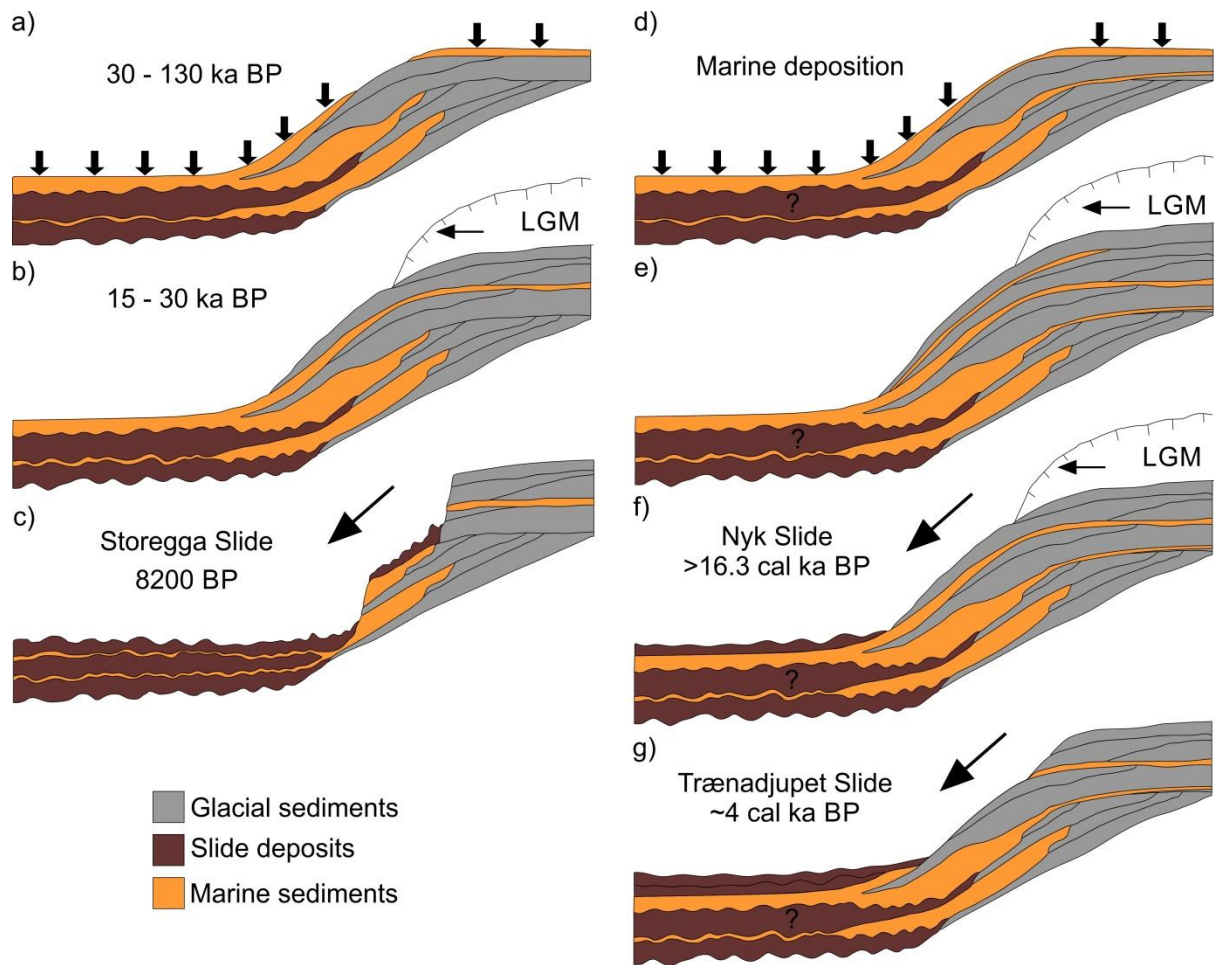
3897

3898 Fig. 28. Schematic model of glaciated margin classification from analysis of glaciated continental
3899 margins in this study.



3900

3901 Fig. 29. Location of the Storegga Slide that comprises $>3,000 \text{ km}^3$ of predominantly glacial material.
 3902 Red dots indicate locations of tsunami deposits associated with the Storegga Slide.
 3903 Tsunami runup heights above sea level are indicated in b). Black bars indicate minimum runup
 3904 heights and grey bars maximum runup heights (Modified from Bondevik et al., 2005 and Talling et
 3905 al., 2014).



3906

3907 Fig. 30. Illustration of the proposed depositional and slide processes that occur in the Storegga Slide
 3908 (a – c) and the Trænadjupet Slide (d – g) areas. a) Deposition of soft marine clays during the last
 3909 interglacial. b) Ice at the shelf edge during the Last Glacial Maximum and the deposition of glacial
 3910 sediments. c) The Storegga Slide. Two older slide scars are filled with marine clays below the
 3911 Storegga Slide scar. Adapted from Bryn et al. (2005). d) Deposition of soft marine clays and
 3912 contouritic sediments. e) Ice at the shelf edge and the deposition of glacial sediments. f) Nyk Slide
 3913 occurs altering the properties of the sediment package on the continental slope. g) The Trænadjupet
 3914 Slide.

3915

3916

3917 **Tables**

3918 **Table 1. Summary of the important steps in glacial evolution of the East Greenland Margin and the**
 3919 **resulting record of sedimentation.**

| Period (Ma) | Ice sheet history | Sedimentation record |
|-------------|--|--|
| 2.58 - 1.3 | Most extensive ice sheet surrounding the Nordic Seas Largest advances from 2.5 - 2.4 Ma and about 2.1 Ma Little evidence of widespread collapses during deglaciation | Dominates IRD signal in the Nordic Seas 2.5 - 2.4 Ma advance marked by regional reflector and glacial debris-flows on Scoresby Sund Trough-Mouth Fan Subsequent advances on Scoresby Sund sector characterised by silty clays with variable IRD content, turbidites and glacial debris-flows limited to the upper slope 5 km progradation of shelf edge |
| 1.3 - 0.7 | Hypothesis 1: relatively stable ice sheet remaining on/near to the continental shelf Hypothesis 2: repeated advances to and retreat from the shelf edge | Glacial debris-flows on the central and southern sides of Scoresby Sund Trough-Mouth Fan Enhanced glacialine sedimentation through meltwater plumes and turbidity currents Submarine channel formation on east Greenland Margin 38 km progradation of the shelf edge 130 m vertical aggradation of the continental shelf |
| 0.7 - 0.13 | Expanded and more stable ice sheet Extent of advances relatively uncertain Saalian Greenland Ice Sheet represents the maximum ice extent reached during the Quaternary | Limited evidence of submarine mass movement occurrence beyond the continental shelf before the Saalian Saalian aged glacial debris-flows on the Scoresby Sund Trough-Mouth Fan and the east Greenland margin Submarine channel system was inactive during the Saalian <5 km progradation of the shelf edge >260 m vertical aggradation of the shelf |
| 0.13 - 0 | Advances during MIS 5d and 5b at least to the inner shelf Advance during MIS 4 (close to MIS 2 limit in Scoresby Sund sector) followed by a limited retreat MIS 3 limited advance and retreat cycles Maximum extent of Late Weichselian ice sheet between 21 - 16 ka BP Expansion to the shelf edge in Northeast and Scoresby Sund sectors; central east Greenland extent is uncertain | Scoresby Sund: Glacial debris-flow emplacement East Greenland margin: Glacial debris-flow emplacement on the upper and mid- continental slope Below 2000 m sedimentological facies dominated by turbidites Laminated silt and mud layers on the upper continental slope and shelf Sedimentation rates peaked during deglaciation between 51 and 79 cm/kyr Channel system cross-cuts glacial debris-flow deposits Northeast sector: Glacial debris-flow emplacement on the upper and mid- continental slope Turbidite deposition on the lower continental slope Submarine landslide headscarp visible in bathymetry |

3920
3921

3922 Table 2. Areas, volumes and ages of known large submarine landslides in the Nordic Sea (adapted
 3923 from Hjelstuen et al. (2007). The volumes reported for PLS-1, PLS-2 and PLS-3 represent minimum
 3924 volumes (Llopart et al., 2015).

| Slide | Area (x 10 ³ km ²) | Volume (x 10 ³ km ³) | Age (Ma) | Reference |
|---------------|--|--|-------------------|--|
| LS-1.1 | 1338.4 | 46.84 | 0.061 - 0.2 | Llopart et al. (2015) |
| LS-2.1 | 95.2 | 2.48 | >0.0225 | Llopart et al. (2015) |
| LS-2.2 | 35.5 | 1.06 | >0.0225 | Llopart et al. (2015) |
| LS-11.1 | 119.9 | 2.06 | | Llopart et al. (2015) |
| LS-11.2 | 52.9 | 1.11 | | Llopart et al. (2015) |
| LS-Kv | 459.1 | 3.67 | | Llopart et al. (2015) |
| PLS-1 | 647.7 | 45.34 | 0.8 - 1.0 | Llopart et al. (2015) |
| PLS-2 | 709 | 127.62 | 0.105 - 0.135 | Llopart et al. (2015) |
| PLS-3 | 240 | 18 | 0.2 - 0.5 | Llopart et al. (2015) |
| BFSC I | 115 | 25.5 | 1.0 - 0.78 | Hjelstuen et al. (2007) |
| BFSC II | 120 | 24.5 | 0.78 - 0.5 | Hjelstuen et al. (2007) |
| BFSC III | 66 | 11.6 | 0.5 - 0.2 | Hjelstuen et al. (2007) |
| Slide B | | | 0.6 - 0.5 | Laberg et al. (1996) |
| Slide A | 12 | 5.1 | 0.6 - 0.5 | Laberg et al. (1996) |
| Bjørnøya | 12.5 | 1.1 | 0.2 - 0.3 | Laberg et al. (1996) Lindberg et al. (2004) |
| Andøya | 9.7 | | Holocene | Laberg et al. (2000) |
| Trænadjupet | 4 - 5 | 0.4 - 0.9 | 0.004 - 0.0035 | Laberg et al. (2002b) |
| Nyk | 4 - 6 | 0.4 - 0.72 | 0.021- 0.016 | Lindberg et al. (2004) |
| Vigrid | 2.5 | | >0.2 | Solheim et al. (2005) |
| Sklinnadjupet | 7.7 | | 0.3 | Solheim et al. (2005) |
| Storegga | 95 | <3.2 | 0.0072 | Hafliðason et al. (2005) |
| R | 6.8 | | 0.3 | Solheim et al. (2005) |
| W | 63.7 | 24.6 | 2.7 - 1.7 | Hjelstuen and Andreassen (2015) |
| S | 72.3 | 15 | 0.5 | Solheim et al. (2005) |
| Tampen | | | 130 | Nygård et al. (2005) |
| Møre | | 1.2 | 0.4 - 0.38 | Nygård et al. (2005) |
| U | 86.7 | 24.6 | 1.7 - 1.1 | Evans et al. (2005) Hjelstuen and Andreassen (2015) |

3925

3926

3927 Table 3. Summary of the important steps in glacial evolution of the Svalbard/Barents Sea margin and
 3928 the resulting record of sedimentation.

| Period (Ma) | Ice sheet history | Sedimentation record |
|-------------|--|--|
| 2.58 - 1.6 | Retreat of initially extensive ice sheet on Svalbard and the northern Barents Sea Subsequent limited advance and retreat of glaciers on Svalbard and in the Northern Barents Sea | Meltwater related increase in sedimentation on Svalbard continental slope Submarine mass movement deposits (not glacial debris-flows) on the Svalbard continental slope Meltwater sediment driven incision of channels into the continental slope Gradual aggradation and progradation of sedimentary wedges |
| 1.6 - 1.3 | Expansion to the shelf edge of glaciers sourced from Svalbard Limited southward expansion of Barents Sea Ice Sheet | Svalbard margin: Period of major glacial debris-flow emplacement Acceleration of sedimentary wedge progradation Deposits are thicker and seismically distinct from previous period Barents Sea margin: Glaciofluvial and glacial marine deposition |
| 1.3 - 0.7 | Advance to and retreat from the shelf edge of Svalbard glaciers First expansion to the shelf edge in the Bear Island Trough of the Barents Sea Ice Sheet | Svalbard margin: Emplacement of glacial debris-flows on the continental shelf Barents Sea margin: 1.3 - 1.0 Ma ? emplacement of glacial debris-flow deposits; rate of sedimentation increased to 130 cm/kyr 1.0 - 0.78 Ma ? emplacement of glacial debris-flow deposits; rate of sedimentation drop to 70 cm/kyr; submarine landslide on Bear Island Trough-Mouth Fan (>25,000 km ³) Change in sedimentation rate hypothesised to be a consequence of Barents Sea shelf submergence |
| 0.7 - 0.13 | Ice sheet expands to the shelf edge during MIS 16, 12, 8 and 6 MIS 14 advance believed to have reached shelf edge of Bear Island Trough but not around Svalbard | Svalbard margin: Glacial debris-flow emplacement (decline in deposit thickness with the adoption of 100 kyr climate cyclicity) Shift from net-erosion to net-accumulation of sediment on the continental shelf Storfjorden Trough-Mouth Fan: Each advance is associated with a package of glacial debris-flows Bear Island Trough-Mouth Fan: Upper and mid-slopes of the trough-mouth fan characterised by glacial debris-flow emplacement; lower slope is characterised by fine-grained turbidites and hemipelagic sediments MIS 12 advance ? 17,650 km ³ of sediment deposited at a rate of 63 cm/ka across the fan MIS 10 and 8 advance ? 7266 km ³ of sediment deposited at a rate of 14 cm/ka across the fan MIS 6 advance ? 4061 km ³ of sediment deposited at a rate of 19 cm/ka Five large submarine landslides on the trough-mouth fan with volumes between 1.1 and 24.5 km ³ |
| 0.13 - 0 | MIS 5d (115 - 105 ka) advance to shelf edge limited to Svalbard MIS 5b (90 - 80 ka BP) advance on Svalbard is less extensive MIS 5b (90 - 80 ka BP) advance in Barents Sea limited to eastern Barents and Kara Seas MIS 4 (70 - 50 ka BP) advance to the shelf edge MIS 2 (32 - 20 cal ka BP) advance to the shelf edge Proposed advance to shelf edge of the Bear Island Trough during MIS 3 (40 - 35 cal ka BP) | Svalbard margin: Deposition of turbidites on the continental slope during MIS 4 (rate of turbidite emplacement was especially high following the initial retreat of the ice) 32 - 24 cal ka BP ice expansion characterised by laminated and massive mud deposition and turbidite emplacement 24 - 20 cal ka BP advance characterised by glacial debris-flow emplacement 20 cal ka BP ? initial retreat of the ice sheet characterised by increased IRD and hemipelagic sedimentation 15.7 - 14.65 cal ka BP ? second phase of retreat characterised by increased IRD <14.65 cal ka BP ? accelerated retreat characterised by deposition of thick, fine-grained laminated mud deposits; rates of sedimentation 1 to 2 orders of magnitude greater than when ice was at the shelf edge Storfjorden Trough-Mouth Fan: Northern/Central Fan ? >50 m of glacial debris-flow deposits emplaced during MIS 2; gully incision into upper slope Southern Fan ? Multiple submarine landslide scars; interlaminated plumite deposits upto 50 m thick interbedded with discontinuous diamicts Bear Island Trough-Mouth Fan: Glacial debris-flow emplacement characterises each advance to the shelf edge Gullies are incised into the upper slope at the margins of the trough-mouth fan <1 m of glacial marine sediments recovered from the upper fan 2400 km ³ of sediment accumulated at 13 cm/ka |

3929
3930

3931 Table 4. Summary of the important steps in glacial evolution of the Norwegian Continental Margin
 3932 and the resulting record of sedimentation.

| Period (Ma) | Ice sheet history | Sedimentation record |
|-------------|---|---|
| 2.58 - 1.1 | <p>Reconstruction 1: Intermediate size ice sheet rarely expanding beyond fjords of western Norway</p> <p>Reconstruction 2: Glaciers regularly advanced to the shelf edge north of the Vøring Plateau Glaciers remained limited in size south of the Vøring Plateau</p> | <p>Slide W occurred between 2.7 and 1.7 Ma and is estimated to have remobilised 24,600 km³</p> <p>Reconstruction 1: No evidence of ice sheet related submarine mass movements Limited delivery of IRD</p> <p>Reconstruction 2: Progradation of sediment wedges in the north where ice reached the shelf edge Little/no influence of ice along southern Norwegian margin</p> |
| 1.1 - 0.7 | <p>First expansion to the shelf edge after 1.1 Ma Subsequent reversion to limited ice sheet extent seen previously</p> | <p>1.1 Ma lacial advance marked by near continuous till layer Glacimarine sedimentation associated with 1.1 Ma advance beyond the shelf edge Retreat of ice sheet is marked by a return of marine sedimentation along the entire margin</p> |
| 0.7 - 0.13 | <p>Advances to the shelf edge during MIS 14, 12, 10 and 6 Uncertainty over whether MIS 8 advance reached the shelf edge or just the mid-continental shelf</p> | <p>MIS 14: Till present on the outer shelf as far south as the Møre Shelf Glacigenic debris-flow emplacement on continental shelf beyond where till is present on the shelf Little/no sedimentary evidence of ice sheet advance south of the Møre Shelf</p> <p>MIS 12: Advance is marked by regional till layer Outer Møre Shelf and continental slope is characterised by marine/glacimarine deposition North Sea Trough-Mouth Fan underwent a major construction phase; 3000 km³ of sediment was deposited, mainly in the form of glacigenic debris-flow deposits Møre submarine landslide (400 - 380 ka BP) reworked 1200 km³ of sediment previously deposited on the North Sea Trough-Mouth Fan</p> <p>MIS 10 - 8: Mid-Norwegian margin? MIS 10 and 8 cannot be clearly distinguished; sequence characterised by strong shelf erosion and glacigenic debris-flow emplacement on the continental slope South Norwegian margin? MIS 10 and 8 clearly distinguishable Two distinct glacigenic till units on the south Vøring and North Sea margin 2600 km³ of sediment emplaced as glacigenic debris-flow deposits on the North Sea Trough-Mouth Fan during MIS 10 3500 km³ of sediment emplaced on the North Sea Trough-Mouth Fan during MIS 8; 2100 km³ through glacimarine processes (ice not at the shelf edge), 1400 km³ by glacigenic debris-flows (ice at the shelf edge) Skinnadjupet (300 ka BP) and R (300 ka BP) landslides occurred during MIS 8</p> <p>MIS 6: Mid-Norwegian margin? deposition of stacked till tongues up to 200 m thick as a result of ice not reaching the shelf edge South Vøring to Northern North Sea margin? extensive till layer deposited to the shelf edge; glacigenic debris-flow emplacement beyond the shelf edge North Sea Trough-Mouth Fan? 2600 km³ of sediment deposited, predominantly by glacigenic debris-flows</p> |
| 0.13 - 0 | <p>MIS 5d (109 - 96 ka BP) advance to coast and into fjords MIS 5b (87 - 82 ka BP) advance to the outer coastline MIS 4 (71 - 57 ka BP) advance to the shelf edge Minor readvance beyond the west Norwegian coastline around (42 cal ka BP)</p> <p>Northern Norway: Ice advanced from 34 cal ka BP, reaching the shelf edge from 24 - 23 cal ka BP Retreat of up to 100 km between 22 and 20 cal ka BP Readvance to the shelf edge from 16 - 14 cal ka BP</p> <p>Mid-Norway: Main expansion to shelf edge began at 23.5 cal ka BP</p> | <p>North Norwegian Continental Shelf (MIS 3 - 1): Earliest dated glacigenic debris-flows emplaced around 34 cal ka BP Plumite deposition around 25,590 14C yr BP Additional glacigenic debris-flow sequences dated to 15.6 ka BP, 19.5 ka BP and 21.7 - 21.1 ka BP; laminated plumites interbed glacigenic debris flow deposits Large numbers of submarine landslides during the Holocene including the Andøya Slide</p> <p>Mid-Norwegian Continental Shelf (MIS 5 - 1): MIS 5 and 4 marine and glacimarine deposition on continental slope reflect withdrawn ice sheet position Two till layers associated with the MIS 2 advance from 22 - 16.5 cal ka BP; glacigenic debris-flows associated with these advances are found on the continental slope Little/no evidence of plumites Two large submarine landslides (Nyk and Trænadjupet) occurred between 21.8 - 19.3 cal ka BP and 5.3 - 3.2 cal ka BP</p> <p>South Vøring Margin (MIS 2 - 1): Three glacigenic units interpreted as glacigenic debris-flows on the continental slope from MIS 2 (21,000, 16,200, 15,700 14C yr BP) Plumite deposits interbed the debris-flow units; deposition rates from Plumites during deglaciation as high as 1750 cm/kyr</p> |